2018

Investigations of Possible Cases of Scurvy in Juveniles from the Kellis 2 Cemetery in the Dakhleh Oasis, Egypt, Through Stable Carbon and Nitrogen Isotopic Analysis of Multiple Tissues

Georgina Chasse
University of Central Florida

INVESTIGATIONS OF POSSIBLE CASES OF SCURVY IN JUVENILES FROM THE KELLIS 2 CEMETERY IN THE DAKHLEH OASIS, EGYPT, THROUGH STABLE CARBON AND NITROGEN ISOTOPIC ANALYSIS OF MULTIPLE TISSUES

by

GEORGINA LUCILLE CHASSE
B.A. University of Central Florida, 2014

A thesis submitted in partial fulfillment of the requirements
for the degree of Master of Arts
in the Department of Anthropology
in the College of Sciences
at the University of Central Florida
Orlando, Florida

Summer Term
2018

ABSTRACT

Vitamin C deficiency, or scurvy, is a disease that can occur in humans at any age and has been seen throughout time. Scurvy affects the production of connective tissues, including collagen, which leads to the many symptoms of the disease, including fatigue, anemia, bleeding gums and lost teeth, skeletal changes, and even death. The Kellis 2 cemetery in the Dakhleh Oasis, Egypt, in use from approximately AD 50-360, contains the remains of many juveniles who exhibit skeletal indicators of scurvy. Tissue samples from juveniles who did (n=31) and did not (n=117) exhibit skeletal indicators of scurvy were analyzed isotopically, with the sample including stable carbon ($\delta^{13}C$) and nitrogen ($\delta^{15}N$) isotope values of bone collagen (scurvy =11, non-scurvy =13), hair (scurvy=21, non-scurvy=112), nail (scurvy =10, non-scurvy =44), and skin (scurvy =19, non-scurvy =59). Intra-tissue comparisons were conducted to determine whether this disease affects $\delta^{13}C$ and $\delta^{15}N$ values sufficiently to distinguish these two groups from one another isotopically. Inter-tissue comparisons between bone collagen and hair were also conducted, with emphasis placed on inter-tissue spacing results and outliers. Mean $\delta^{13}C$ and $\delta^{15}N$ values for each hair segment were compared to look for early isotopic signals of scurvy. No statistically significant differences were found between any intra-tissue scurvy and non-scurvy cohorts and no obvious indications of the onset of scurvy were seen in the hair segment analyses. The inter-tissue spacing results, however, highlighted some interesting patterns in the bone collagen-to-hair values, especially in regards to the identified outliers that are discussed in more detail. While this study did not detect any significant differences between scurvy and non-scurvy cohorts or early isotopic signals of the disease in hair segments, the inter-tissue spacing results

do point to changes between the cohorts that may be attributable to the physiological stress of scurvy and therefore warrants further investigation.

To my family, for their constant love and support in the pursuit of my dream. And especially to my husband, who always believed in me even when I did not believe in myself.

ACKNOWLEDGMENTS

Firstly, I want to thank my advisors, Dr. John Schultz and Dr. Sandra Wheeler, for believing in me and giving me the opportunity to pursue my graduate career. You were both always there to encourage and push me to do my best. And many thanks for your understanding when life took over and delayed this work. Thank you Dr. Sandra Wheeler for always being able to put my mind at ease and explain things to me in order to help ease my anxiety on this long journey. And to Dr. Lana Williams, for sharing your knowledge and expertise both in the classroom and in the laboratory with me. I made a few mistakes along the way, but you never gave up on me. To all of my graduate professors, thank you for passing along your knowledge and giving me the opportunities to improve my writing and for not getting overly annoyed at my long-windedness. To those professors I had the great pleasure to TA for, thank you for sharing tips and advice about the "behind the scenes" aspects of what it is like to be a professor. To the Anthropology Department staff – Lisa Haas and Jennifer Branson – thank you for answering all of my questions about paperwork and what exactly I needed to do with it all. And especially to Lisa Haas for making sure I did not fail to register for classes on time when I was overwhelmed and forgot.

Thank you to everyone who made this research possible, including the Dakhleh Oasis Project, without whom the materials for this study would not have been available. And to Dr. Sandra Wheeler, Dr. Lana Williams, and Dr. Tosha Dupras for making those materials available for me to study. I understand how precious these samples are, and appreciate your willingness to entrust them to me. Dr. Sandra Wheeler, thank you for allowing me to help you investigate a topic you have wanted to study for a long time. And thank you to the many friends and

colleagues I had along the way, especially Jackie, Vu, Lish, and Elizabeth, for always being ready and willing to proofread a paper (or an abstract). You all were as instrumental as our professors in greatly improving my scientific writing skills and I will always remember our long nights in the “bone lab”.

And finally, to my family, for always encouraging me to pursue my education, even when it meant long days and late nights away from you. To my husband, Michael, your support and love has been invaluable to me these past many years. Your understanding of the time required and your willingness to step into the gaps left when I was not able to be at home with our children made all of this possible. To my mother, Rita, without whom this would not have been possible, you will never know just how appreciative I am for you always being there for my boys and your readiness to take on the tasks that were previously mine. And to my precious children, Sean and Connor, I hope that you understand why I was not always home when you got off the bus or when it was bedtime. Know that I always love you, and hope that by witnessing my dedication to something I am passionate about, that you learn the same dedication to your passions.

TABLE OF CONTENTS

LIST OF FIGURES

LIST OF TABLES

CHAPTER 1: INTRODUCTION

The importance of health and disease in humans is not a modern concept. All populations over the course of human history have dealt with diseases that affected their health. The modern analyses that result from the study of ancient health and disease can provide information not only on the diseases affecting a population, but can also provide insight into other aspects of their lives such as socio-economic/status differences, gender differences, or even environmental disasters (Grauer, 2012). The study of ancient health and disease and the extent to which it affected a population is an important goal within bioarchaeology (Brickley and Ives, 2008). One method used by bioarchaeologists to study ancient health and disease is the application of stable isotope analysis of human tissues (Katzenberg, 2008). Stable carbon and nitrogen isotopes are used most often in dietary and nutrition studies, but can also be applied to environmental and physiological studies, such as analysis of patterns and/or evidence of health and disease (Katzenberg, 2008; Schoeninger and Moore, 1992). Bone is generally used in these studies to provide a picture of an individual's or population's diet, health, and disease; this tissue provides a measure of many years of an individual's life, and is thus considered a long-term tissue (Katzenberg, 2008). Soft tissues, such as hair, nail, and skin, however, provide a more focused window into the last months prior to death, and are therefore viewed as short-term tissues (O'Connell and Hedges, 1999; Pollard et al., 2007; White and Schwarcz, 1994; Williams, 2008).

Scurvy, a metabolic bone disease that results from insufficient vitamin C, is a disease that can be present in any human population, as humans are reliant upon their diets for all vitamin C (Allgaier et al., 2012). Clinical data on scurvy indicates that symptoms can appear within 8-12

weeks of the beginning of vitamin C deficiency in the diet (Allgaier et al., 2012), with symptoms progressing from non-specific (e.g. fatigue and lethargy) to more extreme and specific symptoms the longer the deficiency lasts (e.g. presentations within bones, corkscrew hairs, and death) (Agarwal et al., 2015; Allgaier et al., 2012; Polat et al., 2015; Popovich et al., 2009). The majority of scorbutic symptoms are only visible clinically, as they are mostly non-specific or dermatologic in character. Only the most extreme and/or prolonged cases present osteological symptoms, limiting diagnosis of archaeological scurvy cases to those extreme and/or prolonged instances that are then visible on the skeleton and dentition. This study aims to bridge the gap between clinical and archaeological presentations of scurvy through the application of stable isotopic analysis of both long-term and short-term tissues along with osteological indicators of scurvy.

Historical Background

The individuals analyzed in this study are from the Kellis 2 Cemetery in the Dakhleh Oasis, Egypt, and lived and died during the Romano-Christian period, approximately AD 50-360 (Hope, 2003). Due to the high temperatures, alkalinity of the soil, and arid conditions, the individuals interred in the Kellis 2 cemetery exhibit a remarkable degree of skeletal preservation (Dupras and Tocheri, 2007). Additionally, the practice of early Christianity in the region resulted in the burial of all members of the society in the same cemetery, providing researchers with access to individuals from all stages of life (Bowen, 2003). As such, it is possible to investigate ancient health and disease, such as the presence of scurvy, in the juvenile population buried in the Kellis 2 cemetery.

Dakhleh Oasis

The Dakhleh Oasis is located approximately 725 kilometers southwest of Cairo in Egypt (Figure 1). One of five major depressions in the Western Desert, Dakhleh Oasis is 80 kilometers long on its east to west axis and 25 kilometers north to south. The depression is approximately 100 meters below the level of the surrounding desert. The northern portion is bordered by a large escarpment while the southern border is not well-defined (Dupras and Schwarcz, 2001).

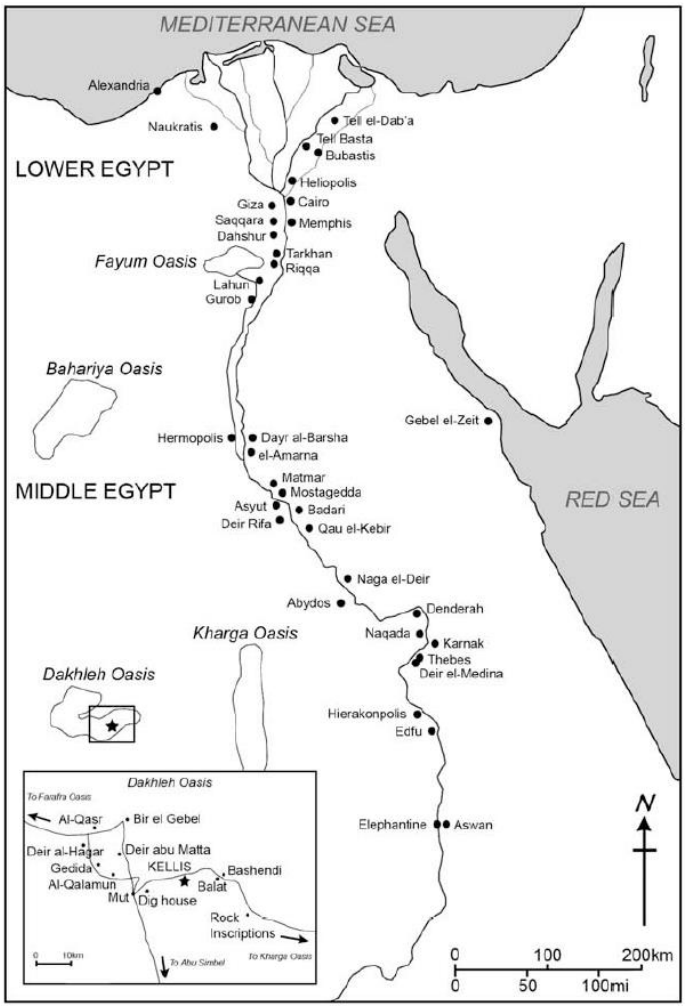

Figure 1: Map of Egypt depicting the location of the Dakhleh Oasis, with the location of Kellis shown in the inset. Map courtesy of the Dakhleh Oasis Project.

The temperatures within the Oasis vary by season. During the winter months, the temperature at midday can reach 25° Celsius while nighttime temperatures can fall as low as -4° Celsius; conversely, temperatures during the summer months typically reach 40-50° Celsius during the day and 19° Celsius at night (Blume et al., 1984; Giddy, 1987). The Dakhleh Oasis experiences very little rainfall, generally receiving only 0.3mm in a year (Schwarcz et al., 1999). As a result, agriculture within the Oasis is reliant on natural springs and wells that tap into the Nubian Sandstone Series, an aquifer that is enclosed in layers of shale (Price, 1985). The humidity between March and September is 23-30% with humidity between October and February reaching 33-50% (Doering and Gericke, 1984; Shalin, 1985). It is believed that the environmental conditions present in the Dakhleh Oasis today are the same as during the Romano-Christian Period (Churcher, 1983, 1993).

Kellis and the Kellis 2 Cemetery

Kellis, an ancient Egyptian city, was located along trading routes that ran through the Egyptian Western Desert and the Dakhleh Oasis (Bowen, 2003; Hope, 2001). The Kellis 2 Cemetery, located along the eastern border of the city, was one of several cemeteries used throughout the existence of the city and was in use during the Late Roman-Early Christian period of occupation. Radiocarbon dating of individuals from the cemetery indicate that it was in use from AD 100-450 (Fairgrieve and Molto, 2000; Stewart et al., 2003), however current archaeological data shows usage from AD 50-360 (Hope, 2003).

The inhabitants of the Dakhleh Oasis relied on agriculture for both subsistence and economic means (Dupras and Schwarcz, 2001). Some of the agricultural products grown in the

Dakhleh Oasis included barley, beans, dates, doum palm nuts, figs, grapes, olives, and wheat (Schwarcz et al., 1999). The dates and olives grown within the Dakhleh Oasis were highly sought after commodities throughout the Nile Valley and Mediterranean area during the Roman period (Bagnall, 1997). The Dakhleh Oasis was also known to produce foods that contained vitamin C (Table 1) (Aufderheide et al., 2003; Dupras, 1999; Thanheiser et al., 2002). The presence of vitamin C-rich foods does not preclude the development of scurvy due to several possible factors such as malabsorption disorders, unequal access to foods, changes to vitamin C content within foods, and personal agency in food choice.

Table 1: Vitamin C, iron, and folate content of select raw foodstuffs grown in the Dakhleh Oasis.

Foods	Vitamin C Content (mg/ 100g)	Iron Content (mg/ 100g)	Folate (µg/ 100g)
Barley, hulled	0.0	3.6	19
Fava Beans	1.4	6.7	423
Dates, medjool	0.0	0.9	15
Figs	2.0	0.37	6
Radishes	14.8	0.34	25
Pomegranates	10.2	0.3	38
Squash	18.0	0.4	30
Honey	0.5	0.42	2
Grapes	3.2	0.36	2
Olives	0.9	6.28	0
Wheat	0.0	3.71	28
Onions	7.4	0.21	19
Turnips	21.0	0.3	15
Apricots	10.0	0.39	9
Peaches	6.6	0.25	4
Lentils	4.5	6.51	479
Goat's Milk	1.3	0.05	1
Cow's Milk	1.5	0.05	5
Human Milk	5.0	0.03	5
Nutrient content from USDA website: https://ndb.nal.usda.gov/ndb/search/list			

Burials within the Kellis 2 Cemetery are single interments, with a few exceptions, placed in an extended supine position with the head facing west, with little to no grave goods, and wrapped in burial shrouds, all of which reflect early Christian burial practices (Birrell, 1999; Bowen, 2003). Tocheri et al. (2005) have suggested that all individuals from ancient Kellis during this time period were buried in the cemetery, and many researchers have found evidence of this in the form of fetal and infant burials, including those with fatal and disfiguring diseases (e.g. Cope, 2008; Cope and Dupras, 2011; Mathews, 2008). The combination of deliberate burial of all members of society, the arid desert environment, and high pH level of the burial matrix

contribute to the exceptional preservation of the individuals interred in the Kellis 2 cemetery (Dupras, 1999; Dupras and Schwarcz, 2001).

Research Aims

The purpose of this research is threefold: 1) an intra-tissue comparison of $\delta^{13}C$ and $\delta^{15}N$ values between those juveniles who exhibit skeletal indicators of scurvy and those who do not, 2) an inter-tissue comparison of $\delta^{13}C$ and $\delta^{15}N$ values between long-term and short-term tissues to determine if they provide different information relating to health status, and 3) a comparison of $\delta^{13}C$ and $\delta^{15}N$ values between hair segments to determine if early isotopic signs of scurvy can be detected. In other words, do the $\delta^{13}C$ and $\delta^{15}N$ values within each tissue differ between those juveniles with and without scurvy? And can the $\delta^{13}C$ and $\delta^{15}N$ values from long-term and short-term tissues be used to bridge the gap between clinical and archaeological symptoms of scurvy so that earlier cases of the disease (i.e., prior to the development of scurvy-like skeletal lesions) can be detected?

Thesis Chapter Summaries

Chapter 2 presents information on scurvy, including historical medical knowledge of the disease and the importance of vitamin C within the human body, as well as processes that may reduce the amount of vitamin C that is bio-available. Typical presentations of scurvy, both in clinical and archaeological settings, are presented along with differential diagnoses for each setting and some difficulties that arise in attempting to diagnosis scurvy in archaeological populations. A brief background on $\delta^{13}C$ and $\delta^{15}N$ analysis is provided, as well as information in

regards to isotopic analysis on the four human tissues used in this study: bone, hair, nail, and skin. A brief explanation of inter-tissue spacing and values found in previous inter-tissue spacing studies is also provided.

Chapter 3 presents the materials and methods for the samples used for analysis in this study. The skeletal sample is introduced and the division into scurvy status and age cohorts is explained, followed by a brief summary of how individuals were separated into the scurvy and non-scurvy cohorts. The subset of the sample prepared for isotopic analysis by the author is described, after which the methods used to prepare the samples for isotopic analysis are listed in step-by-step documentation. The precision and accuracy of the sample are provided with information about statistical analysis methods being presented last.

Chapter 4 presents the results of the $\delta^{13}C$ and $\delta^{15}N$ analysis, starting with preservation data for bone collagen and then hair, nail, and skin samples. The explanation of why some samples were retained for or discarded from further analysis is provided. The $\delta^{13}C$ and $\delta^{15}N$ results for each tissue, scurvy status, and age cohort are presented, along with the mean $\delta^{13}C$ and $\delta^{15}N$ hair segment trends and intra-tissue differences between the scurvy and non-scurvy cohorts. Finally, inter-tissue spacing results are provided and a detailed description of five outliers in regards to inter-tissue spacing is provided.

Chapter 5 presents a discussion of the isotopic analyses, beginning with inter-tissue spacing followed by a discussion of the outliers presented in Chapter 4. The discussion of the intra-tissue scurvy and non-scurvy cohort comparisons follows, with the hair segment comparison discussion being presented last. A brief summary of the discussion is provided at the

end of the chapter. Chapter 6 presents the conclusion of the research, as well as limitations found within the current study and potential topics for future research.

CHAPTER 2: LITERATURE REVIEW

Medical History of Scurvy

Scurvy was first defined in the Ancient Egyptian Ebers Papyrus in approximately 1500 BCE (Pimentel, 2003). Scurvy is a disorder that occurs due to a prolonged deficiency of vitamin C (Agarwal et al., 2015), and may occur as a result of non-consumption of vitamin C-rich foods or malabsorption of necessary levels of vitamin C. Historically, scurvy was considered to be a disease of sailors because they experienced the majority of cases of the disease due to a lack of fresh fruits and vegetables on long voyages (Popovich et al., 2009). The discovery of an effective cure for scurvy is credited to Sir James Lind, a British Navy surgeon (Pimentel, 2003). Lind conducted an experiment in which he divided twelve sailors suffering from scurvy into six groups of two and provided each group with a different possible remedy for the disease. He found that the group who was provided extra citrus fruits as their remedy showed the greatest signs of recovery (Lind, 1753).

Almost a century and a half later, Thomas Barlow (1894) presented a lecture to the Royal College of Physicians of London where he provided evidence that many individuals previously identified as having acute rickets indeed suffered from infantile scurvy. Due to his thorough examination of many infants suffering from the disease, including some post mortem examinations (Barlow, 1894), scurvy in very young children became known as Barlow's disease (Popovich et al., 2009). Barlow found that the one symptom relied heavily upon for the diagnosis of scurvy, "spongy" and/or bleeding gums, may not occur in very young children, especially if their teeth had not yet erupted (Barlow, 1894).

The occurrence of Barlow's disease had increased in the last half of the 1800s (Popovich et al., 2009), however the discovery of this increase did not occur until the 20th century. In 1914, Alfred Hess concluded that heating milk in order to destroy certain infectious bacteria also destroyed the vitamin C in milk (Barr, 2010), thus causing a spike in the cases of infantile scurvy in those who could afford to purchase milk for their infants. It was not until 1931, however, that the antiscorbutic factor in the foods known to fend off scurvy was discovered by Albert Szent-Gyorgyi (Popovich et al., 2009). This factor was labeled hexuronic acid, and later called ascorbic acid, or vitamin C, because of its role in the treatment and prevention of scurvy (Pimentel, 2003). Since the discovery of the key vitamin needed to prevent scurvy, its incidence has drastically decreased in modern society, especially in industrialized societies (Popovich et al., 2009).

Role of Vitamin C in the Human Body

Vitamin C, also known as ascorbic acid, is a necessary nutrient that all humans need for many different bodily functions but are incapable of producing themselves (Allgaier et al., 2012; Polat et al., 2015; Popovich et al., 2009). In other animals, glucose is converted to vitamin C through an enzymatic process that utilizes gulonolactone oxidase, but lacking this ability, humans must acquire the necessary levels of vitamin C through their diets (Agarwal et al., 2015; Polat et al., 2015). This can be achieved through ingestion of vitamin C-rich foods (e.g. citrus fruits, potatoes, broccoli, spinach, and tomatoes) (Allgaier et al., 2012) or vitamin supplements.

Vitamin C is absorbed by the body in the gastrointestinal system, specifically the ileum (Polat et al., 2015). Once absorbed by the body, vitamin C is used in intracellular and extracellular tissues for many different functions (Agarwal et al., 2015) (Table 2). If bodily

tissues do not receive sufficient amounts of vitamin C then they cannot properly carry out their specific tasks, which may result in the onset of scurvy symptoms. The daily recommended amount of vitamin C is 15-75 mg, depending upon age (Agarwal et al., 2015). Since vitamin C is a water-soluble substance, any excess within the body is excreted in the urine (Agarwal et al., 2015; Popovich et al., 2009).

Table 2: Processes within the human body in which vitamin C is an integral component (drawn from Agarwal et al., 2015; Allgaier et al., 2012; Chambial et al., 2013; Pimentel, 2003).

Collagen Synthesis	Iron Absorption
Caratine Biosynthesis	Dopamine to Norepinephrine Conversion
Cholesterol, Cyclic Nucleotide, & Prostaglandin Conversion	Intercellular Connective Tissue, Osteoid, & Dentine Maintenance
Corticosteroid & Aldosterone Synthesis	Vitamin E & Folic Acid Stabilization
Components of Biochemical Reactions (Enzyme Complement, Cofactor, Reducing Agent, Antioxidant, and Co-substrate)	

Factors That Affect Available Vitamin C Levels in the Body

As discussed previously, the Dakhleh Oasis is known to have grown foods that contained differing levels of vitamin C (Table 1). Some of these foods contained sufficient levels of vitamin C to prevent scurvy with minimal consumption required (e.g. radishes, turnips, apricots) while others would have required higher levels of consumption (e.g. fava beans, figs, olives, goat and cow's milk). However, the growth of these foods in the area does not mean the juveniles living in Kellis were necessarily receiving adequate amounts of vitamin C to prevent scurvy. There are several factors that have been found to decrease the amount of vitamin C within food

items or decrease the amount of the ingested vitamin that is actually absorbed by the body. These factors can be divided into three main groups: post-harvest storage and distribution, food preparation/cooking, and internal bodily functions.

Once foods containing vitamin C are harvested, the amount of the vitamin within them begins to decrease. It has been found that storage methods that do not minimize water loss and are at warm or hot temperatures accelerate the loss of vitamin C (Bineesh et al., 2005; Jutkus et al., 2015; Nunes et al., 1998). The hot, arid climate of the Dakhleh Oasis could have decreased the amount of vitamin C within the foodstuffs grown there from the moment they were harvested. Additionally, it has been found that air drying foods such as celery, evidence of which was found in Kellis (Dupras, 1999; Thanheiser et al., 2002), can also cause the level of vitamin C to decrease (Valšíková et al, 2016). Finally, exposure to air and subsequent oxidation after harvest and during storage can cause a loss of vitamin C within foods (Kaewsuksaeng et al., 2011; Rameshkumar et al., 2012). In addition to storage methods causing a loss of vitamin C, it is also possible that vitamin C-rich foods were not being consumed in adequate quantities by the juveniles at Kellis, either due to them not having regular access to these foods or due to them choosing to not consume vitamin C-rich foods.

The second group of factors that can decrease or destroy the amount of vitamin C within foods occurs during preparation and cooking. Preparation of vegetable and fruit matter for cooking by cutting or chopping them into small pieces releases ascorbic acid oxidase, which destroys vitamin C (Davies et al., 1991). Additionally, release of phenolase, the agent within some foods that causes browning when exposed to air, during preparation for cooking also reduces the amount of vitamin C within the food items (Davies et al., 1991). The release of

phenolase and the subsequent interaction with air is another form of oxidation. The process of cooking foods is also responsible for decreasing the amount of vitamin C contained within them. When high temperatures are used for cooking, it destroys the vitamin C within the cooked food, drastically decreasing the amount that can be ingested (Davies et al., 1991; Jutkus et al., 2015). Because vitamin C is water soluble, the use of excess water during boiling leeches the vitamin out of the food and deposits it into the water (Davies et al., 1991). If the water used to boil foods is then discarded, so too is the vitamin C.

Once vitamin C has been ingested, there are endogenous factors that may inhibit absorption of the amounts necessary to prevent the onset of scurvy. These include infections; health issues such as congestive heart failure, kidney, liver, and pancreatic diseases; an over-abundance of some micro-organisms within the digestive system; and other gastrointestinal issues (Table 3)(Davies et al., 1991; Nolan et al., 2015). Systemic infections, such as colds, have been shown to decrease the level of vitamin C within the blood possibly due to oxidation within the body (Davies et al., 1991). Infections within the gastrointestinal tract (e.g. *Giardia intestinalis*, *Cryptosporidium parvum*, *Isospora belli*, *Cyclospora cayetanensis)* can also lead to vitamin C absorption issues due to altering the normal mechanisms of absorption (Nolan et al., 2015). Tuberculosis has also been shown to affect the digestive system (Nolan et al., 2015), and cases of this disease have been found within the Dakhleh Oasis and the Kellis 2 cemetery (Donoghue et al., 2005; Molto, 2002). Several studies (e.g. Innis, 2012; McKeag et al., 2012; Nolan et al., 2015; Song and Kang, 2018) have shown that vitamin C levels within the blood are decreased in individuals suffering from heart failure, kidney disease, liver disease, and pancreatic disease, though whether the deficiency or the disease developed first is unknown. Additionally,

gastrointestinal issues such as Crohn's disease, Celiac disease, lactose intolerance, and inflammatory bowel disease have been found to cause damage to the digestive system that inhibits absorption of the necessary amounts of vitamin C to prevent scurvy (Bickle, 2009; Innis, 2012; Jeejeebhoy and Duerksen, 2018; Nolan et al., 2015; Vagianos et al., 2007). Micronutrient deficiencies also rarely present in isolation (Snoddy et al., 2017), and the interaction of different nutrients have been shown to increase absorption of others (Hallberg et al., 1989; Nolan et al., Sandström, 2001); therefore, a deficiency of other micronutrients may also affect the absorption of vitamin C.

Table 3: Endogenous factors that may affect vitamin C absorption (Bickle, 2009; Davies et al., 1991; Innis, 2012; Jeejeebhoy and Duerksen, 2018; McKeag et al., 2012; Nolan et al., 2015; Song and Kang, 2018; Vagianos et al., 2007).

Factor	**Possible Cause**
Systemic Infection	Oxidation of vitamin C within body
Gastrointestinal Infections	Alteration of normal absorption mechanisms
Tuberculosis	May affect digestive system
Organ Diseases (e.g. heart, kidney, liver, pancreas)	Unknown if disease or vitamin C deficiency occurs first
Gastrointestinal Diseases (e.g. Crohn's, Celiac, lactose intolerance, IBD)	Damage to the digestive system that inhibits proper absorption

Clinical Presentation of Scurvy

Although scurvy is often thought of as a disease of the past, it is still present in the modern world. It is most often seen in populations of developing nations, patients suffering from alcoholism, elderly individuals in isolation, institutionalized individuals, patients with developmental and mental delays, and even people participating in food fads (Allgaier et al.,

2012; Polat et al. 2015). A vitamin C deficiency can be caused by a number of different reasons, including non-access to vitamin C-containing foods, self-imposed dietary restrictions that limit vitamin C intake, and mal-absorption disorders that lower the amount of vitamin C absorbed by the body (Popovich et al., 2009).

If there is a prolonged period of inadequate vitamin C intake or absorption, the body will begin to present symptoms of the disease. Symptoms typically increase in severity the longer the deficiency continues, progressing from non-specific symptoms up to and including death if left untreated (Agarwal et al., 2015; Allgaier et al., 2012). Agarwal et al. (2015) state that there is a progression from non-specific symptoms to clinical symptoms that generally are seen in the skin, dentition, and hair, and finally changes in the skeleton that are visible radiologically.

Multiple researchers have described the progression of symptoms differently, some dividing them into different stages while some divide them by their presentation in individuals. Allgaier et al. (2012) have divided the progression of scurvy into three stages: early, prolonged, and extreme. Each stage presents with different symptoms that worsen as the disease progresses to the next stage, as presented in Table 4. Popovich et al. (2009) have divided scorbutic symptoms into three types of presentations: non-dermatologic, dermatologic, and non-specific. These symptom types overlap with those established by Agarwal et al. (2015). In addition to these three types of symptoms, Popovich et al. (2009) describe severe symptoms that occur if scurvy is left undiagnosed and untreated. These can include seizures; congestive heart failure; cerebral, conjunctival, and intraocular hemorrhages; and death (Popovich et al., 2009).

Table 4: Three stages of scurvy and their respective symptoms as defined by Allgaier et al. (2012).

Stages	Symptoms		
Early Deficiency	Malaise	Fatigue	Lethargy
Prolonged Deficiency	Anemia Myalgia Bone Pain Bruising	Petechiae Perifollicular Hemorrhage Corkscrew Hairs Gingivitis	Poor Wound Healing Mood Changes Depression
Extreme Deficiency	Generalized Edema Severe Jaundice Hemolysis	Acute Spontaneous Bleeding Neuropathy Fever	Convulsions Death

The non-specific symptoms described by Popovich et al. (2009) include some of those listed in Table 4 in both Early and Prolonged Deficiency (e.g. fatigue, myalgia, mood changes/irritability, and depression). Arthralgia, anorexia, weakness, shortness of breath, and weight loss are also included as non-specific symptoms of scurvy (Popovich et al., 2009). Although the above symptoms can be caused by scurvy, their presence, especially when isolated, does not necessarily point toward the disease as their cause.

Once scurvy has progressed further, symptoms begin to develop with a more focused causality. These symptoms fall within Allgaier et al.'s (2012) "prolonged deficiency" category and include both dermatologic and non-dermatologic symptoms. The dermatologic symptoms generally present on the lower limbs, but may also present elsewhere (Alqanatish et al., 2015; Popovich et al., 2009). Several bruising-type symptoms can result from untreated scurvy, including petechiae, ecchymosis, easy bruising, and perifollicular hemorrhage (Fossitt and Kowalski, 2014; Popovich et al., 2009). Scurvy-induced anemia can develop as a result of blood loss from these and other hemorrhages, especially when combined with a decreased iron

absorption and simultaneous deficiency in folic acid, both of which can be caused by scurvy (Pimentel, 2003).

Body hair is also affected by scurvy. One symptom associated with hair is follicular hyperkeratosis which is characterized by cone-shaped, spiky, hyper-keratinized projections at the site of hair follicles (Nadiger, 1980). This symptom, however, often leads to a misdiagnosis of vasculitis due to the frequent occurrence of follicular hyperkeratosis in that disease (Adelman et al., 1994; Polat et al., 2015). Corkscrew hairs are also symptomatic of scurvy, and are caused by broken disulfide bonds within the hair structure leading to a coiled appearance (Popovich et al., 2009).

The non-dermatological symptoms of scurvy occur in the bones and dentition. When presented orally, symptoms include swollen and bleeding gums that may be classified as inflammatory gingivitis and loosened teeth (Agarwal et al., 2015; Alqanatish et al., 2015; Popovich et al., 2009). In order for these symptoms to present, however, the individual must be dentulous (Popovich et al., 2009).

There are many symptoms of scurvy that present within the skeleton of affected individuals, with the symptoms typically presenting symmetrically (Agarwal et al., 2015). Since inadequate vitamin C affects collagen production within the body (Polat et al., 2015), this results in inadequate osteoid formation which in turn affects the development of endochondral bone (Agawarwal et al., 2015). The chain reaction caused by vitamin C deficiency on bone development means osteological symptoms are more common in juveniles due to the rapid growth and regeneration of the matrix within their bones (Polat et al., 2015). General non-dermatological symptoms include subperiosteal hemorrhages that often result in pain within the

bones and joints, weakness in the legs that progressively increases in severity, bone fractures due to brittle bones, and pseudoparalysis (Popovich et al., 2009). Osteological manifestations of scurvy most often occur in the legs, especially in the area of the knee (Polat et al., 2015). In very young children, advanced scurvy may cause the individual to lay in a pithed frog position where the knees and hips are held semi-flexed (Agarwal et al., 2015).

Many of the osteological symptoms of scurvy are visible radiologically, and change the appearance of the affected bone(s). These changes typically occur at the distal end of long bones and often affect the knees and ankles, though the wrists have been found to be affected as well (Agarwal et al., 2015; Noordin et al., 2012). Frequent symptoms of scurvy in these areas can include thinning cortical bone, a White line of Frankel at the metaphyses, a Trümmerfeld zone, Pelkan spurs, and Wimberger ring signs (Agarwal et al., 2015; Noordin et al., 2012; Polat et al., 2015). Table 5 presents more detail on these symptoms and other osteological symptoms that may be present. Additionally, advanced scurvy may also produce epiphysis slippage, or separation, in unfused epiphyses and delayed bone development (Agarwal et al., 2015; Noordin et al., 2012).

Table 5: Details of scorbutic symptoms visible radiologically (drawn from Agarwal et al., 2015; Noordin et al., 2012)

Symptom/Location	Diagnostic Criteria
Cortical Thinning	cortical bone thins and shows in sharp contrast to medullary cavity in radiographs; gives the appearance of a "pencil outline" around diaphyses and epiphyses
White Line of Frankel	area of over-calcified cartilage at metaphyses
Trümmerfeld Zone	area of lessened density of metaphyses on the diaphyseal side of the Frankel Line; appears in later stages of disease, but more specific symptom of scurvy
Pelkan Spurs	projections from periphery of metaphyses; associated with elevation of periosteum
Wimberger Ring Sign	round, opaque shadowy area of growth centers; often surrounded by a white line in epiphyses
Osteopenia	most common osteological symptom; deficient osteoid matrix resulting in less trabeculae than in healthy individual; creates a "ground glass" appearance; nonspecific symptom
Costochondral Junctions	flaring of costochondral junction of ribs 1-8; possibly resulting from fractures acquired during normal breathing; similar to changes as seen in rickets
Skull	marrow hyperplasia resulting from anemia may create secondary symptom of "hair-on-end" appearance; may also cause porotic hyperostosis
Subperiosteal Hemorrhage	bleeding between periosteum and bone; only visible during healing stages of scurvy
Delayed Bone Age	interruption of collagen production may cause delayed development of bones, such as carpals, causing age estimates based on bone development to be inaccurate
Epiphysis Slippage	from the changes within joints, the epiphyses are moved out of their correct locations

Noordin et al. (2012) presented a case study of a 4.5 year-old male originally from Pakistan who presented with scorbutic symptoms after relocating with his parents to Dubai. His initial symptoms included swelling in his joints three months prior to medical attention being

sought. The swelling began after the child exhibited a slight fever, and did not cause any discomfort or restriction of movement. These symptoms progressed to the point of preventing the child from walking or sitting due to pain. Initial tests showed the child suffered from hypochromic anemia and vitamin D deficiency, and he tested negative for septic arthritis. Radiographs were obtained of the affected joints (bilateral wrists and knees), which showed many abnormalities that assisted in the diagnosis of scurvy (Table 6). The child's dietary history indicated that he subsisted only on meat products, and thus did not have any intake of vitamin C since his move to Dubai. After treatment with vitamin C and other supplements (due to other vitamin deficiencies), the child recovered from scurvy.

Table 6: Osteological symptoms seen radiologically in 4.5 year-old male presenting with signs of scurvy in knees and wrists (Noordin et al., 2012).

Knees	**Wrists**
Osteopenia	Osteopenia
Cortical Thinning	White Line of Frankel
White Line of Frankel	Trümmerfeld Zones
Trümmerfeld Zones	Wimberger Ring Sign
Wimberger Ring Sign	Pelkan Spurs
Pelkan Spurs	Epiphysis Slippage
Epiphysis Slippage	Delayed Bone Age

Clinical Differential Diagnosis

The nonspecific nature of many of the symptoms of scurvy cause it to often be misdiagnosed (Polat et al., 2015). Scorbutic symptoms may be mistaken for hematological

diseases, ulcerative gingivitis, vasculitis, infections, medicinal side effects, deep vein thrombosis, other vitamin deficiencies, and even trauma (Pimentel, 2003; Polat et al., 2015). There are many specific diseases and disorders that share symptoms with scurvy that may result in a misdiagnosis (Table 7). Adding to the difficulty in diagnosing scurvy is the fact that it is often found simultaneously with other vitamin deficiencies such as thiamine and vitamin D (Agarwal et al., 2015). The osteological manifestations also simulate some features of malignancy, especially that of leukemia (Agarwal et al., 2015).

Table 7: Differential diagnoses of scorbutic symptoms in clinical settings (drawn from Agarwal et al., 2015; Allgaier et al., 2012; Barlow, 1984; Noordin et al., 2012; Pimentel, 2003).

General Disease/Disorder Type	**Specific Disease/Disorder or Cause**		
Hematologic Abnormalities	Thrombocytopenic Purpura Hematological Malignancies	Disseminated Intravascular Coagulation Vasculitis	Deep Vein Thrombosis
Autoimmune Diseases	Sjogren's Syndrome	Systemic Lupus Erythematosus	Rheumatoid Arthritis
Infections	Septic Arthritis Osteomyelitis	Meningococcemia	Rocky Mountain Spotted Fever
Medication Side Effects	Antiplatelet Agents	Anticoagulants	Nonsteroidal Anti-inflammatory Drugs
Other Vitamin Deficiencies	Vitamin K Deficiency	Vitamin D Deficiency/Rickets	
Other	Child Abuse/Neglect Tumorous Growth	Pediatric Syphilis Trauma	Abscess

In order to assist in remembering the most common presentations of scurvy, Agarwal et al. (2015:104) developed a mnemonic of the 4 H's: **h**emorrhagic signs, **h**yperkeratosis, **h**ematologic abnormalities, and **h**ypochondriasis. In addition to this mnemonic, levels of vitamin

C within bodily fluids (e.g. plasma, urine, and leukocytes) can be tested in an attempt to confirm or exclude scurvy during a differential diagnosis (Agarwal et al., 2015). Agarwal et al. (2015) posit that the best way to diagnosis clinical scurvy is through both clinical methods and radiographic analysis. However, the differential diagnosis of scurvy can be time consuming, difficult, and invasive (Popovich et al., 2009), but it is the only one included in the differential diagnosis list that is resolved by administering vitamin C (Allgaier et al., 2012). Additionally, tests for other vitamin deficiencies should be performed along with tests for scurvy because of the concomitance of multiple vitamin deficiencies (Fossitt and Kowalski, 2014). A prompt and accurate diagnosis of scurvy is important because if left untreated it leads to death, either from infection or sudden death (Pimentel, 2003).

Archaeological Evidence of Scurvy

Although scurvy produces many symptoms while a person is living, the evidence of those symptoms is not always preserved after death and skeletonization. Therefore, when attempting to diagnose scurvy in archaeological populations, symptoms used for clinical diagnosis are largely not applicable. However, clinical knowledge of scurvy can provide information regarding possible locations on an archaeological skeleton that may present evidence of the disease and employing differential diagnostic protocols as used in clinical settings will aid in correctly identifying individuals who suffered from scurvy (Klaus, 2015). It has been found that intermittent or chronic cases of scurvy tend to leave skeletal markers of the disease that correlate with clinical data of vitamin C deficiency (Crandall and Klaus, 2014). The presence of abnormal porotic lesions in these clinically-specified locations and of a specific degree of severity are the

indicators used for the diagnosis of scurvy in archaeological populations (Bourbou, 2014; Brickley and Ives, 2006, 2008; Ortner and Ericksen, 1997; Ortner et al., 2001; Stark, 2014). Initially, the majority of archaeological cases of scurvy were reported in adults, however, due to the work of Ortner and his colleagues, most archaeological cases of scurvy are now found to be in juveniles (Brickley and Ives, 2008). Because of the rapid growth experienced by juveniles, scurvy-like lesions are more likely to be discernable on their skeletons as compared to adults (Ortner et al., 2001; Stark, 2014), with the majority of cases in juveniles being seen in individuals between 5 and 24 months of age (Bourbou, 2014).

Abnormal porosity is the main indication of scurvy on skeletal remains, and periosteal new bone formation may accompany it (Brickley and Ives, 2008). In order for new bone deposition to occur in areas of sub-periosteal bleeding, however, the individual must ingest at least low levels of vitamin C in order for osteoid formation to resume (Brickley and Ives, 2008). Ortner et al. (2001:344) define abnormal porosity as "a localized condition in which fine holes, typically less than 1 mm in diameter, penetrate a compact bone surface." This porosity is a result of chronic bleeding from blood vessels that developed defectively due to scurvy, which causes an inflammatory reaction in the bone and periosteum (Brickley and Ives, 2006; Ortner and Ericksen, 1997; Stark, 2014). The fine holes, or porotic lesions, that are found are the result of increased vascularization in the area in response to the inflammation (Bourbou, 2014). These porotic lesions are typically seen bilaterally in all elements in which they are present within an individual, but may differ in the severity of their presentation (Ortner and Ericksen, 1997; Ortner et al., 2001).

This porosity, however, must be distinguished from normal growth porosity, especially in juveniles (Ortner et al., 2001). Normal growth in juveniles is highly vascular, especially in long bone metaphyses (Scheuer and Black, 2000), resulting in what is considered to be normal porosity with holes being generally larger than 1 mm in diameter (Ortner et al., 2001). Individuals suffering from scurvy present with porotic lesions covering a much larger area than normal growth porosity. Ortner et al. (2001) found that normal porosity extends no more than 10 mm from the metaphyseal end of a long bone. Porosity that extends beyond that can, therefore, be considered abnormal.

Several researchers (e.g. Bourbou, 2014; Brickley and Ives, 2008; Klaus, 2015; Ortner and Ericksen, 1997; Ortner et al., 2001) have described locations typical of porotic lesions found in the skull that they have attributed to cases of scurvy (Table 8). Ortner and colleagues (e.g. Ortner and Ericksen, 1997; Ortner et al., 2001) have found that more often scurvy-like lesions appear in areas near the temporalis muscle. This includes the lateral portions of the greater wings of the sphenoid, the posterior maxilla, the internal surface of the zygomatic, and the medial surface of the coronoid process of the mandible (Netter, 2019). Due to the anterior deep temporal artery being situated between the bone and the temporalis muscle, bleeding from this artery can cause irritation and an inflammatory reaction in the corresponding bones (Ortner and Ericksen, 1997). Bleeding from the posterior superior alveolar artery can also cause lesions on the maxillary alveolar bone superior to the molars (Ortner and Ericksen, 1997). Ortner and Ericksen (1997) have contributed lesions found in these areas to the trauma sustained by the blood vessels supplying the muscles used for chewing or nursing (e.g. temporalis muscle). They indicate that although limb and joint pain may decrease physical activity in advanced cases of scurvy, the

appetite is typically not greatly affected resulting in the use of the chewing muscles and agitation of the underlying blood vessels.

Table 8: Cranial and postcranial locations of typical scurvy skeletal lesions (drawn from Brickley and Ives, 2006, 2008; Bourbou, 2014; Brown and Ortner, 2011; Ortner and Ericksen, 1997; Ortner et al., 2001).

Cranial			
Parietal	Occipital	Frontal	Temporal
Greater Wing of Sphenoid	Medial Coronoid Process of Mandible	Alveola Superior to Molars	Lateral Ramus of Mandible
Hard Palate	Posterior Maxilla	Orbital Roof	Internal Zygomatic
Lateral Orbital Margin		Infraorbital Foramen	
Postcranial			
Scapula - Supraspinous Fossa & Infraspinous Fossa Long Bones - Metaphyses; Occasionally Diaphysis			Ilium

Although the areas associated with the temporalis muscle appear to be the most often affected, additional locations on the cranium can present with porotic lesions (Table 8). The orbital area tends to be affected mainly on the roof (inferior frontal) and the lateral orbital margins of the zygomatic (Bourbou, 2014, Brickley and Ives, 2008; Ortner and Ericksen, 1997; Ortner et al., 2001). The same researchers have also found various instances of abnormal porotic lesions on the hard palate, around the infraorbital foramen of the maxilla, the lateral ascending ramus of the mandible, and other bones of the cranium (parietal, occipital, frontal, and temporal).

The postcranial skeleton has also been found to be affected by abnormal porotic lesions attributed to scurvy, and which generally appear concurrently with those of the skull (Ortner et al., 2001). The most notable postcranial scorbutic lesions occur on the supra- and infra-spinous fossae of the scapula (Ortner et al., 2001). The main arteries that supply the scapular muscles, the

suprascapular artery and circumflex scapular artery, lie between the scapula and the muscles themselves (Netter, 2019). Since these arteries are weakened by vitamin C deficiency in scurvy-afflicted individuals, the normal contractions of the scapular muscles could cause the already defective arteries to bleed (Ortner and Ericksen, 1997; Ortner et al., 2001). As with the area affected by the temporalis muscle, this bleeding could cause an inflammatory response in the bone and increased vascular activity leading to abnormal porotic lesions in the fossae (Ortner and Ericksen, 1997).

Bourbou (2014) has found evidence that the ilium is also affected by scurvy. In her study of four juvenile skeletons found in Byzantine Crete, Greece, she found that one individual exhibited abnormal porotic lesions on the internal and external surfaces of both ilia. This finding of abnormal porotic lesions on the ilium has also been found by Brown and Ortner (2011).

The long bones are also sites of possible abnormal porotic lesions, typically at the metaphyses (Ortner et al., 2001). Due to the rapidity with which juveniles grow, the periosteum can become less tightly attached to the bone which allows for subperiosteal hemorrhage and an inflammatory response by the body, especially at the metaphyses (Ortner and Ericksen, 1997). Additionally, periosteal new bone can be formed along the diaphyses of long bones, however, this typically does not occur when the body is completely devoid of vitamin C (Stark, 2014). This reactive bone formation occurs less often than does abnormal porosity (Ortner et al., 2001), though individuals who suffered from extreme cases of scurvy may be more likely to manifest this periosteal new bone growth (Brickley and Ives, 2006). When evaluating porosity on juvenile long bones, it is pertinent to keep in mind that the metaphyses are normally porous, and thus must be evaluated with the criteria previously discussed.

Differential Diagnosis and Difficulties in Diagnosing Archaeological Scurvy

Differential Diagnosis

There are a small number of conditions and diseases that may present similar skeletal manifestations as scurvy (Ortner et al., 2001). Because of these similarities, Klaus (2015) stresses the importance of using standardized anatomical terminology when describing skeletal lesions in order to limit interobserver error and ambiguity and increase cross-discipline credibility and comparability between samples. The conditions and diseases that present skeletal manifestations most similar to scurvy include normal growth porosity, acute infection, blood disorders, anemia, and rickets (Bourbou, 2015; Brickley and Ives, 2006; Brown and Ortner, 2011; Klaus, 2015; Ortner and Ericksen, 1997; Ortner et al., 2001). The first, and least likely, is that the porotic lesions present may just be normal growth porosity; normal growth porosity, however, does not penetrate the cortical layer of bone as occurs with scurvy-like lesions (Brickley and Ives, 2006). An acute infection, such as osteomyelitis, may present similar lesions to scurvy, however, Brickley and Ives (2006) indicate that osteomyelitis tends to manifest on the diaphysis of long bones with periosteal new bone formation, which does not typically occur with scurvy. Brown and Ortner (2011) also state that some blood disorders, such as hemophilia, may present similar symptoms, but that these disorders usually affect the joints, which is rare for scurvy. They also state that the lesions found on the greater wing of the sphenoid are unlikely to occur in these types of blood disorders.

The two most similar diseases to scurvy are anemia and rickets. These two, as well as scurvy, are diseases of malnutrition, and therefore may possibly be comorbid (Ortner et al.,

2001). However, it is unlikely that more than one of them would present skeletal manifestations at the same time (Ortner et al., 2001). All three are capable of producing abnormal cranial porosity, increasing the importance of determining the type and distribution of the lesions present (Bourbou, 2014). Because of the bilateral nature and symmetry often expressed by scurvy lesions, thorough analysis of all available skeletal elements is essential in diagnosis (Brown and Ortner, 2011).

Although both scurvy and anemia can cause cortical thinning and abnormal porosity of cortical bone (Brickley and Ives, 2006), it is still possible to differentiate between the two. Aside from orbital lesions, the distribution of scorbutic and anemic lesions is typically different (Brown and Ortner, 2011). Even in the orbits, severe anemia should be able to be differentiated from mild scurvy (Brickley and Ives, 2006). The main difference, however, is that anemia causes marrow hyperplasia, which is an enlargement of the marrow within the cranial bone leading to an enlarged diploe (Brickley and Ives, 2006; Brown and Ortner, 2011; Ortner et al., 2001). The lesions located on the greater wing of the sphenoid do not correspond well with this requirement, as this is not an area of the skull that would normally be a place for an increase in hematopoietic marrow (Ortner and Ericksen, 1997). Additionally, scurvy lesions are unlikely to appear isolated in the orbits (Brickley and Ives, 2006).

Rickets has a similar morphology to scurvy within the orbits and ectocranial surfaces (Brickley and Ives, 2006), however, the porotic lesions tend to be very fine in nature in the cranium and ribs (Brown and Ortner, 2011). Additionally, Brown and Ortner (2011) have found that rickets can cause new bone growth endocranially as well, which is uncommon with scurvy, and that the porotic lesions from rickets are not as widespread. However, the main diagnostic

feature of rickets can be found in the postcrania. If present, the long bones, especially those of the legs, are often bowed, a symptom that does not occur in scurvy (Brown and Ortner, 2011).

Due to the similarities in the diseases (especially scurvy, anemia, and rickets), a thorough analysis of all available skeletal elements is important in order to locate all porotic lesions. Identification of the cause of abnormal porotic lesions is unlikely to occur if only isolated bones are available for analysis (Brickley and Ives, 2006). Therefore, it is best to attempt a diagnosis of scurvy on individuals with complete or nearly complete skeletons, as other diseases have more concentrated areas of affectation while scurvy tends to manifest over multiple bones in multiple areas of the body.

Difficulties in Diagnosing Archaeological Cases of Scurvy

In addition to difficulties in completing a differential diagnosis for scurvy on skeletons, other complications exist in detecting this disease in archaeological populations. Ortner and Ericksen (1997:219) have defined four factors that inhibit interpretation of abnormal conditions of archaeological remains: 1) morphological similarities between different pathological processes, 2) differences between clinical presentations and archaeological presentations of a disease, 3) the inability of the researcher to know at what stage of disease progression the individual died, and 4) that different stages of different diseases may resemble one another.

Although knowledge of scurvy dates back to ancient times (Pimentel, 2003), there is a lack of reported cases in the archaeological record, probably due to issues in recognizing the skeletal manifestations of scurvy and differentiating them from other similar diseases (Bourbou, 2014; Crandall and Klaus, 2014), although this is changing. This overlapping of various diseases

makes determining an explicit link between skeletal manifestations and a specific dietary deficiency difficult, if not impossible (Ortner et al., 2001). Brickley and Ives (2006) believe that better understanding of the skeletal manifestations of scurvy in its different stages will assist in properly diagnosing the disease in the archaeological record.

The incomplete nature of juvenile skeletons paired with preservation issues adds another level of difficulty in diagnosing scurvy in archaeological populations (Bourbou, 2014). For example, Ortner and colleagues (Brown and Ortner, 2011; Ortner and Ericksen, 1997; Ortner et al., 2001) posit that the most diagnostic element for determining scurvy is the greater wing of the sphenoid, however, this element is not always well-preserved in the archaeological record (Brickley and Ives, 2006). The Osteological Paradox (Wood et al., 1992) also influences possible diagnoses of scurvy. If individuals in the archaeological record with scurvy died before adequate skeletal markers manifested, they would not be included with those who exhibit the markers of scurvy, which would skew the demographics to depict a lower incidence of scurvy than actually occurred within the population (Ortner et al., 2001).

Finally, Klaus (2015:2) states that "scurvy is one of the most challenging and nuanced disease conditions to diagnose in human skeletal remains." It is this reason that he stresses the importance of proper and standardized anatomical terminology when diagnosing scurvy in archaeological populations. Klaus (2015) has provided three steps he believes will increase the accuracy of paleopathological diagnoses, reduce interobserver error in differential diagnoses, and increase the comparability between paleopathological studies. These three steps are: 1) a better understanding of the behaviors and biology of bone cells, 2) more precise description based on proper anatomical terminology, and 3) performing a systematic differential diagnosis by

applying the manifested skeletal lesions to all the possible diagnoses and ruling them out one by one (Klaus, 2015) (Figure 2).

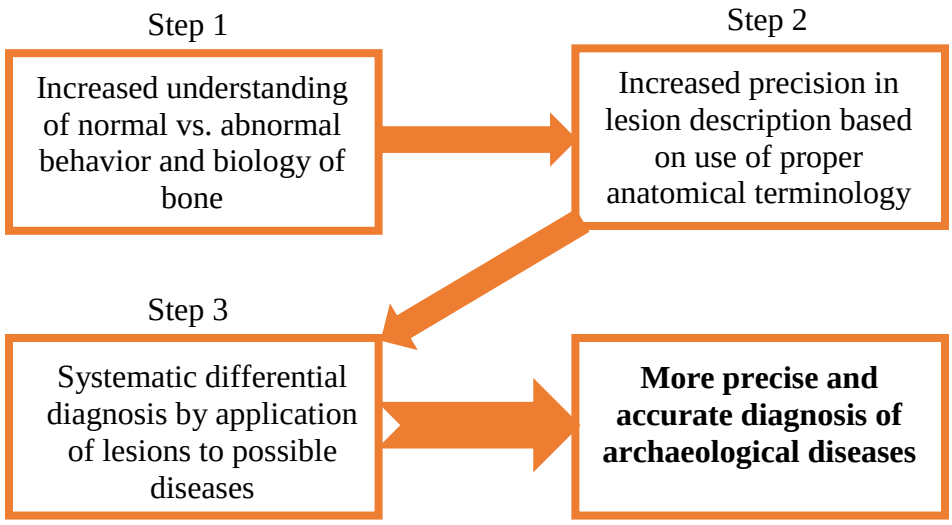

Figure 2: Simple flow chart showing the three steps posited by Klaus (2015) to provide a more accurate and robust differential diagnosis that can be used for various paleopathological analyses, including the diagnosis of scurvy.

Stable Isotopic Analysis

Isotopes are atoms of an element with the same number of protons and electrons but a different number of neutrons (DeNiro, 1987). The positively charged protons and electrically neutral neutrons reside in the nucleus with the negatively charged electrons orbiting them (Pollard et al., 2007). The number of protons and neutrons within the nucleus determines the atomic mass of the atom. However, it is the number of protons that determines the chemical characteristics of the atom and is used to differentiate between elements (Pollard et al., 2007).

Many of the elements have multiple stable (nonradioactive) isotopes that contain the same number of protons but differing numbers of neutrons within their nucleus, though some like phosphorus may only have one stable isotope (DeNiro, 1987; Lambert, 1997). Stable isotopes can be used to test a variety of questions related to past diet, demography, and life history, with those of carbon and nitrogen being used most often in studies involving diet reconstruction because of their abundance in foodstuffs (Katzenberg, 2008).

Because of the differences in weight (mass) of isotopes, the speed in which they react chemically also differs (DeNiro, 1987; Katzenberg, 2008). Isotopes that contain more neutrons are heavier (have a larger mass) and thus react more slowly than the lighter isotopes (Katzenberg, 2008; Lambert, 1997). This difference in mass, and thus reaction time, leads to fractionation, "which occurs when the isotope ratios of the products of a reaction or series of reactions differs from the ratios of the reactants" (DeNiro, 1987:182). This fractionation is what allows researchers to address research questions using stable isotopic analyses (Katzenberg, 2008).

Stable isotope values are represented as a ratio of the sample fractionation to the fractionation of an internationally accepted standard (DeNiro, 1987; Katzenberg, 2008). The international standard to which carbon values are compared is the PeeDee Belemnite Carbonate (PDB) while the nitrogen standard is atmospheric nitrogen (AIR – ambient inhalable reservoir) (DeNiro, 1987; Katzenberg, 2008; Schoeninger and Moore, 1992). The following equations are used to determine the delta (δ) value of the sample compared to the standard in parts per thousand ("per mil", represented by ‰) for carbon (Equation 1) and nitrogen (Equation 2) (DeNiro, 1987; Katzenberg, 2008; Schoeninger and Moore, 1992):

$$\delta^{13}C_{PDB} = \left[\left(\frac{{}^{13}C/{}^{12}C_{Sample}}{{}^{13}C/{}^{12}C_{PDB}} \right) - 1 \right] \times 1000‰ \quad (1)$$

$$\delta^{15}N_{AIR} = \left[\left(\frac{{}^{15}N/{}^{14}N_{Sample}}{{}^{15}N/{}^{14}N_{AIR}} \right) - 1 \right] \times 1000‰ \quad (2)$$

The ratios derived from the previous equations are presented in parts per thousand in order to assist the researcher in distinguishing pertinent patterns and relationships due to the inherently small differences in the sample to standard ratios (Lambert, 1997). The mathematical sign preceding the value produced from the above equations helps to determine whether the sample contains more or less of the heavier isotope in comparison with the standard. If a negative value is produced this shows the sample is isotopically lighter than the standard, and contains less of the heavier isotope (e.g. ^{13}C or ^{15}N), and vice versa (Pollard et al., 2007; Schoeninger and Moore, 1992). If the equation were to produce a value of zero, this would mean the sample and standard were the same.

Carbon Stable Isotopes

Carbon has two stable isotopes: ^{12}C and ^{13}C (Lambert, 1997; Pollard et al., 2007; Schoeninger and Moore, 1992). The lighter isotope, ^{12}C, makes up approximately 99% of natural carbon, while ^{13}C comprises the remaining approximately 1% (Lambert, 1997). The different masses of these two isotopes plays a role in the types of plants that use them during

photosynthesis, and can help to distinguish between the plant types (DeNiro, 1987; Katzenberg, 2008). There are three different types of plants and their corresponding photosynthetic pathways: C_3, C_4, and CAM (crassulacean acid metabolism) (Schoeninger and Moore, 1992).

C_3 plants make up the majority of plants that are used for food, including wheat, rice, beans, tubers, and nuts (DeNiro, 1987). These plants prefer to use the lighter, ^{12}C isotope during photosynthesis (Katzenberg, 2008). This plant type gets its name by the first product it creates during photosynthesis, which is comprised of three carbon atoms (Schoeninger and Moore, 1992). C_3 plants have a $\delta^{13}C$ value that ranges between -20 to -35‰, which is quite a bit lighter than the international standard (Katzenberg, 2008).

C_4 plants include such plants as maize, sorghum, millet, and sugar cane (Schoeninger and Moore, 1992). These plants use the heavier ^{13}C isotope more readily, and as a result they are isotopically heavier than the C_3 plants (Katzenberg, 2008). For these plants, the first product of photosynthesis creates a compound of four carbon atoms, thus giving them their name (Schoeninger and Moore, 1992). The $\delta^{13}C$ value of C_4 plants is typically between -9 and 14‰ (Katzenberg, 2008). Because the $\delta^{13}C$ of C_3 and C_4 plants do not overlap, it is possible to distinguish their consumption through isotopic analysis (Katzenberg, 2008).

The CAM plants include plants such as agave, yucca, pineapple, and prickly pear (DeNiro, 1987). These plants are able to use both the C_3 and C_4 photosynthesis pathways depending on the climate; when it is hot and arid, the plants will switch to the C_4 pathway (Schoeninger and Moore, 1992). Since these plants switch back and forth between the different pathways, their $\delta^{13}C$ values are intermediate between the C_3 and C_4 pathways (Katzenberg, 2008).

Stable carbon isotopes can be used to help differentiate between a terrestrial and marine based diet (Katzenberg, 2008). The major source of carbon for terrestrial plants is atmospheric CO_2 while carbonate within the ocean is the main source for marine plants (Katzenberg, 2008; Schoeninger and Moore, 1992). Because marine carbonate has a $\delta^{13}C$ value of 0‰ while atmospheric CO_2 is approximately -7‰, it may be possible to distinguish individuals subsisting on mainly marine lifeforms from those that survive on terrestrial lifeforms (Katzenberg, 2008), though marine and terrestrial plant life can have overlapping $\delta^{13}C$ values (Schoeninger and Moore, 1992). A note must be made, however, that prior to the Industrial Revolution, the atmospheric CO_2 was slightly more positive, with $\delta^{13}C$ values around -5 to -6‰ (DeNiro, 1987). This information is taken into account when analyzing populations that date to prior to the Industrial Revolution.

Nitrogen Stable Isotopes

Nitrogen, like carbon, has two stable isotopes: ^{14}N and ^{15}N, with the lighter isotope (^{14}N) making up approximately 99.6% of naturally available nitrogen and the heavier isotope (^{15}N) the remaining 0.4% (Pollard et al., 2007). Nitrogen isotope systematics are not as well understood as that of carbon, but it has been found useful in dietary reconstructions (Pollard et al., 2007). The isotopes of nitrogen divide plants into two categories: legumes and nonlegumes (DeNiro, 1987). In addition, trophic levels have an influence on nitrogen isotopes within tissues (Katzenberg, 2008).

Legumes are able to fix nitrogen without fractionation, resulting in a $\delta^{15}N$ value that is close to the international standard (DeNiro, 1987; Lambert, 1997). The standard used for

nitrogen isotopic evaluation is atmospheric nitrogen (AIR), which is set at 0‰ for $\delta^{15}N$ (Lambert, 1997). Legumes are capable of utilizing N_2 from the atmosphere and soil which results in a near 0‰ value (DeNiro, 1987). Nonlegumous plants have a slightly higher $\delta^{15}N$ of approximately 3-10‰, and are only able to acquire nitrogen from soil sources (DeNiro, 1987; Katzenberg, 2008). The $\delta^{15}N$ values of soil nitrogen are more positive than atmospheric N_2, which causes nonlegumous plants to have higher $\delta^{15}N$ values than legumes (DeNiro, 1987). When an animal feeds on these nonlegumous plants, they experience an increase in their own $\delta^{15}N$ values (9-13‰); likewise, when a carnivore feeds on those animals, their $\delta^{15}N$ increases as well (13-16‰) (Katzenberg, 2008; Lambert, 1997). Each successive step up in the food chain equates to an increase of approximately 3‰ to $\delta^{15}N$ values (Milner et al., 2004).

This food-chain effect of successively increasing $\delta^{15}N$ values is referred to as trophic effect (Katzenberg, 2008). It is through analysis of this trophic effect that nitrogen isotopes can be used to study past diets. In addition to determining which trophic level an organism inhabits, $\delta^{15}N$ can also distinguish between terrestrial and marine diets (Pollard et al., 2007). Because the trophic chain of marine animals is much longer than that of terrestrial animals, it is possible to distinguish the $\delta^{15}N$ values of humans who consumed primarily marine resources from those who consumed primarily terrestrial resources (Pollard et al., 2007). The mean $\delta^{15}N$ for terrestrial mammals and birds is approximately +5.9‰ while the mean $\delta^{15}N$ for marine mammals is +15.6‰ (Pollard et al., 2007). It has been found that humans who consume mainly marine resources have $\delta^{15}N$ values that range between +17 and +20‰, which can be distinctly distinguished from those that rely mainly on terrestrial resources with $\delta^{15}N$ values between +6

and +12‰, though the processes behind this trophic level enrichment are not fully understood (Honch et al., 2012; Pollard et al., 2007; Stevens et al., 2010).

In addition to influences from resources, $\delta^{15}N$ values have also been found to be influenced by environmental and physiological factors (Webb et al., 2015). For example, arid environments can cause an enrichment of ^{15}N levels in the animals living there (Dupras and Schwarcz, 2001; Hedges and Reynard, 2007). This enrichment of ^{15}N values is attributed to water stress, as Heaton et al. (1986) found that herbivores living in areas of less rainfall had enriched ^{15}N values when compared to those living in areas of more rainfall. Several theories have been suggested for the cause of this enrichment, extending from being the result of a biological process within the animal itself (Heaton et al., 1986) to increased excretion of ^{15}N-depleted urea (Ambrose and DeNiro, 1987) to a domino-type effect of ^{15}N enriched plants in arid regions (Schwarcz et al., 1999). Whatever the ultimate cause of this ^{15}N enrichment, it has been well-documented that populations living in an arid environment tend to show an increased level of ^{15}N when compared to those living in areas with more precipitation.

Mekota et al. (2009) also found that physiological stress, such as created during a starvation period, can cause an increase in the amount of ^{15}N retained by the body. The bonds of ^{14}N are more easily broken causing it to be more readily excreted by the body, especially during times of physiological stress, and thus causing an enrichment of ^{15}N within the body (Katzenberg and Lovell, 1999). In addition to nutritional stress, pathological diseases have also been shown to affect $\delta^{15}N$ values (Table 9). Due to these potential influences on $\delta^{15}N$ values, care must be taken when analyzing nitrogen isotopic data in order to not overestimate the influence of the diet on the values, especially when evidence of disease or illness is present.

Table 9: Studies of pathological diseases and their effects on $\delta^{15}N$ values.

Study	Pathology	Result
White and Armelagos, 1997	Osteopenia	Pathological individuals have significant increase in $\delta^{15}N$ values
Katzenberg and Lovell, 1999	Osteomyelitis	Increased $\delta^{15}N$ values at lesion sites
Strange, 2006	Tuberculosis	Statistically significant differences between pathological and non-pathological intra-skeletal vertebrae $\delta^{15}N$ values
Olsen, 2013	Osteomyelitis	Significant increase in $\delta^{15}N$ values between intra-skeleton lesion site and distant bone
	Degenerative Disease (osteophytes)	Significant increase in $\delta^{15}N$ values between intra-skeleton lesion site and distant bone
	Fracture Trauma	Significant increase in $\delta^{15}N$ values at fracture site
	Periostitis	No statistically significant difference found in $\delta^{15}N$ values
	Metabolic Disorder (Rickets/Osteomalacia)	No statistically significant difference found in $\delta^{15}N$ values
D'Ortenzio et al., 2015	Long-term Terminal Illness (Cancer)	Elevation of $\delta^{15}N$ values and high trichogram rates in hair samples
	Short-term Illness/Sudden Death (Pneumonia/Stroke)	Little variation in $\delta^{15}N$ values and normal trichogram rates in hair samples
	Infection	Elevation of $\delta^{15}N$ values and high trichogram rates in hair samples
	Fractures	Elevation of $\delta^{15}N$ values and high trichogram rates in hair samples

The last two factors affecting $\delta^{15}N$ values are important aspects in regards to the research conducted for this study because they are both present in the individuals being analyzed. The Dakhleh Oasis is an arid environment with little to no rainfall, and the juveniles being examined exhibited skeletal manifestations of illness at the time of their deaths.

Tissues Used in Stable Isotope Analysis

A variety of tissues can be used when conducting stable isotope analyses on humans (e.g. bone, teeth, hair, skin, etc.) (Williams, 2008). The first tissue used in isotopic studies in archaeology was bone (Katzenberg, 2008). Since bone is one of the best-preserved bodily tissues, it is the most used (Schoeninger and Moore, 1992). Bone is composed of inorganic and organic material (Katzenberg, 2008). The inorganic portion is in the form of the mineral hydroxyapatite while the organic portion is made of protein, mainly collagen (Lambert, 1997). Although collagen is the first portion of bone to degrade, it is still robust enough to allow for collagen collection in archaeological populations (Katzenberg, 2008). The collagen portion of bone can be used to test both carbon and nitrogen stable isotopes, while the hydroxyapatite portion can be used for carbon isotope testing, along with others such as oxygen and strontium (Katzenberg, 2008). Bone is considered to provide information about an individual from the last 10-20 years of their life due to the slow turnover rate of the tissue (Katzenberg, 2008); however, the rate of turnover can be considerably faster in juveniles (Kinaston et al., 2009). The mineral component of bone, when tested for carbon isotopes, is considered to provide an assessment of an individual's overall diet, whereas the collagen portion represents the protein intake (Schoeninger and Moore, 1992).

Hair is another tissue that can be used in isotopic analyses. Hair fibers are composed of the protein keratin (Lubec, 1987) and can be used for both stable carbon and nitrogen isotope analyses (O'Connell and Hedges, 1999). Hair isotopic values have been found to be similar to those found in bone collagen, and likewise, represent the dietary protein values (O'Connell et al., 2001). The nature of hair growth allows for even more defined timelines of isotopic values.

Because hair grows approximately 0.35 millimeters every day (~1 centimeter per month) and does not go through the process of biogenic turnover, samples can be sequentially segmented in order to acquire information from the last several months of an individual's life dependent upon the length of the hair (Barth, 1986; O'Connell and Hedges, 1999; Pollard et al., 2007).

Hair passes through three growth phases before it is shed from the scalp: anagen, catagen, and telogen (Ebling, 1988; Kligman, 1959; Westgate et al., 2013). The anagen phase is a period of active growth within the hair follicle that causes the hair fiber to become longer, with this stage lasting between two to eight years in scalp follicles (Paus and Cotsarelis, 1999). The catagen phase, averaging one to three weeks, is when growth of the hair fiber ceases and is characterized by involution of the follicular bulb, cessation of melanin synthesis, separation of the dermal papilla from the hair fiber, and the formation and upward movement of the club hair (Ebling, 1988; Kligman, 1959; O'Connell and Hedges, 1999; Saitoh et al., 1970; Williams et al., 2011). The telogen phase is a resting phase in which the club hair remains in the epithelial sac where it awaits shedding during subsequent anagen phases or is shed during combing of the hair (Paus and Cotsarelis, 1999; Williams et al., 2011). Only hair in the anagen phase registers an individual's isotopic signatures around their time of death since those in the catagen and telogen phases are no longer physiologically active. It is estimated that approximately 85-90+% of scalp hair is in the anagen phase at any given time with the remainder in the telogen and catagen phases (Dawber and Van Neste, 2004). It is important, therefore, to use only hair that is in the anagen phase when examining isotopic signatures on a "timeline" basis, such as when analyzing diet in the last months prior to death (Williams et al., 2011).

The maximum number of scalp hair follicles for any individual is set at approximately 22 weeks gestation and under normal circumstances no new follicles are added during adult life, although the number may decrease with advancing age (Dawbers and Van Neste, 2004). The average adult human has approximately 100,000 scalp hair follicles (Dawbers and Van Neste, 2004), meaning that at any given time approximately 85,000 to 90,000 are in the anagen growth phase. However, several factors may alter hair's growth cycle causing the distribution of the phases to be different from a "normal" individual. These include intrinsic (e.g. various growth factors, specific hair follicle structures, cytokines, and genes), hormonal (e.g. thyroxine and steroids such as estrogens and androgens) seasonal (e.g. change from spring to fall/winter), and systemic modulators (e.g. severe infection, major trauma, critical illnesses such as renal or liver disease, and vitamin deficiencies) (Ebling, 1988; Williams, 2008, Williams et al., 2011). Williams et al. (2011) found that the isotopic signature in mixed-phase hair is approximately 0-3 months delayed when compared to anagen phase hair from the same individual, and stressed that hair phases should be taken into consideration in hair isotopic analyses performed on individuals with a high telogen phase percentage.

Skin, which is part of the integumentary system (i.e. the outermost organ system of the body), is another tissue that provides isotopic information from a relatively short time period before death (Scanlon and Sanders, 2007; White et al., 1999; Williams, 2008). Skin is composed of two main layers, the epidermis and the dermis, with a third layer, the hypodermis, often included with them (Freinkel and Woodley, 2001; Haake et al., 2001; Scanlon and Sanders, 2007). The main functions of human skin include protection of the individual from the outside environment and other organisms (e.g. bacteria), regulation of internal body temperature,

maintaining proper body water amounts, and sexual attraction to aid in procreating the species (Forslind and Lindberg, 2004; Freinkel and Woodley, 2001; Scanlon and Sanders, 2007).

The three layers of skin are composed of differing majorities of cell types. The hypodermis, the inner-most layer of skin, connects the dermis and epidermis to the underlying muscle and is composed of areolar connective tissue and adipose tissue (Scanlon and Sanders, 2007). Together these tissues contain collagen, elastin, white blood cells, mast cells, and are rich in adipose cells, or fat (Haake et al., 2001; Scanlon and Sanders, 2007). The outer-most layer, the epidermis, is composed of keratinocytes, Langerhans cells, melanocytes, and Merkel cells, with the keratinocytes comprising approximately 90-95% of the epidermal cells (Haake et al., 2001). The middle layer, the dermis, is composed of non-parallel fibers of connective tissue containing collagen and elastin producing fibroblasts (Scanlon and Sanders, 2007). This layer is pliable and provides protection from injuries, as well as houses many accessory structures such as sensory receptors and hair follicles (Haake et al., 2001). Since collagen comprises approximately 75% of the dry weight of skin, with 80-90% of this being Type I collagen (Haake et al., 2001), this layer is most useful in stable isotopic research involving skin (White and Schwarcz, 1994).

Skin, mainly composed of collagen, also includes keratin protein and anywhere from 0.3 to 19% lipids (White, 1991), and therefore represents the protein portion of diet as in other tissues such as bone. Dermal collagen protein has a turnover rate of approximately 2% per day (El-Harake et al., 1998), resulting in the $\delta^{13}C$ and $\delta^{15}N$ values in skin most likely representing the last 1 to 1½ months before death (Williams, 2008). Previous studies have indicated that skin is enriched in ^{13}C by +1-4‰ and ^{15}N by approximately +5‰, relative to dietary protein (White, 1991; White et al., 1999).

Fingernails and toenails, like hair and skin, provide isotopic information from a relatively short period of time before death (White and Schwarcz, 1994; Williams, 2008). Nails function to protect the ends of the fingers and toes and aid in dexterity (Scanlon and Sander, 2007). The whole nail unit can be divided into several different components (Levit and Scher, 2001), with the nail plate being of particular interest in isotopic studies (Grolmusová et al., 2014; Williams, 2008). The nail plate is composed of organic and inorganic components, with the organic components being made up of carbon, nitrogen, and sulfur, while the inorganic components include trace elements and electrolytes (Levit and Scher, 2001). Additionally, the nail plate can include anywhere from 10 to 30% water, dependent upon relative humidity (Levit and Scher, 2001).

The nail plate is produced from cells in the nail matrix, located at the base of the nail plate, that produce keratin proteins, subsequently die, and then become keratinized (Scanlon and Sanders, 2007). These keratins include multiple different types that are differentiated by their isoelectric points (acidic vs. basic), and whether they are ‘hard’ or ‘soft’ (Levit and Scher, 2001). ‘Soft’ keratins are those that are also produced in the epidermal cells of skin and are more easily solubilized, while ‘hard’ keratins are not soluble under the same conditions (Levit and Scher, 2001). It is these keratinized cells that become the nail plate that overlies the nail bed and matrix (de Berker, 2013).

The rate at which nails grow is dependent upon multiple factors (Levit and Scher, 2001; Scanlon and Sanders, 2007), and much research has been done on nail growth rates and the effects of different factors on their growth (e.g. Bean, 1980; Gilchrist and Buxton, 1939; Hamilton et al., 1955; Orentreich et al., 1979; Wu et al., 2012). On average, fingernails grow at a

quicker rate than toenails (Levit and Scher, 2001). In a healthy adult, fingernails grow approximately 3 mm per month, with toenails growing half as slow at approximately 1.5 mm per month (Levit and Scher, 2001; Scanlon and Sanders, 2007). Nail growth rates in juveniles is somewhat quicker than adults, and slows down as age progresses (Hamilton et al., 1955). Although this method of longitudinal length is typically used to calculate nail growth, the calculation of nail plate thickness, which can vary from 0.6 to 1 mm, should also be considered in order to attain a complete picture of nail growth (de Berker, 2013; Levit and Scher, 2001).

Inter-tissue Spacing

Fractionation, as explained previously, causes the stable carbon and nitrogen isotopes taken into the body through diet to differ from those of the diet as well as from tissue to tissue (DeNiro and Epstein, 1978; Krueger and Sullivan, 1984; Lee-Thorp et al., 1989; Norris, 2012; Williams, 2005). This is referred to as diet-tissue spacing and inter-tissue spacing. Diet-tissue spacing was briefly described above. However, inter-tissue spacing is also of importance to this study due to the use of multiple tissues during analysis.

Studies investigating inter-tissue spacing were first conducted as controlled feeding experiments on animals (e.g. Ambrose and Norr, 1993; DeNiro and Epstein; 1978, Krueger and Sullivan, 1984; Tieszen et al., 1983), with studies involving humans following (e.g. Finucane, 2007; O'Connell et al., 2001). These initial studies found that different tissues within the organisms studied were either enriched or depleted in $\delta^{13}C$ and $\delta^{15}N$ relative to each other and their diet. These findings led researchers to determine that multiple tissues, whenever possible, should be utilized in paleodietary studies in order to better determine the dietary components

(DeNiro and Epstein, 1978). Additionally, several factors have been found that affect inter-tissue spacing, including the protein structures of the individual tissues analyzed, the different amino acid make-up of the proteins and their subsequent fractionation, the different turnover rates for tissues, different fractionation effects from the diet, and age (Ambrose and Norr, 1993; Corr et al., 2009; Norris, 2012; O'Connell et al., 2011; Williams et al., 2011).

Detailed studies conducted by Williams (2005) and Norris (2012) have further analyzed inter-tissue spacing (Δ) in humans, including in hair, nail, and skin. Williams (2005) found that fractionation does exist among bone collagen, hair, skin, and nails (Table 10). Norris (2012) also found that differences in tissue spacing exist between the 1 to 4 year (C1), 5 to 10 year (C2), and 11 to 15 year (C3) age cohorts within the Kellis 2 cemetery in regards to $\delta^{13}C$ values (Table 11).

Table 10: Inter-tissue spacing (Δ) of $\delta^{13}C$ and $\delta^{15}N$ values found by Williams (2005) for tissues that are relevant to this study.

	Δ_{BC-H}	Δ_{BC-N}	Δ_{BC-S}	Δ_{H-N}	Δ_{H-S}	Δ_{S-N}
$\delta^{13}C$	1.9 ± 1.4‰	2.0 ± 1.1‰	0.2 ± 1.0‰	0.4 ± 1.0‰	1.6 ± 1.9‰	1.8 ± 1.1‰
$\delta^{15}N$	0.5 ± 1.3‰	0.6 ± 1.2‰	-3.0 ± 1.1‰	-0.7 ± 1.1‰	2.5 ± 1.7‰	1.4 ± 1.7‰

Table 11: Inter-tissue spacing (Δ) of $\delta^{13}C$ values found by Norris (2012:48) in juveniles from the Kellis 2 cemetery, divided by age cohort.

	Δ_{BC-H}	Δ_{BC-N}	Δ_{BC-S}	Δ_{H-N}	Δ_{H-S}	Δ_{S-N}
Overall	0.94 ± 0.14	1.52 ± 0.16	1.46 ± 0.21	0.58 ± 0.10	0.52 ± 0.17	0.06 ± 0.18
C1	0.72 ± 0.29	1.47 ± 0.30	1.31 ± 0.33	0.75 ± 0.14	0.59 ± 0.19	0.16 ±0.21
C2	0.98 ± 0.11	1.39 ±0.16	1.40 ±0.42	0.41 ±0.14	0.42 ± 0.41	0.01 ±0.43
C3	1.49 ± 0.44	2.14 ± 0.49	2.10 ± 0.59	0.65 ± 0.26	0.61 ±0.42	0.04 ±0.47

CHAPTER 3: MATERIALS AND METHODS

Materials

Skeletal Sample and Age Cohorts

A total of 148 juveniles from 24 weeks gestation to 15 years of age were selected for inclusion in this study. Of these, 31 were chosen for inclusion due to the availability of skeletal pathological information indicating possible scurvy status and the presence of at least one of the four tissues analyzed in this study. The remaining 117 juveniles were chosen for inclusion because they did not exhibit skeletal indicators of scurvy and had at least one of the four tissues analyzed in this study. Each individual contributed at least one tissue from bone collagen, hair, nail, or skin, with multiple juveniles contributing two or more tissues. A total of 25 juveniles contributed bone collagen samples, 133 contributed hair samples divided in up to three segments, 54 contributed proximal nail segment samples, and 78 contributed skin samples (Appendix A).

All individuals were previously divided into six age categories as follows: fetal (21-36 weeks gestation), perinatal (37-40 weeks gestation), neonatal (41 weeks gestation to 12 months), C1 (13 months to 4 years), C2 (5 to 10 years), and C3 (11 to 15 years) (Wheeler, 2009; Williams, 2008), with the fetal and perinatal categories being combined for this study. The fetal and perinatal (F&P) cohort contained 37 juveniles, the neonatal cohort contained 49 juveniles, the C1 cohort contained 33 juveniles, the C2 cohort contained 17 juveniles, and the C3 cohort contained 12 juveniles (Table 12).

Table 12: Number of juveniles in each age cohort, divided by scurvy status and the total number of juveniles.

Age Cohort	Scurvy (n)	Non-scurvy (n)	Total (n)
F&P	2	35	37
Neonatal	12	37	49
C1	9	24	33
C2	5	12	17
C3	3	9	12

Scurvy and Non-scurvy Sample

This study consists of two groups of samples, one which contains juveniles with skeletal indications of scurvy and one which contains juveniles with no skeletal indications of scurvy. For the purposes of this thesis, these two groups will be known as the scurvy and non-scurvy cohorts, respectively. The scurvy cohort is comprised of 31 juveniles with ages ranging from 39 weeks gestation to 15 years. The non-scurvy cohort consists of 117 juveniles with ages ranging from the 24 weeks gestation to 15 years. Each tissue included in this study contains both scurvy and non-scurvy juveniles (Table 13).

Table 13: Number of scurvy and non-scurvy juveniles within each tissue analyzed in this study.

Tissue	Scurvy (n)	Non-scurvy (n)	Total
Bone Collagen	11	14	25
Hair	21	112	133
Nail	10	44	54
Skin	19	59	78

Osteological Analysis

Osteological analysis of the juvenile skeletal remains was undertaken by Dr. Sandra Wheeler (2009). Field notes, photographs, and the presence of paleopathological conditions were shared with the author for this study via personal communications. Determinations of the possible presence of scurvy were made by Dr. Wheeler following the methods outlined in published literature on archaeological scurvy (e.g. Brickley and Ives, 2008, 2006; Ortner and colleagues, 2001, 1997). Lesions considered to be pathognomonic of juvenile scurvy in this sample are largely cranial and include cribra orbitalia and new bone formation in the orbits; abnormal pitting on the lateral and orbital surfaces of the greater wings of the sphenoid, zygomatic, posterior maxilla, and anterior mandible; as well as fine layers of new bone formation on the inferior aspect of the mandibular ramus. Some individuals also exhibit endocranial new bone formation and abnormal pitting on the superior and inferior scapular spines. Table 14 indicates the individuals within the sample that exhibit skeletal lesions associated with possible scurvy. Appendix B details the skeletal elements affected while photographs of select skeletal lesions indicating scurvy can be found in Appendix C.

Table 14: Individuals within this study exhibiting skeletal indicators of scurvy, including their age category.

Burial ID	Age Category[1]	Scurvy Status[2]
3	C1	Possible
24	C2	Possible
74	Neo	Possible
258	C2	Possible
260	C3	Possible
290	C3	Possible
295	C3	Possible
299	C1	Possible
326	C1	Possible
328	C1	Possible
336	C2	Possible
347	Neo	Possible
351	C1	Possible
353	Neo	Maybe
356	Neo	Possible
359	C2	Possible
383	C1	Possible
390	Neo	Possible
404	Neo	Possible
419	F&P	Maybe
449	F&P	Possible
519	C1	Possible
520	C2	Possible
545	Neo	Possible
560	C1	Possible
565	Neo	Possible
575A	Neo	Possible
590	Neo	Possible
617	C1	Possible
622	Neo	Possible
626	Neo	Maybe

[1]Age categories: F&P:16 to 40 weeks gestation; Neo: 41 weeks gestation to 12 months; C1: 1 to 4 years; C2: 5 to 10 years; C3:11 to 15 years
[2]Degree to which individual has skeletal indicators of scurvy or other metabolic bone disease, with “possible” indicating a stronger degree of possibility.

Isotopic Sample Prepared by the Author

A total of 43 samples of juvenile tissues from the Kellis 2 cemetery were prepared by the author for inclusion in this research. Each individual was represented by at least one tissue type (bone collagen, hair, skin, and/or nails), with multiple individuals being represented by multiple tissues. Bone collagen was extracted from 24 individuals, with 20 individuals providing enough collagen for isotopic testing, per laboratory regulations. Hair samples were taken from seven individuals in 1cm increments starting at the scalp end of the hair. Four individuals provided two consecutive hair segments, while the remaining three individuals provided one hair segment, resulting in a total of eleven hair samples. These samples were labeled with a "-1" or "-2" at the end of their sample ID to indicate the hair segment (i.e. "-1" indicated the centimeter closest to the scalp and "-2" indicated the next centimeter segment along the hair shaft). One skin sample each from five individuals was also prepared for isotopic analysis. Finally, one proximal fingernail sample from three individuals was also prepared for analysis. The burial ID numbers and tissues prepared for isotopic analysis by the author can be found in Table 15.

Table 15: Burial ID numbers and tissues prepared for isotopic analysis by the author.

Burial ID Number	**Tissues**				
	Bone Collagen	**1st Hair Segment**	**2nd Hair Segment**	**Nail**	**Skin**
3					x
23	x				
38	x				
74		x			
187	x				
260	x				
290		x	x	x	x

Burial ID Number	Tissues				
	Bone Collagen	1st Hair Segment	2nd Hair Segment	Nail	Skin
295	x				
299	x				
325	x				
326	x				
331	x				
336	x				
353				x	
359	x				
383		x	x		
390					x
404				x	
419					x
435	x				
436	x				
449	x				
464	x				
490	x				
520	x				
525	x				
545	x				
551	x				
558	x				
565	x	x			
575A					x
582	x				
590	x	x			
617		x	x		
622		x	x		

In addition to the samples prepared by the author, isotopic data from Williams (2008) was also used. The isotopic data from Williams (2008) represents both wholly distinct individuals from and additional data for some of those individuals prepared by the author. The

preparation methods used for those samples can be found in Williams (2008:81-84, 121-123). Appendix A lists all individuals and their respectively supplied tissues utilized in this study.

Methods

Collagen Extraction from Bone

A modified version of the Longin (1971) method was used to extract collagen from the 24 bone samples prepared by the author. This method has been followed by several recent studies (e.g. East, 2015; Page, 2014; Rumberger, 2016).This sample preparation was completed at the Laboratory for Bioarchaeological Sciences at the University of Central Florida. The samples were processed in two separate batches, however, the procedure used for each batch was the same.

All samples were individually weighed prior to cleaning to obtain approximately 1.0 g of bone (Figure 3). All of the samples were mechanically broken into pieces small enough to fit into a 50 ml centrifuge tube and covered by approximately 10 ml of liquid. After being placed in the centrifuge tubes, the samples were covered with distilled water and ultrasonicated for 10 minutes (Figure 4). This cleaning step was repeated until the decanted water was clear and the bone samples appeared clean. The samples were left uncapped in the centrifuge tubes overnight in a 60° Celsius oven to dry. Once dry, the sample were capped and placed on the counter overnight to cool. Once fully cooled the weight of each sample was taken and recorded for each individual.

Figure 3: Photograph of whole tibia being weighed during first step of collagen extraction.


Figure 4: Photograph of samples being cleaned by ultrasonication.

The samples then underwent lipid extraction. Approximately 10 ml of 2:1 chloroform:methanol solution was added to each centrifuge tube, the tubes were capped, and placed in a fume hood for approximately 20 minutes. The tubes were then balanced with distilled water and spun in a centrifuge at 2400 rpm for 10 minutes. The solution was pipetted off and disposed of in a waste jar. This step was repeated two more times. After the final removal of the 2:1 chloroform:methanol solution, the samples were placed in a fume hood, uncapped, over a weekend to fully dry.

Once dry, approximately 10 ml of 0.5M hydrochloric acid (HCl) was added to each tube. The tubes were capped and placed in a fume hood overnight (Figure 5). The following day the tubes were balanced and spun in a centrifuge at 2400 rpm for 10 minutes, the 0.5M HCl was removed, and approximately 10 ml of new 0.5M HCl was added to each tube, and they were placed in a fume hood. The concentration of HCl was changed to 0.25M after two days due to the speed at which demineralization seemed to be occurring. This step was repeated for all samples in batch 1 until demineralization was completed, which ranged from 4 to 10 acid exchanges and 7 to 15 days. The samples in batch 2 went through the same procedure with the exception of 0.25M HCl acid being used for the entirety of the demineralization process, which ranged from 9 to 20 exchanges (11 to 50 days) with the majority requiring only 9 acid exchanges. All samples were placed in a fume hood in HCl if they were being left only overnight and in the refrigerator in HCl if being left for more than one night (e.g. over a weekend or longer). Once a sample was demineralized, it was placed in distilled water in the refrigerator until the remaining samples from that batch were demineralized.

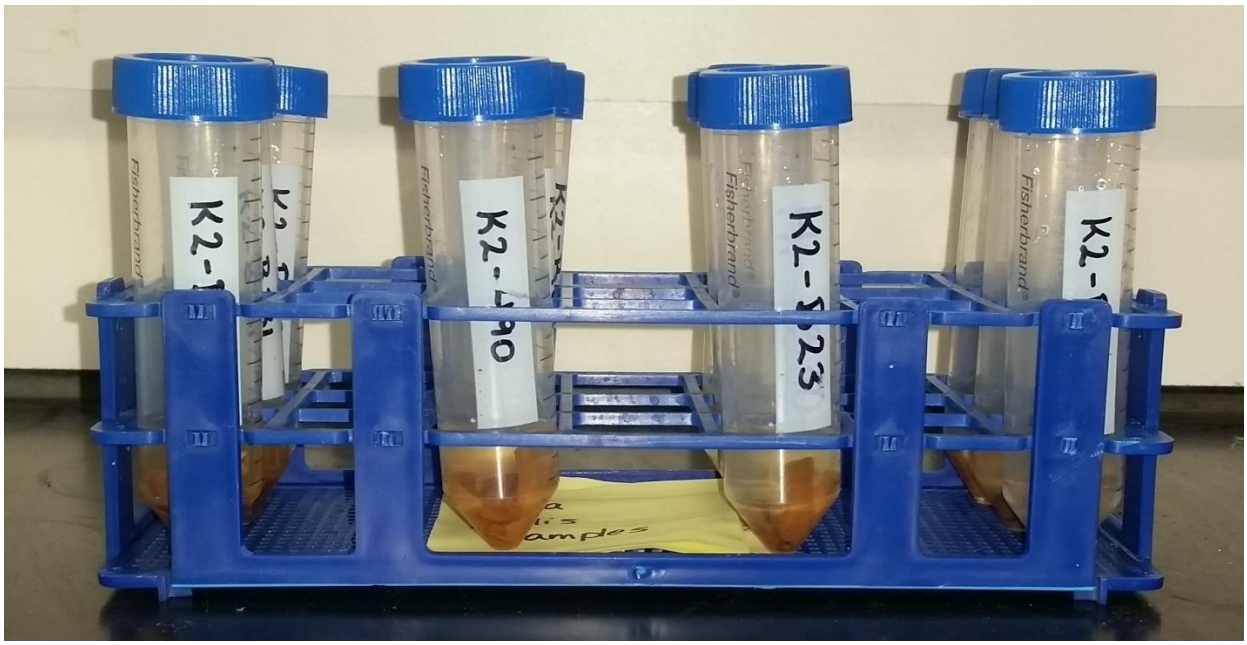

Figure 5: Photograph of bone samples in hydrochloric acid for demineralization.

Once the samples were demineralized, they were rinsed at least three times in distilled water until they reached a pH level between 2.5 and 3.0. Following attainment of the correct pH level, the samples were treated with 0.1M sodium hydroxide (NaOH) to remove any present humic acids. This was accomplished by adding approximately 10 ml of NaOH to each centrifuge tube and gently agitating them every 5 minutes for a total of 20 minutes. The samples were then balanced and spun in a centrifuge at 2400 rpm for 10 minutes. If the color of the NaOH solution in the tube remained clear (i.e. no color change) the solution was pipetted off and approximately 10 ml of distilled water was added. If the NaOH solution exhibited a color change, typically brown in color, then the NaOH was exchanged and the humic acid extraction procedure repeated. Once all samples were free of humic acids, the samples were rinsed at least 6 times in distilled water. After the sixth rinse the pH level was checked, and rinsing was repeated until a pH level between 6.0 and 8.0 was obtained. The final rinse solution was then pipetted off.

Once only the bone collagen remained in the centrifuge tubes (Figure 6), approximately 10 ml of 0.25M HCl was added to each centrifuge tube and spun in the centrifuge at 2400 rpm for 10 minutes. The HCl was then removed and approximately 5 ml of distilled water was added. The pH level was checked for each sample, and adjusted until a pH of 2.5 to 3.0 was reached. The centrifuge tubes were then capped and placed in a 90° Celsius oven overnight. Glass dram vials were each labeled with a sample ID and weighed. The samples were removed from the oven, balanced, and spun in the centrifuge at 2400 rpm for 10 minutes. The collagen solution from each centrifuge tube was pipetted into its corresponding glass dram vial. The glass dram vials were placed, uncapped, in beakers and then into a 90° Celsius oven until completely dry (Figure 7). The glass dram vials were removed from the oven and weighed. The percent collagen yield was then calculated for each sample using equation 3:

$$\%\ \text{Collagen Yield} = \frac{(\text{vial with collagen} - \text{vial without collagen})}{\text{sample original weight}} \times 100 \qquad (3)$$

Figure 6: Photograph of demineralized capitate from burial 582.

Figure 7: Photograph of dried collagen in glass dram vial ready to be weighed for isotopic processing.

The dried collagen was then scraped from the glass dram vials using dental picks. Between 0.540 and 0.560 mg of dried collagen was transferred to tin cups and placed in a labeled tray. Of the initial 24 samples, 20 yielded enough collagen for further analysis.

Preparation of Hair Samples

Scalp hair samples of 1 cm in length were provided by Dr. Lana Williams from the University of Central Florida. The hair samples were placed in glass dram vials and distilled water was added. The samples were ultrasonicated for approximately 30 minutes and the water was removed. The samples were then covered in a 2:1 chloroform:methanol solution overnight to remove any present lipids. The samples were visually evaluated for continued presence of lipids or other residues. All samples were then ultrasonicated in distilled water for 30 minutes. Those that still had lipids present were again soaked in 2:1 chloroform:methanol overnight and rinsed in the ultrasonicator until no evidence of lipids remained. Once all lipids were removed, the samples were rinsed 3 times in distilled water in the ultrasonicator and placed in a 60° Celsius oven to dry for at least 48 hours. Once dried, the hair samples were cut using surgical scissors until very fine. The hair pieces were then weighed into tin cups, with between 0.540 and 0.560 mg of each sample placed in an individual tin cup. The tin cups were then closed and placed into the labeled tray to be sent to the laboratory for analysis.

Preparation of Skin Samples

Naturally desiccated skin samples were provided to the author by Dr. Lana Williams at the University of Central Florida. The samples were cleaned in distilled water in the

ultrasonicator for 30 minutes. They were then soaked in a 2:1 chloroform: methanol solution overnight to remove the remaining lipids (Figure 8). The samples were then rinsed in distilled water in the ultrasonicator for 30 minutes. This length of time in the ultrasonicator began to break down some of the skin samples (Figure 9), so the ultrasonicator time was reduced to 5 minutes, at the advice of Dr. Lana Williams. The soak in 2:1 chloroform:methanol was repeated until the samples were free of lipids. Once all lipids were removed from the skin samples, they were rinsed in distilled water 3 times. The samples were then placed in a 60° Celsius oven, uncapped, overnight. After 24 hours the samples were tested using a glass rod for their stiffness. If the samples were "crunchy", they were pulverized using dental tools. If the samples were not "crunchy", they were frozen for 48 hours and then placed in a 90° Celsius oven for an additional 24 to 48 hours until completely dried. Once the samples were completely dried, they were pulverized using dental tools and weighed into tin cups (between 0.540 and 0.560 mg). The tin cups were closed and placed into the labeled tray to be sent to the laboratory.

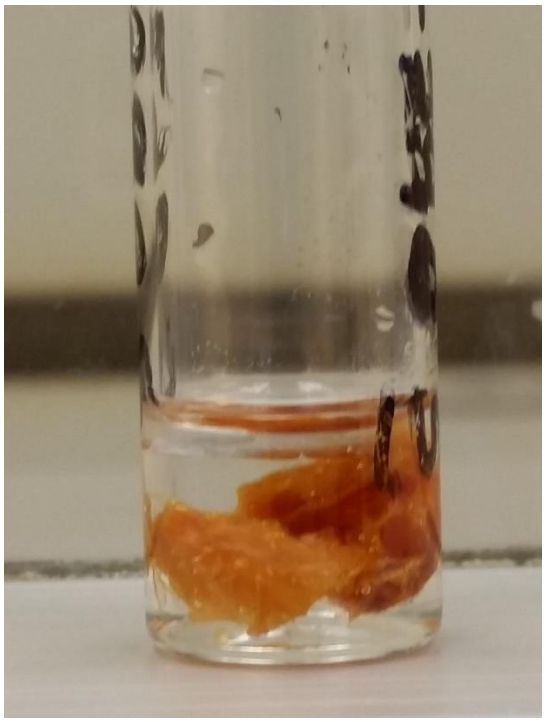

Figure 8: Photograph of skin sample soaking in a 2:1 chloroform: methanol solution to remove lipids.

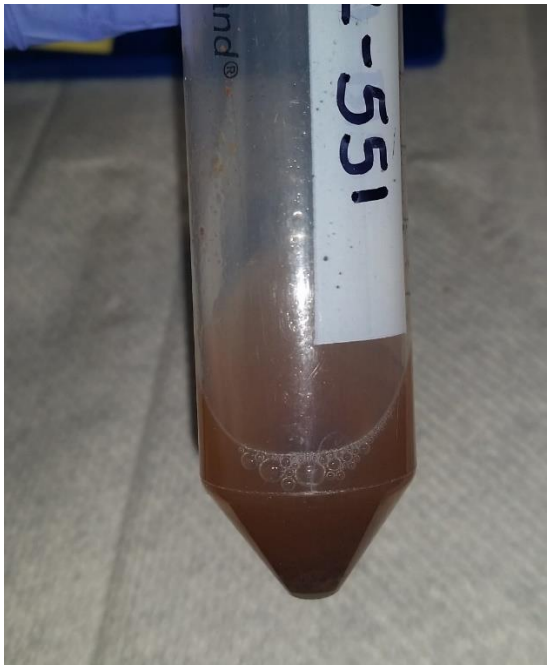

Figure 9: Photograph of skin sample showing break-down of the sample due to the length of time rinsing in the ultrasonicator.

Preparation of Fingernail Samples

The fingernail samples were provided to the author by Dr. Lana Williams at the University of Central Florida. The samples consisted of proximal fingernail segments. The samples were rinsed twice in distilled water in the ultrasonicator for approximately 10 minutes each, until the decanted water was clear. The samples were then covered in a 2:1 chloroform:methanol solution for 1 hour. This was repeated in 30 minute blocks of time until the decanted solution was clear and free of lipid residue (a total of three times for each sample). The samples were then rinsed for approximately 10 minutes in distilled water in the ultrasonicator twice. The samples were then placed in a 60° Celsius oven, uncapped, overnight. The samples were then pulverized using metal dental tools and weighed into tin cups (0.540 to 0.560 mg per tin cup). The tin cups were closed and placed in the labeled tray to be sent to the laboratory.

Precision and Accuracy

The stable carbon and nitrogen isotopes from bone collagen, hair, nail, and skin were analyzed by the Light Stable Isotope Mass Spec Lab in the Department of Geological Sciences at the University of Florida. Precision was calculated by analyzing duplicate samples from four individuals. These duplicate samples included two bone collagen samples, one hair sample, and one nail sample (Table 16). The precision values for $\delta^{13}C$ and $\delta^{15}N$ were ±0.06‰ and ±0.08‰, respectively. Accuracy of the study sample was assessed using laboratory standards. A total of 10 samples of usgs40 were analyzed for accuracy. The average $\delta^{13}C$ value of the standards was -26.39 ± 0.04‰, while the $\delta^{15}N$ was -4.52 ± 0.07‰.

Table 16: Summary of precision values for $\delta^{13}C$ and $\delta^{15}N$ based on duplicate sample analyses.

Sample ID (tissue)	Difference in $\delta^{13}C$ Values	Difference in $\delta^{15}N$ Values
K2-B359 (bone)	0.04	0.02
K2-590 (bone)	0.06	0.01
K2-B617-1 (hair)	0.06	0.01
K2-B353 (nail)	0.09	0.27
Precision	**±0.06**	**±0.08**

Statistical Analysis

All statistical analyses for this study were conducted using the IBM SPSS Statistics 24© software program. Mean, range, minimum and maximum values, and standard deviation, were calculated for the overall sample, scurvy and non-scurvy overall cohorts, and the overall, scurvy, and non-scurvy cohorts for each age cohort (F&P, neonatal, C1, C2, and C3). Box and whisker plots were constructed for each group (where applicable) to examine outliers within the overall sample and each cohort. The whiskers in each box plot indicate the "expected" minimum and maximum values based on that data set, not necessarily the actual minimum and/or maximum values. The outliers, when present, are those isotopic values that fall more than 1.5 times the interquartile range from the first or third quartile value; this method of determining outliers is standard for the IBM SPSS Statistics 24© software program. The Mann-Whitney U non-parametric t-test was used to calculate differences between groups due to unequal variances, small and unequal sample sizes, and some non-normally distributed cohorts. Microsoft Excel 2013© was used to generate all charts and tables.

CHAPTER 4: RESULTS

Bone Collagen Preservation

Four criteria were used to evaluate the preservation of the bone collagen samples prepared for analysis by the author. These include the C:N ratio, collagen yield percentage, %C weight, and %N weight. Table 17 indicates the published values for these criteria that are used to determine if bone collagen samples are well preserved.

Table 17: Published values used to indicate preservation of bone collagen samples for C:N ratio, collagen yield percentage, %C weight, and %N weight.

Criteria	Published Values	Study
C:N Ratio	2.9 - 3.6	Ambrose, 1990; DeNiro, 1985; Schoeninger et al., 1989
% Collagen Yield	Minimum of 2 - 5%	Ambrose, 1990; Lee-Thorp, 2008; van Klinken, 1999
%C Weight	15.3 - 47 %	Ambrose, 1990
%N Weight	5.5 - 17.3%	Ambrose, 1990

A total of 20 bone collagen samples contained enough collagen after preparation for isotopic testing. These samples had C:N ratios that ranged from 3.17 to 3.60, with a mean of 3.23 ± 0.13, with all samples falling within the published values for being well preserved. The C:N ratios in Williams (2008) for those samples utilized in this study that were not prepared by the author had a mean of 3.25 ± 0.06. The % collagen yield from these samples ranged from 0.46% to 36.06%, with a mean of 14.03 ± 9.55%. Four samples had % collagen yield values less than 2% . While most studies use a low-end cutoff value for collagen yield, due to the effect scurvy has on collagen production, a low collagen yield alone was not deemed enough to warrant

exclusion from this study. The %C weight ranged from 14.65% to 44.51%, with a mean of 41.34 ± 6.54%, with only one sample having a too-low value. The %N weight ranged from 4.75% to 16.30%, with a mean of 15.00 ± 2.58%, again with only one sample having a too-low value. The preservation values for each bone collagen sample can be viewed in Appendix D.

Each of the above listed preservation criteria were considered in order to determine the preservation of each bone collagen sample prepared for this study by the author. Multiple preservation values were considered in order to determine if each sample was preserved well enough to limit erroneous isotopic analysis values due to degradation or contamination. Samples were only discarded if more than one value was outside of the published acceptable values listed in Table 17. The procedures for determining the preservation level of bone collagen samples used in this study that were prepared and analyzed for previous research can be found in Williams (2008:123).

Hair, Nail and Skin Preservation

Three criteria were used to evaluate the preservation of the 11 hair and three nail samples prepared for analysis by the author. These include the C:N ratio, %C weight, and %N weight. Table 18 indicates the published values for these criteria that are used to determine if hair and nail samples are well preserved. The listed values for %C and %N weight are for those of hair, however, since the same α-keratin is used to produce both hair and nail, it results in the same %C and %N weight. At this time, there are no published standard preservation values for skin samples (Lamb, 2016; Williams, 2008), so the five skin C:N ratio, %C weight, and %N weight are provided here for comparative purposes.

Table 18: Published values used to indicate preservation of hair and nail samples for C:N ratio, %C weight, and %N weight.

Criteria	Published Values	Study
C:N Ratio	3.0 – 3.8	O'Connell and Hedges, 1999; O'Connell et al., 2001
%C Weight	50.65%	Rutherford and Hawk, 1907
%N Weight	17.14%	Rutherford and Hawk, 1907

The hair samples had C:N ratios that ranged from 3.53 to 3.69, with a mean of 3.58 ± 0.06, with all samples falling within the published values for being well preserved. The C:N ratios in Williams (2008) for those hair samples utilized in this study that were not prepared by the author had a mean of 3.6 ± 0.11. The hair %C weight ranged from 41.66% to 45.56%, with a mean of 43.61 ± 1.17. The %N weight ranged from 13.54% to 14.78%, with a mean of 14.20 ± 0.41. The %C and %N weight values of the sample are slightly less than those in the published literature. The preservation values for each hair sample can be viewed in Appendix D.

The nail samples had C:N ratios that ranged from 3.72 to 3.86, with a mean of 3.78 ± 0.08, with one sample having a value slightly higher than the published literature. The C:N ratios in Williams (2008) for those nail samples utilized in this study that were not prepared by the author had a mean of 3.73 ± 0.38. The nail %C weight ranged from 42.18% to 43.78%, with a mean of 43.02 ± 0.80%. The %N weight ranged from 13.22% to 13.43%, with a mean of 13.29 ± 0.12%. Again, these values are slightly less than those in the published literature. The preservation values for each nail sample can be viewed in Appendix D.

The skin samples had C:N ratios that ranged from 3.51 to 4.85, with a mean of 3.88 ± 0.57. The C:N ratios in Williams (2008) for those skin samples utilized in this study that were not prepared by the author had a mean of 3.25 ± 0.06. The skin %C weight ranged from 31.43%

to 51.48%, with a mean of 43.83 ± 7.53%. The %N weight ranged from 9.34% to 15.35%, with a mean of 13.32 ± 2.52. The values for each skin sample can be viewed in Appendix D.

As with bone collagen, each of the above listed preservation criteria were considered in order to determine the preservation of each hair and nail sample prepared for this study by the author. Multiple preservation values were considered in order to determine if each sample was preserved well enough to limit erroneous isotopic analysis values due to degradation or contamination. No hair or nail samples had more than one criteria outside of the published values, therefore no hair or nail samples were discarded from further analysis. The procedures for determining the preservation level of the hair and nail samples used in this study that were prepared and analyzed for previous research can be found in Williams (2008:123).

Explanation of Retained and Discarded Samples

Six juveniles in total had at least one preservation value fall outside of the published ranges listed in Tables 17 and 18. Of these, only sample 325 (bone collagen) presented with multiple values outside of the acceptable ranges, including low %C and %N weights, low collagen yield, and a borderline high C:N ratio. Therefore, this sample was determined to not be well preserved and was therefore excluded from further statistical analyses.

The remaining five samples each had only one preservation value outside of the published ranges. Sample 435 (bone collagen) produced a very low collagen yield (0.46%), but provided acceptable %C and %N concentrations and C:N ratio. This sample was kept in the analysis because it has been found that the isotopic composition may remain intact even when a low percentage of the original amount of collagen is retained (Lee-Thorp, 2008). Additionally,

this sample was retained in the study because low collagen yield could result in elimination of an individual who exhibited signs of scurvy as it affects the formation of collagen in the body. Samples 449 and 525 (both bone collagen) produced low collagen yields (1.24% and 1.70%, respectively) but had acceptable %C and %N concentrations and C:N ratios. Sample 290 (nail) produced acceptable %C and %N concentrations, but did have a slightly high C:N ratio (3.86). However, because this value was within the standard deviation of the nail sample, it was retained in the study. Sample 575A (skin) produced an unusually high C:N ratio but was not excluded from the study since there currently is no accepted standard of C:N ratio values for this body tissue.

Stable Carbon Isotope Results

Bone Collagen

A total of 24 bone collagen samples were analyzed for $\delta^{13}C$ values. All descriptive statistics (mean, minimum, maximum, and standard deviation) for $\delta^{13}C$ values from bone collagen can be found in Table 19. The $\delta^{13}C$ values of bone collagen for these individuals can be found in Appendix E (Table 56).

Table 19: Descriptive statistics for $\delta^{13}C$ values for bone collagen. Each category's statistics are first presented as an overall representation, followed by those individuals who exhibited skeletal indicators of scurvy and then those who did not. Entries of "-" indicate not enough data available to calculate the statistic.

		N	Mean	Min	Max	Standard Deviation
Entire Sample	**Overall**	24	-18.8	-19.5	-17.6	0.4
	Scurvy	11	-18.9	-19.5	-18.2	0.5
	Non-scurvy	13	-18.8	-19.3	-17.6	0.4
F&P	**Overall**	2	-18.9	-19.3	-18.4	0.6
	Scurvy	1	-18.4	-	-	-
	Non-scurvy	1	-19.3	-	-	-
Neo	**Overall**	4	-18.6	-18.9	-18.3	0.2
	Scurvy	2	-18.5	-18.6	-18.3	0.2
	Non-scurvy	2	-18.8	-18.9	-18.6	0.2
C1	**Overall**	10	-18.7	-19.3	-17.6	0.5
	Scurvy	3	-18.9	-19.3	-18.2	0.6
	Non-scurvy	7	-18.6	-19.1	-17.6	0.5
C2	**Overall**	5	-19.0	-19.2	-18.8	0.2
	Scurvy	3	-19.0	-19.2	-18.8	0.2
	Non-scurvy	2	-19.1	-19.2	-19.0	0.1
C3	**Overall**	3	-19.3	-19.5	-19.1	0.2
	Scurvy	2	-19.4	-19.5	-19.2	0.2
	Non-scurvy	1	-19.1	-	-	-

The $\delta^{13}C$ values for the entire sample ranged from -19.5‰ to -17.6‰, with a mean value of -18.8 ± 0.5‰. Of the 24 bone collagen samples, 11 individuals exhibited skeletal indicators of scurvy. The $\delta^{13}C$ values for this cohort ranged from -19.5‰ to -18.2‰, with a mean value of -18.9 ± 0.4‰. The remaining 13 individuals did not exhibit skeletal indicators of scurvy. The $\delta^{13}C$ values for this second cohort ranged from -19.3‰ to -17.6‰, with a mean value of -18.8 ± 0.4‰. There was no statistically significant difference between the mean scurvy and non-scurvy

$\delta^{13}C$ values for the overall bone collagen samples (p=0.705) (Appendix F). The $\delta^{13}C$ and $\delta^{15}N$ values of the scurvy and non-scurvy cohorts are shown in Figure 10.

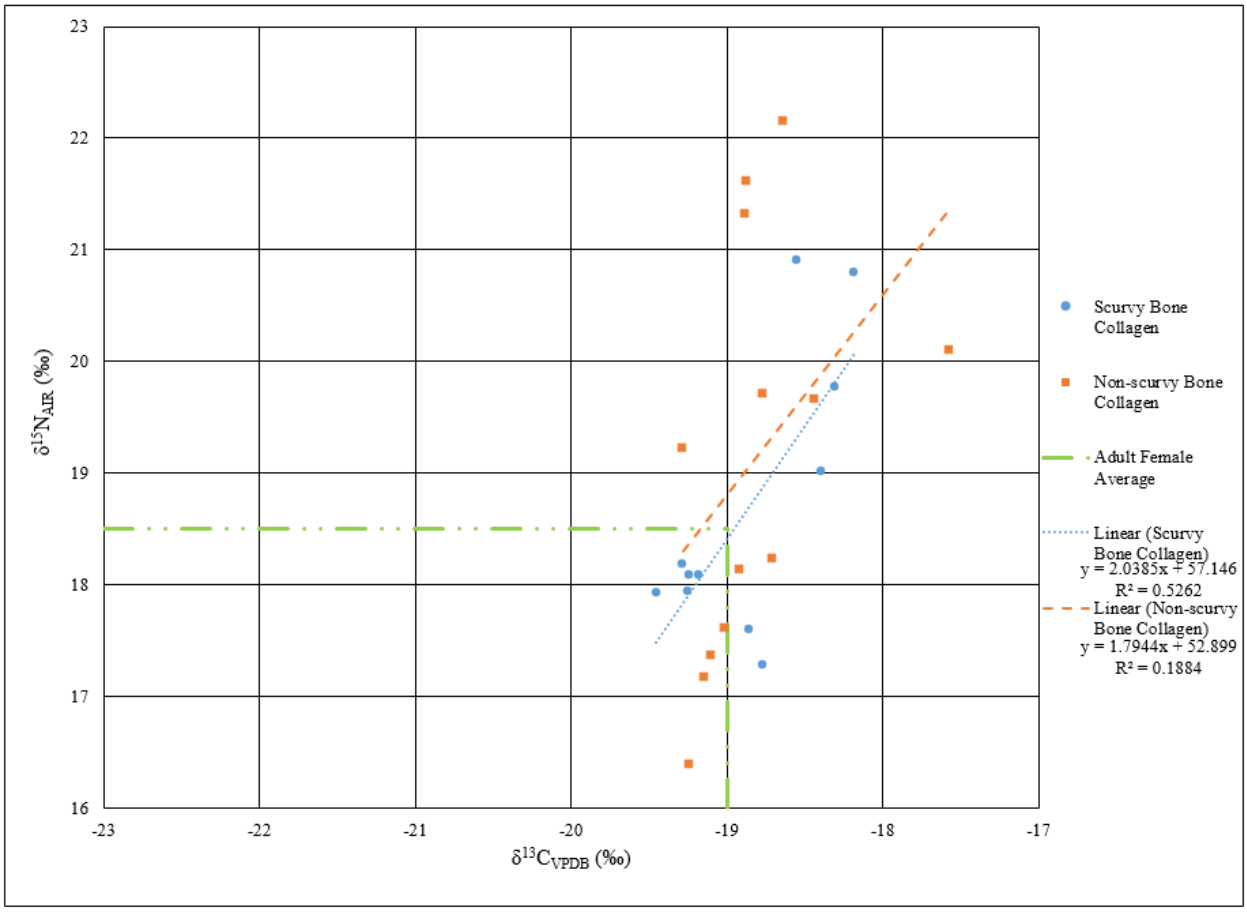

Figure 10: Scatter plot of $\delta^{13}C$ and $\delta^{15}N$ values for the overall bone collagen cohort.

When the $\delta^{13}C$ values for bone collagen were plotted by age, a general trend can be seen. Both the scurvy and non-scurvy cohorts show a general trend of more negative $\delta^{13}C$ values as age increases (Figure 11).

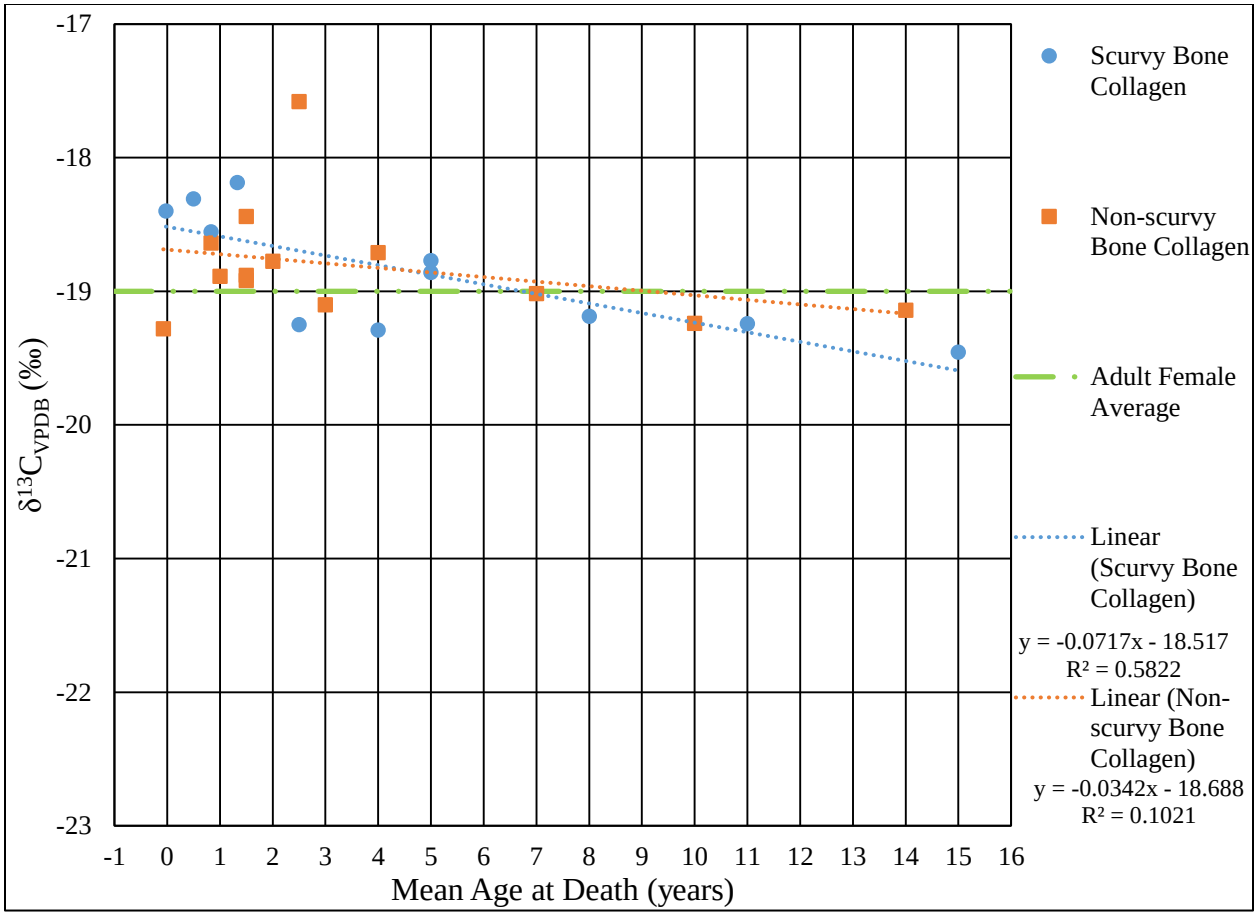

Figure 11: Bone collagen $\delta^{13}C$ values plotted by mean age.

The results for $\delta^{13}C$ values were also divided based on the age at death cohorts previously described. The fetal and perinatal (F&P) cohort represented by bone collagen consisted of two individuals, one who exhibited skeletal indicators of scurvy and one who did not, with $\delta^{13}C$ values of -18.4‰ and -19.3‰, respectively. The $\delta^{13}C$ values for the F&P cohort had a mean value of -18.9 ± 0.6‰. There was no statistically significant difference between the mean scurvy and non-scurvy $\delta^{13}C$ values for the F&P bone collagen cohort (p=0.317) (Appendix G). The $\delta^{13}C$ and $\delta^{15}N$ values of the F&P scurvy and non-scurvy cohorts are shown in Figure 12. The neonatal cohort represented by bone collagen consisted of four individuals, two who exhibited skeletal

indicators of scurvy and two who did not. The $\delta^{13}C$ values for the entire neonatal cohort ranged from -18.9‰ to -18.3‰, with a mean value of -18.6 ± 0.2‰. The $\delta^{13}C$ values for those neonatal cohort individuals who exhibited skeletal indicators of scurvy ranged from -18.5‰ to -18.3‰, with a mean value of -18.4 ± 0.2‰. The $\delta^{13}C$ values for those neonatal cohort individuals who did not present with skeletal indicators of scurvy ranged from -18.9‰ to -18.6‰, with a mean value of -18.8 ± 0.2‰. There was no statistically significant difference between the mean scurvy and non-scurvy $\delta^{13}C$ values for the neonatal bone collagen samples (p=0.221) (Appendix G). The $\delta^{13}C$ and $\delta^{15}N$ values of the neonatal scurvy and non-scurvy cohorts are shown in Figure 12.

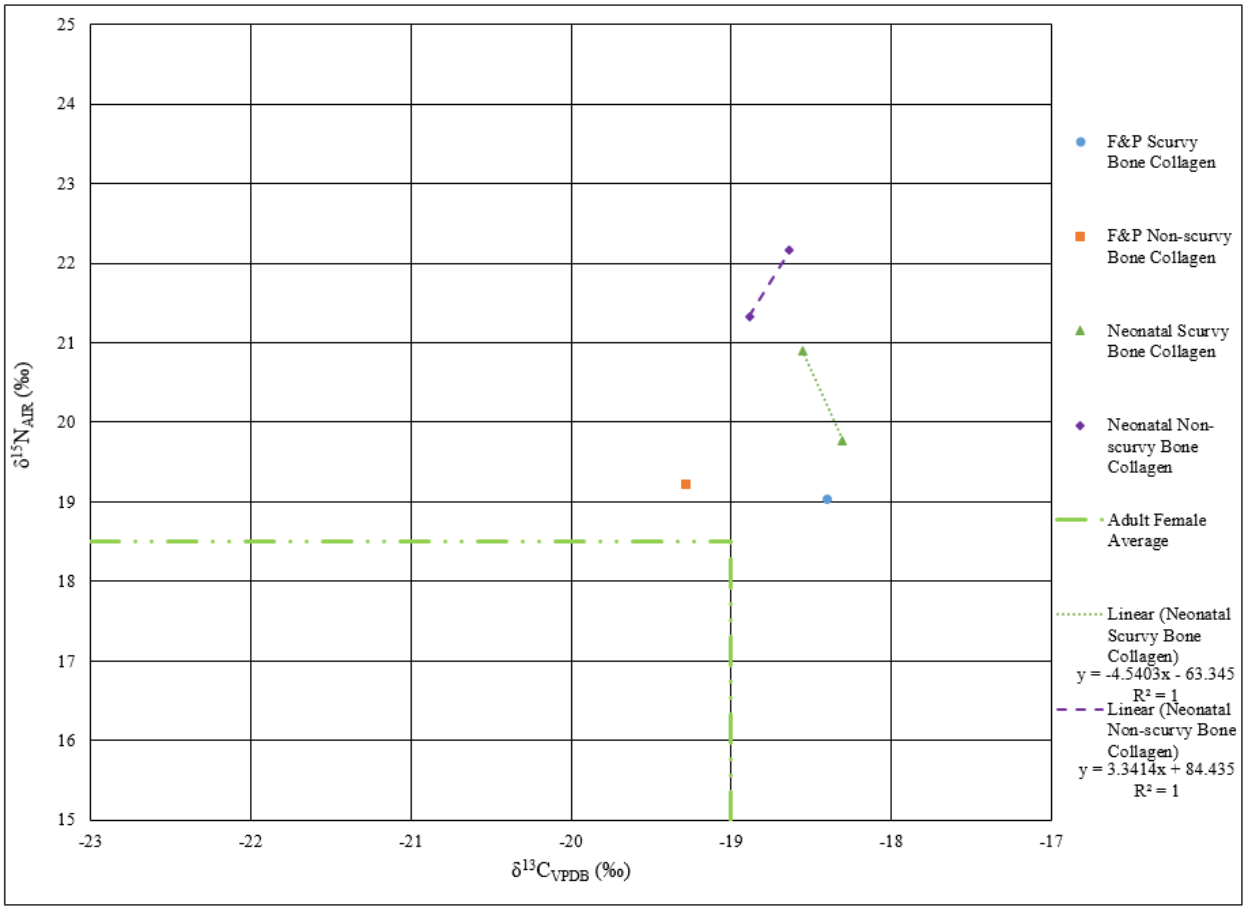

Figure 12: Scatter plot of $\delta^{13}C$ and $\delta^{15}N$ values for the F&P and neonatal bone collagen cohorts, separated by scurvy status.

The C1 cohort represented by bone collagen consisted of ten individuals, three who exhibited skeletal indicators of scurvy and seven who did not. The $\delta^{13}C$ values for the entire C1 cohort ranged from -19.3‰ to -17.6‰, with a mean value of -18.7 ± 0.5‰. The $\delta^{13}C$ values for those C1 cohort individuals who exhibited skeletal indicators of scurvy ranged from -19.3‰ to -18.2‰, with a mean value of -18.9 ± 0.6‰. The $\delta^{13}C$ values for those C1 cohort individuals who did not present with skeletal indicators of scurvy ranged from -19.1‰ to -17.6‰, with a mean value of -18.6 ± 0.5‰. One outlier (burial 71) was present in this cohort with a more enriched $\delta^{13}C$ value (Figure 13). There was no statistically significant difference between the

mean scurvy and non-scurvy $\delta^{13}C$ values for the C1 bone collagen samples (p=0.302) (Appendix G). The $\delta^{13}C$ and $\delta^{15}N$ values of the C1 scurvy and non-scurvy cohorts are shown in Figure 14.

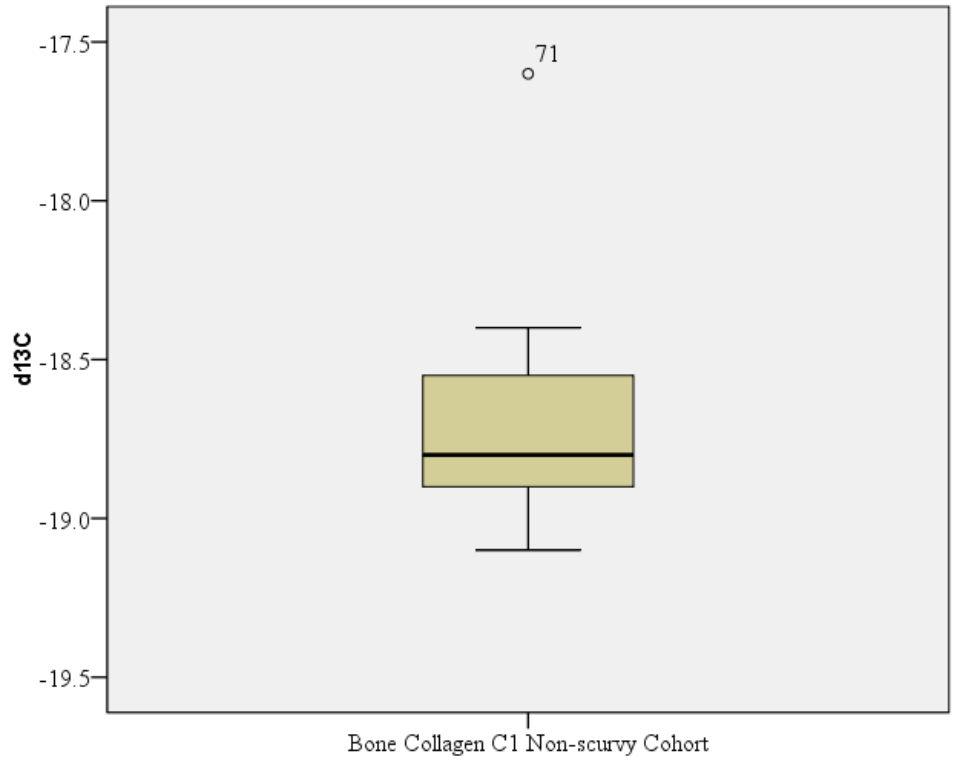

Figure 13: Box and whisker plot for $\delta^{13}C$ indicating the outlier for the C1 non-scurvy bone collagen cohort.

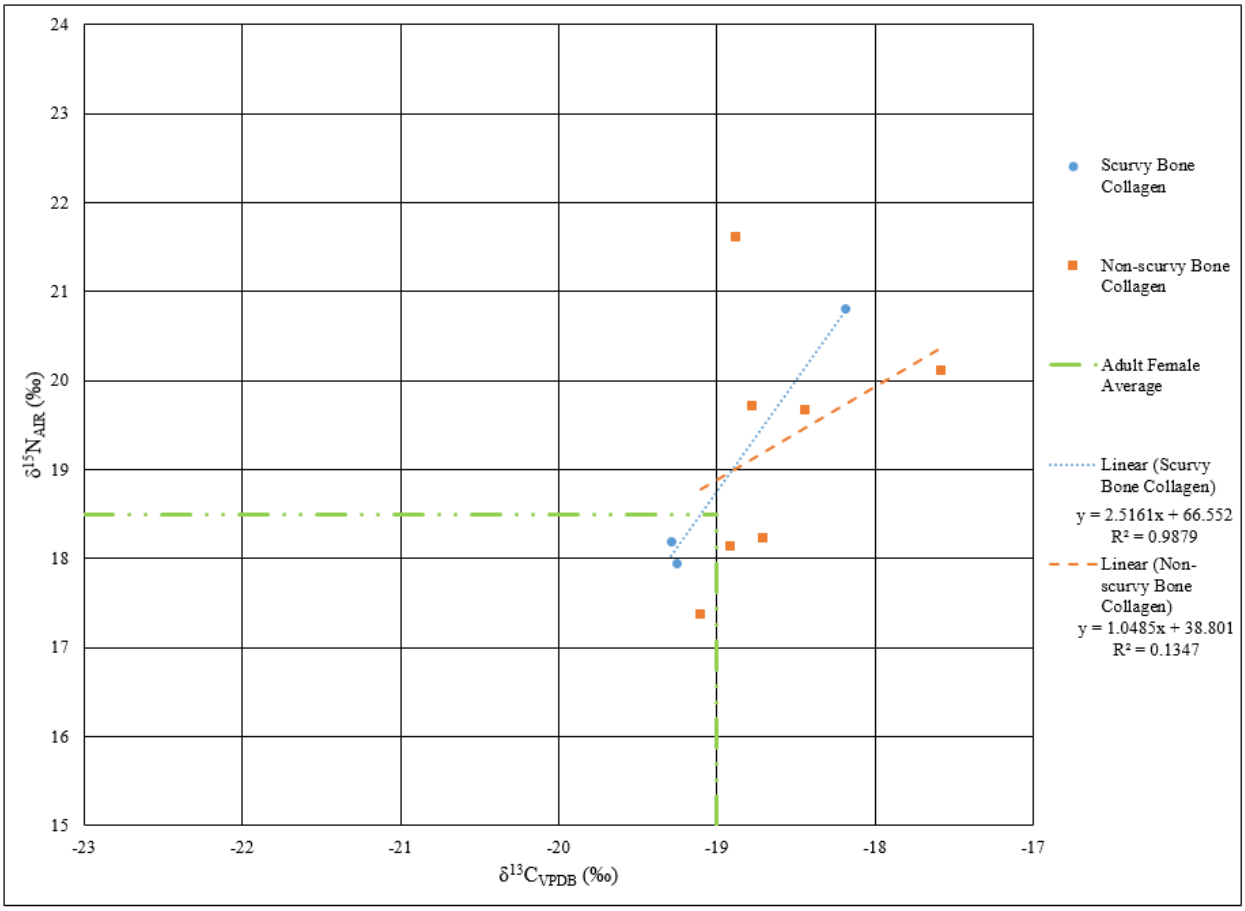

Figure 14: Scatter plot of $\delta^{13}C$ and $\delta^{15}N$ values for the C1 bone collagen cohort.

The C2 cohort represented by bone collagen consisted of five individuals, three who exhibited skeletal indicators of scurvy and two who did not. The $\delta^{13}C$ values for the entire C2 cohort ranged from -19.2‰ to -18.8‰, with a mean value of -19.0 ± 0.2‰. The $\delta^{13}C$ values for those C2 cohort individuals who exhibited skeletal indicators of scurvy ranged from -19.2‰ to -18.8‰, with a mean value of -19.0 ± 0.2‰. The $\delta^{13}C$ values for those C2 cohort individuals who did not present with skeletal indicators of scurvy ranged from -19.2‰ to -19.0‰, with a mean value of -19.1 ± 0.1‰. There was no statistically significant difference between the mean scurvy

and non-scurvy $\delta^{13}C$ values for the C2 bone collagen samples (p=0.374) (Appendix G). The $\delta^{13}C$ and $\delta^{15}N$ values of the C2 scurvy and non-scurvy cohorts are shown in Figure 15.

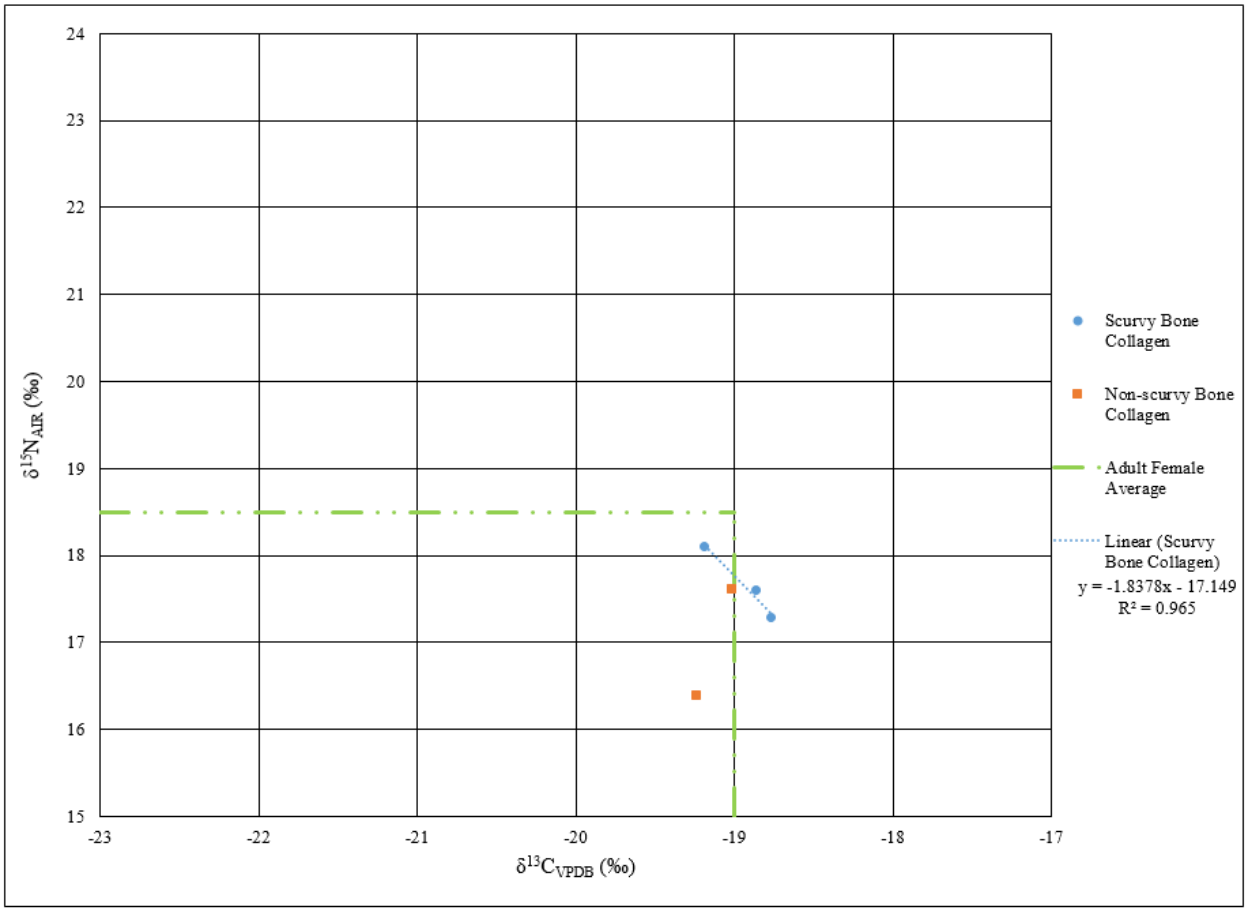

Figure 15: Scatter plot of $\delta^{13}C$ and $\delta^{15}N$ values for the C2 bone collagen cohort.

The C3 cohort represented by bone collagen consisted of three individuals, two who exhibited skeletal indicators of scurvy and one who did not. The $\delta^{13}C$ values for the entire C3 cohort ranged from -19.5‰ to -19.1‰, with a mean value of -19.3 ± 0.2‰. The $\delta^{13}C$ values for those C3 cohort individuals who exhibited skeletal indicators of scurvy ranged from -19.5‰ to -19.2‰, with a mean value of -19.4 ± 0.2‰. The $\delta^{13}C$ value for the C3 individual who did not exhibit skeletal indicators of scurvy was -19.1‰. There was no statistically significant difference

between the mean scurvy and non-scurvy $\delta^{13}C$ values for the C3 bone collagen samples (p=0.221) (Appendix G). The $\delta^{13}C$ and $\delta^{15}N$ values of the C3 scurvy and non-scurvy cohorts are shown in Figure 16.

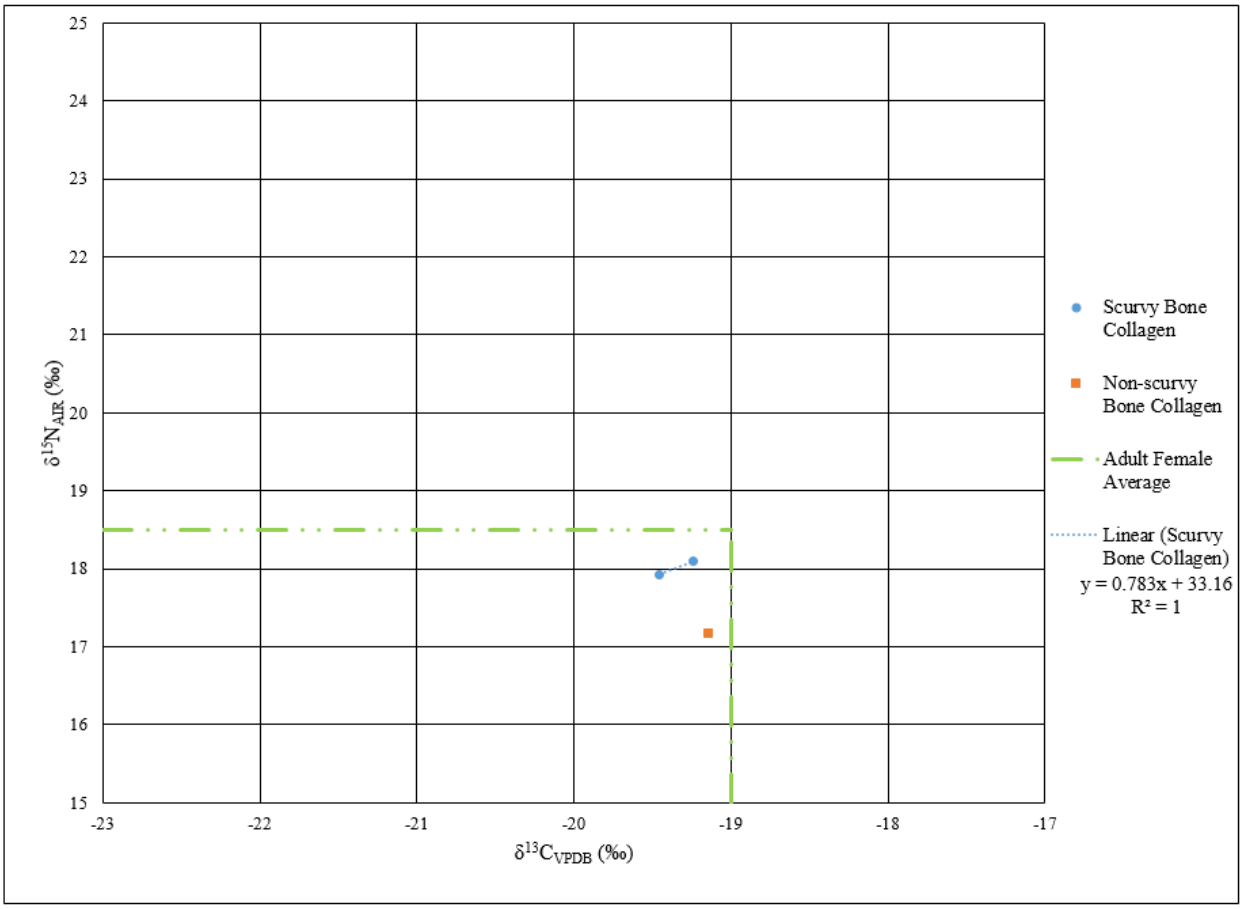

Figure 16: Scatter plot of $\delta^{13}C$ and $\delta^{15}N$ values for the C3 bone collagen cohort.

Hair

A total of 133 juveniles, represented by one to three hair segments (measuring 1cm in length each), were analyzed for $\delta^{13}C$ values. There were 67 juveniles who provided only one hair

segment, 26 who provided two segments, and 40 who provided three segments. Descriptive statistics (mean, minimum, maximum, and standard deviation) for the $\delta^{13}C$ values of each of the first three hair segments were calculated separately and can be found in Tables 20-22. The $\delta^{13}C$ values for up to the first three hair segments for these individuals can be found in Appendix E (Table 57). The overall descriptive and statistical tests for each hair segment are presented first. Then, in order to see trends over the last three months of life, the mean of each scurvy and non-scurvy segment for each age cohort is presented together.

Table 20: Descriptive statistics for $\delta^{13}C$ for first hair segments. Each category's statistics are first presented as an overall representation, followed by those individuals who exhibited skeletal indicators of scurvy and then those who did not. Entries of "-" indicate not enough data to calculate statistic.

		N	Mean	Min	Max	Standard Deviation
Entire Sample	**Overall**	133	-19.5	-22.7	-17.7	0.8
	Scurvy	21	-19.4	-21.1	-18.3	0.6
	Non-scurvy	112	-19.5	-22.7	-17.7	0.8
F&P	**Overall**	-	-	-	-	-
	Scurvy	-	-	-	-	-
	Non-scurvy	35	-19.9	-21.7	-18.9	0.8
Neo	**Overall**	42	-19.2	-22.7	-18.0	0.8
	Scurvy	7	-18.9	-19.4	-18.3	0.4
	Non-scurvy	35	-19.3	-22.7	-18.0	0.8
C1	**Overall**	30	-19.3	-21.2	-17.7	0.7
	Scurvy	7	-19.3	-19.7	-18.8	0.4
	Non-scurvy	23	-19.3	-21.2	-17.7	0.8
C2	**Overall**	15	-19.7	-20.2	-19.2	0.3
	Scurvy	4	-19.9	-20.2	-19.6	0.3
	Non-scurvy	11	-19.7	-20.2	-19.2	0.3
C3	**Overall**	11	-19.8	-21.1	-19.2	0.5
	Scurvy	3	-20.3	-21.1	-19.5	0.8
	Non-scurvy	8	-19.7	-20.1	-19.2	0.3

Table 21: Descriptive statistics for $\delta^{13}C$ for second hair segments. Each category's statistics are first presented as an overall representation, followed by those individuals who exhibited skeletal indicators of scurvy (scorbutic) and then those who did not (nonscorbutic). Entries of "-" indicate not enough data to calculate statistic.

		N	Mean	Min	Max	Standard Deviation
Entire Sample	**Overall**	66	-19.3	-20.5	-18.1	0.6
	Scurvy	15	-19.5	-20.5	-18.2	0.6
	Non-scurvy	51	-19.3	-20.5	-18.1	0.5
F&P	**Overall**	-	-	-	-	-
	Scurvy	-	-	-	-	-
	Non-scurvy	7	-19.4	-20.5	-19.0	0.5
Neo	**Overall**	17	-19.0	-19.5	-18.2	0.4
	Scurvy	4	-18.8	-19.2	-18.2	0.5
	Non-scurvy	13	-19.0	-19.5	-18.5	0.3
C1	**Overall**	23	-19.3	-20.5	-18.1	0.6
	Scurvy	5	-19.5	-20.5	-18.9	0.6
	Non-scurvy	18	-19.3	-20.4	-18.1	0.6
C2	**Overall**	10	-19.7	-20.4	-19.1	0.4
	Scurvy	3	-19.9	-20.2	-19.5	0.4
	Non-scurvy	7	-19.6	-20.4	-19.1	0.4
C3	**Overall**	9	-19.7	-20.4	-19.3	0.4
	Scurvy	3	-19.9	-20.4	-19.3	0.6
	Non-scurvy	6	-19.6	-20.2	-19.3	0.4

Table 22: Descriptive statistics for $\delta^{13}C$ for third hair segments. Each category's statistics are first presented as an overall representation, followed by those individuals who exhibited skeletal indicators of scurvy and then those who did not. Entries of "-" indicate not enough data to calculate statistic.

		N	Mean	Min	Max	Standard Deviation
Entire Sample	**Overall**	40	-19.5	-21.2	-17.9	0.6
	Scurvy	8	-19.8	-21.2	-18.7	0.8
	Non-scurvy	32	-19.4	-20.4	-17.9	0.6
F&P	**Overall**	-	-	-	-	-
	Scurvy	-	-	-	-	-
	Non-scurvy	3	-19.0	-19.5	-18.4	0.6
Neo	**Overall**	-	-	-	-	-
	Scurvy	-	-	-	-	-
	Non-scurvy	6	-19.2	-19.9	-18.2	0.6
C1	**Overall**	15	-19.5	-21.2	-17.9	0.8
	Scurvy	3	-19.7	-21.2	-18.7	1.3
	Non-scurvy	12	-19.4	-20.4	-17.9	0.7
C2	**Overall**	8	-19.7	-20.4	-19.0	0.5
	Scurvy	3	-20.0	-20.4	-19.6	0.4
	Non-scurvy	5	-19.5	-20.2	-19.0	0.5
C3	**Overall**	8	-19.6	-20.1	-19.1	0.3
	Scurvy	2	-19.7	-20.1	-19.3	0.6
	Non-scurvy	6	-19.6	-20.0	-19.1	0.3

The $\delta^{13}C$ values for the overall first hair segment ranged from -22.7‰ to -17.7‰, with a mean value of -19.5 ± 0.8‰. The 21 juveniles who exhibited skeletal indicators of scurvy had $\delta^{13}C$ values that ranged from -21.1‰ to -18.3‰, with a mean value of -19.4 ± 0.6‰. The 112 juveniles who did not exhibit skeletal indicators of scurvy had $\delta^{13}C$ values that ranged from -22.7‰ to -17.7‰, with a mean value of -19.5 ± 0.8‰. There was no statistically significant difference between the mean scurvy and non-scurvy $\delta^{13}C$ values for the overall first hair segment

samples (p=0.667) (Appendix F). The $\delta^{13}C$ and $\delta^{15}N$ values of the overall first hair segment scurvy and non-scurvy cohorts are shown in Figure 17.

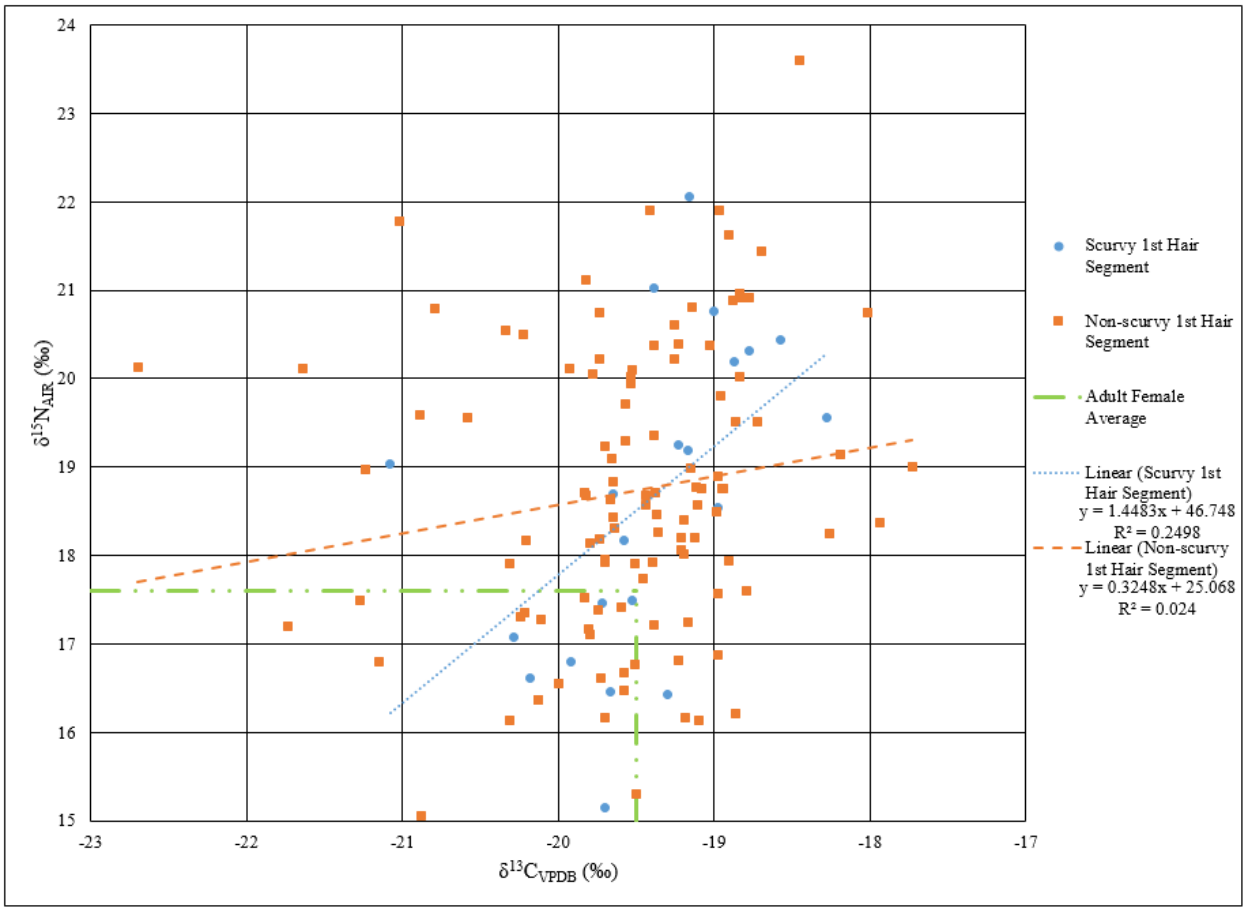

Figure 17: Scatter plot of $\delta^{13}C$ and $\delta^{15}N$ values for the overall first hair segment cohort.

The $\delta^{13}C$ values for the overall second hair segment ranged from -20.5‰ to -18.1‰, with a mean value of -19.3 ± 0.6‰. The 15 individuals who exhibited skeletal indicators of scurvy had $\delta^{13}C$ values that ranged from -20.5‰ to -18.2‰, with a mean value of -19.5 ± 0.6‰. The remaining 51 individuals who did not present with skeletal indicators of scurvy had $\delta^{13}C$ values that ranged from -20.5‰ to -18.1‰, with a mean value of -19.3 ± 0.5‰. There was no statistically significant difference between the mean scurvy and non-scurvy $\delta^{13}C$ values for the

overall second hair segment samples (p=0.443) (Appendix F). The $\delta^{13}C$ and $\delta^{15}N$ values of the overall second hair segment scurvy and non-scurvy cohorts are shown in Figure 18.

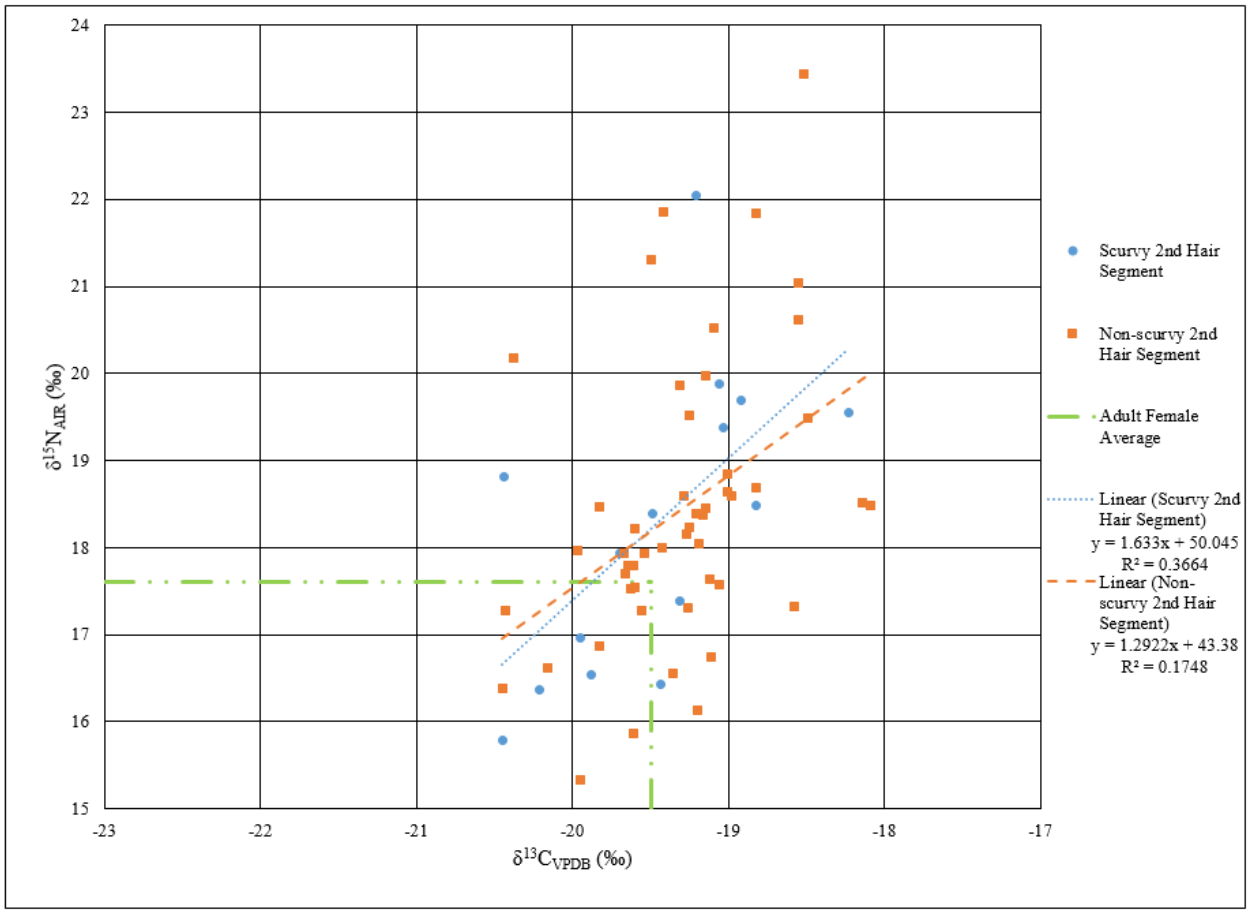

Figure 18: Scatter plot of $\delta^{13}C$ and $\delta^{15}N$ values for the overall second hair segment cohort.

The $\delta^{13}C$ values for the overall third hair segment ranged from -21.2‰ to -17.9‰, with a mean value of -19.5 ± 0.6‰. Eight individuals exhibited skeletal indicators of scurvy and had $\delta^{13}C$ values that ranged from -21.2‰ to -18.7‰, with a mean value of -19.8 ± 0.8‰. The remaining 32 individuals who did not present with skeletal indicators of scurvy had $\delta^{13}C$ values that ranged from -20.4‰ to -17.9‰, with a mean value of -19.4 ± 0.6‰. There was no

statistically significant difference between the mean scurvy and non-scurvy $\delta^{13}C$ values for the overall third hair segment samples (p=0.160) (Appendix F). The $\delta^{13}C$ and $\delta^{15}N$ values of the overall third hair segment scurvy and non-scurvy cohorts are shown in Figure 19.

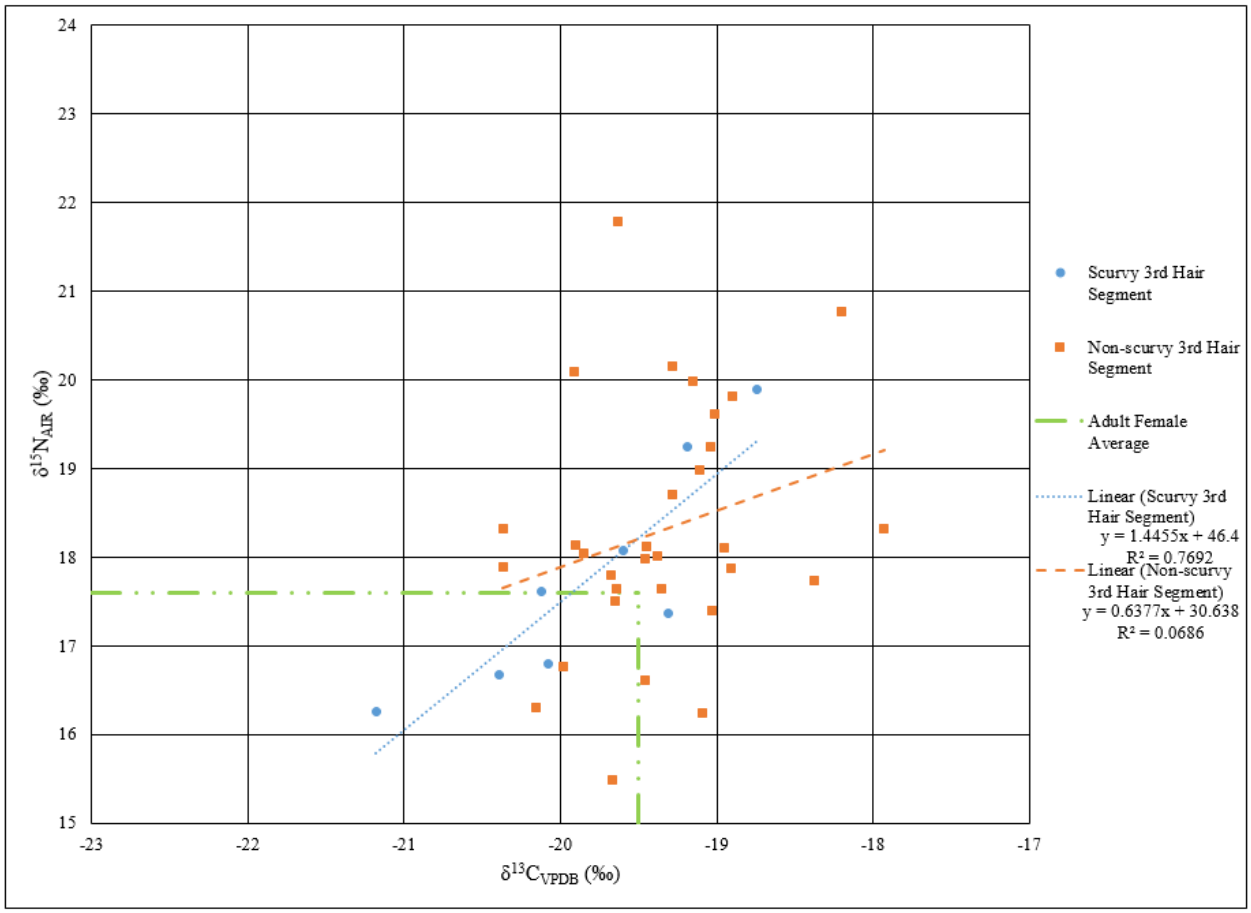

Figure 19: Scatter plot of $\delta^{13}C$ and $\delta^{15}N$ values for the overall third hair segment cohort.

When the $\delta^{13}C$ values for each hair segment were plotted by age, some patterns were found. For the $\delta^{13}C$ values within the first hair segment, the range of values is greatest in the younger ages with a tapering effect occurring as age increases (Figures 20). The second and third hair segments for $\delta^{13}C$ values experience a similar effect, but not to the same extent as the first hair segment (Figures 21 and 22). When a linear trend line is plotted for the scurvy and non-

scurvy $\delta^{13}C$ values for the third hair segment, both the equations and r^2 values are very similar (Figure 22).

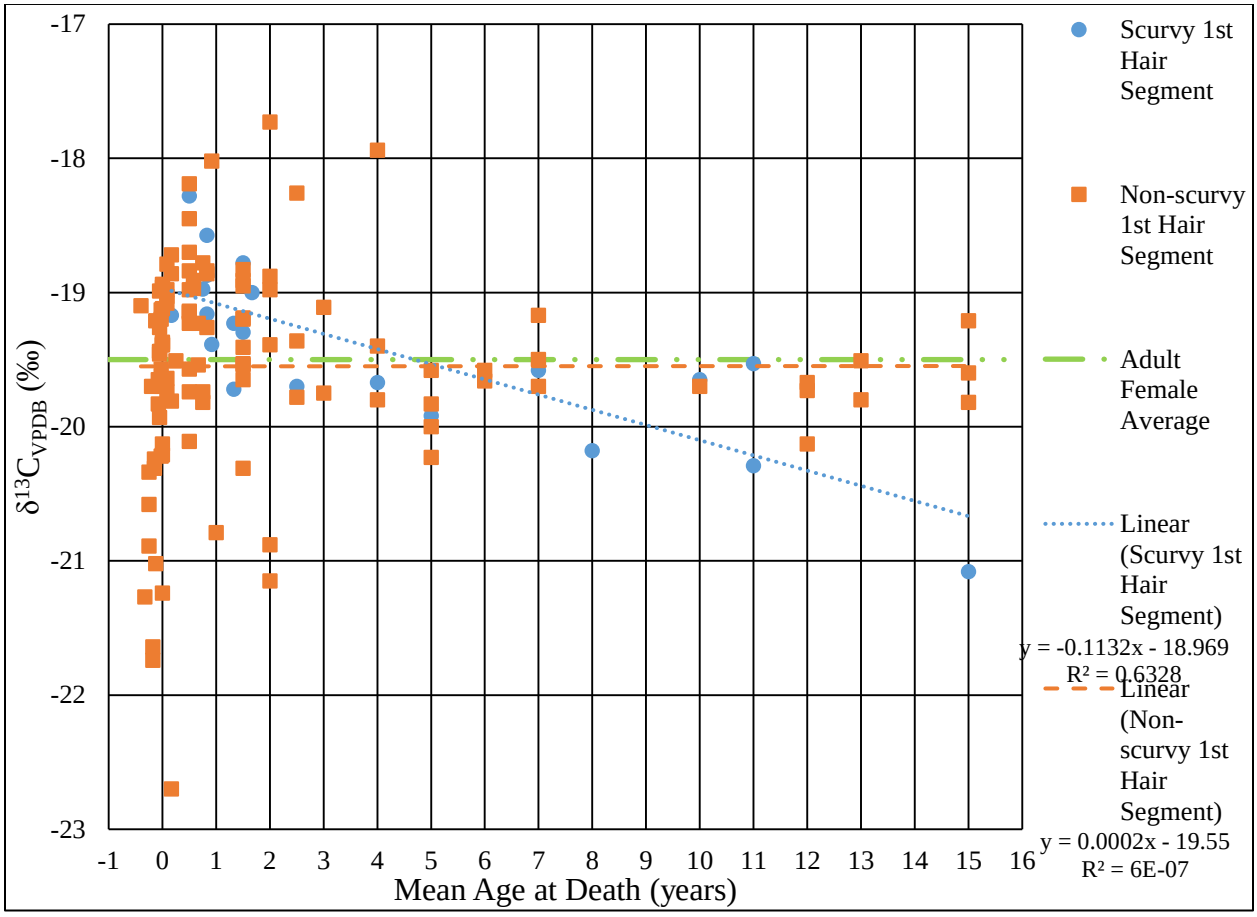

Figure 20: First hair segment $\delta^{13}C$ values plotted by mean age.

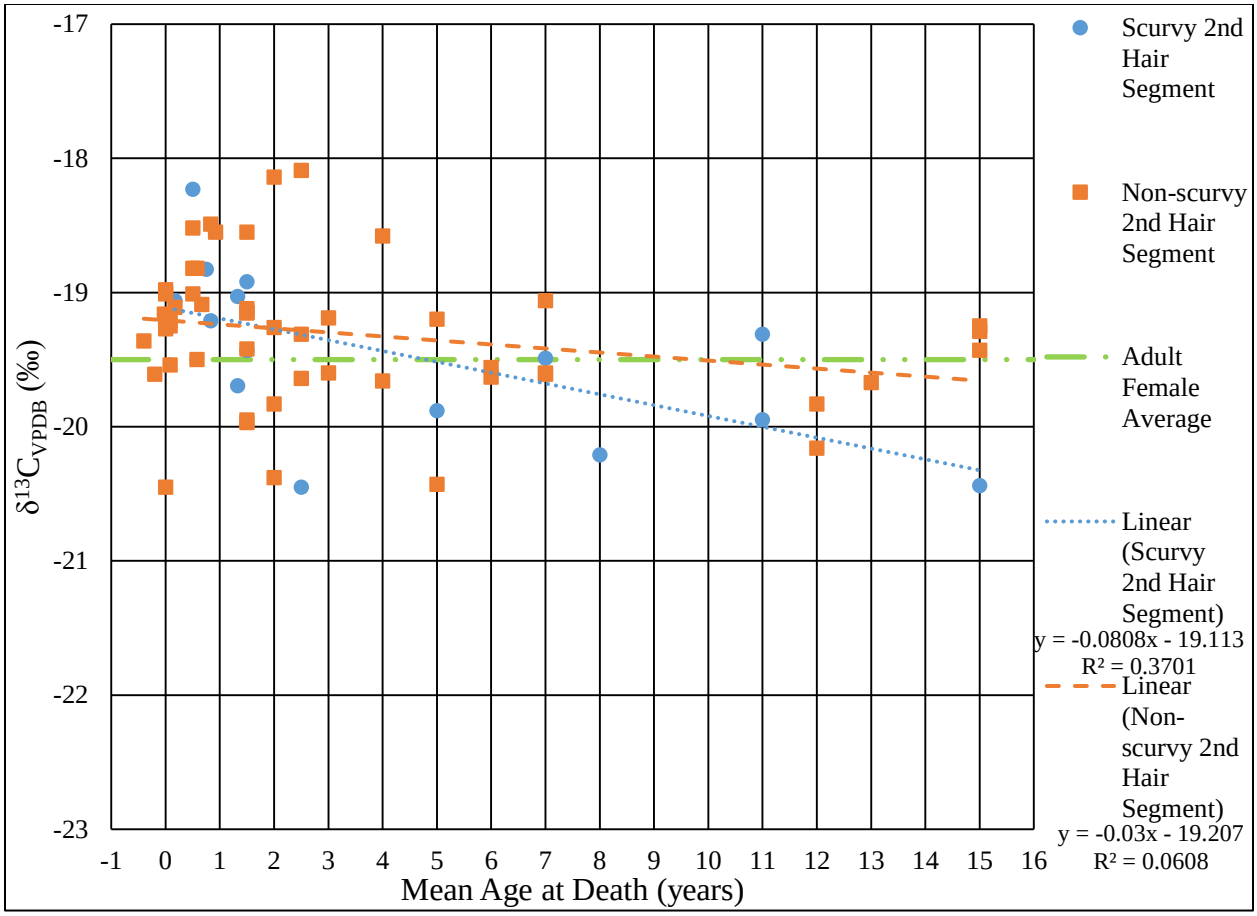

Figure 21: Second hair segment $\delta^{13}C$ values plotted by mean age.

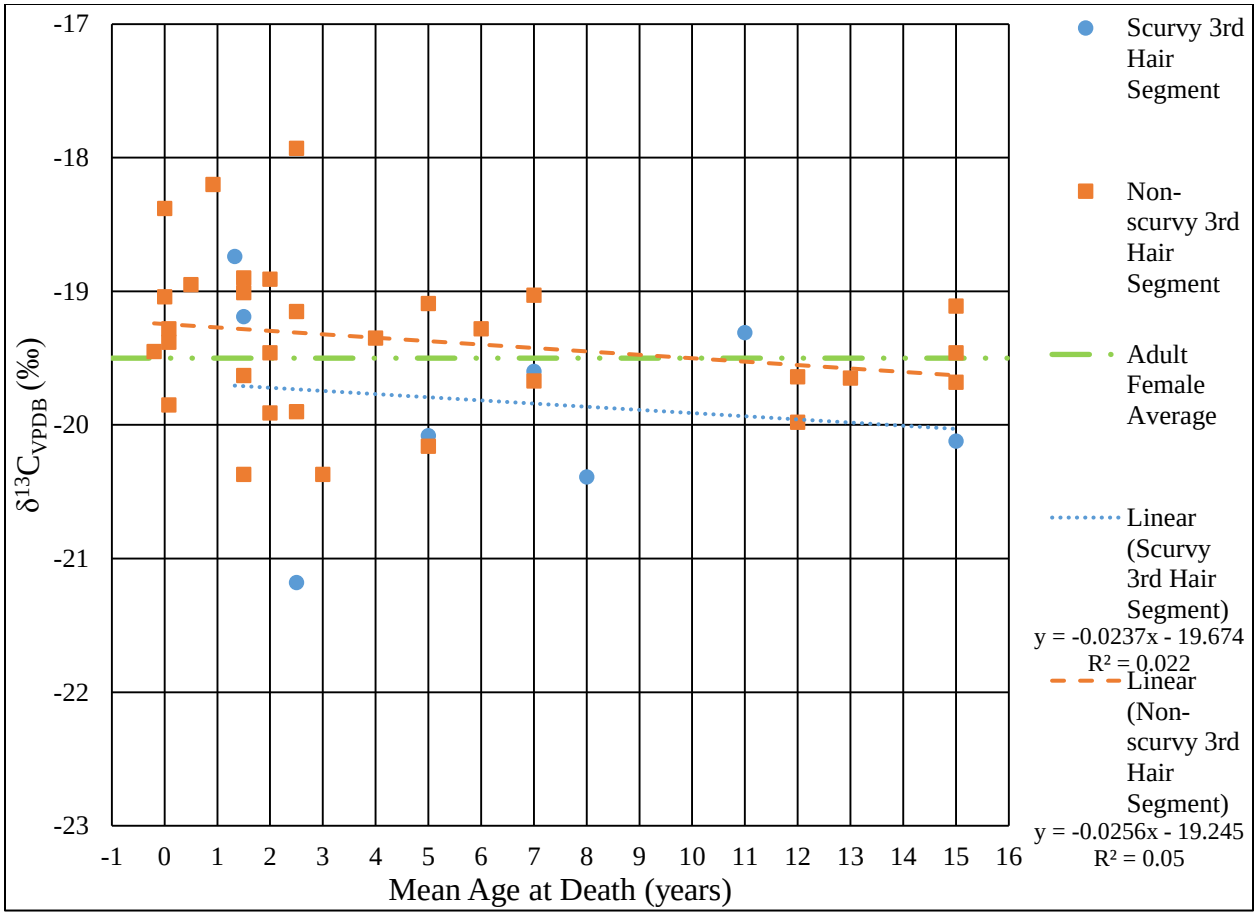

Figure 22: Third hair segment $\delta^{13}C$ values plotted by mean age.

The F&P cohort first, second, and third hair segments were represented by 35, seven, and three non-scurvy juveniles, respectively. The $\delta^{13}C$ values for the first hair segment ranged from -21.7‰ to -18.9‰, with a mean value of -19.9 ± 0.8‰. Two outliers (burials 130 and 292) were present, both with less enriched $\delta^{13}C$ values (Figure 23). The $\delta^{13}C$ values for the second hair segment ranged from -20.5‰ to -19.0‰, with a mean value of -19.4 ± 0.5‰. One outlier (burial 599) was present in this cohort with a less enriched $\delta^{13}C$ value (Figure 24). The $\delta^{13}C$ values for the third hair segment ranged from -19.5‰ to -18.4‰, with a mean value of -19.0 ± 0.6‰. The scatter plot of all juveniles for the first, second, and third F&P hair segments can be found in

Appendix H (Figure 94). The F&P cohort for each hair segment was also averaged in order to show trends in $\delta^{13}C$ values for this cohort over the last three months of life, which shows a slight decrease of $\delta^{13}C$ values over this time period (Figure 25). The difference between the third and first hair segment $\delta^{13}C$values is not statistically significant ($p = 0.57$).

Figure 23: Box and whisker plot for $\delta^{13}C$ indicating the outliers for the F&P overall (non-scurvy) first hair segment cohort.

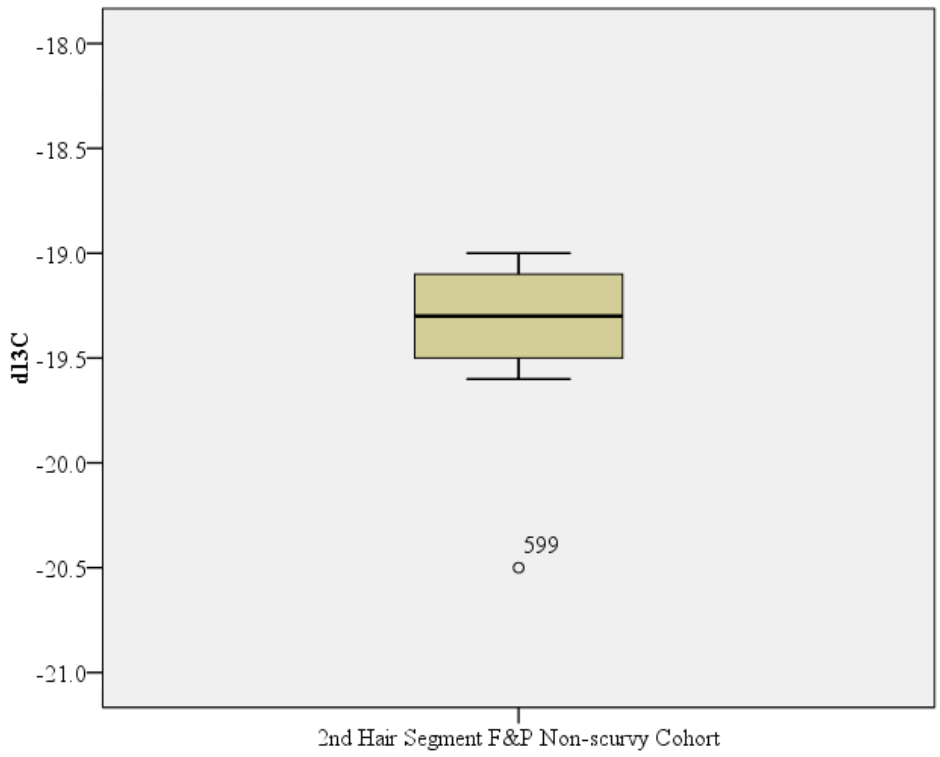

Figure 24: Box and whisker plot for $\delta^{13}C$ indicating the outlier for the F&P overall (non-scurvy) second hair segment cohort.

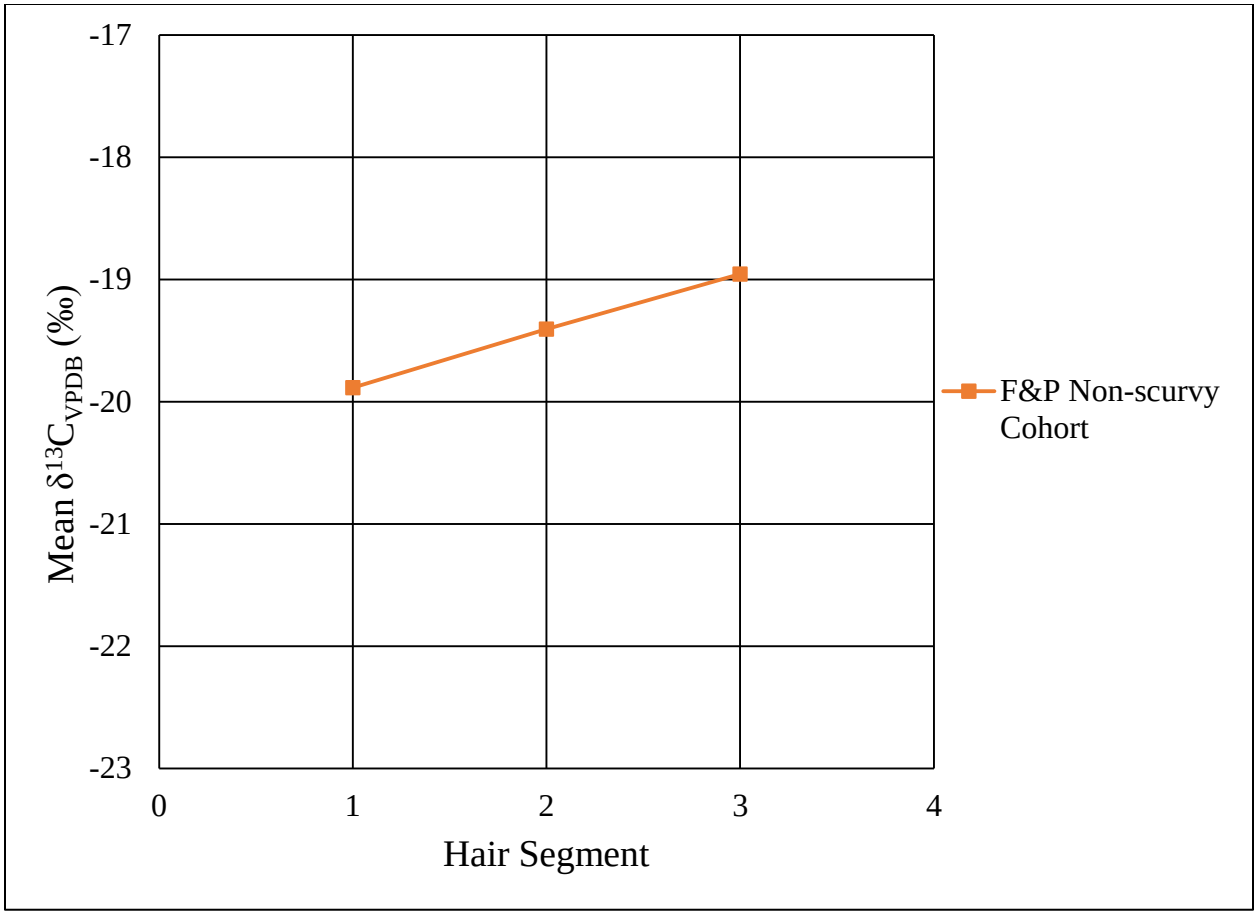

Figure 25: Averaged $\delta^{13}C$ values for each hair segment of the F&P cohort showing trends in the last three months of life.

The neonatal cohort first, second, and third hair segments were represented by 42, 17, and six scurvy and/or non-scurvy juveniles, respectively. The $\delta^{13}C$ values for the overall first hair segment ranged from -22.7‰ to -18.0‰, with a mean value of -19.2 ± 0.8‰. Two outliers (burials 206 and 596) were present in this cohort, both with less enriched $\delta^{13}C$ values (Figure 26). The $\delta^{13}C$ values for the scurvy cohort (n = 7) ranged from -19.4‰ to -18.3‰, with a mean value of -18.9 ± 0.4‰. The $\delta^{13}C$ values for the non-scurvy cohort (n = 35) ranged from -22.7‰ to -18.0‰, with a mean value of -19.3 ± 0.8‰. One outlier (burial 596) was present in this cohort with a less enriched $\delta^{13}C$ value (Figure 27). There was no statistically significant

difference between the mean scurvy and non-scurvy $\delta^{13}C$ values for the neonatal first hair segment samples ($p = 0.361$) (Appendix G). The scatter plot of all juveniles for the neonatal first hair segment can be found in Appendix H (Figure 95).

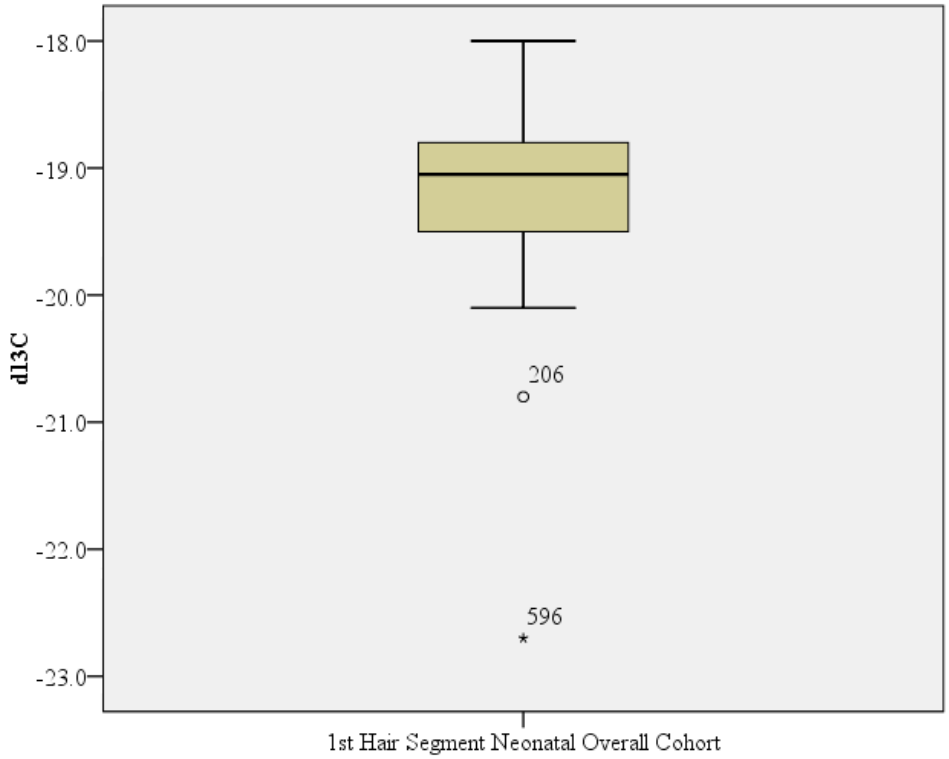

Figure 26: Box and whisker plot for $\delta^{13}C$ indicating the outliers for the neonatal overall first hair segment cohort.

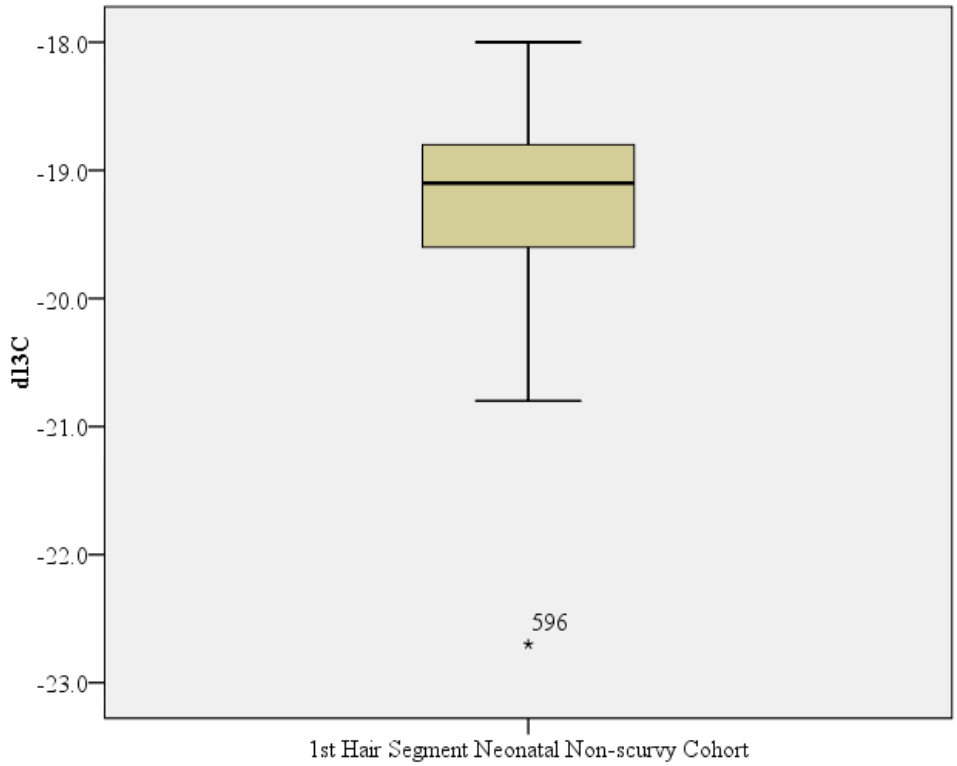

Figure 27: Box and whisker plot for $\delta^{13}C$ indicating the outlier for the neonatal non-scurvy first hair segment cohort.

The $\delta^{13}C$ values for the neonatal overall second hair segment ranged from -19.5‰ to -18.2‰, with a mean value of -19.0 ± 0.4‰. One outlier (burial 347) was present in this cohort with a more enriched $\delta^{13}C$ value (Figure 28). The $\delta^{13}C$ values for the scurvy cohort (n= 4) ranged from -19.2‰ to -18.2‰, with a mean value of -18.8 ± 0.5‰. The $\delta^{13}C$ values for the non-scurvy cohort (n = 13) ranged from -19.5‰ to -18.5‰, with a mean value of -19.0 ± 0.3‰. There was no statistically significant difference between the mean scurvy and non-scurvy $\delta^{13}C$ values for the neonatal second hair segment samples (p = 0.567) (Appendix G). The scatter plot of all juveniles for the neonatal second hair segment can be found in Appendix H (Figure 95)

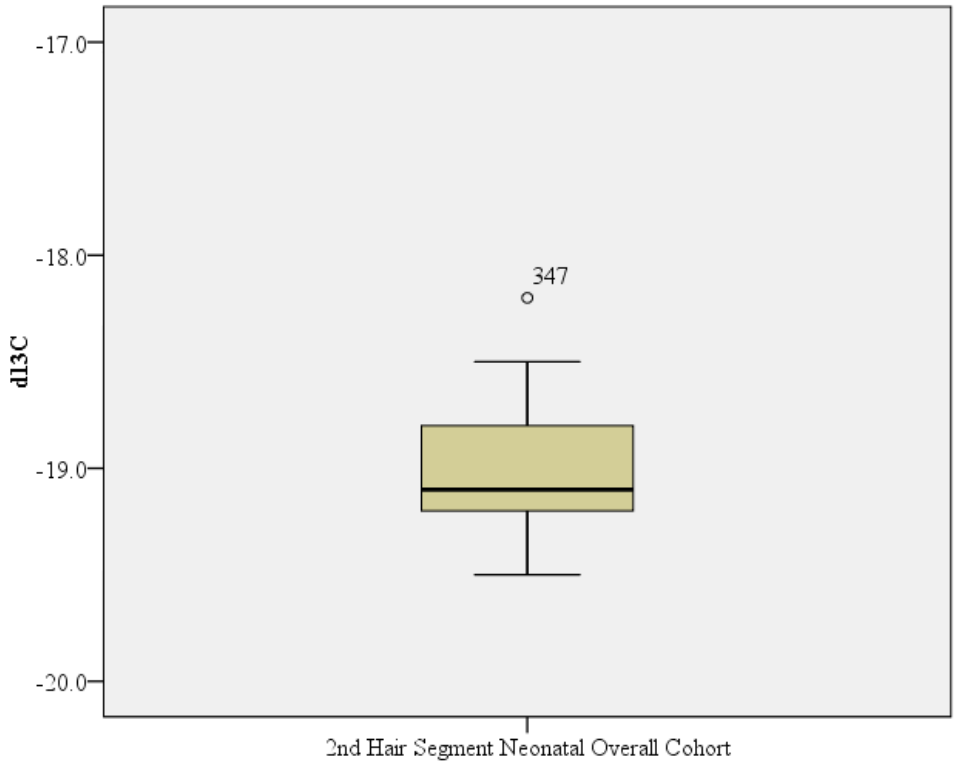

Figure 28: Box and whisker plot for $\delta^{13}C$ indicating the outlier for the neonatal overall second hair segment cohort.

The $\delta^{13}C$ values for the overall (non-scurvy) third hair segment (n = 6) ranged from -19.9‰ to -18.2‰, with a mean value of -19.2 ± 0.6‰. One outlier (burial 538) was present in this cohort with a more enriched $\delta^{13}C$ value (Figure 29). The scatter plot of all juveniles for the neonatal third hair segment can be found in Appendix H (Figure 95)

Figure 29: Box and whisker plot for $\delta^{13}C$ indicating the outlier for the neonatal non-scurvy third hair segment cohort.

The neonatal cohort for each hair segment was also averaged in order to show trends in $\delta^{13}C$ values for this cohort over the last three months of life. The scurvy cohort shows a slight decrease in $\delta^{13}C$ values in the last two months of life, while the non-scurvy cohort shows a slight increase in $\delta^{13}C$ values between the third and second months and a decrease from the second to the last month of life. (Figure 30). The difference between the scurvy second and first hair segment was not statistically significant ($p = 0.567$). The difference between the non-scurvy third and second hair segment was not statistically significant ($p = .0290$). The difference between the non-scurvy second and first hair segment was not statistically significant ($p = 0.300$). The difference between the non-scurvy third and first hair segment was not statistically significant ($p = 0.657$).

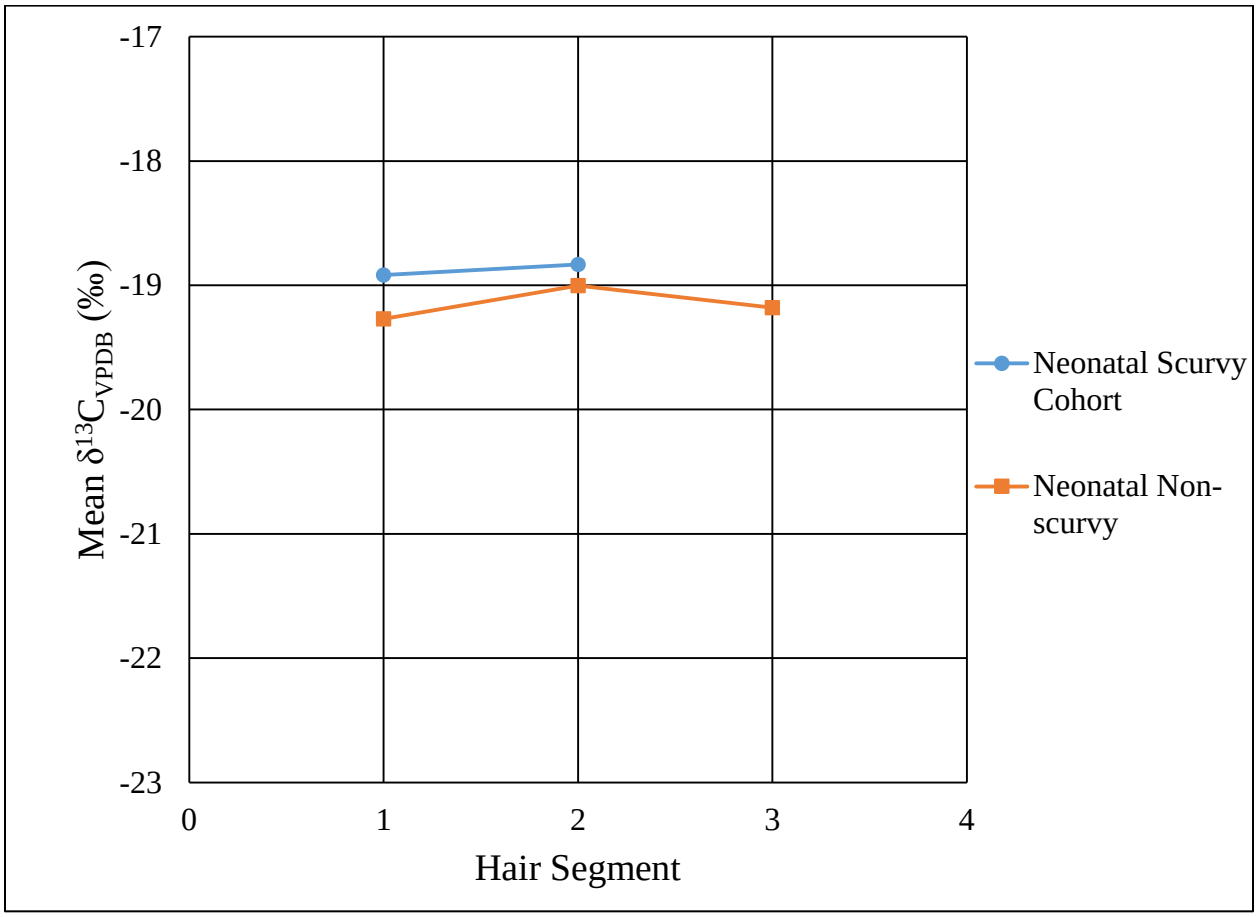

Figure 30: Averaged $\delta^{13}C$ values for each hair segment of the neonatal scurvy and non-scurvy cohorts showing trends in the last three months of life.

The C1 cohort first, second, and third hair segments were represented by 30, 23, and 15 scurvy and non-scurvy juveniles, respectively. The $\delta^{13}C$ values for the overall first hair segment ranged from -21.2‰ to -17.7‰, with a mean value of -19.3 ± 0.7‰. Four outliers were present in this cohort, two with more enriched $\delta^{13}C$ values (burials 330 and 487) and two with less enriched $\delta^{13}C$ values (burials 23 and 619) (Figure 31). The $\delta^{13}C$ values for the scurvy cohort (n = 7) ranged from -19.7‰ to -18.8‰, with a mean value of -19.3 ± 0.4‰. The $\delta^{13}C$ values for the non-scurvy cohort (n = 23) ranged from -21.2‰ to -17.7‰, with a mean value of -19.3 ± 0.8‰.

Two outliers were present, one with a more enriched $\delta^{13}C$ value (burial 487) and one with a less enriched $\delta^{13}C$ values (burial 23) (Figure 32). There was no statistically significant difference between the mean scurvy and non-scurvy $\delta^{13}C$ values for the C1 first hair segment samples ($p = 0.980$) (Appendix G). The scatter plot of all juveniles for the C1 first hair segment can be found in Appendix H (Figure 96).

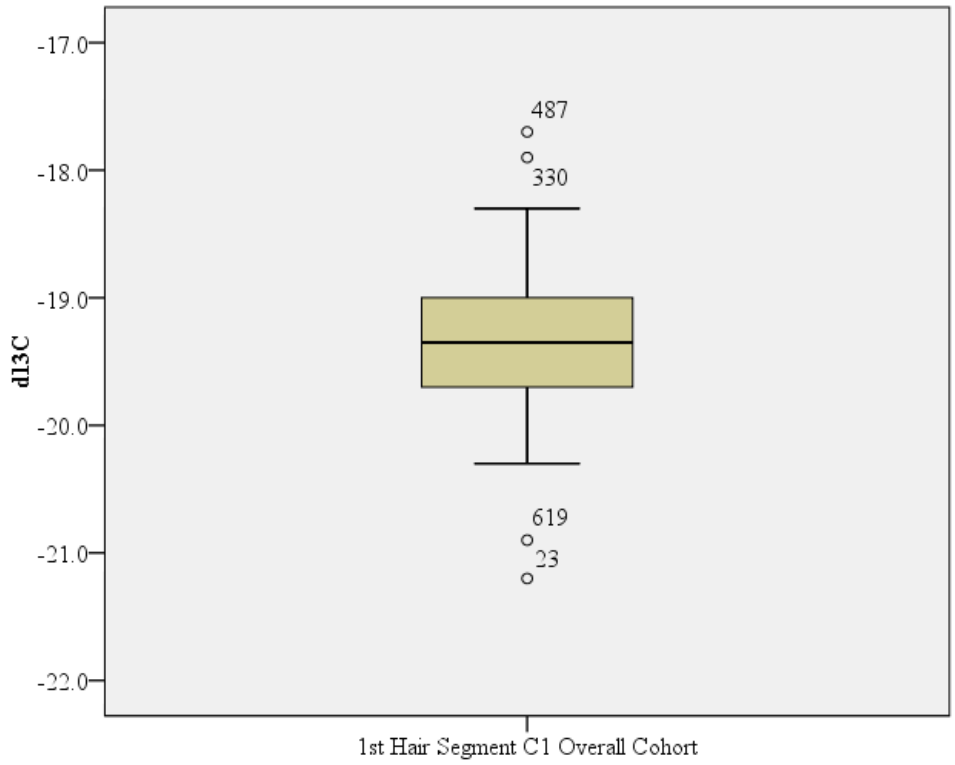

Figure 31: Box and whisker plot for $\delta^{13}C$ indicating the outliers for the C1 overall first hair segment cohort.

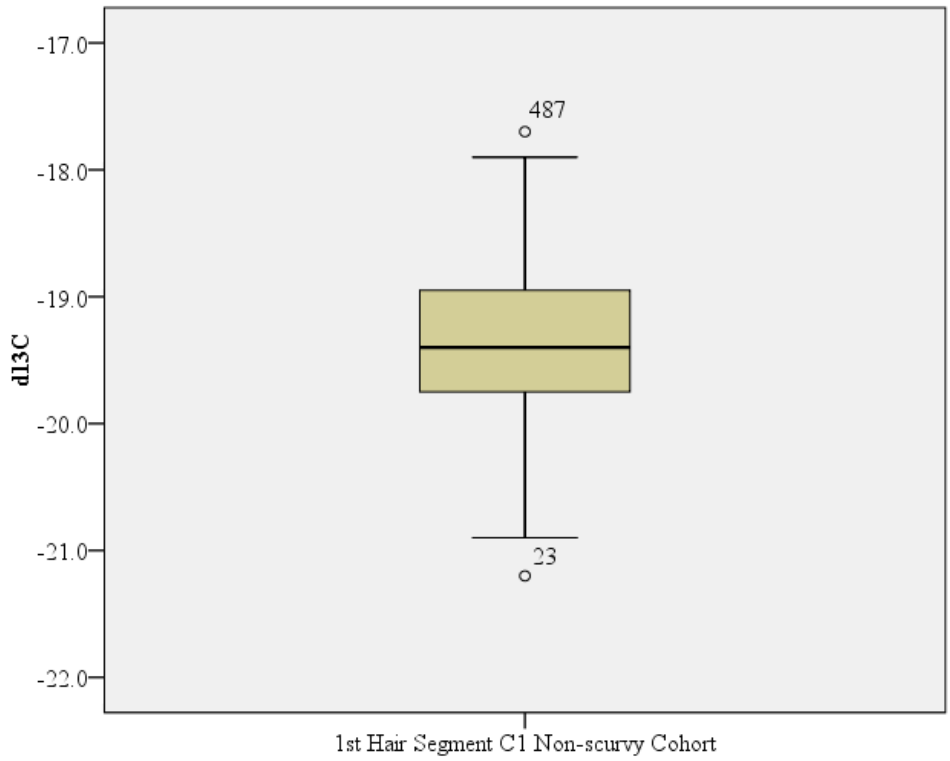

Figure 32: Box and whisker plot for $\delta^{13}C$ indicating the outliers for the C1 non-scurvy first hair segment cohort.

The $\delta^{13}C$ values for the overall second hair segment ranged from -20.5‰ to -18.1‰, with a mean value of -19.3 ± 0.6‰. The $\delta^{13}C$ values for the scurvy cohort (n = 5) ranged from -20.5‰ to -18.9‰, with a mean value of -19.5 ± 0.6‰. The $\delta^{13}C$ values for the non-scurvy cohort (n = 18) ranged from -20.4‰ to -18.1‰, with a mean value of -19.3 ± 0.6‰. Two outliers (burials 71 and 487) were present in this cohort, both with more enriched $\delta^{13}C$ values (Figure 33). There was no statistically significant difference between the mean scurvy and non-scurvy $\delta^{13}C$ values for the C1 second hair segment samples (p = 0.709) (Appendix G). The scatter plot of all juveniles for the C1 second hair segment can be found in Appendix H (Figure 96).

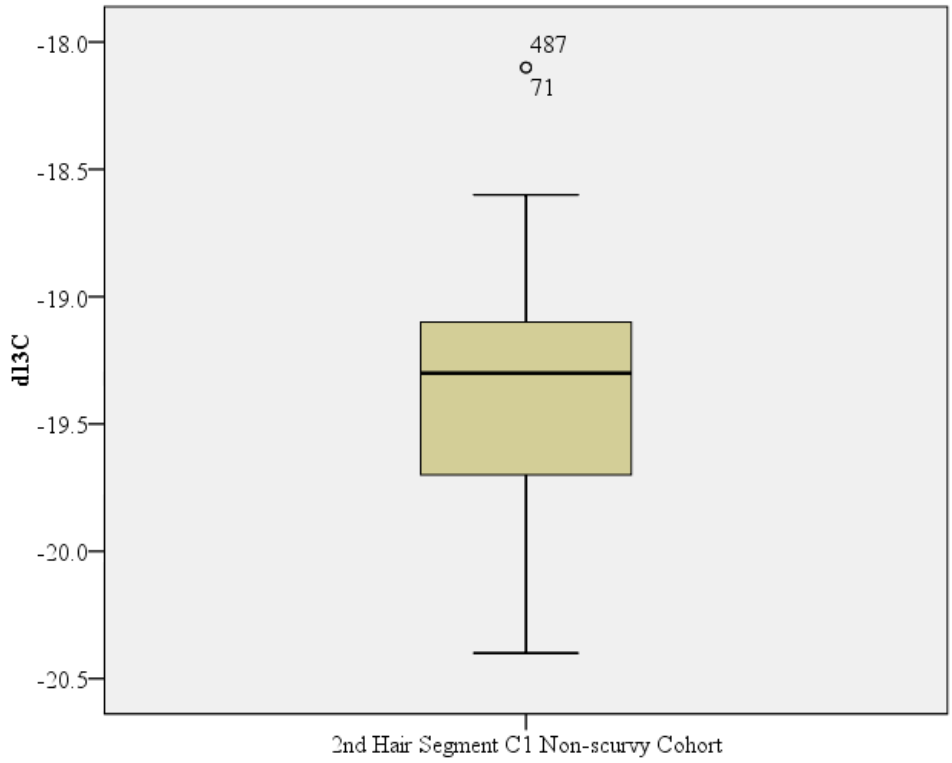

Figure 33: Box and whisker plot for $\delta^{13}C$ indicating the outliers for the C1 non-scurvy second hair segment cohort.

The $\delta^{13}C$ values for the overall third hair segment ranged from -21.2‰ to -17.9‰, with a mean value of -19.5 ± 0.8‰. The $\delta^{13}C$ values for the scurvy cohort (n = 3) ranged from -21.2‰ to -18.7‰, with a mean value of -19.7 ± 1.3‰. The $\delta^{13}C$ values for the non-scurvy cohort (n = 12) ranged from -20.4‰ to -17.9‰, with a mean value of -19.4 ± 0.7‰. There was no statistically significant difference between the mean scurvy and non-scurvy $\delta^{13}C$ values for the C1 third hair segment samples (p=0.942) (Appendix G). The scatter plot of all juveniles for the C1 third hair segment can be found in Appendix H (Figure96).

The C1 cohort for each hair segment was also averaged in order in order to show trends in $\delta^{13}C$ values for this cohort over the last three months of life. The scurvy cohort shows a slight increase in $\delta^{13}C$ over the last three months of life, while the non-scurvy cohort shows a very

slight increase in $\delta^{13}C$ values between the third and second months and no change from the second to the last month of life (Figure34). The difference between the scurvy third and first hair segments was not statistically significant ($p = 0.817$). The difference between the non-scurvy third and first hair segments was not statistically significant ($p = 0.577$).

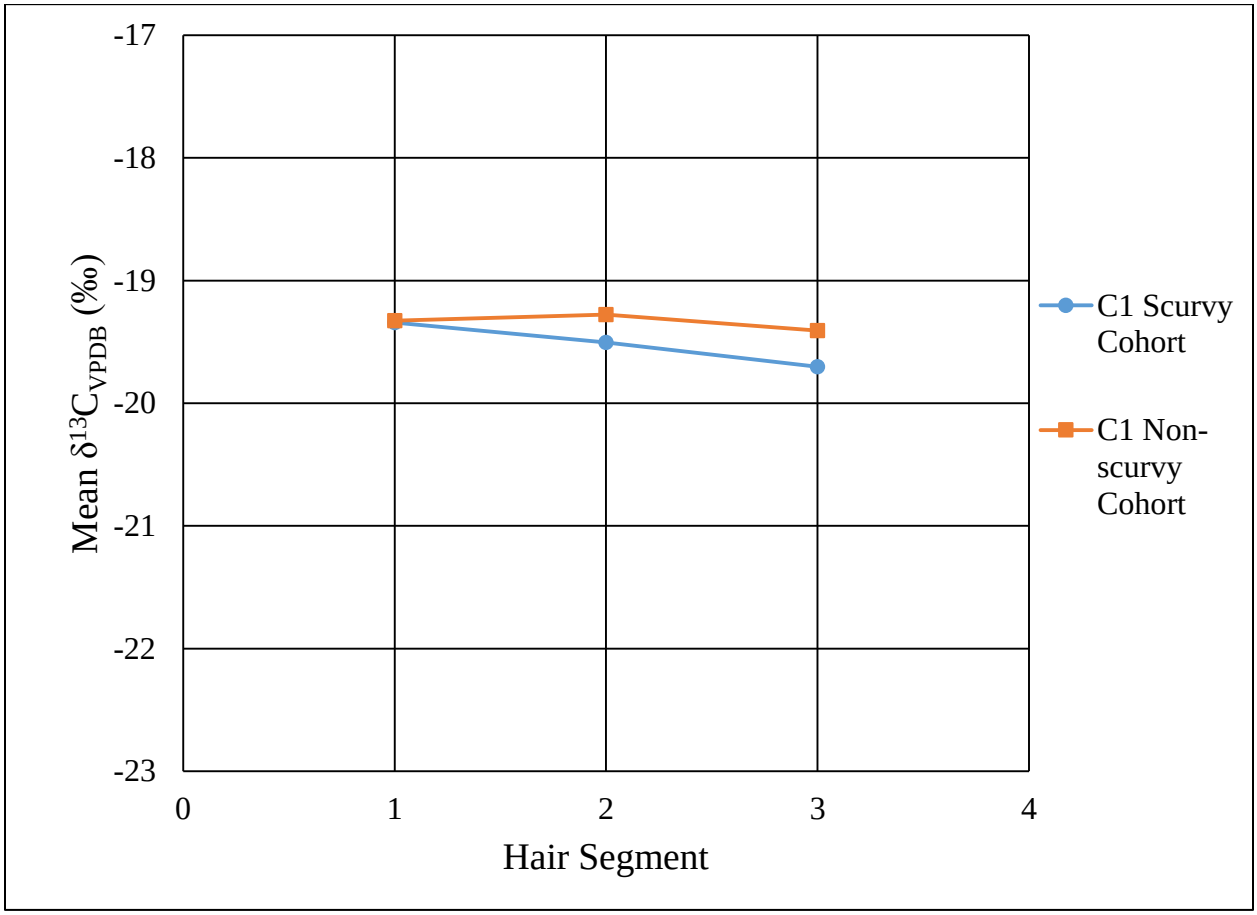

Figure 34: Averaged $\delta^{13}C$ values for each hair segment of the C1 scurvy and non-scurvy cohorts showing trends in the last three months of life.

The C2 cohort first, second, and third hair segments were represented by 15, ten, and eight scurvy and non-scurvy juveniles, respectively. The $\delta^{13}C$ values for the overall first hair segment ranged from -20.2‰ to -19.2‰, with a mean value of -19.7 ± 0.3‰. One outlier with a

more enriched $\delta^{13}C$ value (burial 374) was present in this cohort (Figure 35). The $\delta^{13}C$ values for the scurvy cohort (n = 4) ranged from -20.2‰ to -19.6‰, with a mean value of -19.9 ± 0.3‰. The $\delta^{13}C$ values for the non-scurvy cohort (n = 11) ranged from -20.2‰ to -19.2‰, with a mean value of -19.7 ± 0.3‰. Two outliers were present in this cohort, one with a more enriched $\delta^{13}C$ value (burial 374) and one with a less enriched $\delta^{13}C$ value (burial 163) (Figure 36). There was no statistically significant difference between the mean scurvy and non-scurvy $\delta^{13}C$ values for the C2 first hair segment samples (p = 0.290) (Appendix G). The scatter plot of all juveniles for the C2 first hair segment can be found in Appendix H (Figure 97).

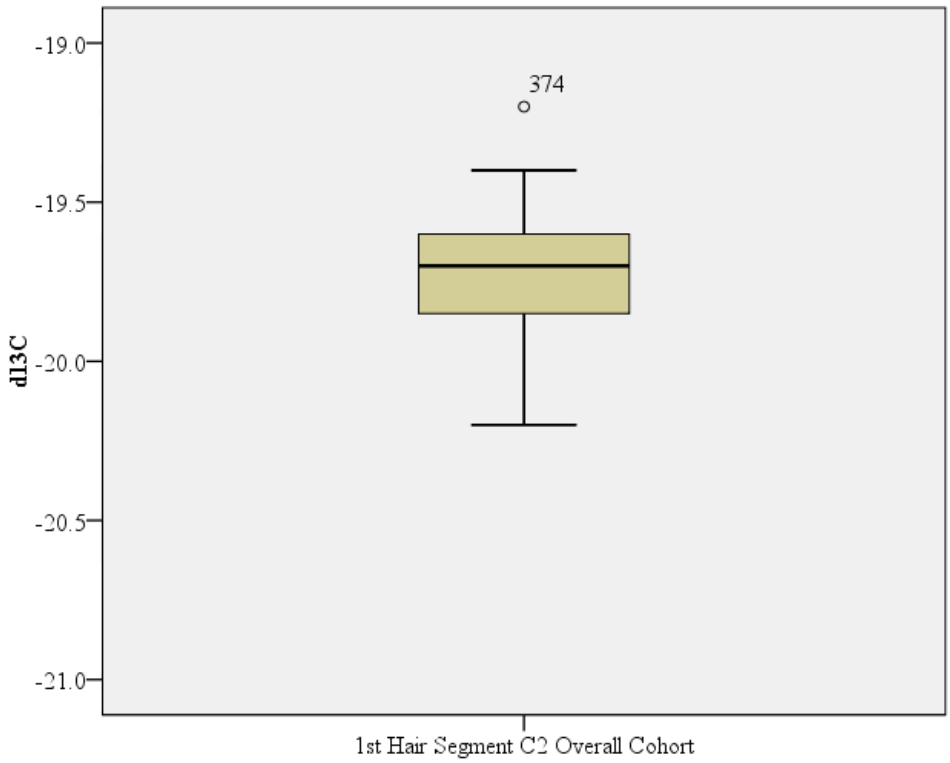

Figure 35: Box and whisker plot for $\delta^{13}C$ indicating the outlier for the C2 overall first hair segment cohort.

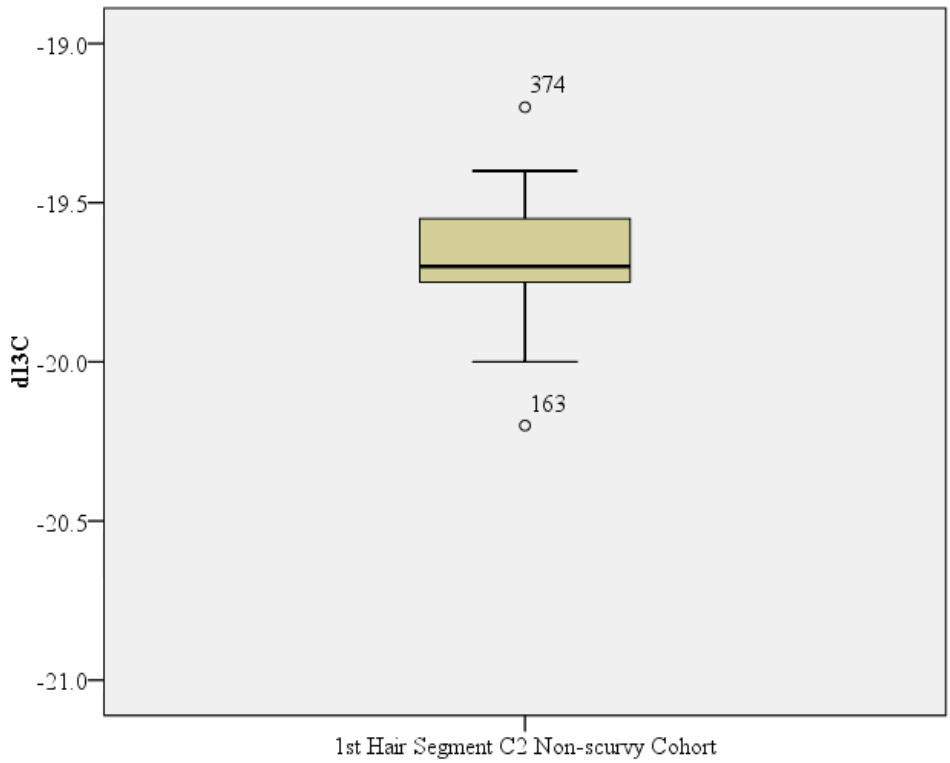

Figure 36: Box and whisker plot for $\delta^{13}C$ indicating the outliers for the C2 non-scurvy first hair segment cohort.

The $\delta^{13}C$ values for the overall second hair segment ranged from -20.4‰ to -19.1‰, with a mean value of -19.7 ± 0.4‰. The $\delta^{13}C$ values for the scurvy cohort (n = 3) ranged from -20.2‰ to -19.5‰, with a mean value of -19.9 ± 0.4‰. The $\delta^{13}C$ values for the non-scurvy cohort (n = 7) ranged from -20.4‰ to -19.1‰, with a mean value of -19.6 ± 0.4‰. One outlier with a less enriched $\delta^{13}C$ value (burial 584) was present in this subsample (Figure 37). There was no statistically significant difference between the mean scurvy and non-scurvy $\delta^{13}C$ values for the C2 second hair segment samples (p = 0.410) (Appendix G). The scatter plot of all juveniles for the C2 second hair segment can be found in Appendix H (Figure 97).

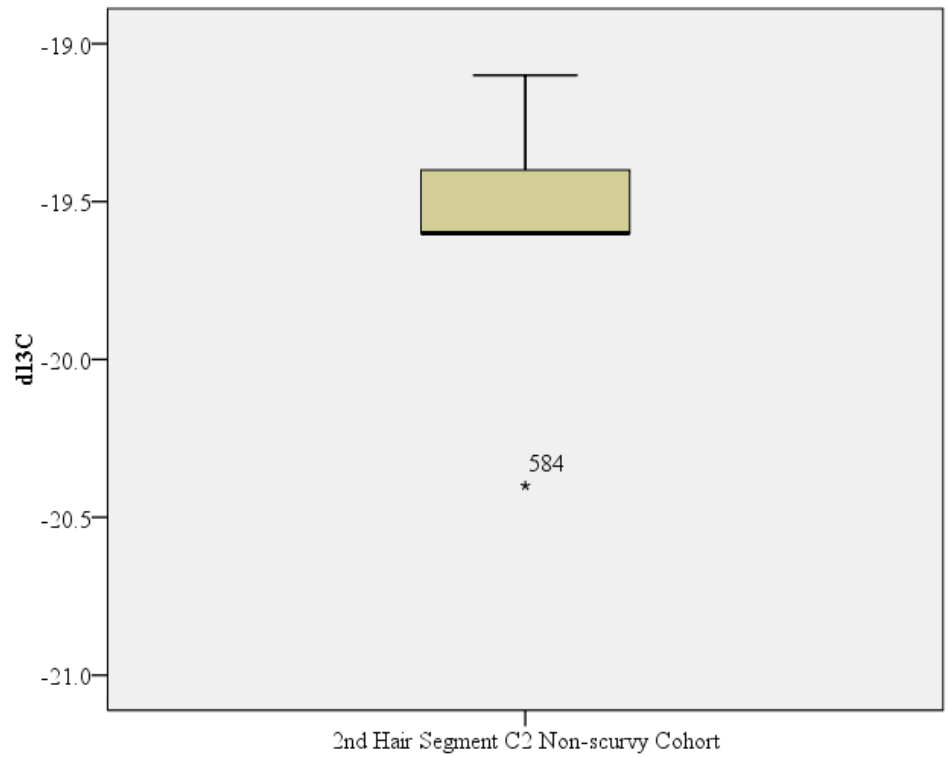

Figure 37: Box and whisker plot for $\delta^{13}C$ indicating the outlier for the C2 non-scurvy second hair segment cohort.

The $\delta^{13}C$ values for the overall third hair segment ranged from -20.4‰ to -19.0‰, with a mean value of -19.7 ± 0.5‰. The $\delta^{13}C$ values for the scurvy cohort (n = 3) ranged from -20.4‰ to -19.6‰, with a mean value of -20.0 ± 0.4‰. The $\delta^{13}C$ values for the non-scurvy cohort (n = 5) ranged from -20.2‰ to -19.0‰, with a mean value of -19.5 ± 0.5‰. There was no statistically significant difference between the mean scurvy and non-scurvy $\delta^{13}C$ values for the C2 third hair segment samples (p = 0.180) (Appendix G). The scatter plot of all juveniles for the C2 third hair segment can be found in Appendix H (Figure 97).

The C2 cohort for each hair segment was also averaged in order to show trends in $\delta^{13}C$ values for this cohort over the last three months of life. The scurvy cohort shows a slight increase in $\delta^{13}C$ values over the last three months of life, while the non-scurvy cohort shows a slight

decrease in $\delta^{13}C$ values over the last three months of life (Figure 38). The difference between the scurvy third and first hair segments was not statistically significant ($p = 0.593$). The difference between the non-scurvy third and first hair segments was not statistically significant ($p = 0.278$).

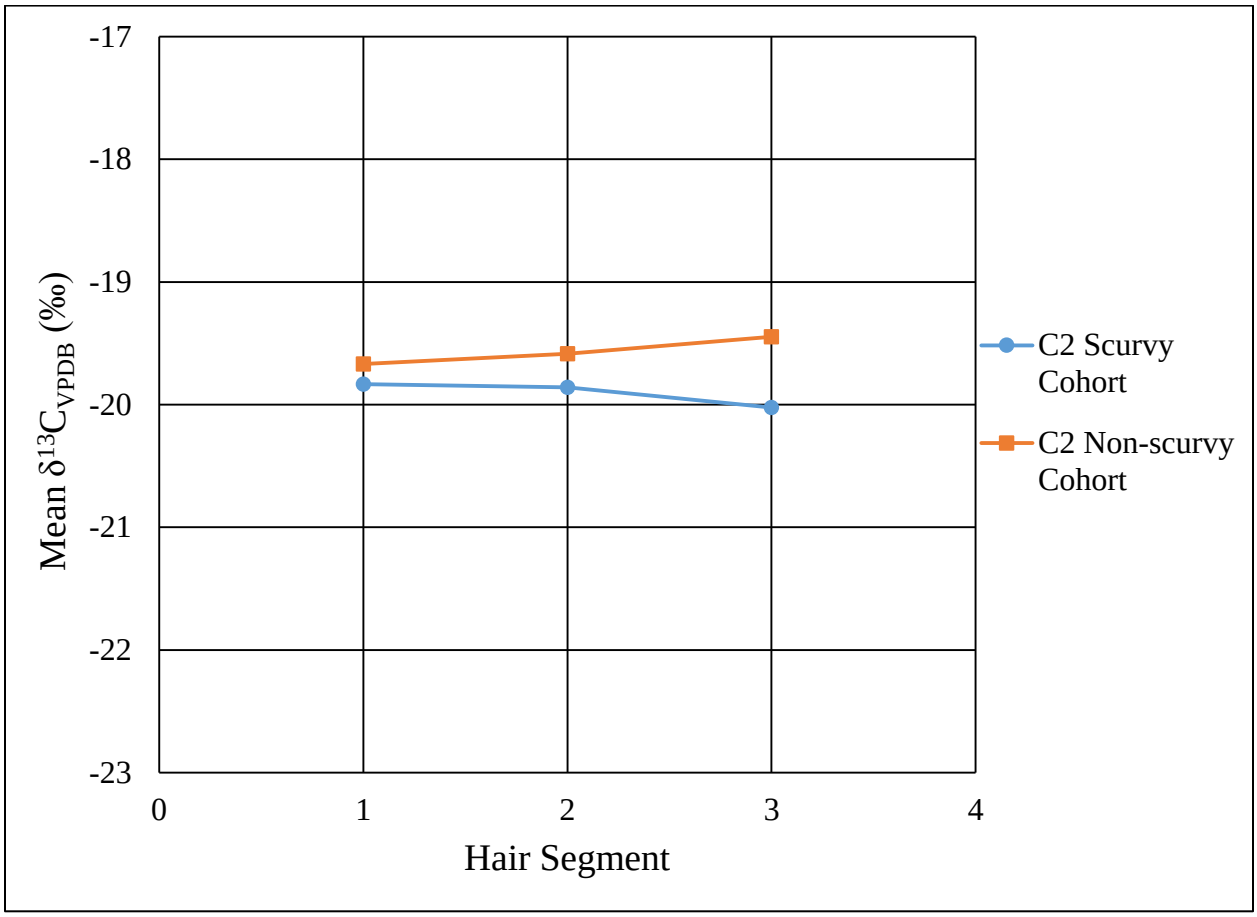

Figure 38: Averaged $\delta^{13}C$ values for each hair segment of the C2 scurvy and non-scurvy cohorts showing trends in the last three months of life.

The C3 cohort first, second, and third hair segments were represented by 11, nine, and eight scurvy and non-scurvy juveniles, respectively. The $\delta^{13}C$ values for the overall first hair segment ranged from -21.1‰ to -19.2‰, with a mean value of -19.8 ± 0.5‰. One outlier (burial 260) was present in this cohort with a less enriched $\delta^{13}C$ value (Figure 39). The $\delta^{13}C$ values for

the scurvy cohort (n = 3) ranged from -21.1‰ to -19.5‰, with a mean value of -20.3 ± 0.8‰. The $\delta^{13}C$ values for the non-scurvy cohort (n = 8) ranged from -20.1‰ to -19.2‰, with a mean value of -19.7 ± 0.3‰. There was no statistically significant difference between the mean scurvy and non-scurvy $\delta^{13}C$ values for the C3 first hair segment samples (p = 0.258) (Appendix G). The scatter plot of all juveniles for the C3 first hair segment can be found in Appendix H (Figure 98).

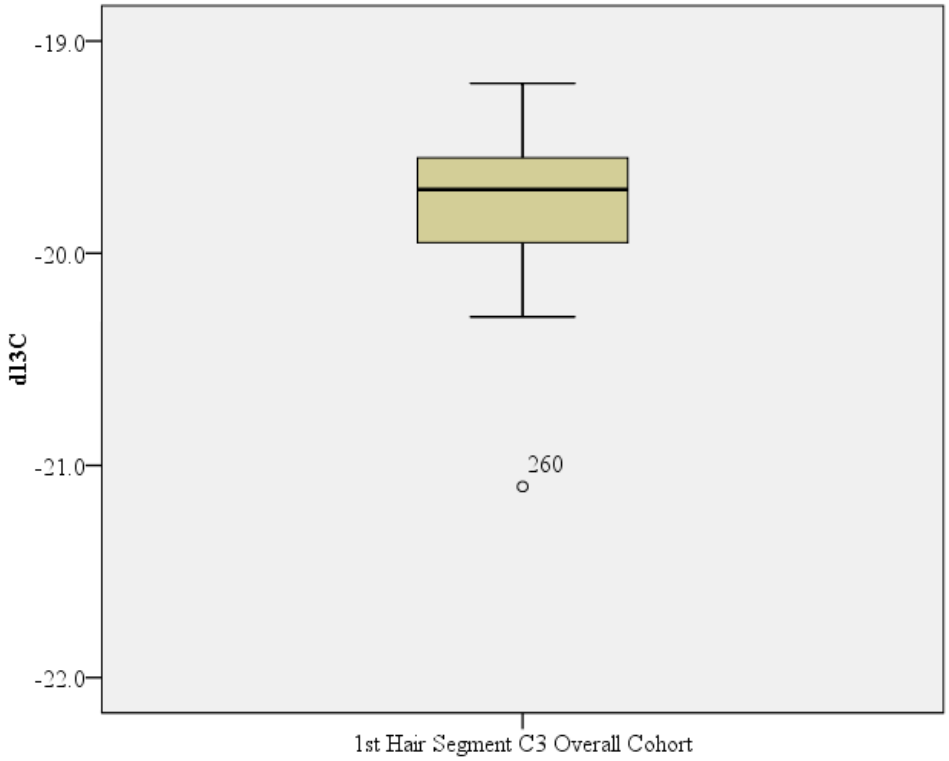

Figure 39: Box and whisker plot for $\delta^{13}C$ indicating the outlier for the C3 overall first hair segment cohort.

The $\delta^{13}C$ values for the overall second hair segment ranged from -20.4‰ to -19.3‰, with a mean value of -19.7 ± 0.4‰. The $\delta^{13}C$ values for the scurvy cohort (n = 3) ranged from -20.4‰ to -19.3‰, with a mean value of -19.9 ± 0.6‰. The $\delta^{13}C$ values for the non-scurvy cohort (n = 6) ranged from -20.2‰ to -19.3‰, with a mean value of -19.6 ± 0.4‰. There was no statistically

significant difference between the mean scurvy and non-scurvy $\delta^{13}C$ values for the C3 second hair segment samples ($p = 0.431$) (Appendix G). The scatter plot of all juveniles for the C3 second hair segment can be found in Appendix H (Figure 98).

The $\delta^{13}C$ values for the overall third hair segment ranged from -20.1‰ to -19.1‰, with a mean value of -19.6 ± 0.3‰. The $\delta^{13}C$ values for the scurvy cohort ($n = 2$) ranged from -20.1‰ to -19.3‰, with a mean value of -19.7 ± 0.6‰. The $\delta^{13}C$ values for the non-scurvy cohort ($n = 6$) ranged from -20.0‰ to -19.1‰, with a mean value of -19.6 ± 0.3‰. One outlier (burial 239) was present in this cohort with a more enriched $\delta^{13}C$ value (Figure 40). There was no statistically significant difference between the mean scurvy and non-scurvy $\delta^{13}C$ values for the C3 third hair segment samples ($p = 0.737$) (Appendix G). The scatter plot of all juveniles for the C3 third hair segment can be found in Appendix H (Figure 98).

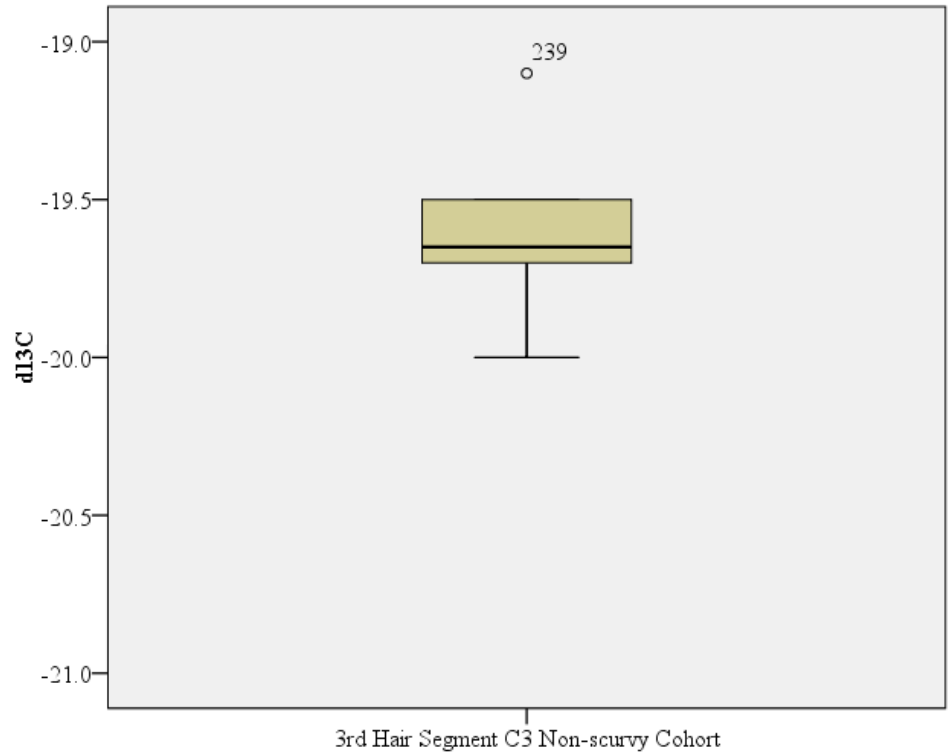

Figure 40: Box and whisker plot for $\delta^{13}C$ indicating the outlier for the C3 non-scurvy third hair segment cohort.

The C3 cohort for each hair segment was also averaged in order to show trends in $\delta^{13}C$ values for this cohort over the last three months of life. The scurvy cohort shows a slight decrease in $\delta^{13}C$ values over the last three months of life, while the non-scurvy cohort $\delta^{13}C$ remained fairly constant over the last three months of life with only a 0.1‰ increase from the second to first hair segment (Figure 41). The difference between the scurvy third and first hair segments was not statistically significant ($p = 0.248$). The difference between the non-scurvy third and first hair segments was not statistically significant ($p = 0.513$).

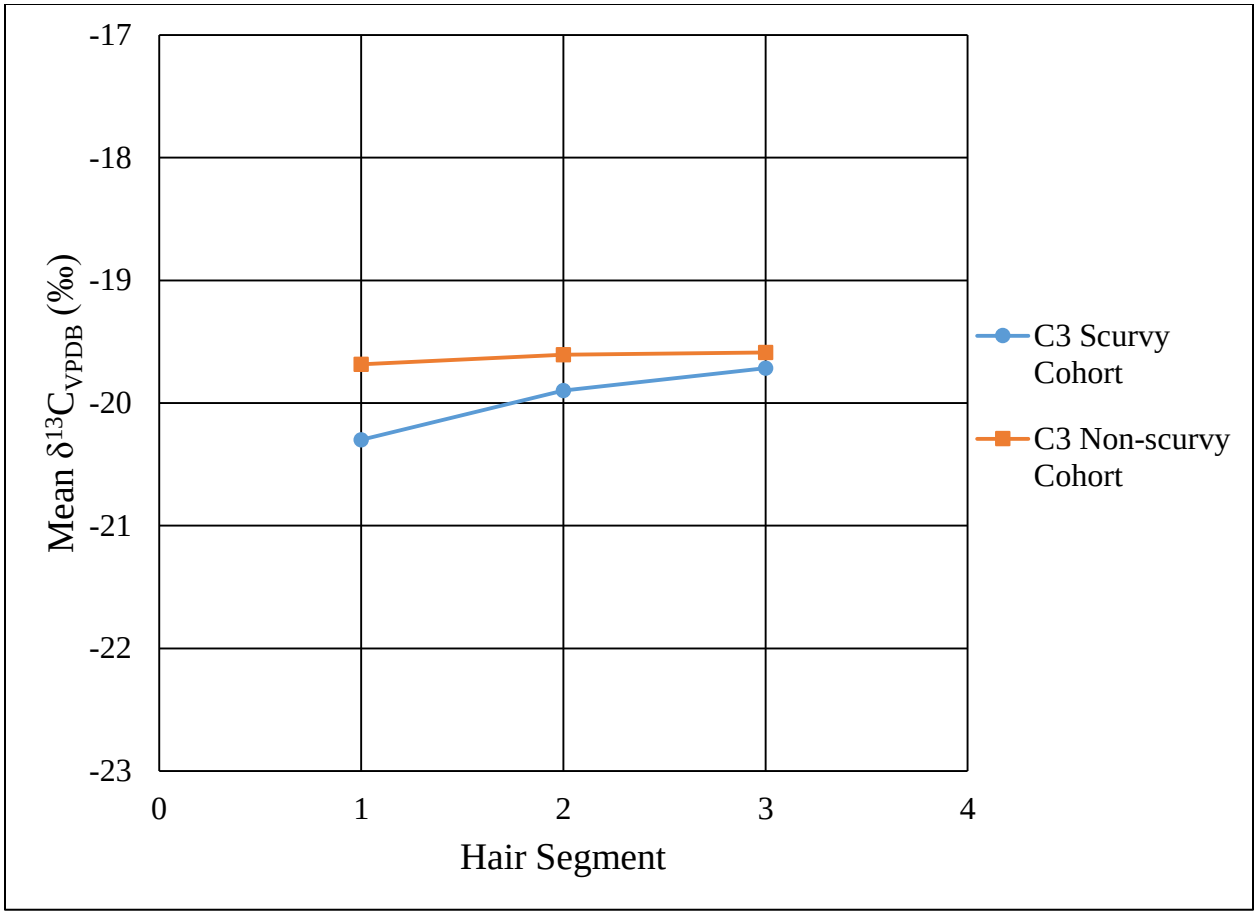

Figure 41: Averaged $\delta^{13}C$ values for each hair segment of the C3 scurvy and non-scurvy cohorts showing trends in the last three months of life.

Nail

A total of 54 individuals represented by proximal nail samples were analyzed for $\delta^{13}C$ values. Descriptive statistics (mean, minimum, maximum, and standard deviation) were calculated for the proximal nail segments. The descriptive statistics for $\delta^{13}C$ values from the nails can be found in Table 23. The $\delta^{13}C$ values for proximal nail segments can be found in Appendix E (Table 58).

Table 23: Descriptive statistics for $\delta^{13}C$ for proximal nail segments. Each category's statistics are first presented as an overall representation, followed by those individuals who exhibited skeletal indicators of scurvy and then those who did not. Entries of "-" indicate not enough data to calculate statistic.

		N	Mean	Min	Max	Standard Deviation
Entire Sample	**Overall**	54	-19.8	-22.5	-18.1	0.7
	Scurvy	10	-19.7	-20.7	-18.1	0.8
	Non-scurvy	44	-19.8	-22.5	-18.4	0.7
F&P	**Overall**	-	-	-	-	-
	Scurvy	-	-	-	-	-
	Non-scurvy	4	-19.5	-20.5	-18.7	0.7
Neo	**Overall**	18	-19.4	-20.4	-18.1	0.5
	Scurvy	3	-18.9	-19.5	-18.1	0.7
	Non-scurvy	15	-19.5	-20.4	-18.4	0.4
C1	**Overall**	18	-20.0	-22.5	-19.0	0.8
	Scurvy	4	-19.7	-19.9	-19.5	0.2
	Non-scurvy	14	-20.1	-22.5	-19.0	0.9
C2	**Overall**	10	-20.1	-20.7	-18.6	0.6
	Scurvy	2	-20.3	-20.7	-19.9	0.6
	Non-scurvy	8	-20.0	-20.6	-18.6	0.6
C3	**Overall**	4	-20.5	-20.8	-20.2	0.3
	Scurvy	1	-20.7	-	-	-
	Non-scurvy	3	-20.4	-20.8	-20.2	0.3

The $\delta^{13}C$ values for the proximal nail segment of the entire sample ranged from -22.5‰ to -18.1‰, with a mean value of -19.8 ± 0.7‰. The ten individuals who exhibited skeletal indicators of scurvy had $\delta^{13}C$ values that ranged from -20.7‰ to -18.1‰, with a mean value of -19.7 ± 0.8‰. The 44 individuals who did not exhibit skeletal indicators of scurvy had $\delta^{13}C$ values that ranged from -22.5‰ to -18.4‰, with a mean value of -19.8 ± 0.7‰. There was no statistically significant difference between the mean scurvy and non-scurvy $\delta^{13}C$ values for the

overall proximal nail segment samples (p=0.631) (Appendix F). The scatter plot of $\delta^{13}C$ and $\delta^{15}N$ values for the overall proximal nail segment cohort can be seen in Figure 42.

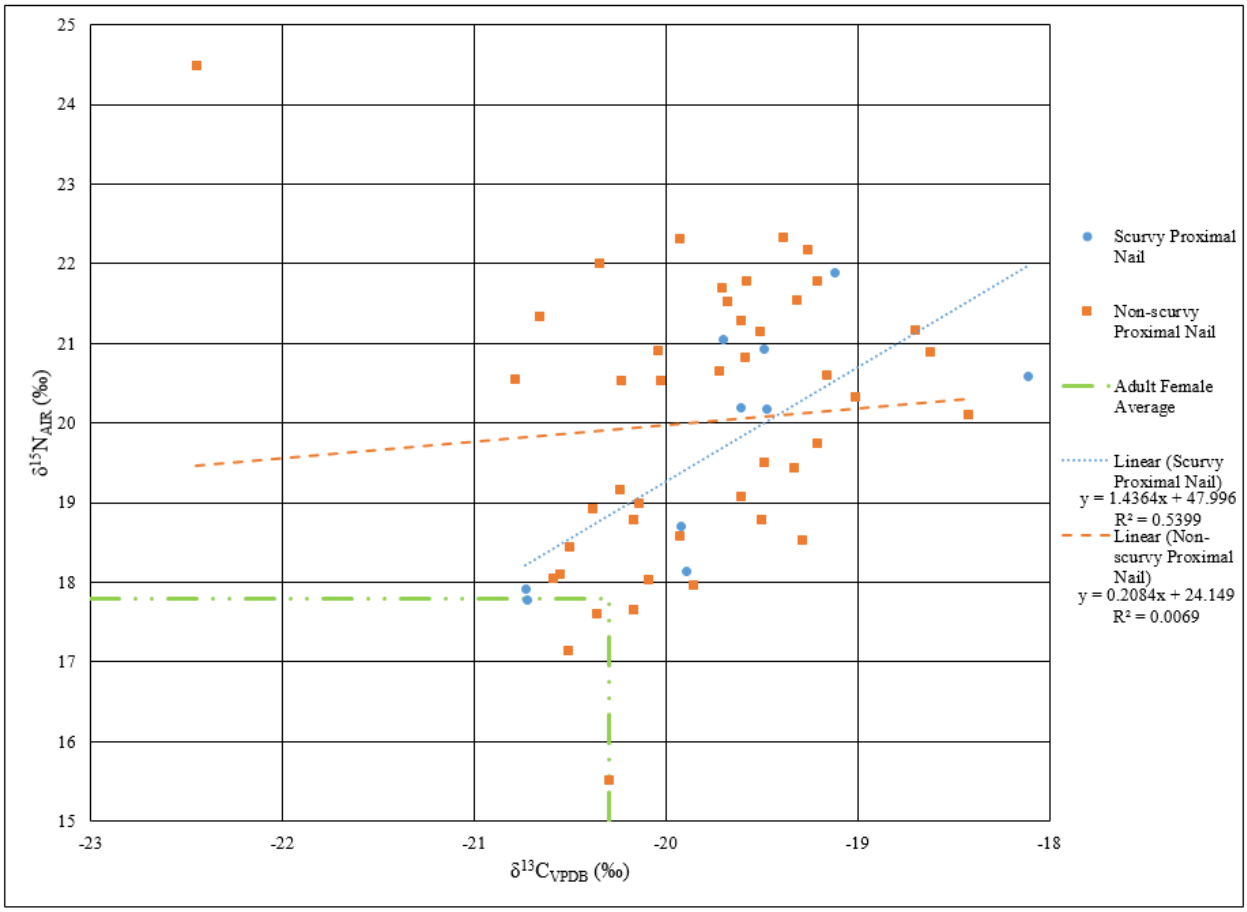

Figure 42: Scatter plot of $\delta^{13}C$ and $\delta^{15}N$ values for the overall proximal nail segment cohort.

When the $\delta^{13}C$ values for the proximal nail segment were plotted by age, a similar trend to other tissues can be seen. The younger ages exhibited a greater range in $\delta^{13}C$ values, with the range decreasing as age increases (Figure 43).

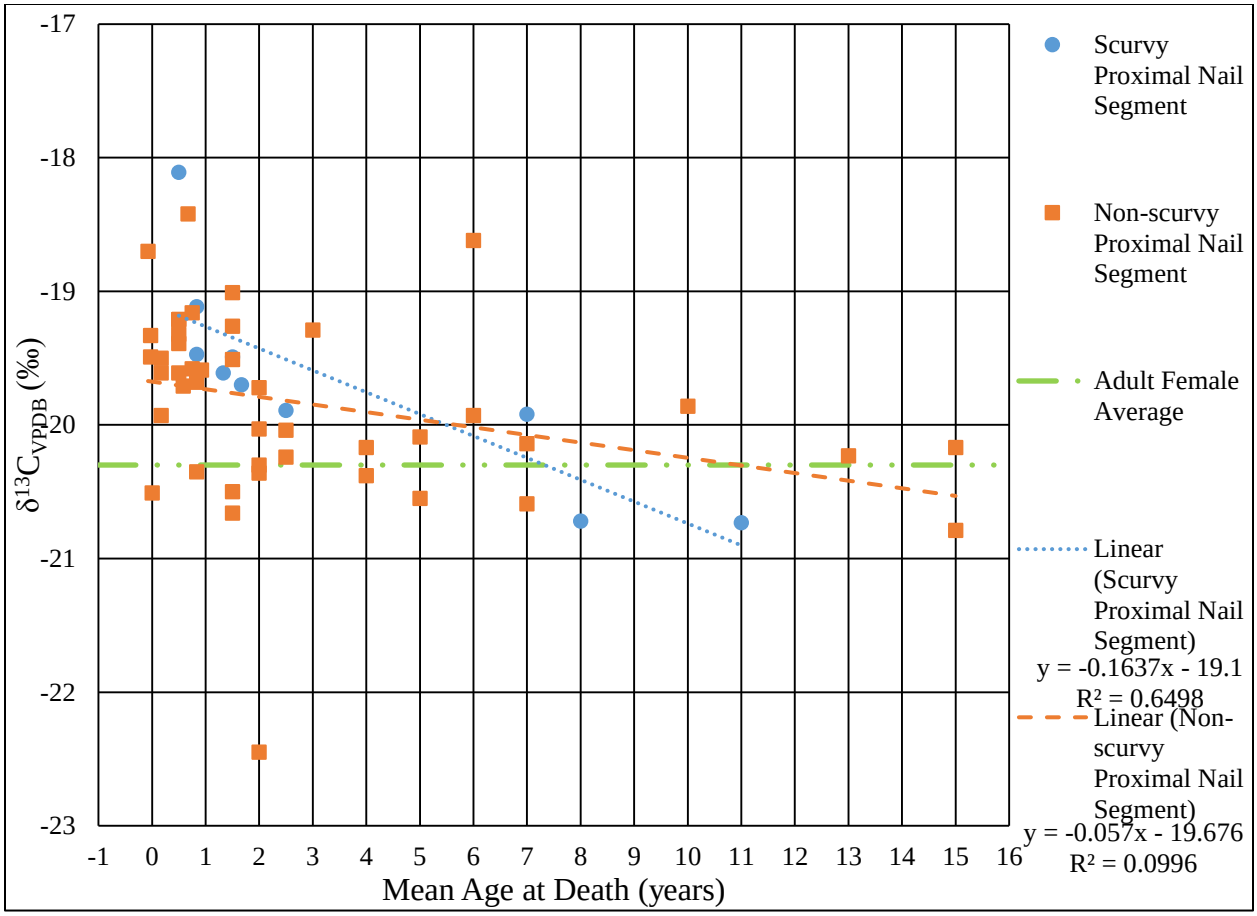

Figure 43: Proximal nail segment average $\delta^{13}C$ values plotted by mean age.

The F&P cohort represented by the proximal nail segment consisted of four individuals, none of which exhibited skeletal indicators of scurvy. The $\delta^{13}C$ for F&P cohort ranged from -20.5‰ to -18.7‰, with a mean value of -19.5 ± 0.7‰. The scatter plot of $\delta^{13}C$ and $\delta^{15}N$ values for the F&P proximal nail segment cohort can be seen in Figure 44. The neonatal cohort represented by the proximal nail segment consisted of 18 individuals, three who exhibited skeletal indicators of scurvy and 15 who did not. The $\delta^{13}C$ for the neonatal cohort ranged from -20.4‰ to -18.1‰, with a mean value of -19.4 ± 0.5‰. The $\delta^{13}C$ values for those neonatal cohort individuals who exhibited skeletal indicators of scurvy ranged from -19.5‰ to -18.1‰, with a

mean value of -18.9 ± 0.7‰. The $\delta^{13}C$ values for those neonatal cohort individuals who did not present with skeletal indicators of scurvy ranged from -20.4‰ to -18.4‰, with a mean value of -19.5 ± 0.4‰. There was no statistically significant difference between the mean scurvy and non-scurvy $\delta^{13}C$ values for the neonatal proximal nail segment samples (p=0.073) (Appendix G). The scatter plot of $\delta^{13}C$ and $\delta^{15}N$ values for the neonatal proximal nail segment cohort can be seen in Figure 45

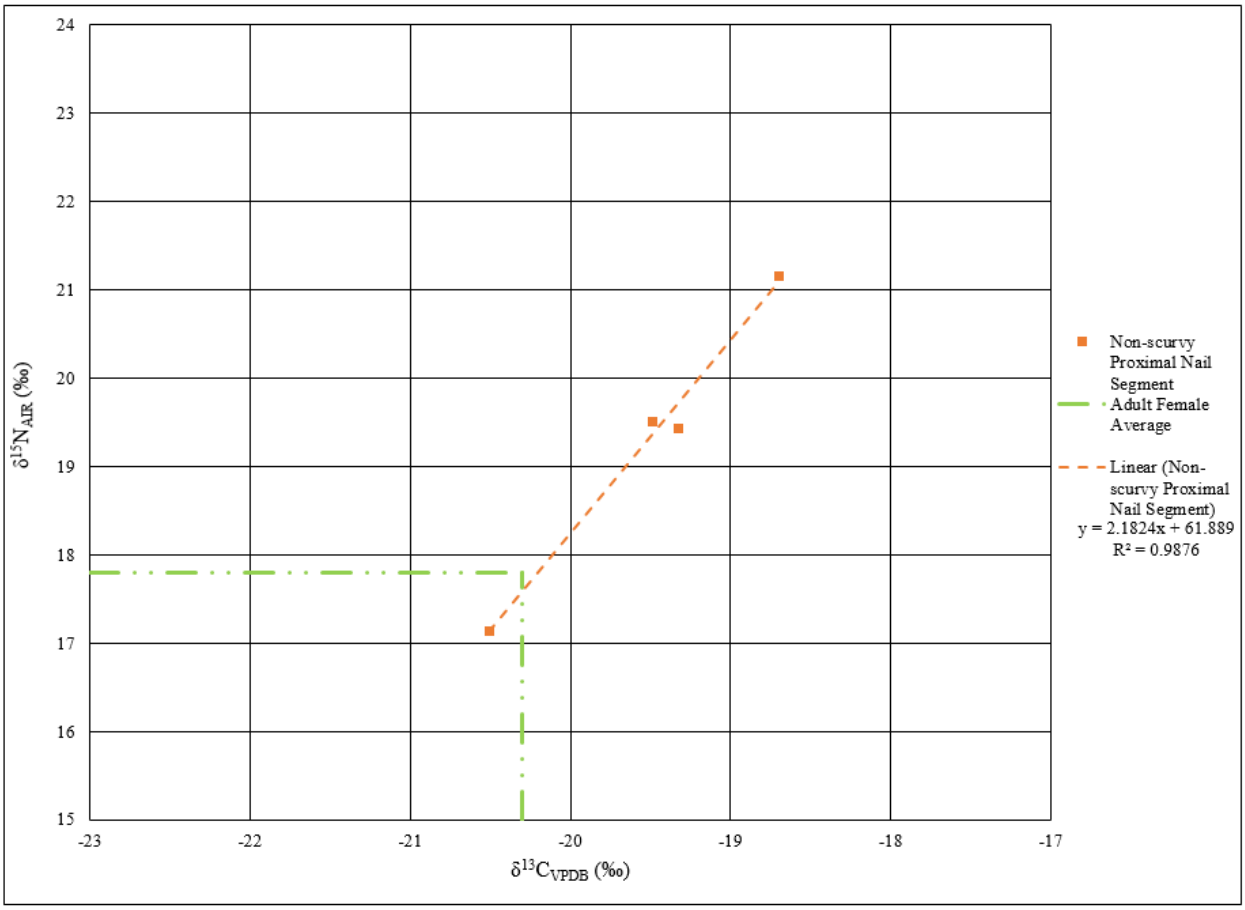

Figure 44: Scatter plot of $\delta^{13}C$ and $\delta^{15}N$ values for the F&P proximal nail segment cohort.

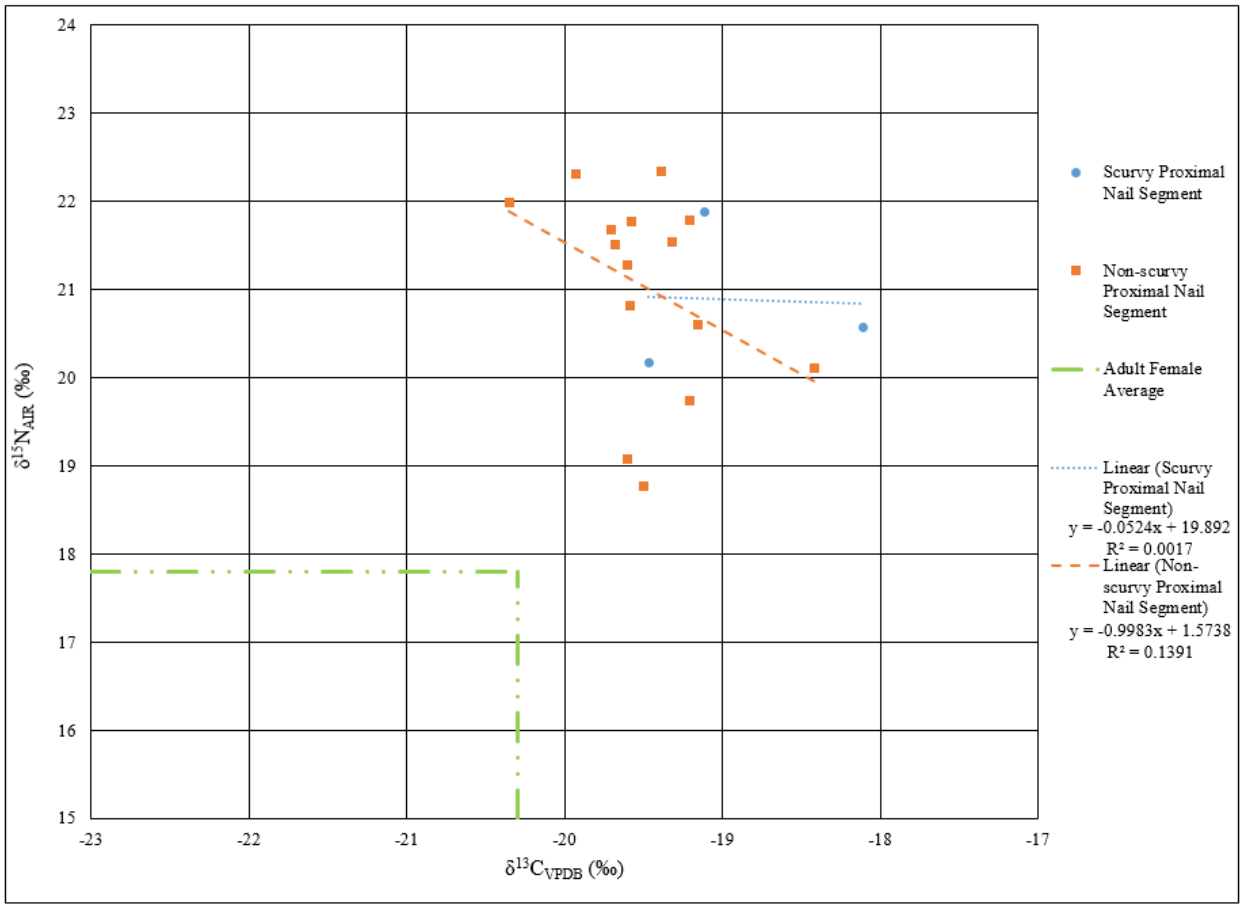

Figure 45: Scatter plot of $\delta^{13}C$ and $\delta^{15}N$ values for the neonatal proximal nail segment cohort.

The C1 cohort represented by the proximal nail segment consisted of 18 individuals, four who exhibited skeletal indicators of scurvy and 14 who did not. The $\delta^{13}C$ values for the entire C1 cohort ranged from -22.5‰ to -19.0‰, with a mean value of -20.0 ± 0.8‰. The $\delta^{13}C$ values for those C1 cohort individuals who exhibited skeletal indicators of scurvy ranged from -19.9‰ to -19.5‰, with a mean value of -19.7 ± 0.2‰. The $\delta^{13}C$ values for those C1 cohort individuals who did not present with skeletal indicators of scurvy ranged from -22.5‰ to -19.0‰, with a mean value of -20.1 ± 0.9‰. There was no statistically significant difference between the mean scurvy and non-scurvy $\delta^{13}C$ values for the C1 proximal nail segment samples (p=0.242)

(Appendix G). The scatter plot of $\delta^{13}C$ and $\delta^{15}N$ values for the C1 proximal nail segment cohort can be seen in Figure 46.

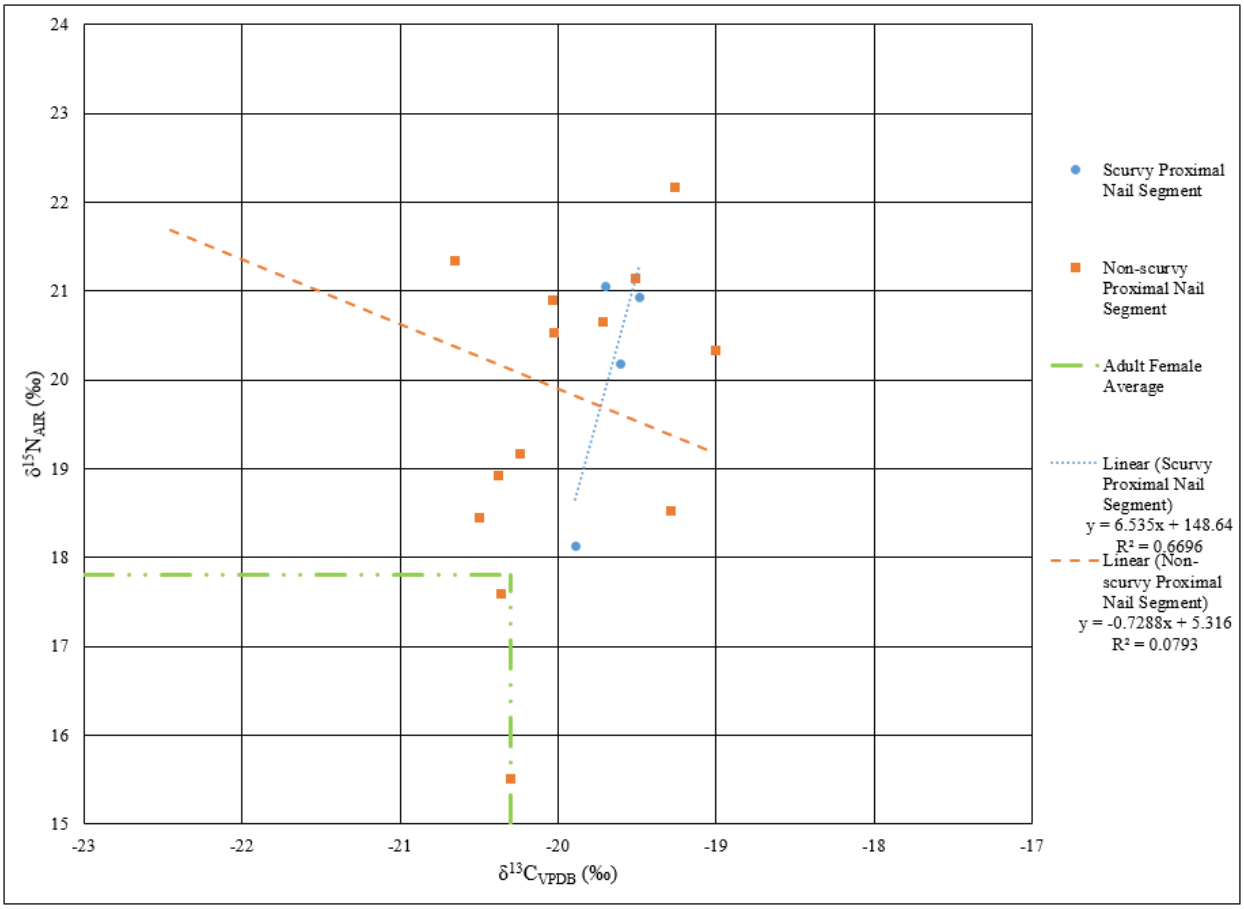

Figure 46: Scatter plot of $\delta^{13}C$ and $\delta^{15}N$ values for the C1 proximal nail segment cohort.

The C2 cohort represented by the proximal nail segment consisted of ten individuals, two who exhibited skeletal indicators of scurvy and eight who did not. The $\delta^{13}C$ values for the entire C2 cohort ranged from -20.7‰ to -18.6‰, with a mean value of -20.1 ± 0.6‰. The $\delta^{13}C$ values for those C2 cohort individuals who exhibited skeletal indicators of scurvy ranged from -20.7‰ to -19.9‰, with a mean value of -20.3 ± 0.6‰. The $\delta^{13}C$ values for those C2 cohort individuals who did not present with skeletal indicators of scurvy ranged from -20.6‰ to -18.6‰, with a

mean value of -20.0 ± 0.6‰. There was no statistically significant difference between the mean scurvy and non-scurvy $\delta^{13}C$ values for the C2 proximal nail segment samples (p=0.595) (Appendix G). The scatter plot of $\delta^{13}C$ and $\delta^{15}N$ values for the C2 proximal nail segment cohort can be seen in Figure 47.

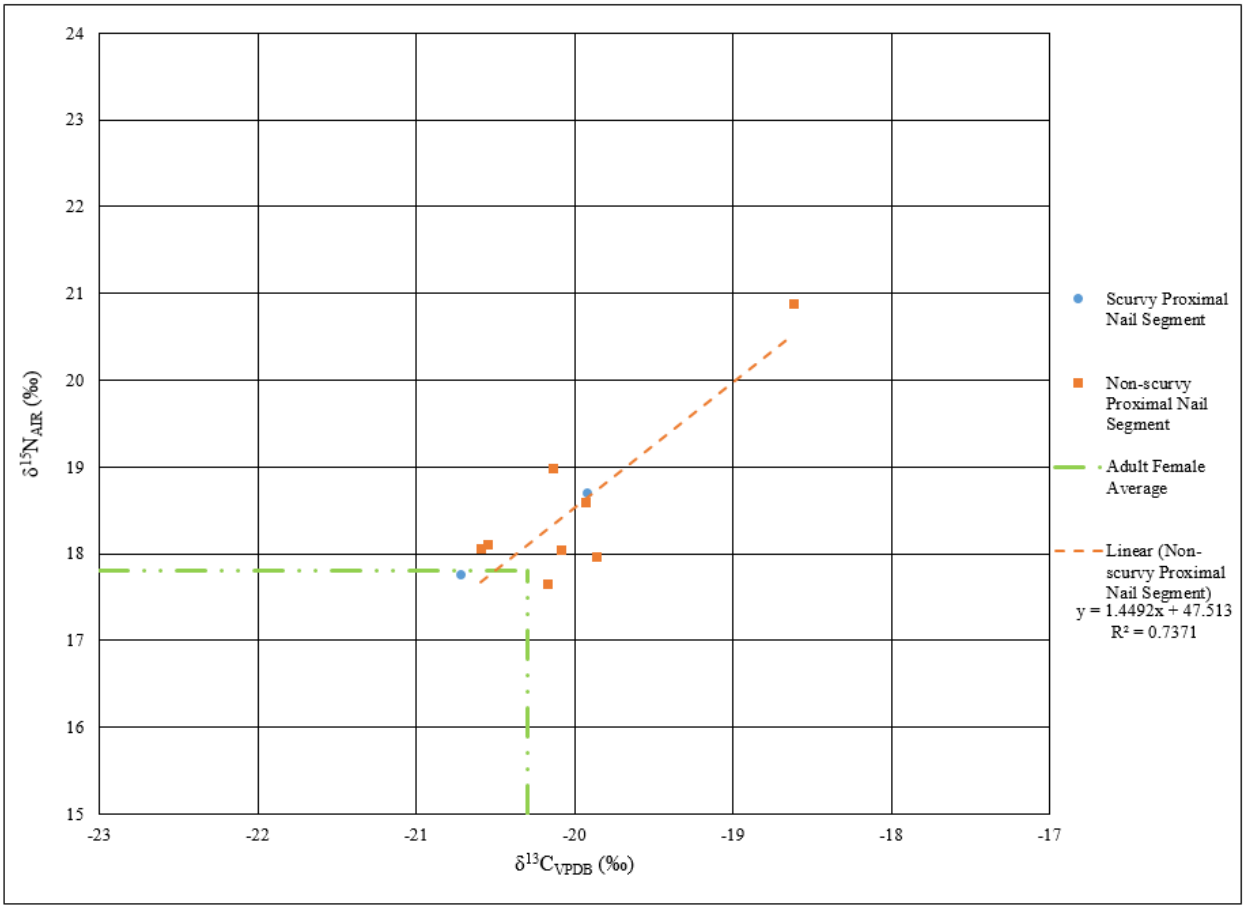

Figure 47: Scatter plot of $\delta^{13}C$ and $\delta^{15}N$ values for the C2 proximal nail segment cohort.

The C3 cohort represented by the proximal nail segment consisted of four individuals, one who exhibited skeletal indicators of scurvy and three who did not. The $\delta^{13}C$ values for the entire C3 cohort ranged from -20.8‰ to -20.2‰, with a mean value of -20.5 ± 0.3‰. The $\delta^{13}C$ values for the C3 cohort individual who exhibited skeletal indicators of scurvy was -20.7‰. The

$\delta^{13}C$ values for those C3 cohort individuals who did not present with skeletal indicators of scurvy ranged from -20.8‰ to -20.2‰, with a mean value of -20.4 ± 0.3‰. There was no statistically significant difference between the mean scurvy and non-scurvy $\delta^{13}C$ values for the C3 proximal nail segment samples (p=0.637) (Appendix G). The scatter plot of $\delta^{13}C$ and $\delta^{15}N$ values for the C3 proximal nail segment cohort can be seen in Figure 48.

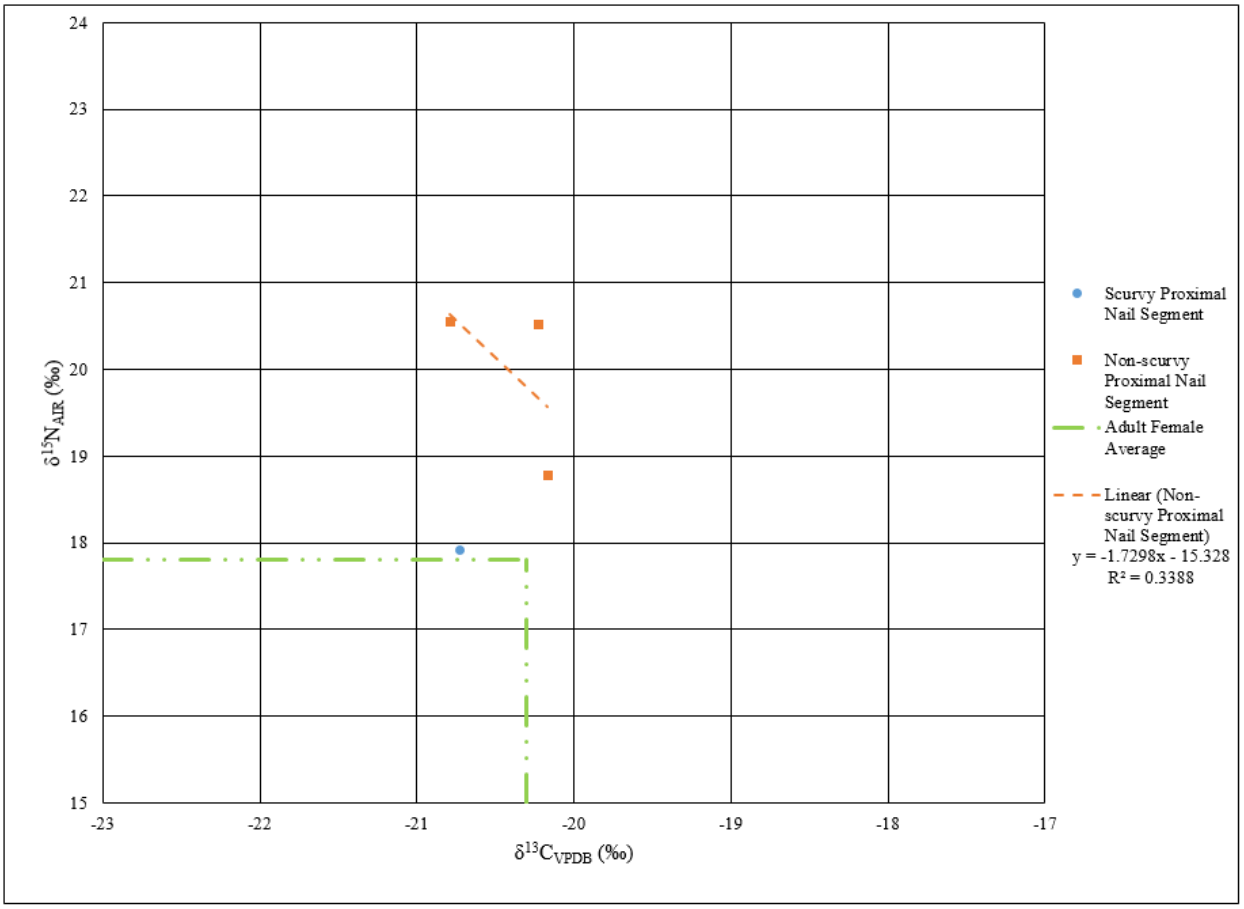

Figure 48: Scatter plot of $\delta^{13}C$ and $\delta^{15}N$ values for the C3 proximal nail segment cohort.

Skin

A total of 78 skin samples, each representing one individual, were analyzed for $\delta^{13}C$ values. All descriptive statistics (mean, minimum, maximum, and standard deviation) for $\delta^{13}C$ values from skin can be found in Table 24. The $\delta^{13}C$ values of skin for applicable individuals can be found in Appendix E (Table 59).

Table 24: Descriptive statistics for $\delta^{13}C$ for skin. Each category's statistics are first presented as an overall representation, followed by those individuals who exhibited skeletal indicators of scurvy and then those who did not. Entries of "-" indicate not enough data to calculate statistic.

		N	Mean	Min	Max	Standard Deviation
Entire Sample	**Overall**	78	-20.0	-22.7	-18.5	0.9
	Scurvy	19	-20.0	-22.2	-18.7	0.9
	Non-scurvy	59	-20.1	-22.7	-18.5	0.9
F&P	**Overall**	9	-20.6	-21.8	-19.6	0.7
	Scurvy	1	-19.6	-	-	-
	Non-scurvy	8	-20.7	-21.8	-20.0	0.6
Neo	**Overall**	28	-19.9	-22.7	-18.7	0.9
	Scurvy	5	-19.7	-20.9	-18.7	1.0
	Non-scurvy	23	-19.9	-22.7	-19.1	0.9
C1	**Overall**	22	-19.9	-21.7	-18.6	0.8
	Scurvy	6	-19.8	-21.7	-19.1	1.0
	Non-scurvy	16	-19.9	-20.9	-18.6	0.7
C2	**Overall**	11	-20.1	-22.4	-18.8	1.2
	Scurvy	4	-20.6	-22.2	-19.6	1.1
	Non-scurvy	7	-19.8	-22.4	-18.8	1.3
C3	**Overall**	8	-20.3	-22.0	-18.5	1.0
	Scurvy	3	-20.2	-20.6	-19.6	0.5
	Non-scurvy	5	-20.4	-22.0	-18.5	1.3

The $\delta^{13}C$ values for the overall skin sample ranged from -22.7‰ to -18.5‰, with a mean value of -20.0 ± 0.9‰. Of the 78 individuals whose skin was analyzed, a total of 19 individuals exhibited skeletal indicators of scurvy. The $\delta^{13}C$ values for this cohort ranged from -22.2‰ to -18.7‰, with a mean value of -20.0 ± 0.9‰. The remaining 59 individuals did not exhibit skeletal indicators of scurvy. The $\delta^{13}C$ values for this second cohort ranged from -22.7‰ to -18.5‰, with a mean value of -20.1 ± 0.9‰. There was no statistically significant difference between the mean scurvy and non-scurvy $\delta^{13}C$ values for the overall skin samples (p=0.744) (Appendix F). The scatter plot of $\delta^{13}C$ and $\delta^{15}N$ values for the overall skin sample can be seen in Figure 49.

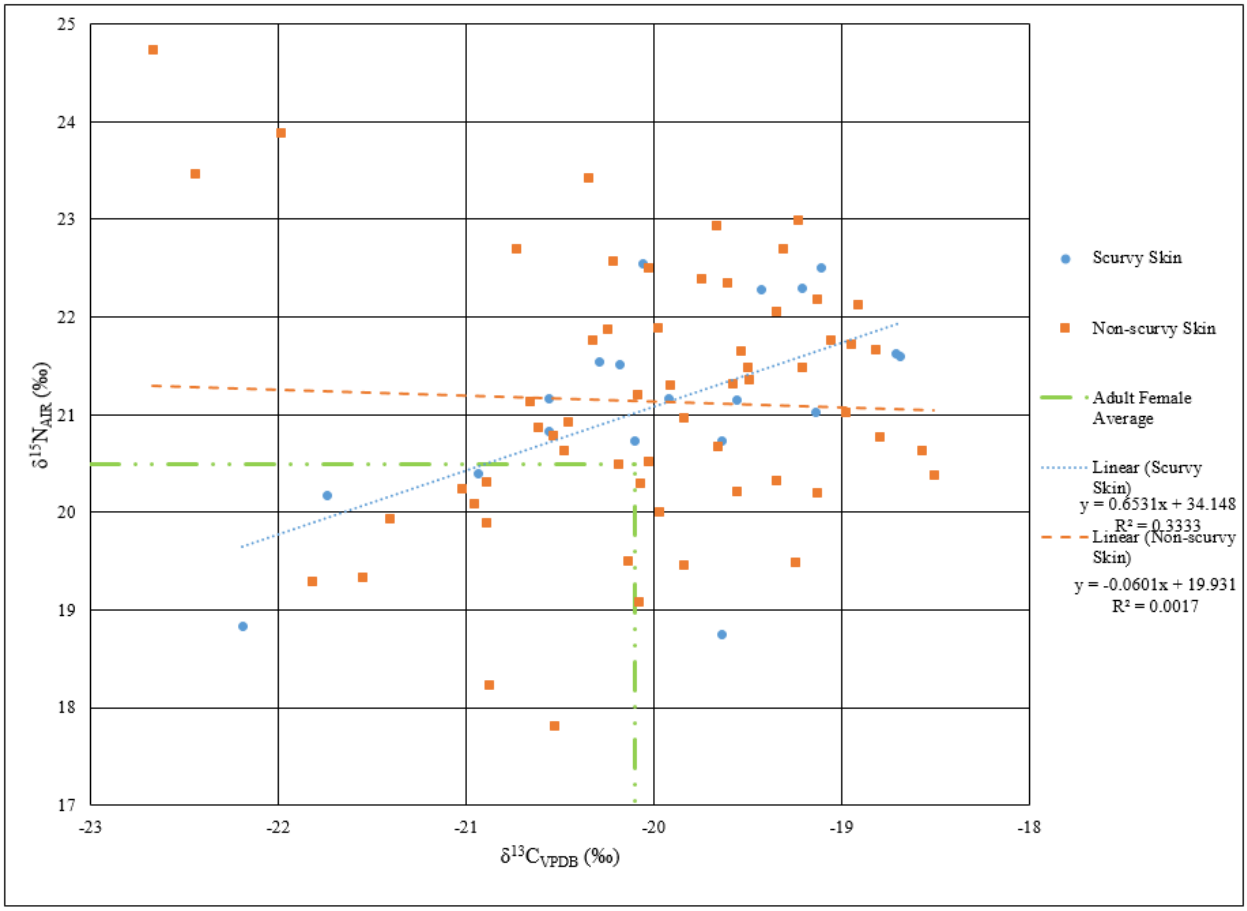

Figure 49: Scatter plot of $\delta^{13}C$ and $\delta^{15}N$ values for the overall skin cohort.

When the $\delta^{13}C$ values for skin were plotted by age, less adherence to any trend is seen (Figure 50). While the range of $\delta^{13}C$ values decreases as age increases, the individual $\delta^{13}C$ values are much more widely dispersed from both their respective scurvy and non-scurvy linear trend lines and the adult female average.

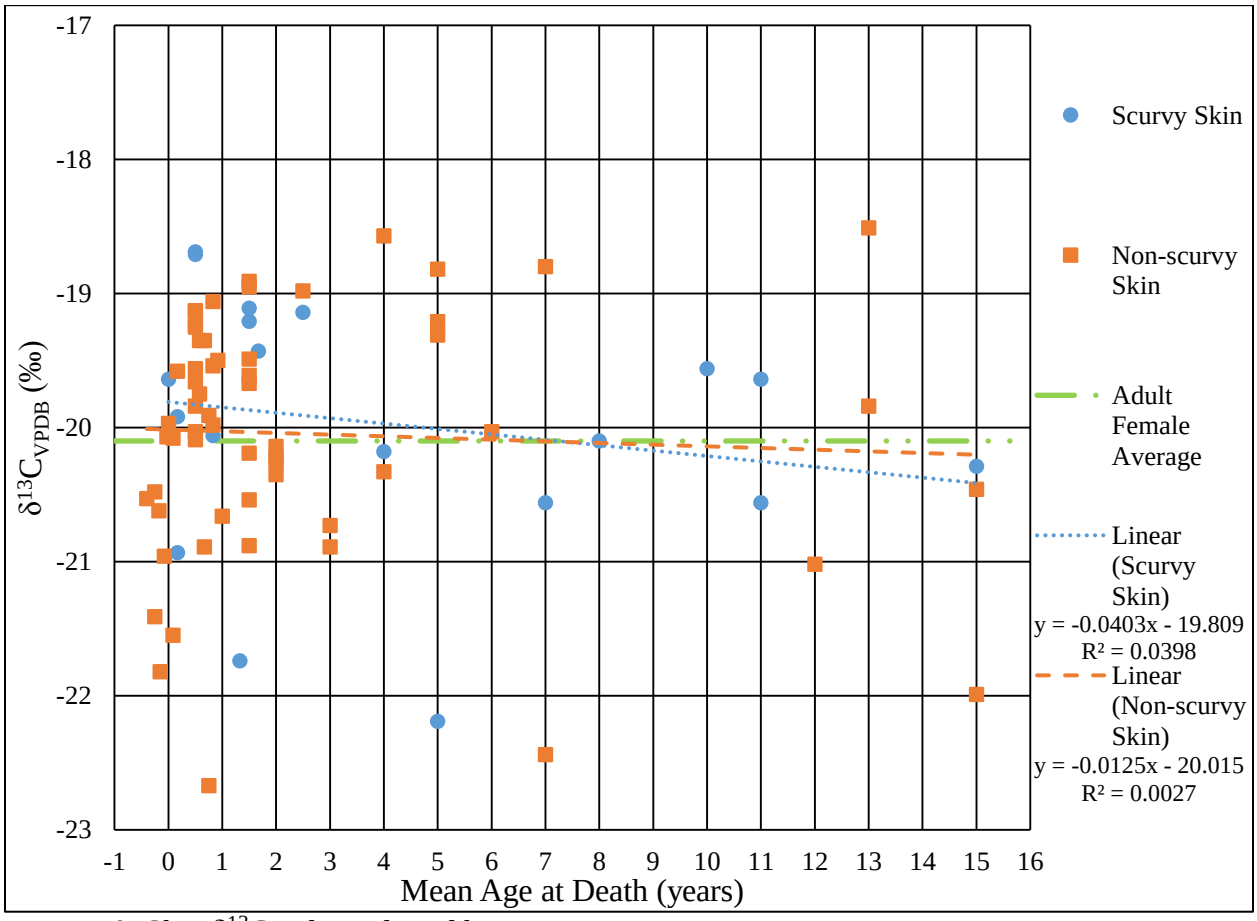

Figure 50: Skin $\delta^{13}C$ values plotted by mean age.

The $\delta^{13}C$ values for skin were again divided into age at death cohorts. The F&P cohort represented by skin consisted of nine individuals, one who exhibited skeletal indicators of scurvy and eight who did not. The $\delta^{13}C$ for F&P cohort ranged from -21.8‰ to -19.6‰, with a mean value of -20.6 ± 0.7‰. The $\delta^{13}C$ values for the F&P cohort individual who exhibited skeletal

indicators of scurvy was -19.6‰. The $\delta^{13}C$ values for those F&P cohort individuals who did not present with skeletal indicators of scurvy ranged from -21.8‰ to -20.0‰, with a mean value of -20.7 ± 0.6‰. There was no statistically significant difference between the mean scurvy and non-scurvy $\delta^{13}C$ values for the F&P skin samples (p=0.120) (Appendix G). The scatter plot of $\delta^{13}C$ and $\delta^{15}N$ values for the F&P skin cohort can be seen in Figure 51. The neonatal cohort represented by skin consisted of 28 individuals, five who exhibited skeletal indicators of scurvy and 23 who did not. The $\delta^{13}C$ for the neonatal cohort ranged from -22.7‰ to -18.7‰, with a mean value of -19.9 ± 0.9‰. The $\delta^{13}C$ values for those neonatal cohort individuals who exhibited skeletal indicators of scurvy ranged from -20.9‰ to -18.7‰, with a mean value of -19.7 ± 1.0‰. The $\delta^{13}C$ values for those neonatal cohort individuals who did not present with skeletal indicators of scurvy ranged from -22.7‰ to -19.1‰, with a mean value of -19.9 ± 0.9‰. There was no statistically significant difference between the mean scurvy and non-scurvy $\delta^{13}C$ values for the neonatal skin samples (p=0.787) (Appendix G). The scatter plot of $\delta^{13}C$ and $\delta^{15}N$ values for the neonatal skin sample can be seen in Figure 52.

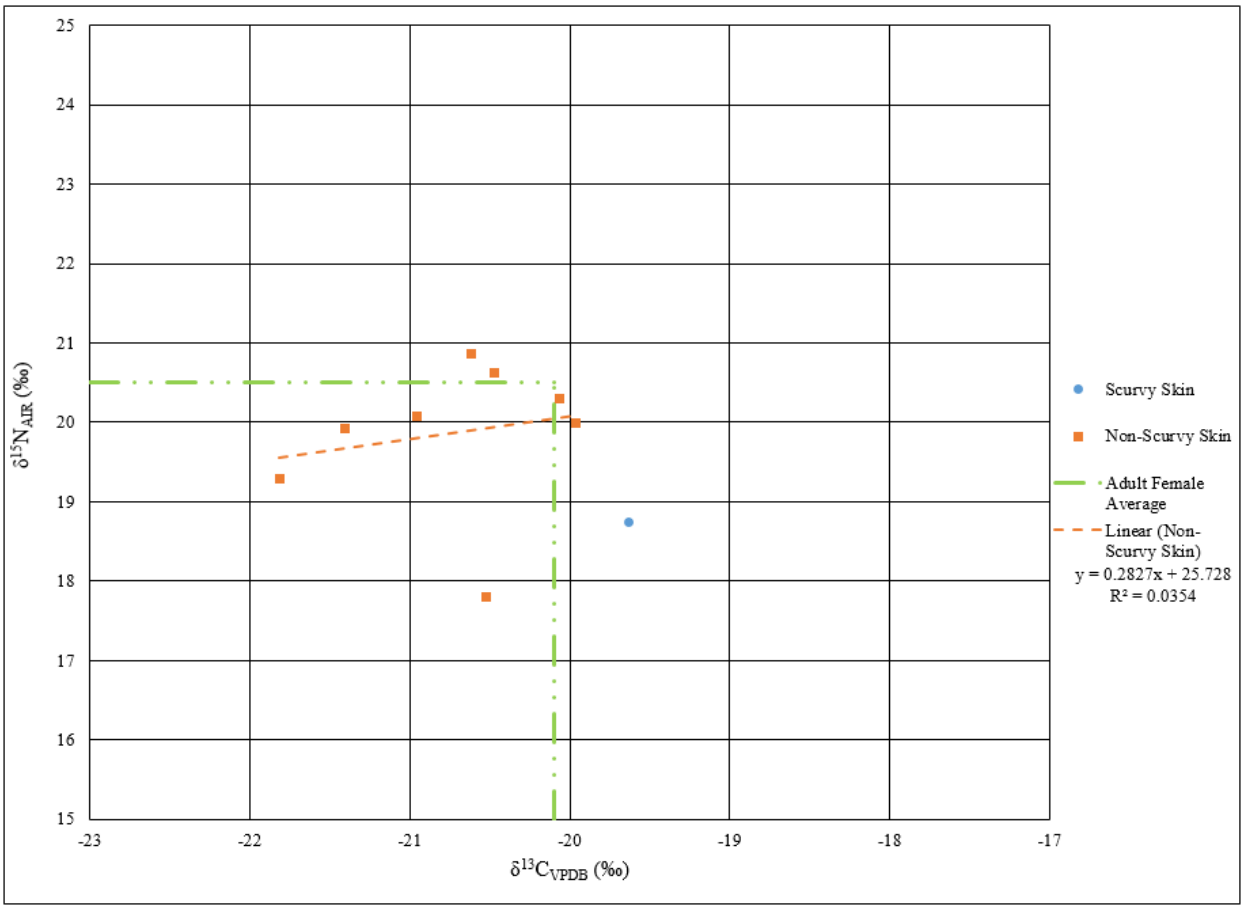

Figure 51: Scatter plot of $\delta^{13}C$ and $\delta^{15}N$ values for the F&P skin cohort.

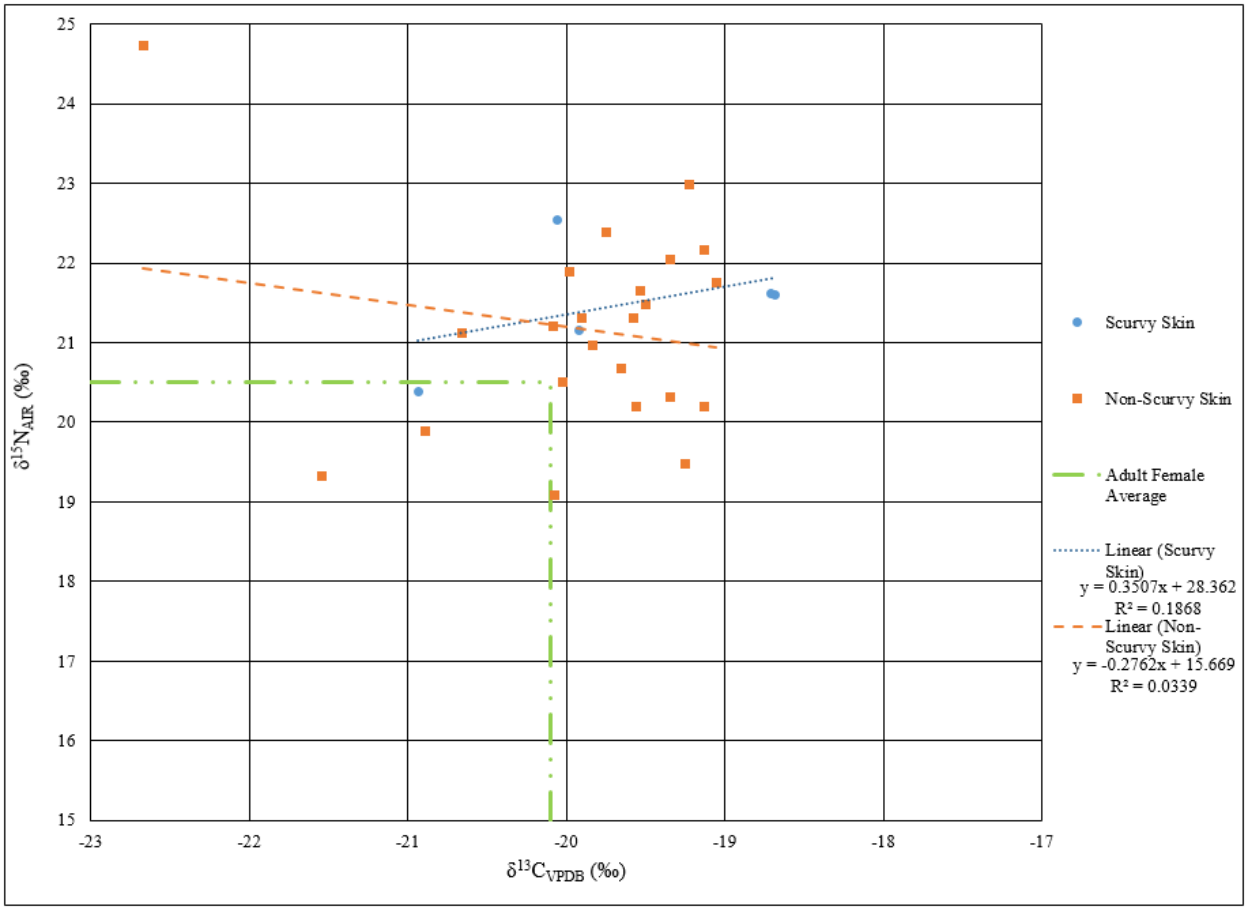

Figure 52: Scatter plot of $\delta^{13}C$ and $\delta^{15}N$ values for the neonatal skin cohort.

The C1 cohort represented by skin consisted of 22 individuals, six who exhibited skeletal indicators of scurvy and 16 who did not. The $\delta^{13}C$ values for the entire C1 cohort ranged from -21.7‰ to -18.6‰, with a mean value of -19.9 ± 0.8‰. The $\delta^{13}C$ values for those C1 cohort individuals who exhibited skeletal indicators of scurvy ranged from -21.7‰ to -19.1‰, with a mean value of -19.8 ± 1.0‰. The $\delta^{13}C$ values for those C1 cohort individuals who did not present with skeletal indicators of scurvy ranged from -20.9‰ to -18.6‰, with a mean value of -19.9 ± 0.7‰. There was no statistically significant difference between the mean scurvy and non-

scurvy $\delta^{13}C$ values for the C1 skin samples (p=0.605) (Appendix G). The scatter plot of $\delta^{13}C$ and $\delta^{15}N$ values for the C1 skin sample can be seen in Figure 53.

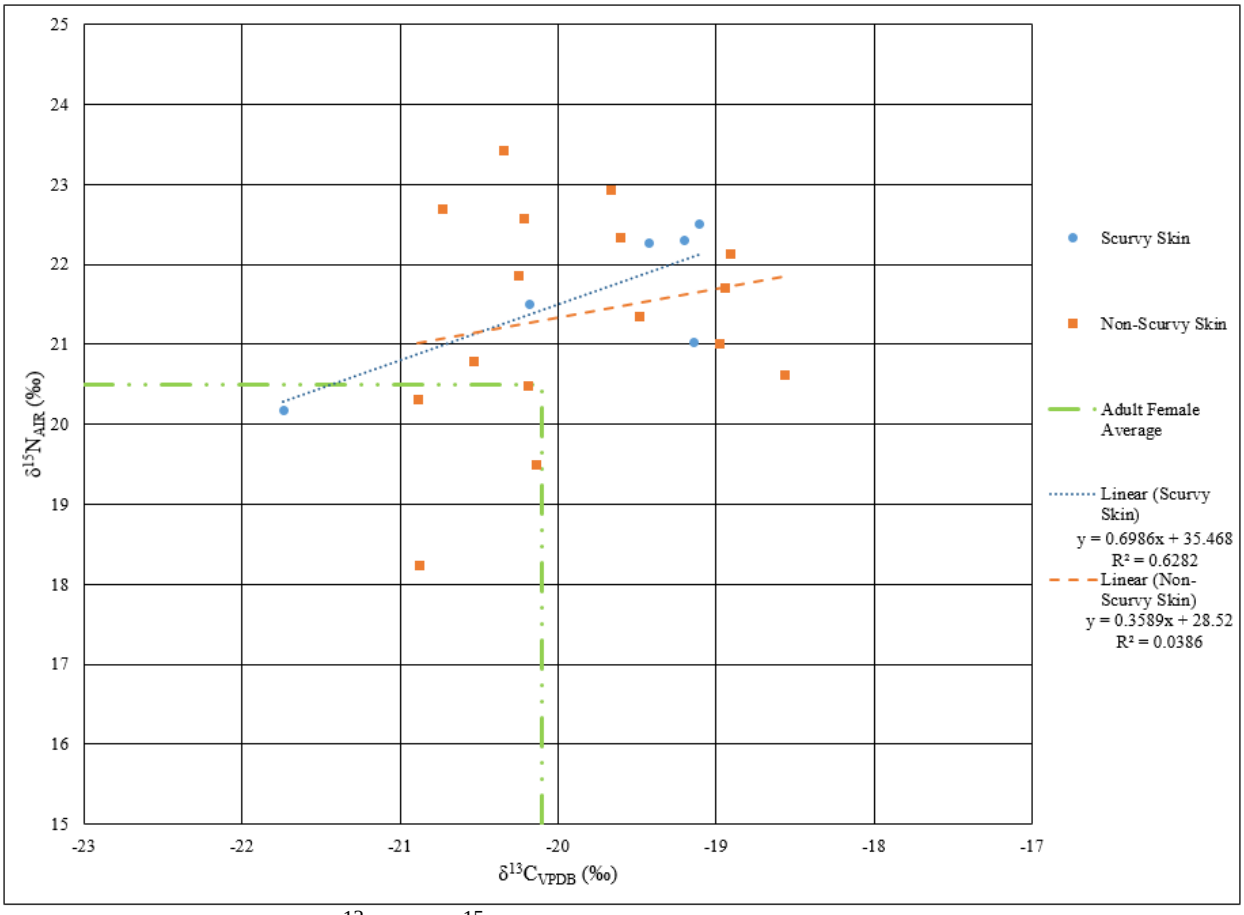

Figure 53: Scatter plot of $\delta^{13}C$ and $\delta^{15}N$ values for the C1 skin cohort.

The C2 cohort represented by skin consisted of 11 individuals, four who exhibited skeletal indicators of scurvy and seven who did not. The $\delta^{13}C$ values for the entire C2 cohort ranged from -22.4‰ to -18.8‰, with a mean value of -20.1 ± 1.2‰. The $\delta^{13}C$ values for those C2 cohort individuals who exhibited skeletal indicators of scurvy ranged from -22.2‰ to -19.6‰, with a mean value of -20.6 ± 1.1‰. The $\delta^{13}C$ values for those C2 cohort individuals who did not present with skeletal indicators of scurvy ranged from -22.4‰ to -18.8‰, with a mean

value of -19.8 ± 1.3‰. There was no statistically significant difference between the mean scurvy and non-scurvy $\delta^{13}C$ values for the C2 skin samples (p=0.185) (Appendix G). The scatter plot of $\delta^{13}C$ and $\delta^{15}N$ values for the C2 skin sample can be seen in Figure 54.

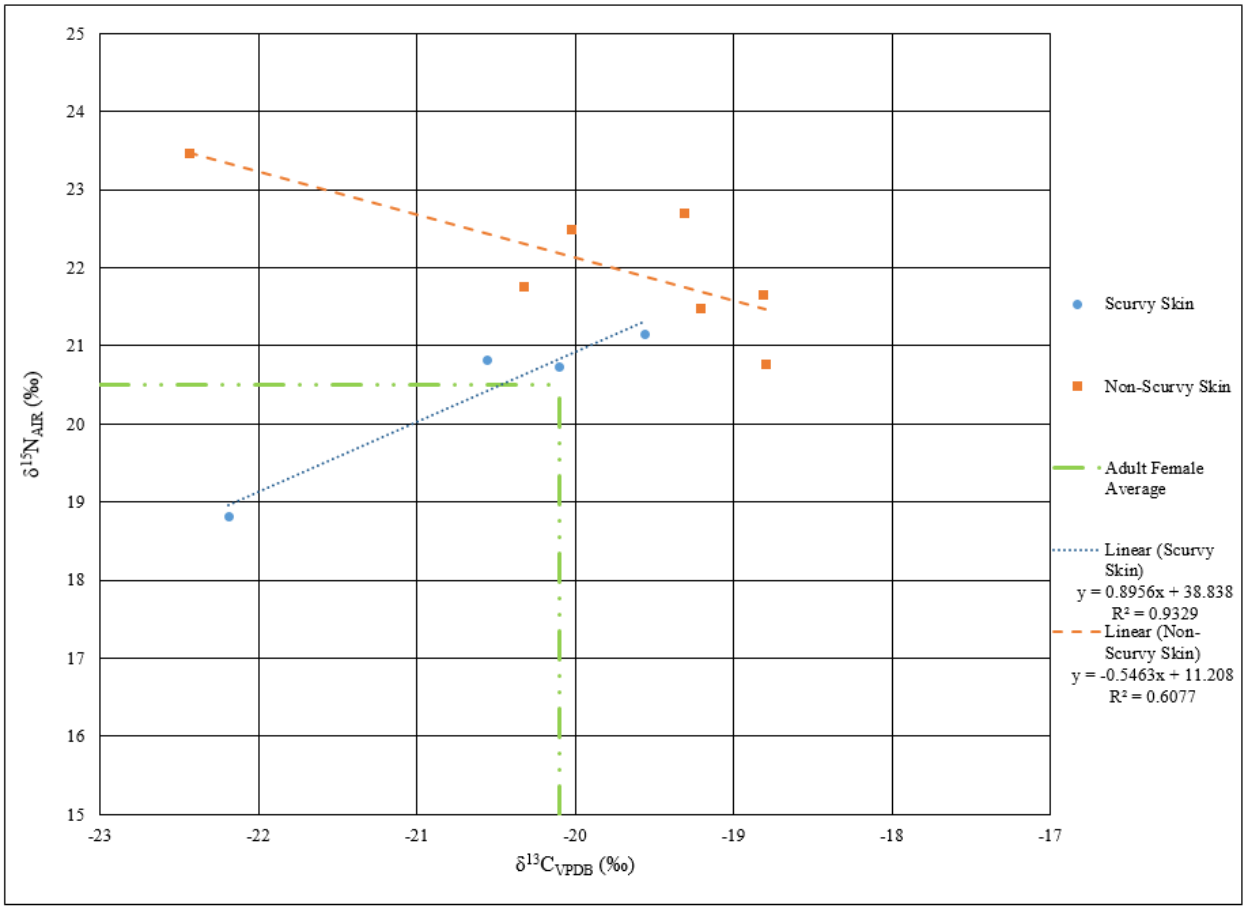

Figure 54: Scatter plot of $\delta^{13}C$ and $\delta^{15}N$ values for the C2 skin cohort.

The C3 cohort represented by skin consisted of eight individuals, three who exhibited skeletal indicators of scurvy and five who did not. The $\delta^{13}C$ values for the entire C3 cohort ranged from -22.0‰ to -18.5‰, with a mean value of -20.3 ± 1.0‰. The $\delta^{13}C$ values for those C3 cohort individuals who exhibited skeletal indicators of scurvy ranged from -20.6‰ to -19.6‰, with a mean value of -20.2 ± 0.5‰. The $\delta^{13}C$ values for those C3 cohort individuals who

did not present with skeletal indicators of scurvy ranged from -22.0‰ to -18.5‰, with a mean value of -20.4 ± 1.3‰. There was no statistically significant difference between the mean scurvy and non-scurvy $\delta^{13}C$ values for the C3 skin samples (p=0.655) (Appendix G). The scatter plot of $\delta^{13}C$ and $\delta^{15}N$ values for the C3 skin sample can be seen in Figure 55.

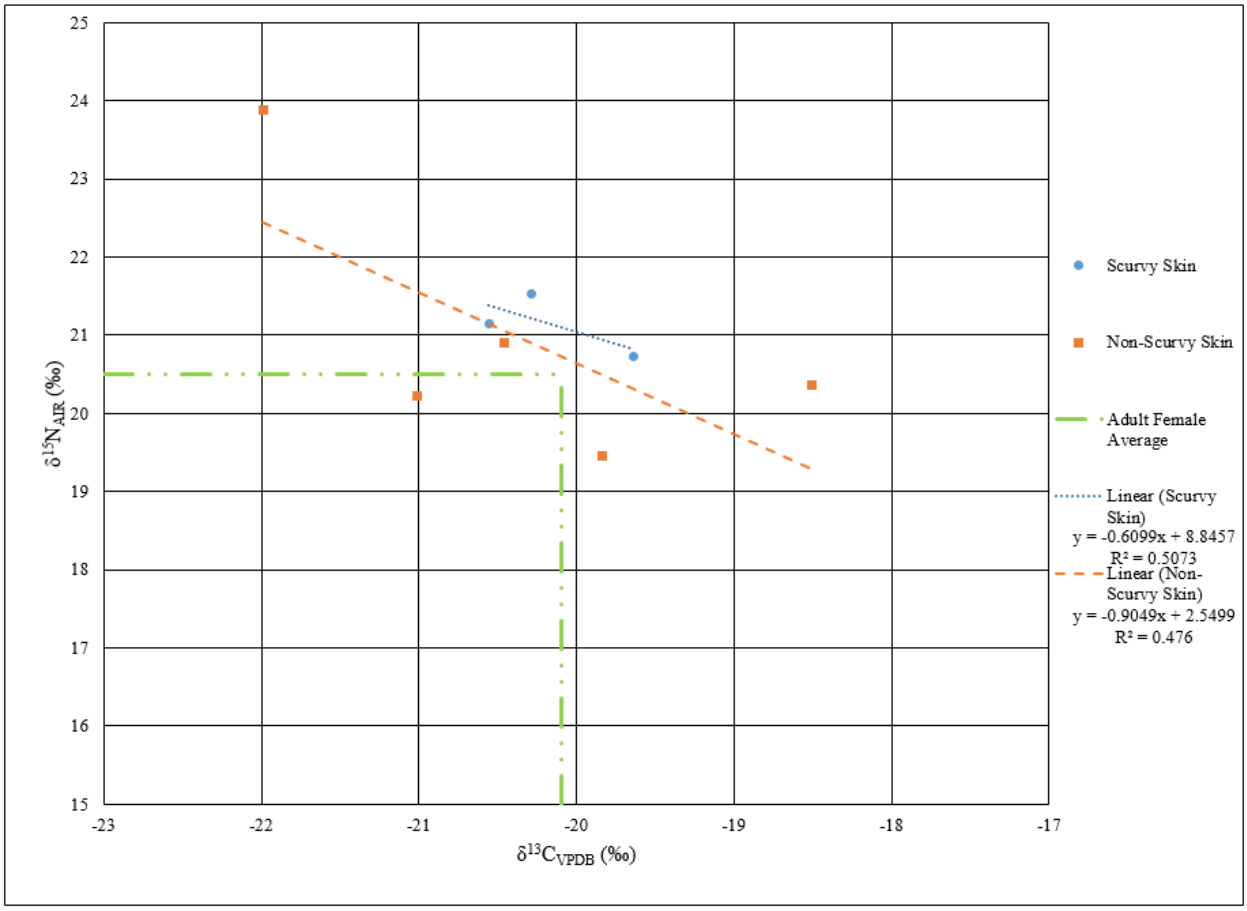

Figure 55: Scatter plot of $\delta^{13}C$ and $\delta^{15}N$ values for the C3 skin cohort.

Intra-tissue $\delta^{13}C$ Differences between Scurvy and Non-Scurvy Cohorts

The differences between mean $\delta^{13}C$ values of the scurvy and non-scurvy cohorts within each tissue and age cohort were compared for significant differences. The differences can be found in Tables 25 - 30.The difference in mean $\delta^{13}C$ values between the overall bone collagen scurvy and non-scurvy samples was -0.1‰. The difference in mean $\delta^{13}C$ values between the F&P bone collagen scurvy and non-scurvy samples was 0.9‰. The difference in mean $\delta^{13}C$ values between the neonatal bone collagen scurvy and non-scurvy samples was 0.3‰. The difference in mean $\delta^{13}C$ values between the C1 bone collagen scurvy and non-scurvy samples was -0.3‰. The difference in mean $\delta^{13}C$ values between the C2 bone collagen scurvy and non-scurvy samples was 0.1‰. The difference in mean $\delta^{13}C$ values between the C3 bone collage scurvy and non-scurvy samples was -0.3‰.

Table 25: Differences between mean $\delta^{13}C$ values of the scurvy and non-scurvy bone collagen samples, both as an overall sample and within each age cohort.

	Scurvy Samples		Non-Scurvy Samples		Δ Scurvy - Non-Scurvy
Age Cohort	Number of Individuals	Mean $\delta^{13}C$ (‰)	Number of Individuals	Mean $\delta^{13}C$ (‰)	Mean $\delta^{13}C$ (‰)
Overall	11	-18.9	13	-18.8	-0.1
F&P	1	-18.4	1	-19.3	0.9
Neonatal	2	-18.5	2	-18.8	0.3
C1	3	-18.9	7	-18.6	-0.3
C2	3	-19.0	2	-19.1	0.1
C3	2	-19.4	1	-19.1	-0.3

The difference in mean $\delta^{13}C$ values between the overall first hair segment scurvy and non-scurvy samples was 0.1‰. The difference in mean $\delta^{13}C$ values between the neonatal first

hair segment scurvy and non-scurvy samples was 0.4‰. The difference in mean $\delta^{13}C$ values between the C1 first hair segment scurvy and non-scurvy samples was 0.1‰. The difference in mean $\delta^{13}C$ values between the C2 first hair segment scurvy and non-scurvy samples was -0.3‰. The difference in mean $\delta^{13}C$ values between the C3 first hair segment scurvy and non-scurvy samples was -0.6‰.

Table 26: Differences between mean $\delta^{13}C$ values of the scurvy and non-scurvy first hair segment samples, both as an overall sample and within each age cohort.

	Scurvy Samples		Non-Scurvy Samples		Δ Scurvy - Non-Scurvy
Age Cohort	Number of Individuals	Mean $\delta^{13}C$ (‰)	Number of Individuals	Mean $\delta^{13}C$ (‰)	Mean $\delta^{13}C$ (‰)
Overall	21	-19.4	112	-19.5	0.1
F&P	0	-	38	-19.8	-
Neonatal	7	-18.9	32	-19.3	0.4
C1	7	-19.3	24	-19.4	0.1
C2	4	-19.9	10	-19.6	-0.3
C3	3	-20.3	8	-19.7	-0.6

The difference in mean $\delta^{13}C$ values between the overall second hair segment scurvy and non-scurvy samples was -0.2‰. The difference in mean $\delta^{13}C$ values between the neonatal second hair segment scurvy and non-scurvy samples was 0.1‰. The difference in mean $\delta^{13}C$ values between the C1 second hair segment scurvy and non-scurvy samples was -0.2‰. The difference in mean $\delta^{13}C$ values between the C2 second hair segment scurvy and non-scurvy samples was -0.4‰. The difference in mean $\delta^{13}C$ values between the C3 second hair segment scurvy and non-scurvy samples was -0.3‰.

Table 27: Differences between mean $\delta^{13}C$ values of the scurvy and non-scurvy second hair segment samples, both as an overall sample and within each age cohort.

	Scurvy Samples		Non-Scurvy Samples		Δ Scurvy - Non-Scurvy
Age Cohort	Number of Individuals	Mean $\delta^{13}C$ (‰)	Number of Individuals	Mean $\delta^{13}C$ (‰)	Mean $\delta^{13}C$ (‰)
Overall	15	-19.5	51	-19.3	-0.2
F&P	-	-	9	-19.4	-
Neonatal	4	-18.8	11	-18.9	0.1
C1	5	-19.5	19	-19.3	-0.2
C2	3	-19.9	6	-19.5	-0.4
C3	3	-19.9	6	-19.6	-0.3

The difference in mean $\delta^{13}C$ values between the overall third hair segment scurvy and non-scurvy samples was -0.4‰. Since the neonatal cohort did not include any individuals exhibiting signs of scurvy with a third hair segment, a difference could not be calculated. The difference in mean $\delta^{13}C$ values between the C1 third hair segment scurvy and non-scurvy samples was -0.2‰. The difference in mean $\delta^{13}C$ values between the C2 third hair segment scurvy and non-scurvy samples was -0.7‰. The difference in mean $\delta^{13}C$ values between the C3 third hair segment scurvy and non-scurvy samples was -0.1‰.

Table 28: Differences between mean $\delta^{13}C$ values of the scurvy and non-scurvy third hair segment samples, both as an overall sample and within each age cohort.

	Scurvy Samples		Non-Scurvy Samples		Δ Scurvy - Non-Scurvy
Age Cohort	Number of Individuals	Mean $\delta^{13}C$ (‰)	Number of Individuals	Mean $\delta^{13}C$ (‰)	Mean $\delta^{13}C$ (‰)
Overall	8	-19.8	32	-19.4	-0.4
F&P	-	-	5	-19.1	-
Neonatal	-	-	4	-19.0	-
C1	3	-19.7	13	-19.5	-0.2
C2	3	-20.0	4	-19.3	-0.7
C3	2	-19.7	6	-19.6	-0.1

The difference in mean $\delta^{13}C$ values between the overall proximal nail segment scurvy and non-scurvy samples was 0.1‰. The difference in mean $\delta^{13}C$ values between the neonatal proximal nail segment scurvy and non-scurvy samples was 0.6‰. The difference in mean $\delta^{13}C$ values between the C1 proximal nail segment scurvy and non-scurvy samples was 0.5‰. The difference in mean $\delta^{13}C$ values between the C2 proximal nail segment scurvy and non-scurvy samples was -0.4‰. The difference in mean $\delta^{13}C$ values between the C3 proximal nail segment scurvy and non-scurvy samples was -0.3‰.

Table 29: Differences between mean $\delta^{13}C$ values of the scurvy and non-scurvy proximal nail segment samples, both as an overall sample and within each age cohort.

	Scurvy Samples		Non-Scurvy Samples		Δ Scurvy - Non-Scurvy
Age Cohort	Number of Individuals	Mean $\delta^{13}C$ (‰)	Number of Individuals	Mean $\delta^{13}C$ (‰)	Mean $\delta^{13}C$ (‰)
Overall	10	-19.7	44	-19.8	0.1
F&P	-	-	4	-19.5	-
Neonatal	3	-18.9	15	-19.5	0.6
C1	4	-19.7	15	-20.2	0.5
C2	2	-20.3	7	-19.9	-0.4
C3	1	-20.7	3	-20.4	-0.3

The difference in mean $\delta^{13}C$ values between the overall skin scurvy and non-scurvy samples was 0.1‰. The difference in mean $\delta^{13}C$ values between the F&P skin scurvy and non-scurvy samples was 1.1‰. The difference in mean $\delta^{13}C$ values between the neonatal skin scurvy and non-scurvy samples was 0.2‰. The difference in mean $\delta^{13}C$ values between the C1 skin scurvy and non-scurvy samples was 0.1‰. The difference in mean $\delta^{13}C$ values between the C2 skin scurvy and non-scurvy samples was -0.8‰. The difference in mean $\delta^{13}C$ values between the C3 skin scurvy and non-scurvy samples was 0.2‰.

Table 30: Differences between mean $\delta^{13}C$ values of the scurvy and non-scurvy skin samples, both as an overall sample and within each age cohort.

	Scurvy Samples		Non-Scurvy Samples		Δ Scurvy - Non-Scurvy
Age Cohort	Number of Individuals	Mean $\delta^{13}C$ (‰)	Number of Individuals	Mean $\delta^{13}C$ (‰)	Mean $\delta^{13}C$ (‰)
Overall	19	-20.0	59	-20.1	0.1
F&P	1	-19.6	8	-20.7	1.1
Neonatal	5	-19.7	23	-19.9	0.2
C1	6	-19.8	16	-19.9	0.1
C2	4	-20.6	7	-19.8	-0.8
C3	3	-20.2	5	-20.4	0.2

Stable Nitrogen Isotope Results

Bone Collagen

A total of 24 bone collagen samples were analyzed for $\delta^{15}N$ values. All descriptive statistics (mean, minimum, maximum, and standard deviation) for $\delta^{15}N$ values from bone collagen can be found in Table 31. The $\delta^{15}N$ values of bone collagen for all individuals can be found in Appendix E (Table 56).

Table 31 Descriptive statistics for $\delta^{15}N$ values for bone collagen. Each category's statistics are first presented as an overall representation, followed by those individuals who exhibited skeletal indicators of scurvy and those who did not. Entries of "-" indicate not enough data available to calculate the statistic.

		N	Mean	Min	Max	Standard Deviation
Entire Sample	**Overall**	24	18.9	16.4	22.2	1.6
	Scurvy	11	18.7	17.3	20.9	1.3
	Non-scurvy	13	19.1	16.4	22.2	1.8
F&P	**Overall**	2	19.1	19.0	19.2	0.1
	Scurvy	1	19.0	-	-	-
	Non-scurvy	1	19.2	-	-	-
Neo	**Overall**	4	21.1	19.8	22.2	1.0
	Scurvy	2	20.4	19.8	20.9	0.8
	Non-scurvy	2	21.8	21.3	22.2	0.6
C1	**Overall**	10	19.2	17.4	21.6	1.4
	Scurvy	3	19.0	17.9	20.8	1.6
	Non-scurvy	7	19.3	17.4	21.6	1.4
C2	**Overall**	5	17.4	16.4	18.1	0.6
	Scurvy	3	17.7	17.3	18.1	0.4
	Non-scurvy	2	17.0	16.4	17.6	0.8
C3	**Overall**	3	17.7	17.2	18.1	0.5
	Scurvy	2	18.0	17.9	18.1	0.1
	Non-scurvy	1	17.2	-	-	-

The $\delta^{15}N$ values for the entire sample ranged from 16.4‰ to 22.2‰, with a mean value of 18.9 ± 1.6‰. Of these 24 samples, 11 individuals exhibited skeletal indicators of scurvy. The $\delta^{15}N$ values for this cohort ranged from 17.3‰ to 20.9‰, with a mean value of 18.7 ± 1.3‰. The remaining 13 individuals did not exhibit skeletal indicators of scurvy. The $\delta^{15}N$ values for this second cohort ranged from 16.4‰ to 22.2‰, with a mean value of 19.1 ± 1.8‰. There was no statistically significant difference between the mean scurvy and non-scurvy $\delta^{15}N$ values for

the overall bone collagen samples (p = 0.622) (Appendix F).). The $\delta^{13}C$ and $\delta^{15}N$ values of the scurvy and non-scurvy cohorts are shown in Figure 10.

When the $\delta^{15}N$ values for bone collagen were plotted by age, a general trend can be seen. The scurvy and non-scurvy cohorts both show a trend of decreasing $\delta^{15}N$ values as age increases (Figure 56).

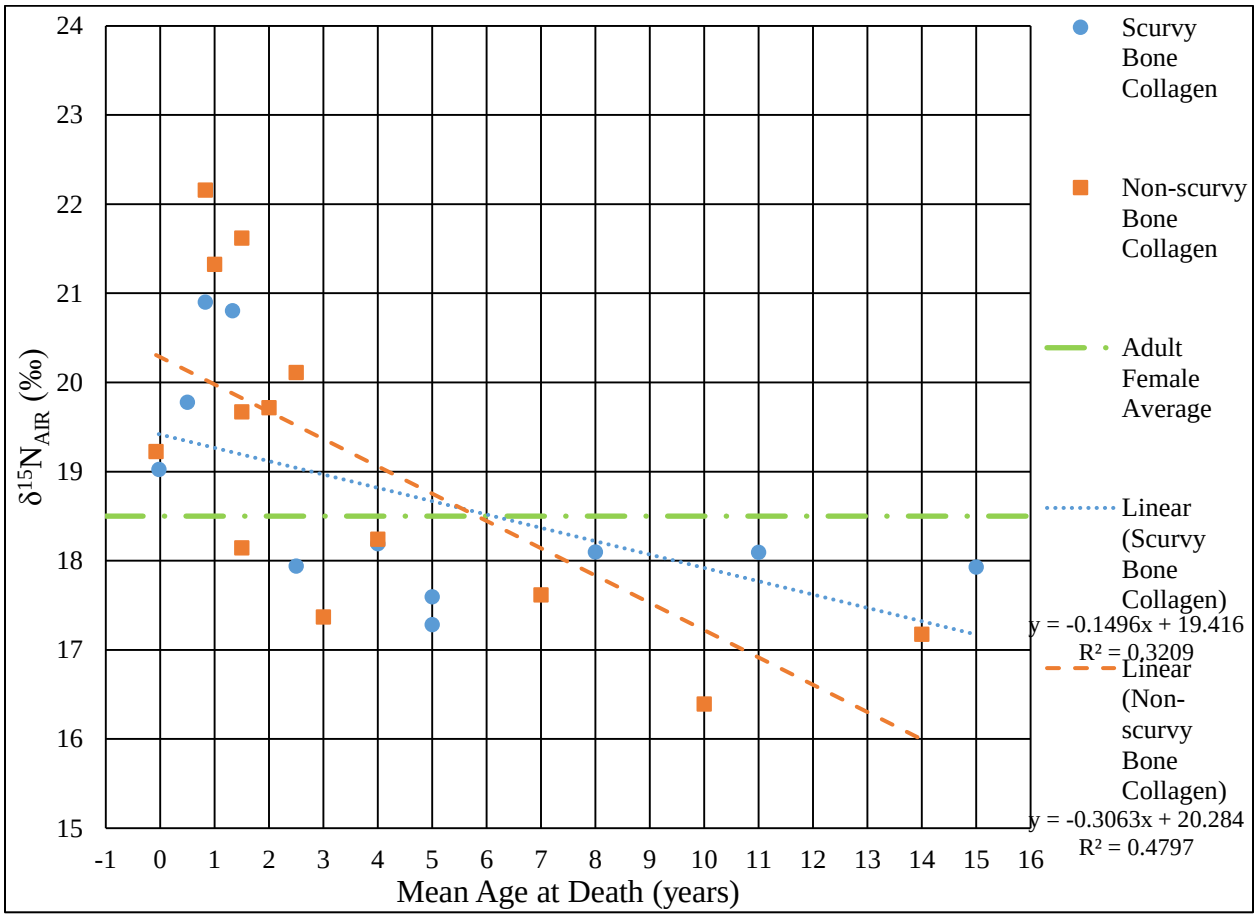

Figure 56: Bone collagen $\delta^{15}N$ values plotted by mean age.

The results for $\delta^{15}N$ values were also divided based on age at death cohorts. The fetal and perinatal (F&P) cohort represented by bone collagen consisted of two individuals, one who exhibited skeletal indicators of scurvy and one who did not, with $\delta^{15}N$ values of 19.0‰ and

19.2‰, respectively. The $\delta^{15}N$ values for the F&P cohort had a mean value of 19.1 ± 0.1‰. There was no statistically significant difference between the mean scurvy and non-scurvy $\delta^{15}N$ values for the F&P bone collagen samples (p = 0.317) (Appendix G). The $\delta^{13}C$ and $\delta^{15}N$ values of the F&P scurvy and non-scurvy cohorts are shown in Figure 12. The neonatal cohort represented by bone collagen consisted of four individuals, two who exhibited skeletal indicators of scurvy and two who did not. The $\delta^{15}N$ values for the entire neonatal cohort ranged from 19.8‰ to 22.2‰, with a mean value of 21.1 ± 1.0‰. The $\delta^{15}N$ values for those neonatal cohort individuals who exhibited skeletal indicators of scurvy ranged from 19.8‰ to 20.9‰, with a mean value of 20.4 ± 0.8‰. The $\delta^{15}N$ values for those neonatal cohort individuals who did not exhibit skeletal indicators of scurvy ranged from 21.3‰ to 22.2‰, with a mean value of 21.8 ± 0.6‰. There was no statistically significant difference between the mean scurvy and non-scurvy $\delta^{15}N$ values for the neonatal bone collagen samples (p = 0.121) (Appendix G). The $\delta^{13}C$ and $\delta^{15}N$ values of the neonatal scurvy and non-scurvy cohorts are shown in Figure 12.

The C1 cohort represented by bone collagen consisted of ten individuals, three who exhibited skeletal indicators of scurvy and seven who did not. The $\delta^{15}N$ values for the entire C1 cohort ranged from 17.4‰ to 21.6‰, with a mean value of 19.2 ± 1.4‰. The $\delta^{15}N$ values for those C1 cohort individuals who exhibited skeletal indicators of scurvy ranged from 17.9‰ to 20.8‰, with a mean value of 19.0 ± 1.6‰. The $\delta^{15}N$ values for those C1 cohort individuals who did not exhibit skeletal indicators of scurvy ranged from 17.4‰ to 21.6‰, with a mean value of 19.3 ± 1.4‰. There was no statistically significant difference between the mean scurvy and non-scurvy $\delta^{15}N$ values for the C1 bone collagen samples (p = 0.819) (Appendix G). The $\delta^{13}C$ and $\delta^{15}N$ values of the C1 scurvy and non-scurvy cohorts are shown in Figure 14.

The C2 cohort represented by bone collagen consisted of five individuals, three who exhibited skeletal indicators of scurvy and two who did not. The $\delta^{15}N$ values for the entire C2 cohort ranged from 16.4‰ to 18.1‰, with a mean value of 17.4 ± 0.6‰. Two outliers were present in this cohort, one with a more enriched $\delta^{15}N$ value (burial 520) and one with a less enriched $\delta^{15}N$ value (burial 582) (Figure 57). The $\delta^{15}N$ values for those C2 cohort individuals who exhibited skeletal indicators of scurvy ranged from 17.3‰ to 18.1‰, with a mean value of 17.7 ± 0.4‰. The $\delta^{15}N$ values for those C2 cohort individuals who did not exhibit skeletal indicators of scurvy ranged from 16.4‰ to 17.6‰, with a mean value of 17.0 ± 0.8‰. There was no statistically significant difference between the mean scurvy and non-scurvy $\delta^{15}N$ values for the C2 bone collagen samples ($p = 0.374$) (Appendix G). The $\delta^{13}C$ and $\delta^{15}N$ values of the C2 scurvy and non-scurvy cohorts are shown in Figure 15.

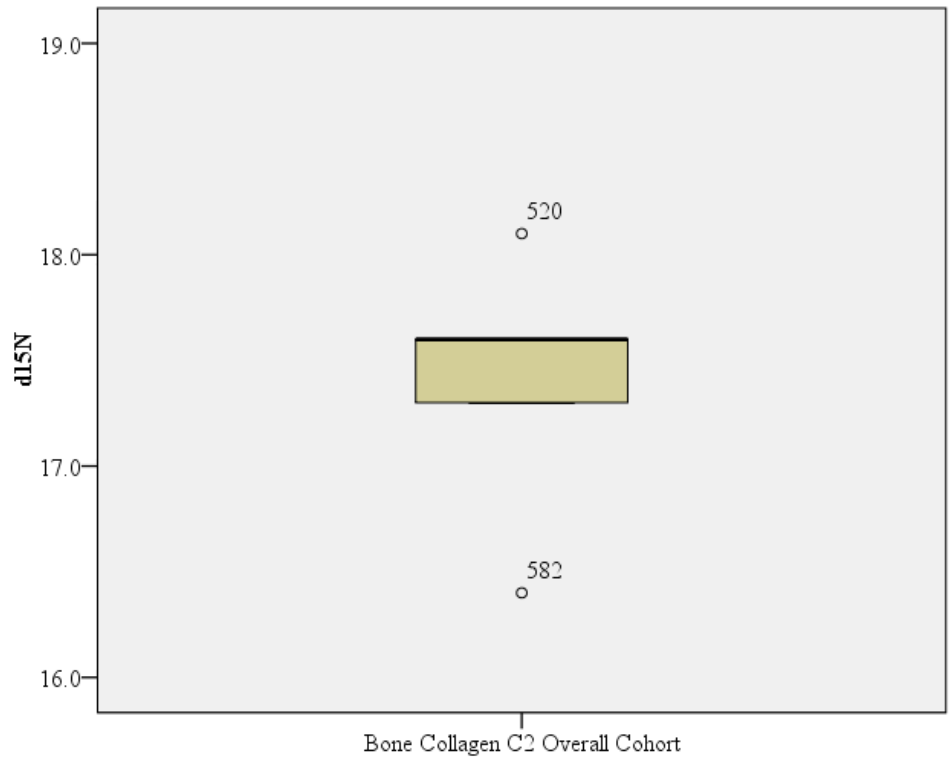

Figure 57: Box and whisker plot for $\delta^{15}N$ indicating the outliers for the C2 bone collagen cohort.

The C3 cohort represented by bone collagen consisted of three individuals, two who exhibited skeletal indicators of scurvy and one who did not. The $\delta^{15}N$ values for the entire C3 cohort ranged from 17.2‰ to 18.1‰, with a mean value of 17.7± 0.5‰. The $\delta^{15}N$ values for those C3 cohort individuals who exhibited skeletal indicators of scurvy ranged from 17.9‰ to 18.1‰, with a mean value of 18.0 ± 0.1‰. The $\delta^{15}N$ value for the C3 individual who did not exhibit skeletal indicators of scurvy was 17.2‰. There was no statistically significant difference between the mean scurvy and non-scurvy $\delta^{15}N$ values for the C3 bone collagen samples ($p = 0.221$) (Appendix G). The $\delta^{13}C$ and $\delta^{15}N$ values of the C3 scurvy and non-scurvy cohorts are shown in Figure 16.

Hair

A total of 132 individuals represented by one to three hair segments (measuring 1cm in length each), were analyzed for $\delta^{15}N$ values. There were 67 juveniles who provided only one hair segment, 26 who provided two segments, and 39 who provided three segments. Descriptive statistics (mean, minimum, maximum, and standard deviation) for the $\delta^{15}N$ values of each of the first three hair segments were calculated separately and can be found in Tables 32 - 34. The $\delta^{15}N$ values for up to the first three hair segments for these individuals can be found in Appendix E (Table 57). The overall descriptive and statistical tests for each hair segment are presented first. Then, in order to see trends over the last three months of life, the mean of each segment for each age cohort is presented together.

Table 32: Descriptive statistics for $\delta^{15}N$ values for the first hair segment. Each category's statistics are first presented as an overall representation, followed by those individuals who exhibited skeletal indicators of scurvy and those who did not. Entries of "-" indicate not enough data available to calculate the statistic.

		N	Mean	Min	Max	Standard Deviation
Entire Sample	**Overall**	132	18.7	15.1	23.6	1.7
	Scurvy	21	18.6	15.2	22.1	1.8
	Non-scurvy	111	18.7	15.1	23.6	1.6
F&P	**Overall**	-	-	-	-	-
	Scurvy	-	-	-	-	-
	Non-scurvy	35	18.6	16.1	21.8	1.3
Neo	**Overall**	41	19.7	16.2	23.6	1.6
	Scurvy	7	20.1	18.5	22.1	1.2
	Non-scurvy	34	19.6	16.2	23.6	1.7
C1	**Overall**	30	18.5	15.1	21.9	1.7
	Scurvy	7	18.0	15.2	20.8	2.1
	Non-scurvy	23	18.7	15.1	21.9	1.6
C2	**Overall**	15	17.5	15.3	20.5	1.3
	Scurvy	4	17.6	16.6	18.7	1.0
	Non-scurvy	11	17.4	15.3	20.5	1.4
C3	**Overall**	11	17.6	16.4	19.0	0.9
	Scurvy	3	17.9	17.1	19.0	1.0
	Non-scurvy	8	17.5	16.4	18.7	0.9

Table 33: Descriptive statistics for $\delta^{15}N$ values for the second hair segment. Each category's statistics are first presented as an overall representation, followed by those individuals who exhibited skeletal indicators of scurvy and those who did not. Entries of "-" indicate not enough data available to calculate the statistic.

		N	Mean	Min	Max	Standard Deviation
Entire Sample	**Overall**	65	18.4	15.3	23.4	1.6
	Scurvy	15	18.2	15.8	22.0	1.7
	Non-scurvy	50	18.4	15.3	23.4	1.6
F&P	**Overall**	-	-	-	-	-
	Scurvy	-	-	-	-	-
	Non-scurvy	7	17.8	16.4	18.9	1.0
Neo	**Overall**	16	19.8	16.7	23.4	1.7
	Scurvy	4	20.0	18.5	22.0	1.5
	Non-scurvy	12	19.7	16.7	23.4	1.9
C1	**Overall**	23	18.3	15.3	21.9	1.6
	Scurvy	5	17.8	15.8	19.7	1.7
	Non-scurvy	18	18.5	15.3	21.9	1.6
C2	**Overall**	10	17.1	15.9	18.4	0.9
	Scurvy	3	17.1	16.4	18.4	1.1
	Non-scurvy	7	17.1	15.9	18.2	0.8
C3	**Overall**	9	17.9	16.6	18.8	0.8
	Scurvy	3	17.7	17.0	18.8	0.9
	Non-scurvy	6	18.0	16.6	18.6	0.7

Table 34: Descriptive statistics for $\delta^{15}N$ values for the third hair segment. Each category's statistics are first presented as an overall representation, followed by those individuals who exhibited skeletal indicators of scurvy and those who did not. Entries of "-" indicate not enough data available to calculate the statistic.

		N	Mean	Min	Max	Standard Deviation
Entire Sample	**Overall**	39	18.2	15.5	21.8	1.4
	Scurvy	8	17.8	16.3	19.9	1.3
	Non-scurvy	31	18.3	15.5	21.8	1.4
F&P	**Overall**	-	-	-	-	-
	Scurvy	-	-	-	-	-
	Non-scurvy	3	18.3	17.7	19.2	0.8
Neo	**Overall**	-	-	-	-	-
	Scurvy	-	-	-	-	-
	Non-scurvy	5	19.0	18.0	20.8	1.4
C1	**Overall**	15	18.8	16.3	21.8	1.5
	Scurvy	3	18.5	16.3	19.9	1.9
	Non-scurvy	12	18.8	16.6	21.8	1.4
C2	**Overall**	8	17.0	15.5	18.7	1.1
	Scurvy	3	17.2	16.7	18.1	0.8
	Non-scurvy	5	16.8	15.5	18.7	1.3
C3	**Overall**	8	17.7	16.8	19.0	0.6
	Scurvy	2	17.5	17.4	17.6	0.1
	Non-scurvy	6	17.8	16.8	19.0	0.7

The $\delta^{15}N$ values for the overall first hair segment ranged from 15.1‰ to 23.6‰, with a mean value of 18.7 ± 1.7‰. The 21 juveniles who exhibited skeletal indicators of scurvy had $\delta^{15}N$ values that ranged from 15.2‰ to 22.1‰, with a mean value of 18.6 ± 1.8‰. The 111 individuals who did not exhibit skeletal indicators of scurvy had $\delta^{15}N$ values that ranged from 15.1‰ to 23.6‰, with a mean value of 18.7 ± 1.6‰. There was no statistically significant difference between the mean scurvy and non-scurvy $\delta^{15}N$ values for the overall first hair segment

samples (p = 0.879) (Appendix F). The $\delta^{13}C$ and $\delta^{15}N$ values of the overall first hair segment scurvy and non-scurvy cohorts are shown in Figure 17.

When the $\delta^{15}N$ values for each hair segment were plotted by age, all hair cohorts exhibited a greater range in $\delta^{15}N$ values in the younger ages with the range decreasing as age increased (Figures 58 - -60). Additionally, for all hair cohorts, the change in average $\delta^{15}N$ values between age cohorts follows a pattern of increasing between the F&P and neonatal cohorts, decreasing between the neonatal and C1 cohorts, decreasing between the C1 and C2 cohorts, and increasing between the C2 and C3 cohorts (Table 35).

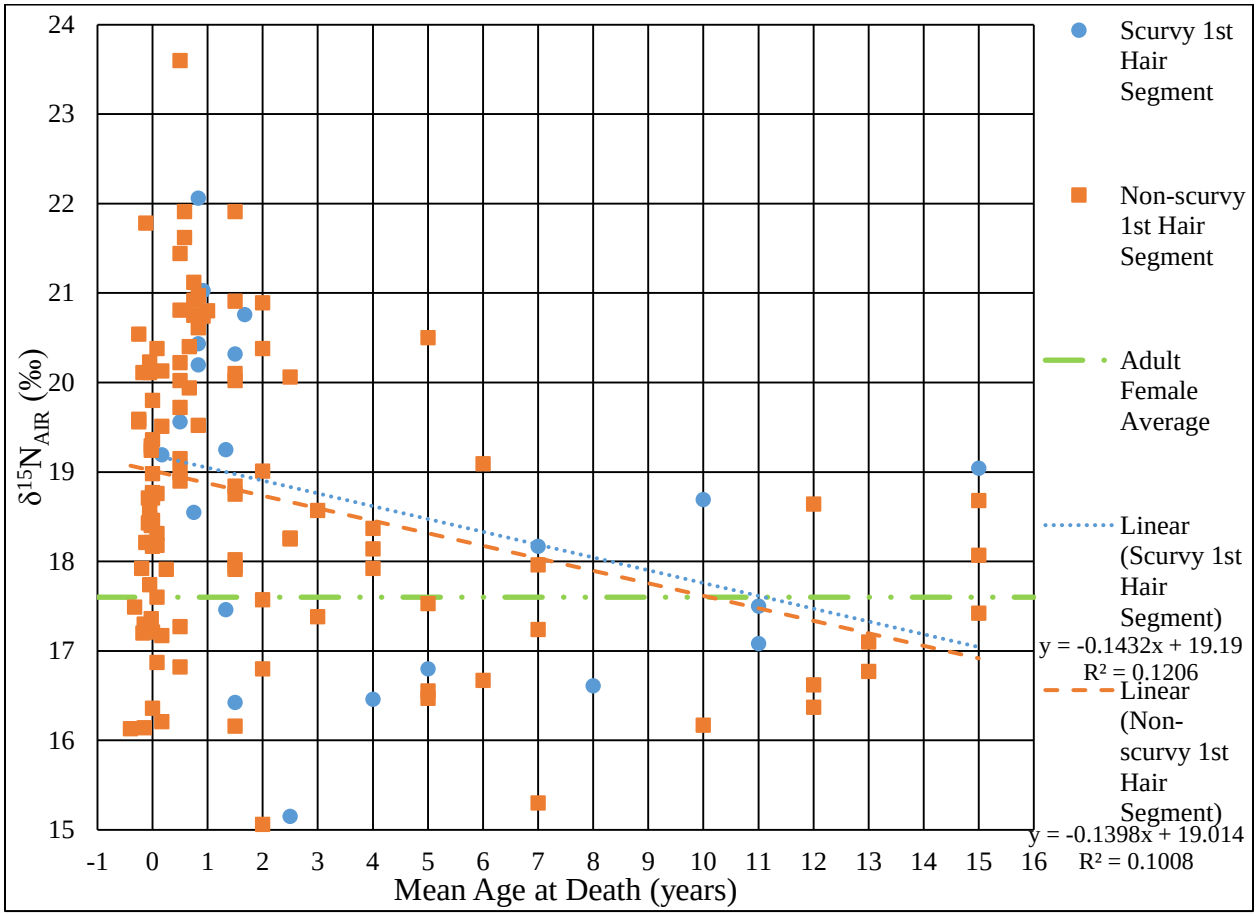

Figure 58: First hair segment $\delta^{15}N$ values plotted by mean age.

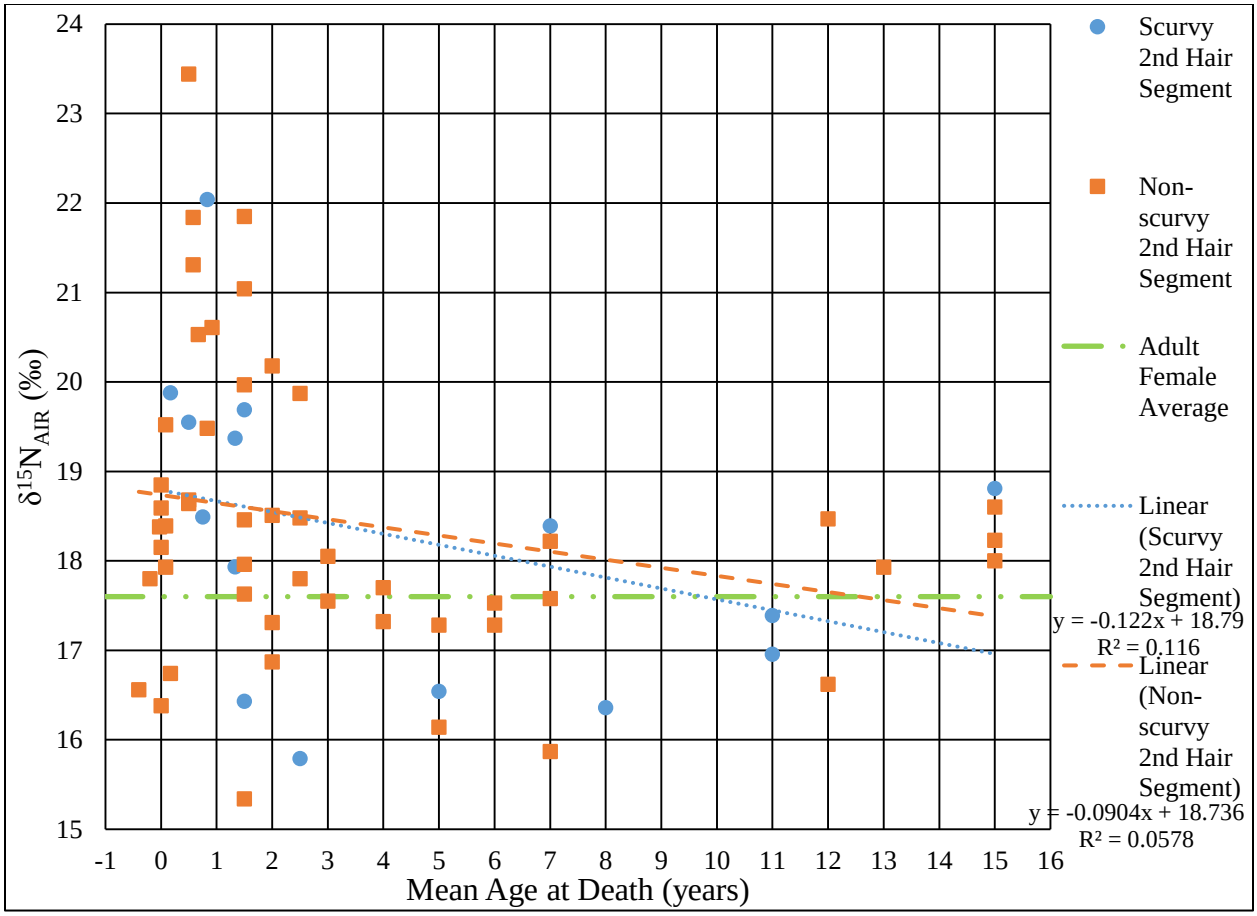

Figure 59: Second hair segment $\delta^{15}N$ values plotted by mean age.

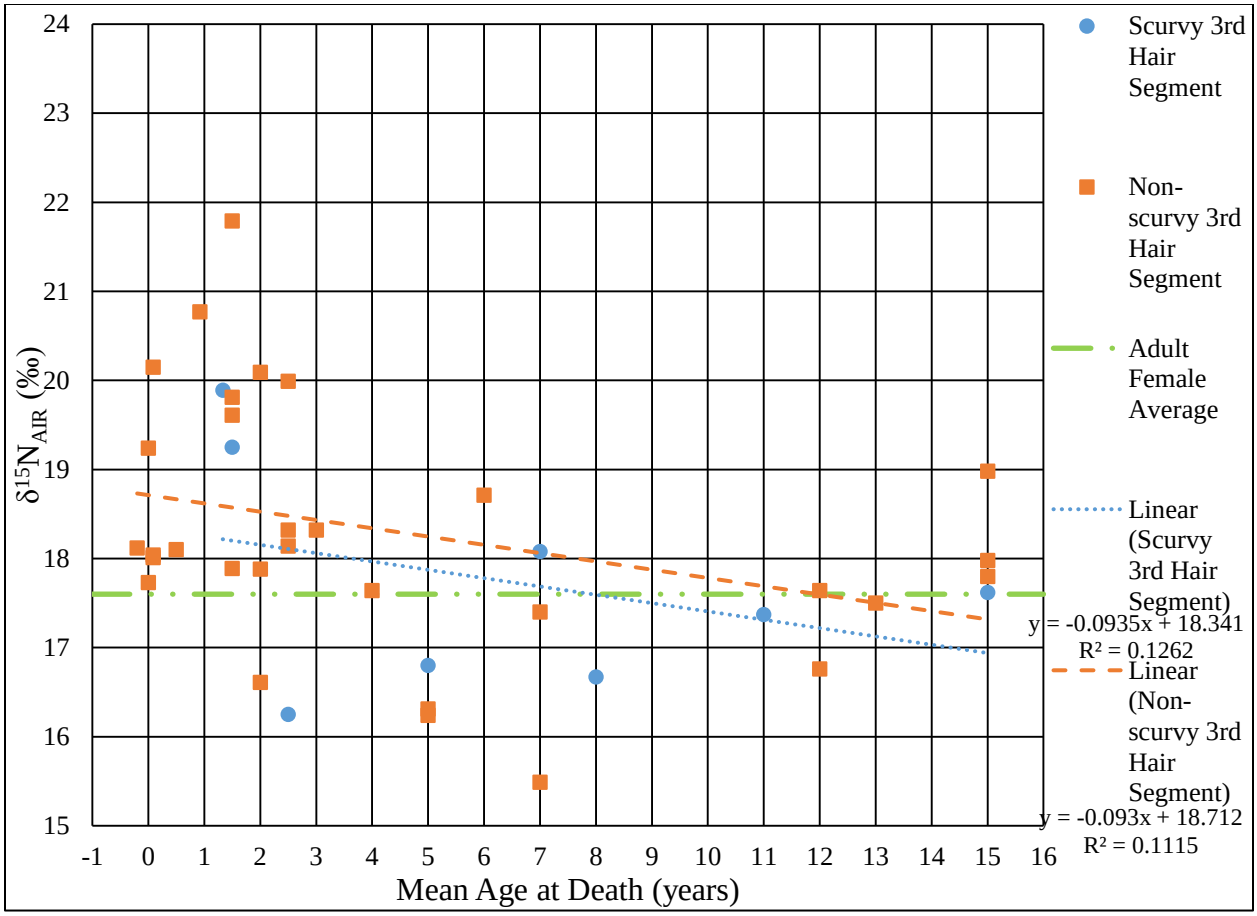

Figure 60: Third hair segment $\delta^{15}N$ values plotted by mean age.

Table 35: Average $\delta^{15}N$ values, in ‰, for the first, second, and third hair segments for each age cohort. The arrow next to the $\delta^{15}N$ values (except the F&P cohort) in each sample column indicates either a decrease (⬇) or increase (⬆) in average $\delta^{15}N$ value from the cohort above.

	1st Segment (‰)	2nd Segment (‰)	3rd Segment (‰)
F&P	18.6	18.1	18.7
Neonatal	19.8 ⬆	20.0 ⬆	19.0
C1	18.5 ⬇	18.3 ⬇	18.6 ⬇
C2	17.5 ⬇	17.1 ⬇	17.1 ⬇
C3	17.6 ⬆	17.9 ⬆	17.7 ⬆

The $\delta^{15}N$ values for the overall second hair segment ranged from 15.3‰ to 23.4‰, with a mean value of 18.4 ± 1.6‰. The 15 individuals who exhibited skeletal indicators of scurvy had $\delta^{15}N$ values that ranged from 15.8‰ to 22.0‰, with a mean value of 18.2 ± 1.7‰. The remaining 50 individuals who did not exhibit skeletal indicators of scurvy had $\delta^{15}N$ values that ranged from 15.3‰ to 23.4‰, with a mean value of 18.4 ± 1.6‰. There was no statistically significant difference between the mean scurvy and non-scurvy $\delta^{15}N$ values for the overall second hair segment samples ($p = 0.761$) (Appendix F). The $\delta^{13}C$ and $\delta^{15}N$ values of the overall second hair segment scurvy and non-scurvy cohorts are shown in Figure 18.

The $\delta^{15}N$ values for the overall third hair segment ranged from 15.5‰ to 21.8‰, with a mean value of 18.2 ± 1.4‰. Eight individuals exhibited skeletal indicators of scurvy and had $\delta^{15}N$ values that ranged from 16.3‰ to 19.9‰, with a mean value of 17.8 ± 1.3‰. The remaining 31 individuals who did not present with skeletal indicators of scurvy had $\delta^{15}N$ values that ranged from 15.5‰ to 21.8‰, with a mean value of 18.3 ± 1.4‰. There was no statistically significant difference between the mean scurvy and non-scurvy $\delta^{15}N$ values for the overall third hair segment samples ($p = 0.265$) (Appendix F). The $\delta^{13}C$ and $\delta^{15}N$ values of the overall third hair segment scurvy and non-scurvy cohorts are shown in Figure 19.

The F&P cohort first, second, and third hair segments were represented by 35, seven, and three non-scurvy juveniles, respectively. The $\delta^{15}N$ values for the first hair segment ranged from 16.1‰ to 21.8‰, with a mean value of 18.6 ± 1.3‰. One outlier (burial 428) was present in this cohort with a more enriched $\delta^{15}N$ value (Figure 61). The $\delta^{15}N$ values for the second hair segment ranged from 16.4‰ to 18.9‰, with a mean value of 17.8 ± 1.0‰. The $\delta^{15}N$ values for the third hair segment ranged from 17.7‰ to 19.2‰, with a mean value of 18.3 ± 0.8‰. The scatter plots

of all juveniles for the first, second, and third F&P hair segments can be found in Appendix H (Figure 94). The F&P cohort for each hair segment was also averaged in order to show trends in $\delta^{15}N$ values for this cohort over the last three months of life, which shows a slight decrease of $\delta^{15}N$ values between the third and second hair segment and then a slight increase in $\delta^{15}N$ values from the second to the first hair segment (Figure 62). The difference between the third and second hair segment $\delta^{15}N$ values is not statistically significant ($p = 0.732$). The difference between the second and first hair segment $\delta^{15}N$ values is not statistically significant ($p = 0.156$). The difference between the third and first hair segment $\delta^{15}N$ values is not statistically significant ($p = 0.607$).

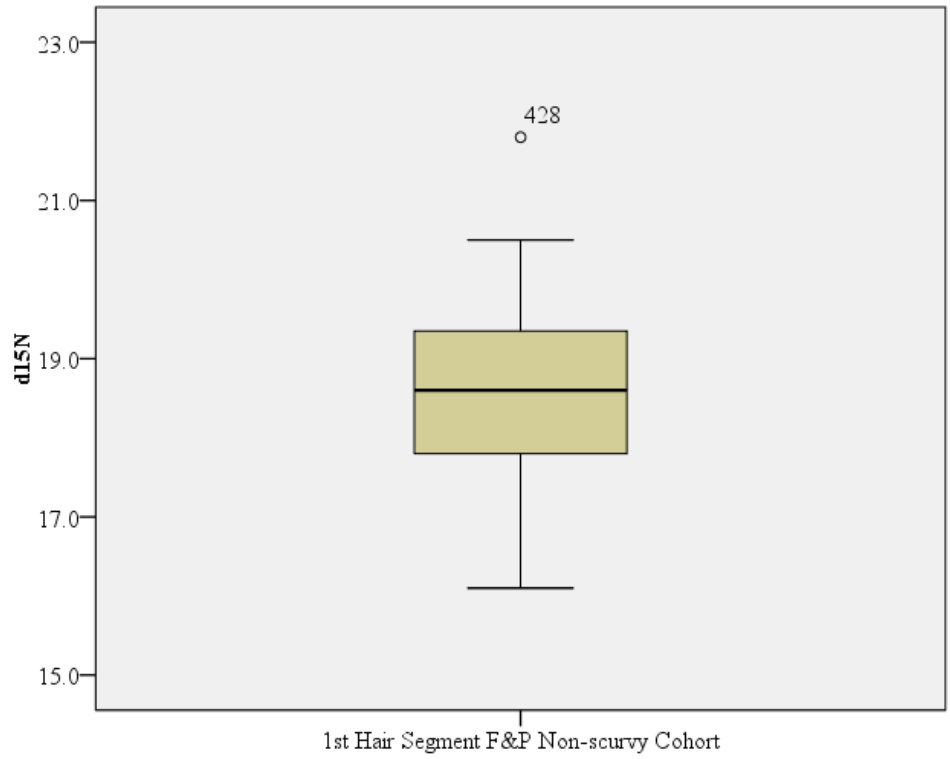

Figure 61: Box and whisker plot for $\delta^{15}N$ indicating the outlier for the F&P overall (non-scurvy)first hair segment non-scurvy cohort.

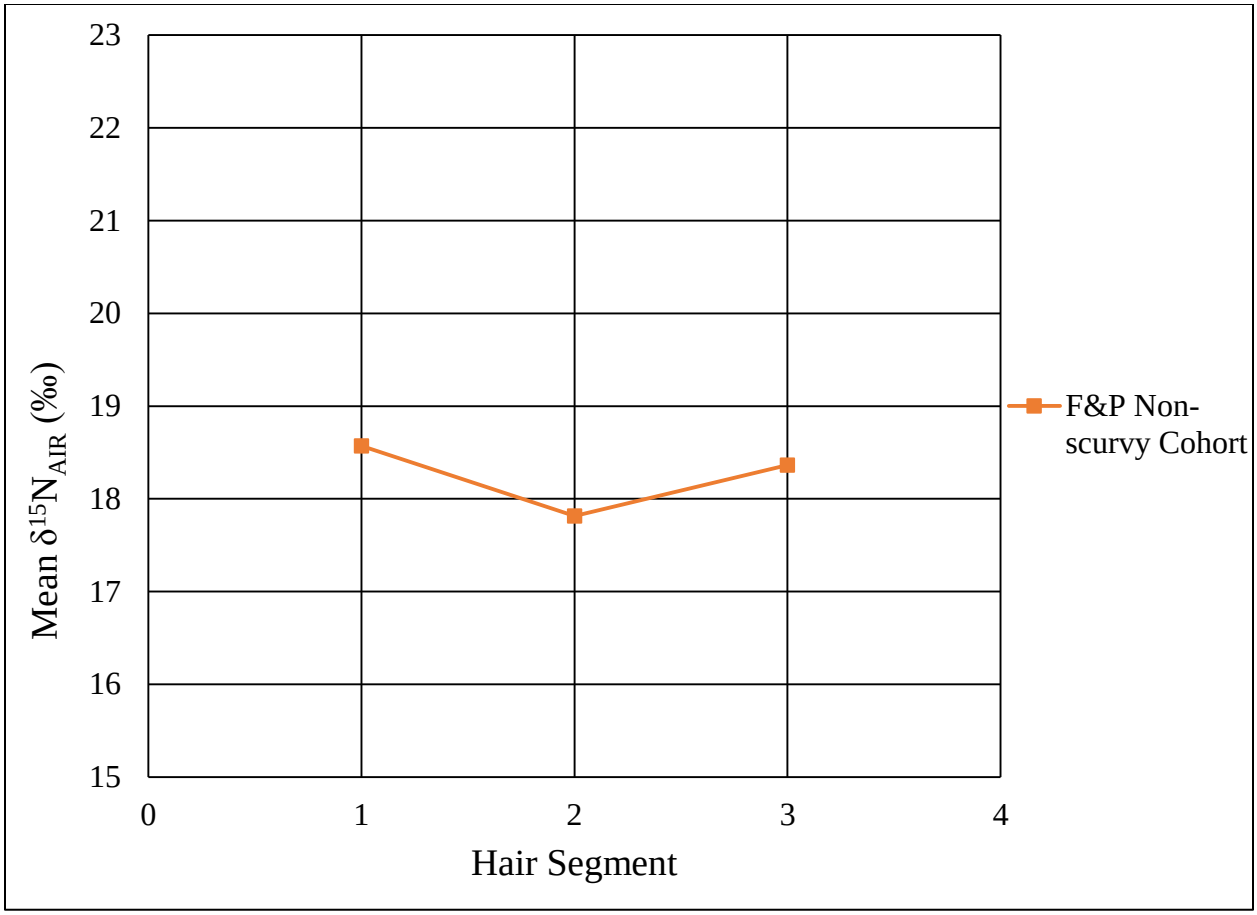

Figure 62: Averaged $\delta^{15}N$ values for each hair segment of the F&P cohort showing trends in the last three months of life.

The neonatal cohort first, second, and third hair segments were represented by 41, 16, and five scurvy and/or non-scurvy juveniles, respectively. The $\delta^{15}N$ values for the overall first hair segment ranted from 16.2‰ to 23.6‰, with a mean value of 19.7 ± 1.6‰. The $\delta^{15}N$ values for the scurvy cohort (n = 7) ranged from 16.2‰ to 23.6‰, with a mean value of 19.7 ± 1.6‰. The $\delta^{15}N$ values for the non-scurvy cohort (n = 34) ranged from 18.5‰ to 22.1‰, with a mean value of 20.1 ± 1.2‰. There was no statistically significant difference between the mean scurvy and non-scurvy $\delta^{15}N$ values for the neonatal first hair segment samples (p = 0.499) (Appendix G).

The scatter plot of all juveniles for the neonatal first hair segment can be found in Appendix H (Figure 95).

The $\delta^{15}N$ values for the neonatal overall second hair segment ranged from 16.7‰ to 23.4‰, with a mean value of 19.8 ± 1.7‰. The $\delta^{15}N$ values for the scurvy cohort (n = 4) ranged from 18.5‰ to 22.0‰, with a mean value of 20.0 ± 1.5‰. The $\delta^{15}N$ values for the non-scurvy cohort (n = 12) ranged from 16.7‰ to 23.4‰, with a mean value of 19.7 ± 1.9‰. There was no statistically significant difference between the mean scurvy and non-scurvy $\delta^{15}N$ values for the neonatal second hair segment samples (p = 0.627) (Appendix G). The scatter plot of all juveniles for the neonatal second hair segment can be found in Appendix H (Figure 95)

The $\delta^{15}N$ values for the overall (non-scurvy) third hair segment (n = 5) ranged from 18.0‰ to 20.8‰, with a mean value of 19.0 ± 1.4‰. The scatter plot of all juveniles for the neonatal third hair segment can be found in Appendix H (Figure95).

The neonatal cohort for each hair segment was also averaged in order to show trends in $\delta^{15}N$ values for this cohort over the last three months of life. The scurvy cohort shows a slight increase in $\delta^{15}N$ values in the last two months of life, while the non-scurvy cohort shows an increase in $\delta^{15}N$ values between the third and second months and a slight decrease from the second to the last month of life (Figure 63). The difference between the scurvy second and first hair segment was not statistically significant (p = 0.704). The difference between the non-scurvy third and second hair segment was not statistically significant (p = 0.398). The difference between the non-scurvy second and first hair segment was not statistically significant (p = 0.960). The difference between the non-scurvy third and first hair segment was not statistically significant (p = 0.424).

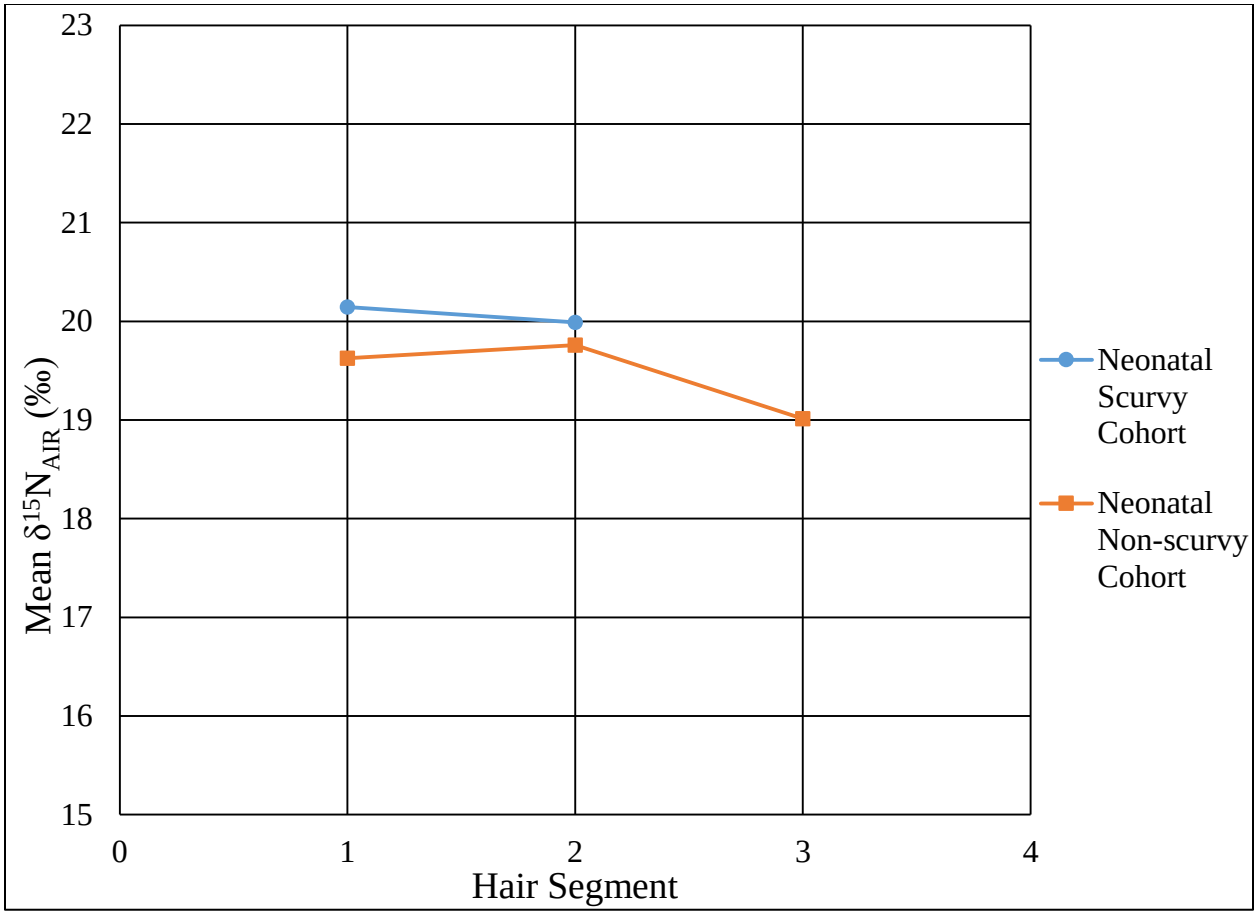

Figure 63: Averaged $\delta^{15}N$ values for each hair segment of the neonatal scurvy and non-scurvy cohorts showing trends in the last three months of life.

The C1 cohort first, second, and third hair segments were represented by 30, 23, and 15 scurvy and non-scurvy juveniles, respectively. The $\delta^{15}N$ values for the overall first hair segment ranged from 15.1‰ to 21.9‰, with a mean value of 18.5 ± 1.7‰. The $\delta^{15}N$ values for the scurvy cohort (n = 7) ranged from 15.2‰ to 20.8‰, with a mean value of 18.0 ± 2.1‰. The $\delta^{15}N$ values for the non-scurvy cohort (n = 23) ranged from 15.1‰ to 21.9‰, with a mean value of 18.7 ± 1.6‰. There was no statistically significant difference between the mean scurvy and non-scurvy $\delta^{15}N$ values for the C1 first hair segment samples (p = 0.418) (Appendix G). The scatter plot of all juveniles for the C1 first hair segment can be found in Appendix H (Figure 96).

The $\delta^{15}N$ values for the overall second hair segment ranged from 15.3‰ to 21.9‰, with a mean value of 18.3 ±‰1.6. The $\delta^{15}N$ values for the scurvy cohort (n = 5) ranged from 15.8‰ to 19.7‰, with a mean value of 17.8 ± 1.7‰. The $\delta^{15}N$ values for the non-scurvy cohort (n = 18) ranged from 15.3‰ to 21.9‰, with a mean value of 18.5 ± 1.6‰. There was no statistically significant difference between the mean scurvy and non-scurvy $\delta^{15}N$ values for the C1 second hair segment samples (p = 0.502) (Appendix G). The scatter plot of all juveniles for the C1 second hair segment can be found in Appendix H (Figure 96).

The $\delta^{15}N$ values for the overall third hair segment ranged from 16.3‰ to 21.8‰, with a mean value of 18.8 ± 1.5‰. The $\delta^{15}N$ values for the scurvy cohort (n = 3) ranged from 16.3‰ to 19.9‰, with a mean value of 18.5 ± 1.9‰. The $\delta^{15}N$ values for the non-scurvy cohort (n = 12) ranged from 16.6‰ to 21.8‰, with a mean value of 18.8 ± 1.4‰. There was no statistically significant difference between the mean scurvy and non-scurvy $\delta^{15}N$ values for the C1 third hair segment samples (p = 0.772) (Appendix G). The scatter plot of all juveniles for the C1 third hair segment can be found in Appendix H (Figure 96).

The C1 cohort for each hair segment was also averaged in order to create a plot showing the trend in $\delta^{15}N$ values for this cohort over the last three months of life. Both the scurvy and non-scurvy cohorts show a decrease in $\delta^{15}N$ values between the third and second months and a slight increase in $\delta^{15}N$ values between the second and the last month of life (Figure 64). The difference between the scurvy third and second hair segments was not statistically significant (p = 0.655). The difference between the scurvy second and first hair segments was not statistically significant (p = 0.871). The difference between the non-scurvy third and second hair segments

was not statistically significant (p = 0.498). The difference between the non-scurvy second and first hair segments was not significant (p = 0.430).

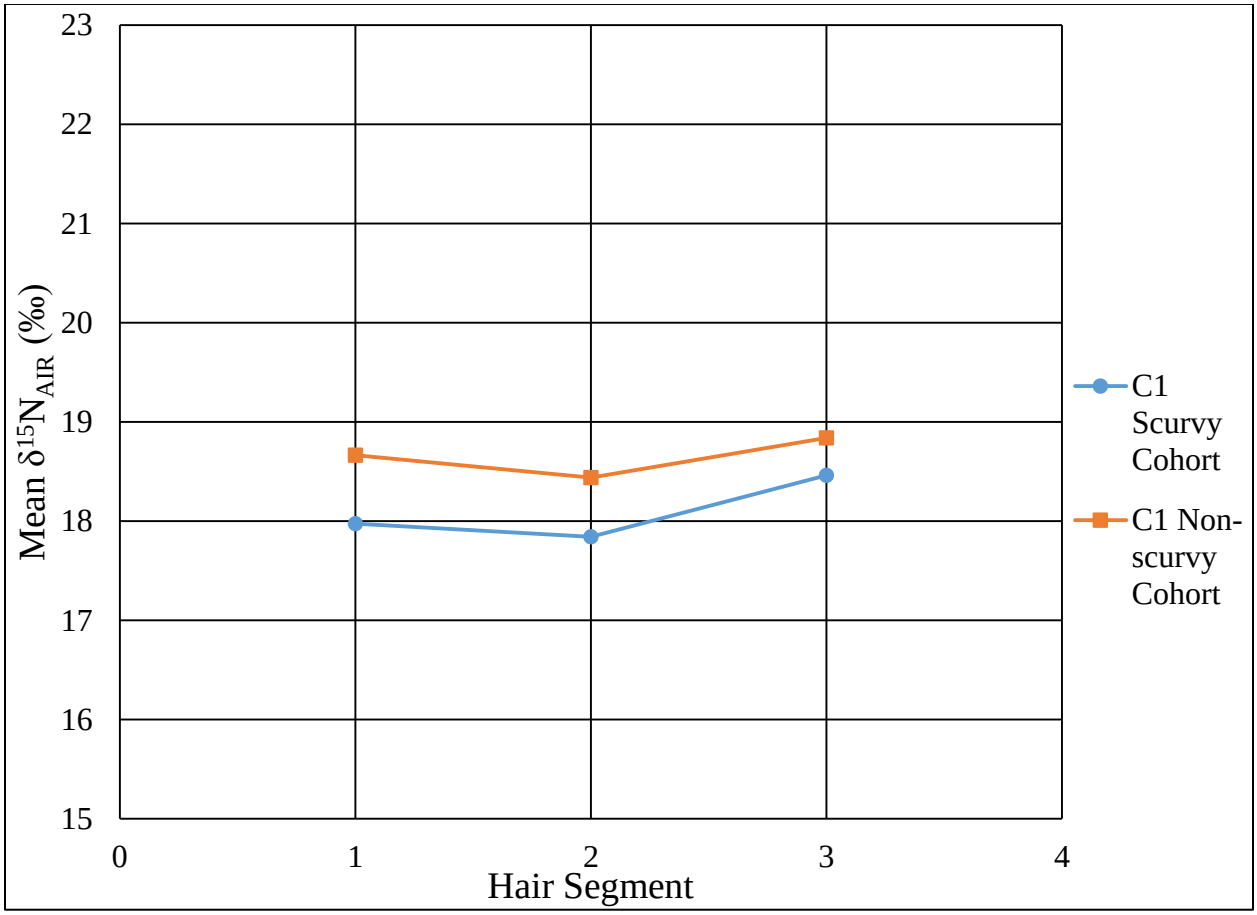

Figure 64: Averaged $\delta^{15}N$ values for each hair segment of the C1 scurvy and non-scurvy cohorts showing trends in the last three months of life.

The C2 cohort first, second, and third hair segments were represented by 15, ten, and eight scurvy and non-scurvy juveniles, respectively. The $\delta^{15}N$ values for the overall first hair segment ranged from 15.3‰ to 20.5‰, with a mean value of 17.5 ± 1.3‰. One outlier (burial 163) was present in this cohort with a more enriched $\delta^{15}N$ value (Figure 65). The $\delta^{15}N$ values for the scurvy cohort (n = 4) ranged from 16.6‰ to 18.7‰, with a mean value of 17.6 ± 1.0‰. The

$\delta^{15}N$ values for the non-scurvy cohort (n = 11) ranged from 15.3‰ to 20.5‰, with a mean value of 17.4 ± 1.4‰. One outlier (burial 163) was present in this cohort with a more enriched $\delta^{15}N$ value (Figure 66). There was no statistically significant difference between the mean scurvy and non-scurvy $\delta^{15}N$ values for the C2 first hair segment samples (p = 0.557) (Appendix G). The scatter plot of all juveniles for the C2 first hair segment can be found in Appendix H (Figure 97).

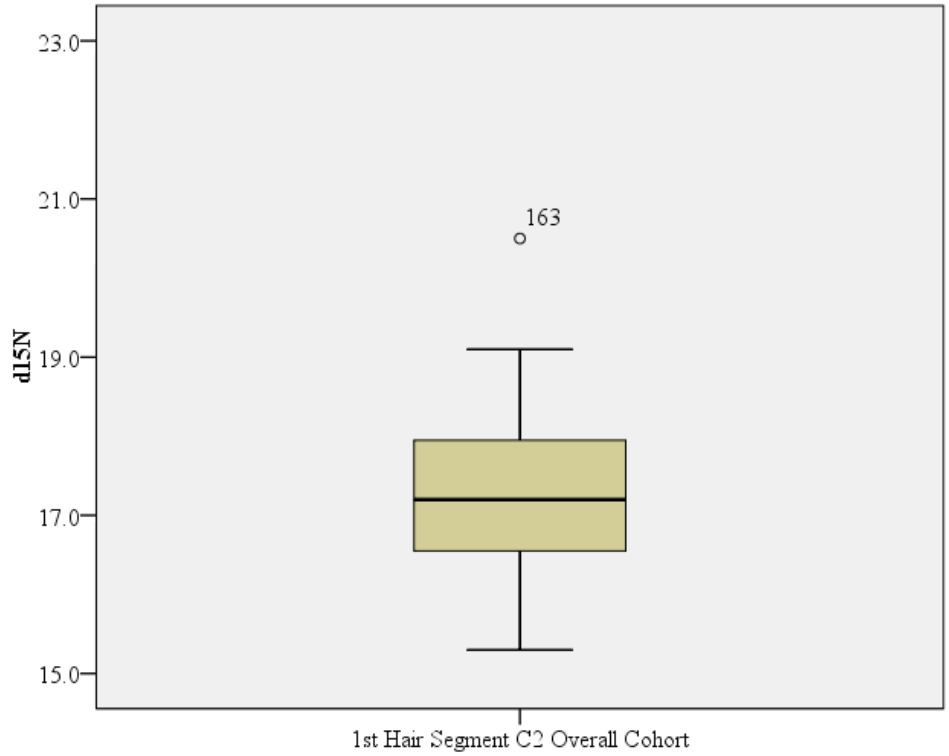

Figure 65: Box and whisker plot for $\delta^{15}N$ indicating the outlier for the C2 overall first hair segment cohort.

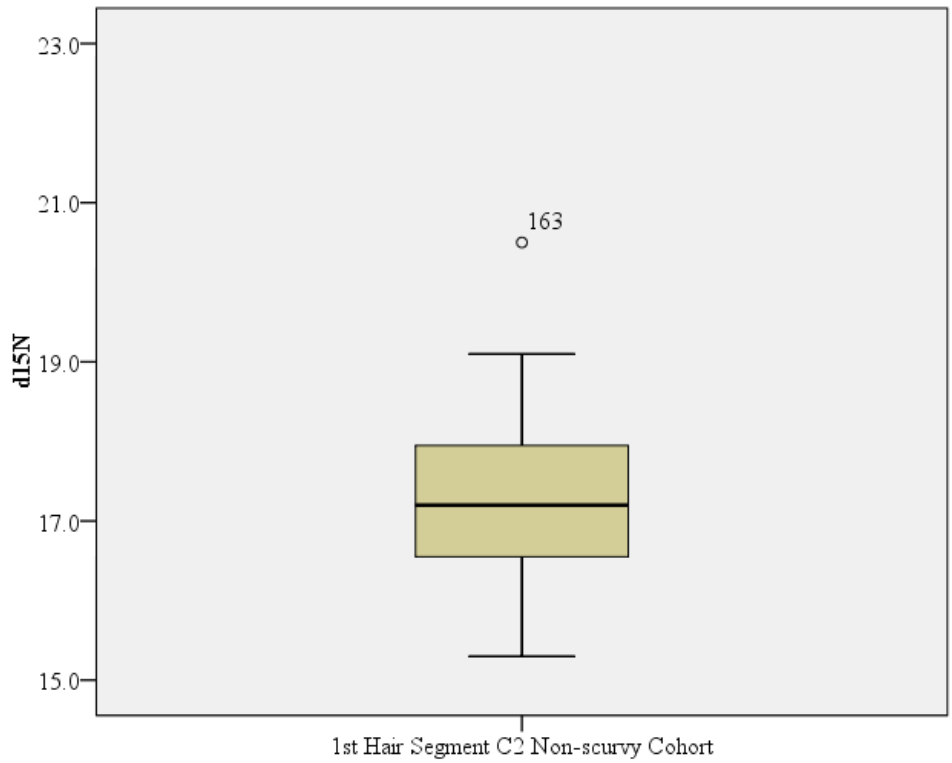

Figure 66: Box and whisker plot for $\delta^{15}N$ indicating the outlier for the C2 non-scurvy first hair segment cohort.

The $\delta^{15}N$ values for the overall second hair segment ranged from 15.9‰ to 18.4‰, with a mean value of 17.1 ± 0.9‰. The $\delta^{15}N$ values for the scurvy cohort (n = 3) ranged from 16.4‰ to 18.4‰, with a mean value of 17.1 ± 1.1‰. The $\delta^{15}N$ values for the non-scurvy cohort (n = 7) ranged from 15.9‰ to 18.2‰, with a mean value of 17.1 ± 0.8‰. There was no statistically significant difference between the mean scurvy and non-scurvy $\delta^{15}N$ values for the C2 second hair segment samples (p = 0.909) (Appendix G). The scatter plot of all juveniles for the C2 second hair segment can be found in Appendix H (Figure 97).

The $\delta^{15}N$ values for the overall third hair segment ranged from 15.5‰ to 18.7‰, with a mean value of 17.0 ± 1.1‰. The $\delta^{15}N$ values for the scurvy cohort (n = 3) ranged from 16.7‰ to 18.1‰, with a mean value of 17.2 ± 0.8‰. The $\delta^{15}N$ values for the non-scurvy cohort (n = 5)

ranged from 15.5‰ to 18.7‰, with a mean value of 16.8 ± 1.3‰. There was no statistically significant difference between the mean scurvy and non-scurvy $\delta^{15}N$ values for the C2 third hair segment samples ($p = 0.456$) (Appendix G). The scatter plot of all juveniles for the C2 third hair segment can be found in Appendix H (Figure 97).

The C2 cohort for each hair segment was also averaged in order to create a plot showing the trend in $\delta^{15}N$ values for this cohort over the last three months of life. The scurvy cohort shows a slight decrease between the third and second months and then an increase between the second and first months, while the non-scurvy cohort shows an increase over the last three months of life (Figure 67). The difference between the scurvy third and second hair segments was not statistically significant ($p = 0.513$). The difference between the scurvy second and first hair segments was not statistically significant ($p = 0.289$). The difference between the scurvy third and first hair segment is not statistically significant ($p = 0.593$). The difference between the non-scurvy third and first hair segments was not statistically significant ($p = 0.684$).

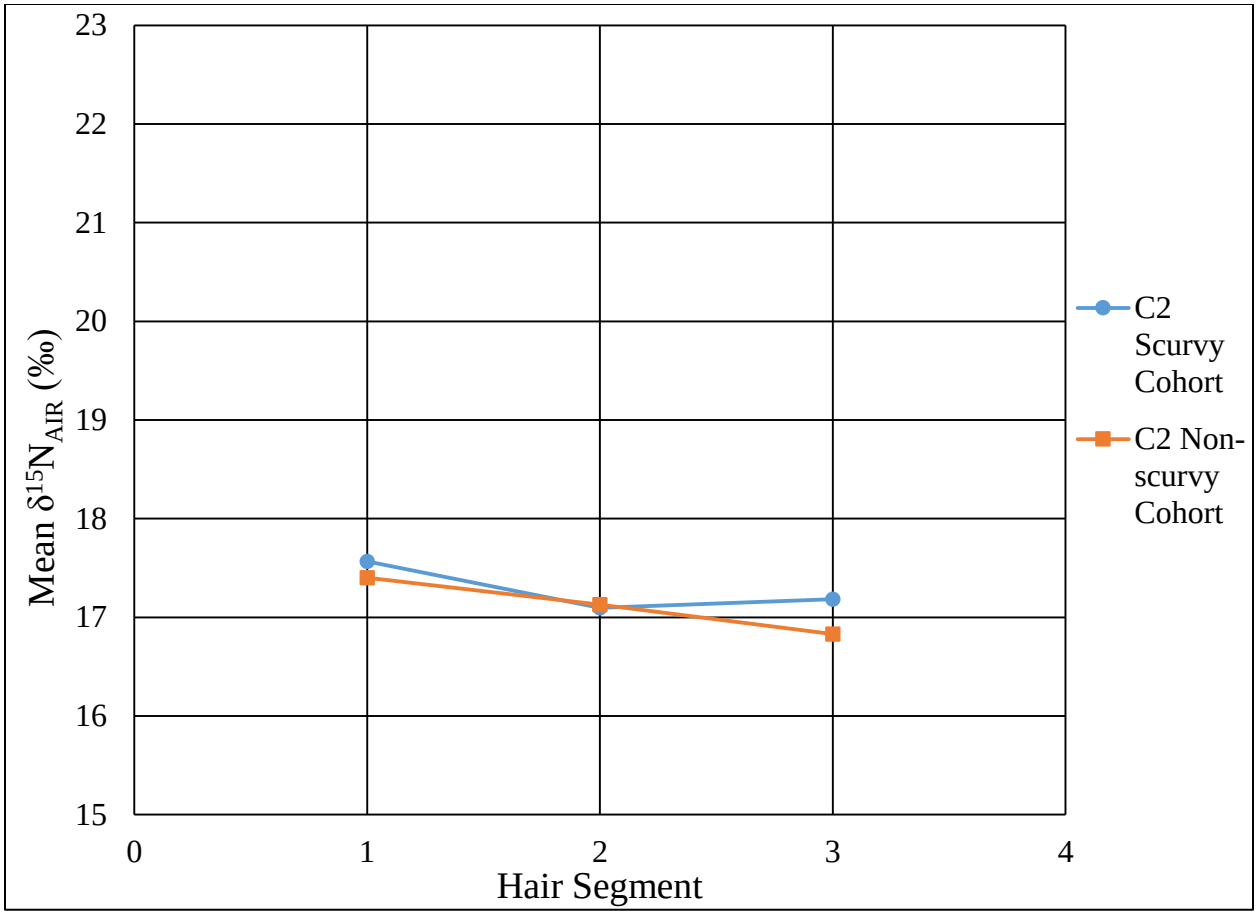

Figure 67: Averaged $\delta^{15}N$ values for each hair segment of the C2 scurvy and non-scurvy cohorts showing trends in the last three months of life.

The C3 cohort first, second, and third hair segments were represented by 11, nine, and eight scurvy and non-scurvy juveniles, respectively. The $\delta^{15}N$ values for the overall first hair segment ranged from 16.4‰ to 19.0‰, with a mean value of 17.6 ± 0.9‰. The $\delta^{15}N$ values for the scurvy cohort (n = 3) ranged from 17.1‰ to 19.0‰, with a mean value of 17.9 ± 1.0‰. The $\delta^{15}N$ values for the non-scurvy cohort (n = 8) ranged from 16.4‰ to 18.7‰, with a mean value of 17.5 ± 0.9‰. There was no statistically significant difference between the mean scurvy and non-scurvy $\delta^{15}N$ values for the C3 first hair segment samples (p = 0.357) (Appendix G). The scatter plot of all juveniles for the C3 first hair segment can be found in Appendix H (Figure 98).

The $\delta^{15}N$ values for the overall second hair segment ranged from 16.6‰ to 18.8‰, with a mean value of 17.9 ± 0.8‰. The $\delta^{15}N$ values for the scurvy cohort (n = 3) ranged from 17.0‰ to 18.8‰, with a mean value of 17.7 ± 0.9‰. The $\delta^{15}N$ values for the non-scurvy cohort (n = 6) ranged from 16.6‰ to 18.6‰, with a mean value of 18.0 ± 0.7‰. One outlier (burial 149) was present in this cohort with a less enriched $\delta^{15}N$ value (Figure 68). There was no statistically significant difference between the mean scurvy and non-scurvy $\delta^{15}N$ values for the C3 second hair segment samples (p = 0.796) (Appendix G). The scatter plot of all juveniles for the C3 second hair segment can be found in Appendix H (Figure 98).

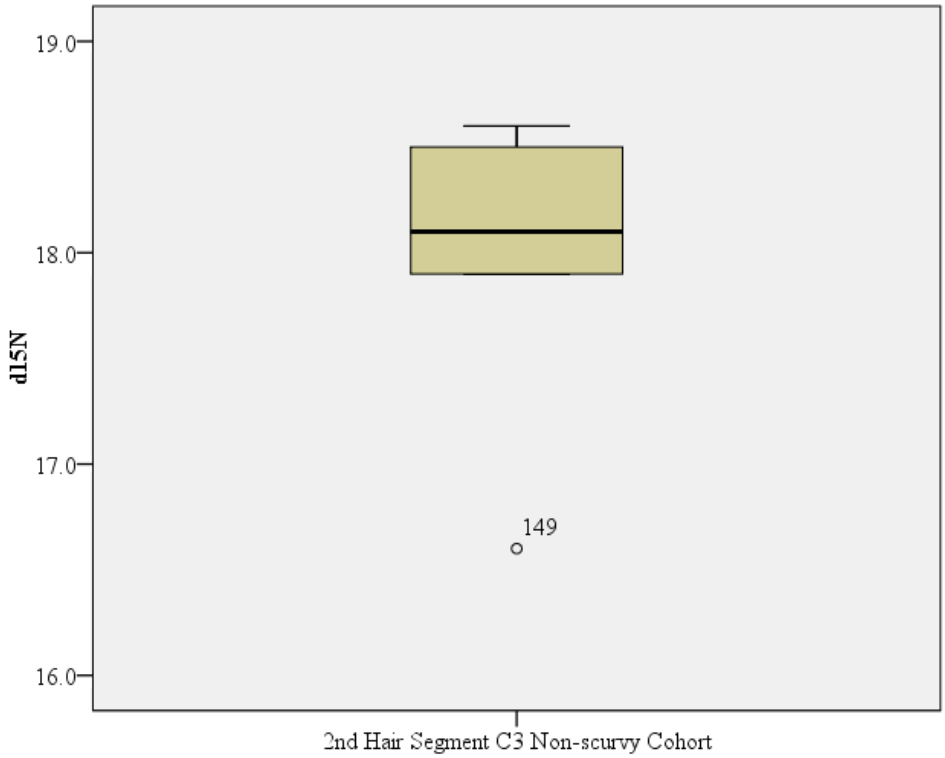

Figure 68: Box and whisker plot for $\delta^{15}N$ indicating the outlier for the C3 non-scurvy second hair segment cohort.

The $\delta^{15}N$ values for the overall third hair segment ranged from 16.8‰ to 19.0‰, with a mean value of 17.7 ± 0.6‰. One outlier (burial 239) was present in this cohort with a more enriched $\delta^{15}N$ value (Figure 69). The $\delta^{15}N$ values for the scurvy cohort (n = 2) ranged from 17.4‰ to 17.6‰, with a mean value of 17.5 ± 0.1‰. The $\delta^{15}N$ values for the non-scurvy cohort (n = 6) ranged from 16.8‰ to 19.0‰, with a mean value of 17.8 ± 0.7‰. One outlier (burial 239) was present in this cohort with a more enriched $\delta^{15}N$ value (Figure 70). There was no statistically significant difference between the mean scurvy and non-scurvy $\delta^{15}N$ values for the C3 third hair segment samples (p = 0.402) (Appendix G). The scatter plot of all juveniles for the C3 third hair segment can be found in Appendix H (Figure 98).

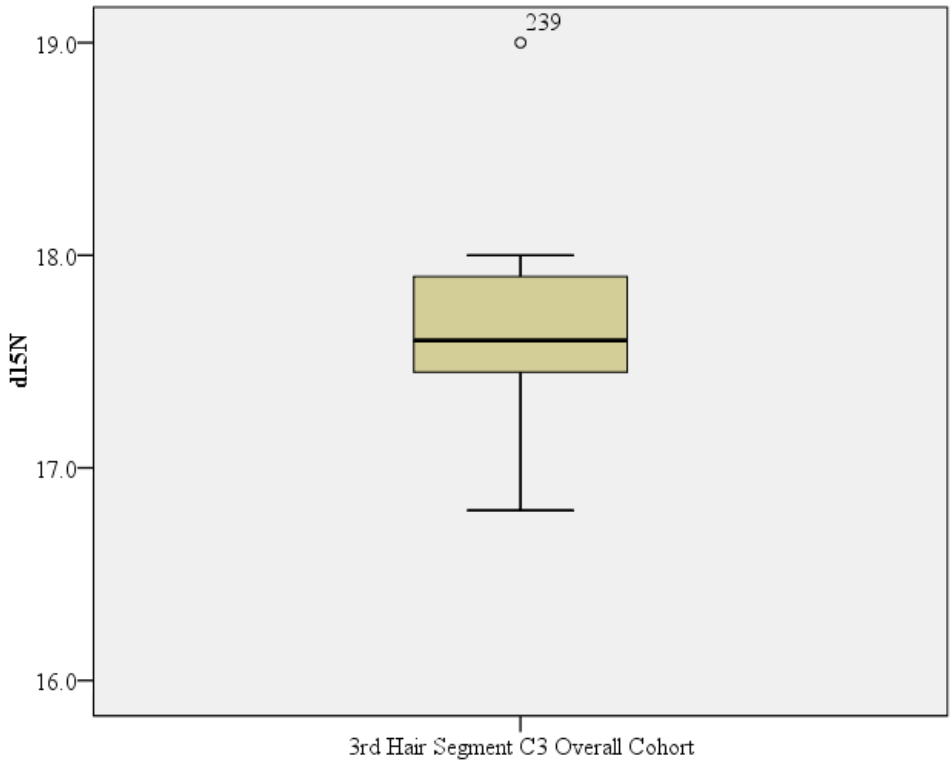

Figure 69: Box and whisker plot for $\delta^{15}N$ indicating the outlier for the C3 overall third hair segment cohort.

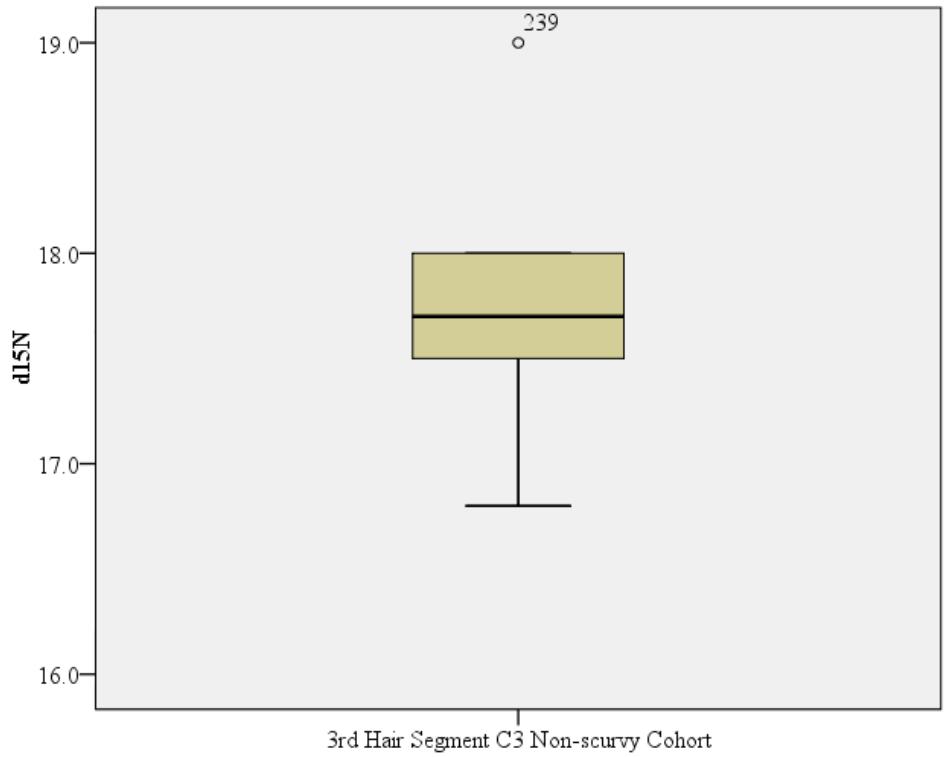

Figure 70: Box and whisker plot for $\delta^{15}N$ indicating the outlier for the C3 non-scurvy third hair segment cohort.

The C3 cohort for each hair segment was also averaged in order to create a plot showing the trend in $\delta^{15}N$ values for this cohort over the last three months of life. The scurvy cohort shows a slight increase in $\delta^{15}N$ values over the last three months of life, while the non-scurvy cohort $\delta^{15}N$ values show a slight increase from the third to second months and a decrease from the second to the last month of life (Figure 71). The difference between the scurvy third and first hair segments was not statistically significant ($p = 1.000$). The difference between the non-scurvy third and second hair segments was not statistically significant ($p = 0.378$). The difference between the non-scurvy second and first hair segments was not statistically significant ($p = 0.438$). The difference between the non-scurvy third and first hair segments was not statistically significant ($p = 0.401$).

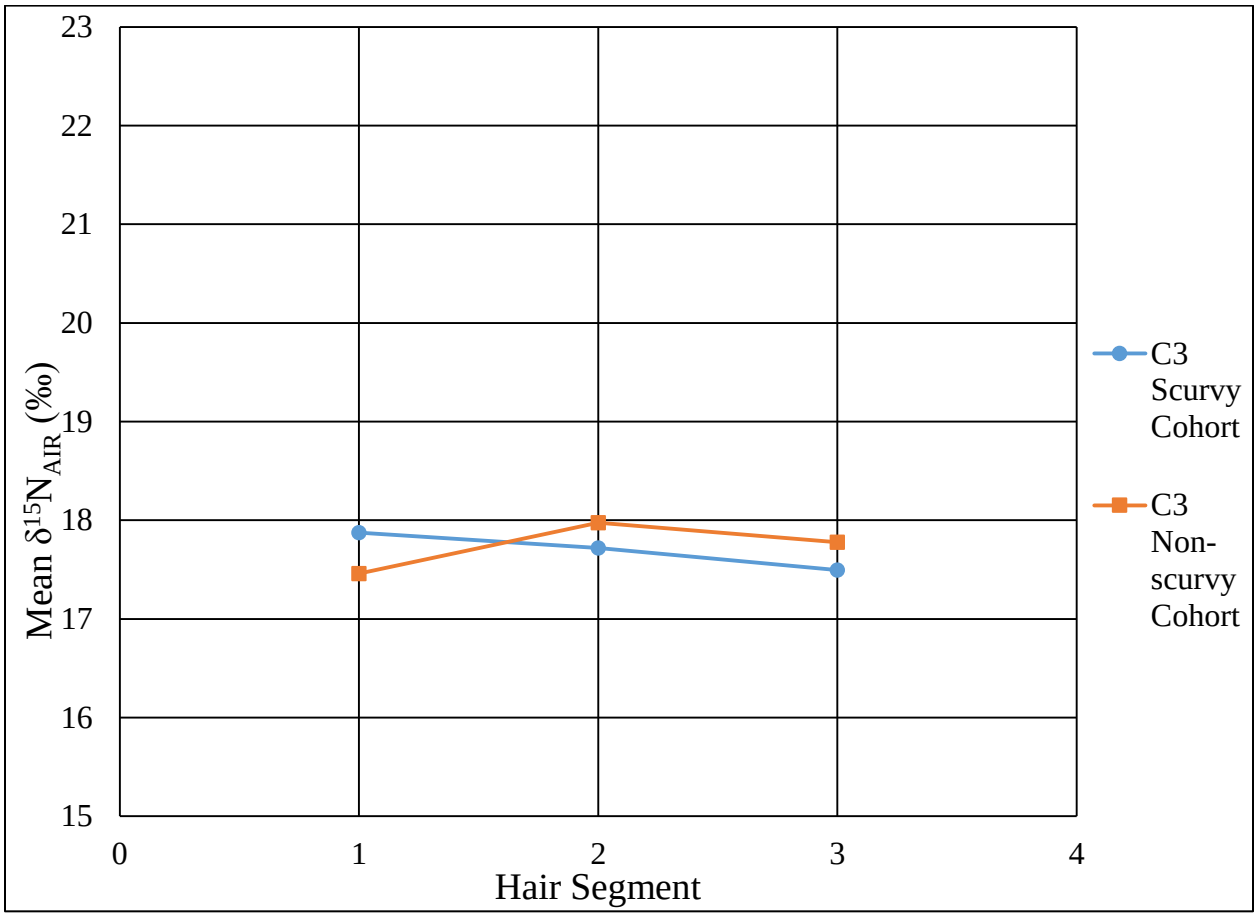

Figure 71: Averaged $\delta^{15}N$ values for each hair segment of the C3 scurvy and non-scurvy cohorts showing trends in the last three months of life.

Nail

A total of 54 individuals represented by proximal nail samples were analyzed for $\delta^{15}N$ values. The descriptive statistics (mean, minimum, maximum, and standard deviation) were calculated for the proximal nail segments separately. The descriptive statistics for $\delta^{15}N$ values

from the nails can be found in Table 36. The $\delta^{15}N$ values for proximal nail segments can be found in Appendix E (Table 58).

Table 36: Descriptive statistics for $\delta^{15}N$ values for the proximal nail segment. Each category's statistics are first presented as an overall representation, followed by those individuals who exhibited skeletal indicators of scurvy and those who did not. Entries of "-" indicate not enough data available to calculate the statistic.

		N	Mean	Min	Max	Standard Deviation
Entire Sample	**Overall**	54	20.0	15.5	24.5	1.7
	Scurvy	10	19.7	17.8	21.9	1.5
	Non-scurvy	44	20.0	15.5	24.5	1.8
Fetal & Perinatal	**Overall**	-	-	-	-	-
	Scurvy	-	-	-	-	-
	Non-scurvy	4	19.3	17.2	21.2	1.6
Neonatal	**Overall**	18	21.0	18.8	22.3	1.1
	Scurvy	3	20.9	20.2	21.9	0.9
	Non-scurvy	15	21.0	18.8	22.3	1.1
C1	**Overall**	18	20.0	15.5	24.5	2.0
	Scurvy	4	20.1	18.1	21.1	1.4
	Non-scurvy	14	20.0	15.5	24.5	2.2
C2	**Overall**	10	18.5	17.7	20.9	0.9
	Scurvy	2	18.3	17.8	18.7	0.6
	Non-scurvy	8	18.6	17.7	20.9	1.0
C3	**Overall**	4	19.5	17.9	20.6	1.3
	Scurvy	1	17.9	-	-	-
	Non-scurvy	3	20.0	18.8	20.6	1.0

The $\delta^{15}N$ values for the proximal nail segment of the entire sample (n = 54) ranged from 15.5‰ to 24.5‰, with a mean value of 20.0 ± 1.7‰. The ten individuals who exhibited skeletal indicators of scurvy had $\delta^{15}N$ values that ranged from 17.8‰ to 21.9‰, with a mean value of 19.7 ± 1.5‰. The 44 individuals who did not exhibit skeletal indicators of scurvy had $\delta^{15}N$

values that ranged from 15.5‰ to 24.5‰, with a mean value of 20.0 ± 1.8‰. There was no statistically significant difference between the mean scurvy and non-scurvy $\delta^{15}N$ values for the overall proximal nail segment samples (p = 0.518) (Appendix F). The scatter plot of $\delta^{13}C$ and $\delta^{15}N$ values for the overall proximal nail segment sample can be seen in Figure 42.

When the $\delta^{15}N$ values for the proximal nail segment were plotted by age, the younger ages exhibited a greater range while the range decreased as age increased (Figure 72). The same trend as found in hair samples in regards to increasing and decreasing average $\delta^{15}N$ values between age cohorts can be seen in the proximal nail segment cohorts (Table 37).

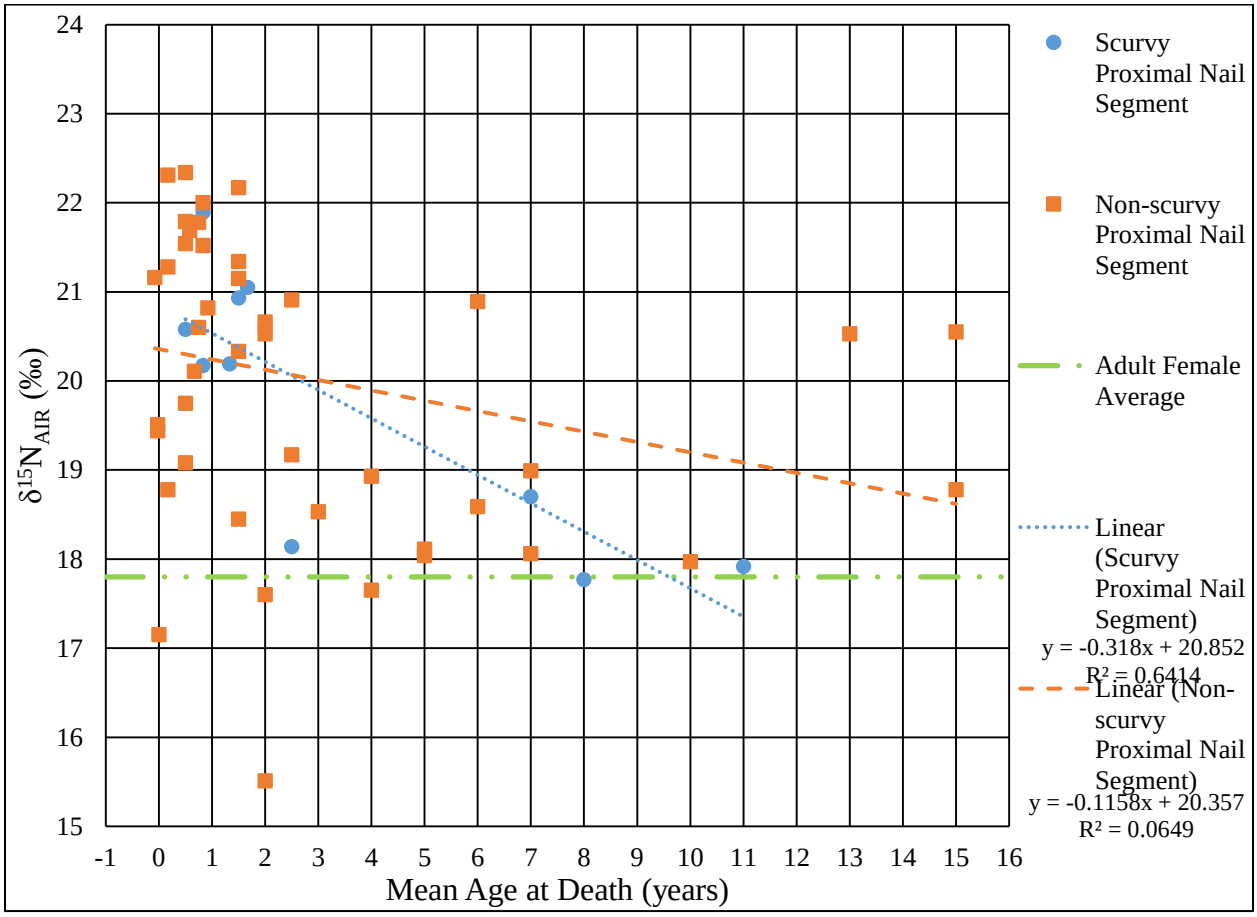

Figure 72: Proximal nail segment average $\delta^{15}N$ values plotted by mean age.

Table 37: Average $\delta^{15}N$ values, in ‰, for the proximal nail segment for each age cohort. The arrow next to the $\delta^{15}N$ values (except the F&P cohort) in each sample column indicates either a decrease (⬇) or increase (⬆) in average $\delta^{15}N$ value from the cohort above.

	Proximal Nail Segment (‰)
F&P	19.3
Neonatal	21.0⬆
C1	20.4⬇
C2	18.3⬇
C3	19.4⬆

The F&P cohort represented by the proximal nail segment consisted of four individuals, none of which exhibited skeletal indicators of scurvy. The $\delta^{15}N$ for F&P cohort ranged from 17.2‰ to 21.2‰, with a mean value of 19.3 ± 1.6‰. The scatter plot of $\delta^{13}C$ and $\delta^{15}N$ values for the F&P proximal nail segment cohort can be seen in Figure 44. The neonatal cohort represented by the proximal nail segment consisted of 18 individuals, three who exhibited skeletal indicators of scurvy and 15 who did not. The $\delta^{15}N$ for the neonatal cohort ranged from 18.8‰ to 22.3‰, with a mean value of 21.0 ± 1.1‰. The $\delta^{15}N$ values for those neonatal cohort individuals who exhibited skeletal indicators of scurvy ranged from 20.2‰ to 21.9‰, with a mean value of 20.9 ± 0.9‰. The $\delta^{15}N$ values for those neonatal cohort individuals who did not exhibit skeletal indicators of scurvy ranged from 18.8‰ to 22.3‰, with a mean value of 21.0 ± 1.1‰. There was no statistically significant difference between the mean scurvy and non-scurvy $\delta^{15}N$ values for the neonatal proximal nail segment samples ($p = 0.812$) (Appendix G). The scatter plot of $\delta^{13}C$ and $\delta^{15}N$ values for the neonatal proximal nail segment cohort can be seen in Figure 45.

The C1 cohort represented by the proximal nail segment consisted of 18 individuals, four who exhibited skeletal indicators of scurvy and 14 who did not. The $\delta^{15}N$ values for the entire C1

cohort ranged from 15.5‰ to 24.5‰, with a mean value of 20.0 ± 2.0‰. The $\delta^{15}N$ values for those C1 cohort individuals who exhibited skeletal indicators of scurvy ranged from 18.1‰ to 21.1‰, with a mean value of 20.1 ± 1.4‰. The $\delta^{15}N$ values for those C1 cohort individuals who did not exhibit skeletal indicators of scurvy ranged from 15.5‰ to 24.5‰, with a mean value of 20.0 ± 2.2‰. There was no statistically significant difference between the mean scurvy and non-scurvy $\delta^{15}N$ values for the C1 proximal nail segment samples ($p = 0.958$) (Appendix G). The scatter plot of $\delta^{13}C$ and $\delta^{15}N$ values for the C1 proximal nail segment cohort can be seen in Figure 46.

The C2 cohort represented by the proximal nail segment consisted of ten individuals, two who exhibited skeletal indicators of scurvy and eight who did not. The $\delta^{15}N$ values for the entire C2 cohort ranged from 17.7‰ to 20.9‰, with a mean value of 18.5 ± 0.9‰. The $\delta^{15}N$ values for those C2 cohort individuals who exhibited skeletal indicators of scurvy ranged from 17.8‰ to 18.7‰, with a mean value of 18.3 ± 0.6‰. The $\delta^{15}N$ values for those C2 cohort individuals who did not exhibit skeletal indicators of scurvy ranged from 17.7‰ to 20.9‰, with a mean value of 18.6 ± 1.0‰. There was no statistically significant difference between the mean scurvy and non-scurvy $\delta^{15}N$ values for the C2 proximal nail segment samples ($p = 0.793$) (Appendix G). The scatter plot of $\delta^{13}C$ and $\delta^{15}N$ values for the C2 proximal nail segment cohort can be seen in Figure 47.

The C3 cohort represented by the proximal nail segment consisted of four individuals, one who exhibited skeletal indicators of scurvy and three who did not. The $\delta^{15}N$ values for the entire C3 cohort ranged from 17.9‰ to 20.6‰, with a mean value of 19.5 ± 1.3‰. The $\delta^{15}N$ value for the C3 cohort individual who exhibited skeletal indicators of scurvy was 17.9‰. The

$\delta^{15}N$ values for those C3 cohort individuals who did exhibit with skeletal indicators of scurvy ranged from 18.8‰ to 20.6‰, with a mean value of 20.0 ± 1.0‰. There was no statistically significant difference between the mean scurvy and non-scurvy $\delta^{15}N$ values for the C3 proximal nail segment samples ($p = 0.180$) (Appendix G). The scatter plot of $\delta^{13}C$ and $\delta^{15}N$ values for the C3 proximal nail segment cohort can be seen in Figure 48.

Skin

A total of 78 skin samples, each representing one individual, were analyzed for $\delta^{15}N$ values. All descriptive statistics for $\delta^{15}N$ values from skin can be found in Table 38. The $\delta^{15}N$ values of skin for applicable individuals can be found in Appendix E (Table 59).

Table 38: Descriptive statistics for $\delta^{15}N$ values for skin. Each category's statistics are first presented as an overall representation, followed by those individuals who exhibited skeletal indicators of scurvy and those who did not. Entries of "-" indicate not enough data available to calculate the statistic.

		N	Mean	Min	Max	Standard Deviation
Entire Sample	**Overall**	78	21.1	17.8	24.7	1.3
	Scurvy	19	21.1	18.7	22.5	1.1
	Non-scurvy	59	21.1	17.8	24.7	1.4
F&P	**Overall**	9	19.7	17.8	20.9	1.0
	Scurvy	1	18.7	-	-	-
	Non-scurvy	8	19.9	17.8	20.9	1.0
Neo	**Overall**	28	21.2	19.1	24.7	1.2
	Scurvy	5	21.5	20.4	22.5	0.8
	Non-scurvy	23	21.2	19.1	24.7	1.3
C1	**Overall**	22	21.4	18.2	23.4	1.2
	Scurvy	6	21.6	20.2	22.5	0.9
	Non-scurvy	16	21.4	18.2	23.4	1.4
C2	**Overall**	11	21.5	18.8	23.5	1.2
	Scurvy	4	20.4	18.8	21.2	1.1
	Non-scurvy	7	22.1	20.8	23.5	0.9
C3	**Overall**	8	21.0	19.5	23.9	1.3
	Scurvy	3	21.1	20.7	21.5	0.4
	Non-scurvy	5	21.0	19.5	23.9	1.7

The $\delta^{15}N$ values for skin of the overall sample ranged from 17.8‰ to 24.7‰, with a mean value of 21.1 ± 1.3‰. Of the 78 individuals whose skin was analyzed, a total of 19 individuals exhibited skeletal indicators of scurvy. The $\delta^{15}N$ values for this cohort ranged from 18.7‰ to 22.5‰, with a mean value of 21.1 ± 1.1‰. The remaining 59 individuals did not exhibit skeletal indicators of scurvy. The $\delta^{15}N$ values for this second cohort ranged from 17.8‰ to 24.7‰, with a mean value of 21.1 ± 1.4‰. There was no statistically significant difference between the mean scurvy and non-scurvy $\delta^{15}N$ values for the overall skin samples ($p = 0.907$)

(Appendix F). The scatter plot of $\delta^{13}C$ and $\delta^{15}N$ values for the overall skin sample can be seen in Figure 49.

When the $\delta^{15}N$ values for skin were plotted by age, there was again less adherence to any trend seen (Figure 73). While the range of $\delta^{15}N$ values decreases as age increases, the individual $\delta^{15}N$ values are much more widely dispersed from both their respective scurvy and non-scurvy linear trend lines and the adult female average.

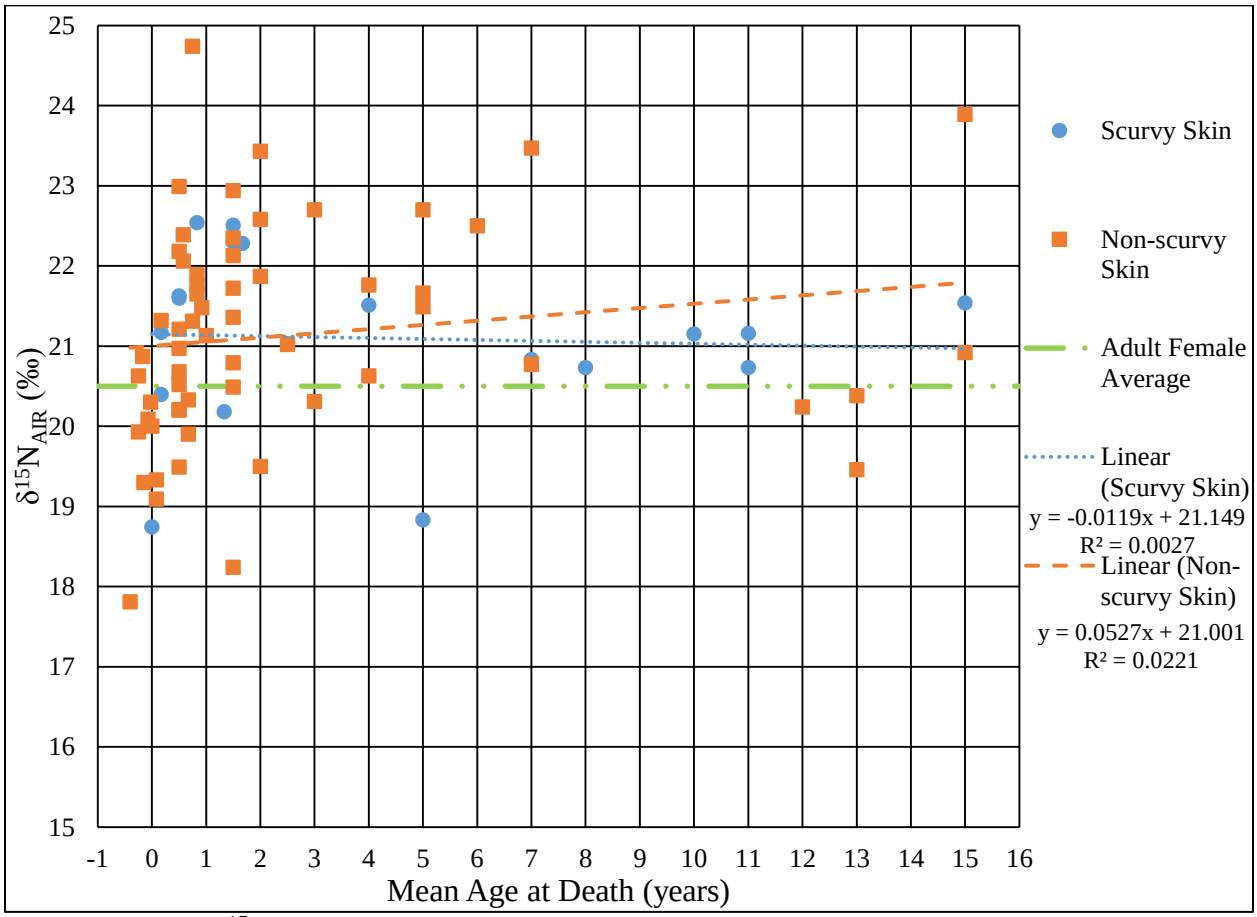

Figure 73: Skin $\delta^{15}N$ values plotted by mean age.

The $\delta^{15}N$ values for skin were again divided into age at death cohorts. The F&P cohort represented by skin consisted of nine individuals, one who exhibited skeletal indicators of scurvy

and eight who did not. The $\delta^{15}N$ values for F&P cohort ranged from 17.8‰ to 20.9‰, with a mean value of 19.7 ± 1.0‰. The $\delta^{15}N$ value for the F&P cohort individual who exhibited skeletal indicators of scurvy was 18.7‰. The $\delta^{15}N$ values for those F&P cohort individuals who did not exhibit skeletal indicators of scurvy ranged from 17.8‰ to 20.9‰, with a mean value of 19.9 ± 1.0‰. There was no statistically significant difference between the mean scurvy and non-scurvy $\delta^{15}N$ values for the F&P skin samples ($p = 0.245$) (Appendix G). The scatter plot of $\delta^{13}C$ and $\delta^{15}N$ values for the F&P skin cohort can be seen in Figure 51. The neonatal cohort represented by skin consisted of 28 individuals, five who exhibited skeletal indicators of scurvy and 23 who did not. The $\delta^{15}N$ for the entire neonatal cohort ranged from 19.1‰ to 24.7‰, with a mean value of 21.2 ± 1.2‰. The $\delta^{15}N$ values for those neonatal cohort individuals who exhibited skeletal indicators of scurvy ranged from 20.4‰ to 22.5‰, with a mean value of 21.5 ± 0.8‰. The $\delta^{15}N$ values for those neonatal cohort individuals who did not exhibit skeletal indicators of scurvy ranged from 19.1‰ to 24.7‰, with a mean value of 21.2 ± 1.3‰. There was no statistically significant difference between the mean scurvy and non-scurvy $\delta^{15}N$ values for the neonatal skin samples ($p = 0.471$) (Appendix G). The scatter plot of $\delta^{13}C$ and $\delta^{15}N$ values for the neonatal skin cohort can be seen in Figure 52.

The C1 cohort represented by skin consisted of 22 individuals, six who exhibited skeletal indicators of scurvy and 16 who did not. The $\delta^{15}N$ values for the entire C1 cohort ranged from 18.2‰ to 23.4‰, with a mean value of 21.4 ± 1.2‰. The $\delta^{15}N$ values for those C1 cohort individuals who exhibited skeletal indicators of scurvy ranged from 20.2‰ to 22.5‰, with a mean value of 21.6 ± 0.9‰. The $\delta^{15}N$ values for those C1 cohort individuals who did not exhibit skeletal indicators of scurvy ranged from 18.2‰ to 23.4‰, with a mean value of 21.4 ± 1.4‰.

There was no statistically significant difference between the mean scurvy and non-scurvy $\delta^{15}N$ values for the C1 skin samples ($p = 0.854$) (Appendix G). The scatter plot of $\delta^{13}C$ and $\delta^{15}N$ values for the C1 skin cohort can be seen in Figure 53.

The C2 cohort represented by skin consisted of 11 individuals, four who exhibited skeletal indicators of scurvy and seven who did not. The $\delta^{15}N$ values for the entire C2 cohort ranged from 18.8‰ to 23.5‰, with a mean value of 21.5 ± 1.2‰. The $\delta^{15}N$ values for those C2 cohort individuals who exhibited skeletal indicators of scurvy ranged from 18.8‰ to 21.2‰, with a mean value of 20.4 ± 1.1‰. The $\delta^{15}N$ values for those C2 cohort individuals who did not exhibit skeletal indicators of scurvy ranged from 20.8‰ to 23.5‰, with a mean value of 22.1 ± 0.9‰. There was a statistically significant difference between the mean scurvy and non-scurvy $\delta^{15}N$ values for the C2 skin samples ($p = 0.018$) (Appendix G). The scatter plot of $\delta^{13}C$ and $\delta^{15}N$ values for the C2 skin cohort can be seen in Figure 54.

The C3 cohort represented by skin consisted of eight individuals, three who exhibited skeletal indicators of scurvy and five who did not. The $\delta^{15}N$ values for the entire C3 cohort ranged from 19.5‰ to 23.9‰, with a mean value of 21.0 ± 1.3‰. The $\delta^{15}N$ values for those C3 cohort individuals who exhibited skeletal indicators of scurvy ranged from 20.7‰ to 21.5‰, with a mean value of 21.1 ± 0.4‰. The $\delta^{15}N$ values for those C3 cohort individuals who did not exhibit skeletal indicators of scurvy ranged from 19.5‰ to 23.9‰, with a mean value of 21.0 ± 1.7‰. There was no statistically significant difference between the mean scurvy and non-scurvy $\delta^{15}N$ values for the C3 skin samples ($p = 0.297$) (Appendix G). The scatter plot of $\delta^{13}C$ and $\delta^{15}N$ values for the C3 skin cohort can be seen in Figure 55.

Intra-tissue $\delta^{15}N$ Differences between Scurvy and Non-Scurvy Cohorts

The differences between mean $\delta^{15}N$ values of the scurvy and non-scurvy subsamples within each tissue and age cohort were compared for significant differences. The differences can be found in Tables 39-44 .The difference in mean $\delta^{15}N$ values between the overall bone collagen scurvy and non-scurvy samples was -0.4‰. The difference in mean $\delta^{15}N$ values between the F&P bone collagen scurvy and non-scurvy samples was -0.2‰. The difference in mean $\delta^{15}N$ values between the neonatal bone collagen scurvy and non-scurvy samples was -1.4‰. The difference in mean $\delta^{15}N$ values between the C1 bone collagen scurvy and non-scurvy samples was -0.3‰. The difference in mean $\delta^{15}N$ values between the C2 bone collagen scurvy and non-scurvy samples was 0.7‰. The difference in mean $\delta^{15}N$ values between the C3 bone collage scurvy and non-scurvy samples was 0.8‰.

Table 39: Differences between mean $\delta^{15}N$ values of the scurvy and non-scurvy bone collagen samples, both as an overall sample and within each age cohort.

	Scurvy Samples		Non-Scurvy Samples		Δ Scurvy - Non-Scurvy
Age Cohort	Number of Individuals	Mean $\delta^{15}N$ (‰)	Number of Individuals	Mean $\delta^{15}N$ (‰)	Mean $\delta^{15}N$ (‰)
Overall	11	18.7	13	19.1	-0.4
F&P	1	19.0	1	19.2	-0.2
Neonatal	2	20.4	2	21.8	-1.4
C1	3	19.0	7	19.3	-0.3
C2	3	17.7	2	17.0	0.7
C3	2	18.0	1	17.2	0.8

The difference in mean $\delta^{15}N$ values between the overall first hair segment scurvy and non-scurvy samples was -0.1‰. The difference in mean $\delta^{15}N$ values between the neonatal first hair segment scurvy and non-scurvy samples was 0.4‰. The difference in mean $\delta^{15}N$ values

between the C1 first hair segment scurvy and non-scurvy samples was -0.6‰. The difference in mean $\delta^{15}N$ values between the C2 first hair segment scurvy and non-scurvy samples was 0.1‰. The difference in mean $\delta^{15}N$ values between the C3 first hair segment scurvy and non-scurvy samples was 0.4‰.

Table 40 Differences between mean $\delta^{15}N$ values of the scurvy and non-scurvy first hair segment samples, both as an overall sample and within each age cohort.

	Scurvy Samples		Non-Scurvy Samples		Δ Scurvy - Non-Scurvy
Age Cohort	Number of Individuals	Mean $\delta^{15}N$ (‰)	Number of Individuals	Mean $\delta^{15}N$ (‰)	Mean $\delta^{15}N$ (‰)
Overall	21	18.6	111	18.7	-0.1
F&P	-	-	38	18.6	-
Neonatal	7	20.1	31	19.7	0.4
C1	7	18.0	24	18.6	-0.6
C2	4	17.6	10	17.5	0.1
C3	3	17.9	8	17.5	0.4

The difference in mean $\delta^{15}N$ values between the overall second hair segment scurvy and non-scurvy samples was -0.2‰. The difference in mean $\delta^{15}N$ values between the neonatal second hair segment scurvy and non-scurvy samples was 0.1‰. The difference in mean $\delta^{15}N$ values between the C1 second hair segment scurvy and non-scurvy samples was -0.6‰. The difference in mean $\delta^{15}N$ values between the C2 second hair segment scurvy and non-scurvy samples was 0.7‰. The difference in mean $\delta^{15}N$ values between the C3 second hair segment scurvy and non-scurvy samples was 0.8‰.

Table 41: Differences between mean $\delta^{15}N$ values of the scurvy and non-scurvy second hair segment samples, both as an overall sample and within each age cohort.

	Scurvy Samples		Non-Scurvy Samples		Δ Scurvy - Non-Scurvy
Age Cohort	Number of Individuals	Mean $\delta^{15}N$ (‰)	Number of Individuals	Mean $\delta^{15}N$ (‰)	Mean $\delta^{15}N$ (‰)
Overall	15	18.2	50	18.4	-0.2
F&P	-	-	9	18.1	-
Neonatal	4	20.0	10	19.9	0.1
C1	5	17.8	19	18.4	-0.6
C2	3	17.1	6	17.1	0
C3	3	17.7	6	18.0	-0.3

The difference in mean $\delta^{15}N$ values between the overall third hair segment scurvy and non-scurvy samples was -0.5‰. Since the neonatal cohort did not include any individuals exhibiting signs of scurvy with a third hair segment, a difference could not be calculated. The difference in mean $\delta^{15}N$ values between the C1 third hair segment scurvy and non-scurvy samples was -0.1‰. The difference in mean $\delta^{15}N$ values between the C2 third hair segment scurvy and non-scurvy samples was 0.2‰. The difference in mean $\delta^{15}N$ values between the C3 third hair segment scurvy and non-scurvy samples was -0.3‰.

Table 42: Differences between mean $\delta^{15}N$ values of the scurvy and non-scurvy third hair segment samples, both as an overall sample and within each age cohort.

	Scurvy Samples		Non-Scurvy Samples		Δ Scurvy - Non-Scurvy
Age Cohort	Number of Individuals	Mean $\delta^{15}N$ (‰)	Number of Individuals	Mean $\delta^{15}N$ (‰)	Mean $\delta^{15}N$ (‰)
Overall	8	17.8	31	18.3	-0.5
F&P	-	-	5	18.6	-
Neonatal	-	-	3	19.0	-
C1	3	18.5	13	18.6	-0.1
C2	3	17.2	4	17.0	0.2
C3	2	17.5	6	17.8	-0.3

The difference in mean $\delta^{15}N$ values between the overall proximal nail segment scurvy and non-scurvy samples was -0.3‰. The difference in mean $\delta^{15}N$ values between the neonatal proximal nail segment scurvy and non-scurvy samples was -0.1‰. The difference in mean $\delta^{15}N$ values between the C1 proximal nail segment scurvy and non-scurvy samples was 0.2‰. The difference in mean $\delta^{15}N$ values between the C2 proximal nail segment scurvy and non-scurvy samples was -0.3‰. The difference in mean $\delta^{15}N$ values between the C3 proximal nail segment scurvy and non-scurvy samples was -2.1‰.

Table 43: Differences between mean $\delta^{15}N$ values of the scurvy and non-scurvy proximal nail segment samples, both as an overall sample and within each age cohort.

	Scurvy Samples		Non-Scurvy Samples		Δ Scurvy - Non-Scurvy
Age Cohort	Number of Individuals	Mean $\delta^{15}N$ (‰)	Number of Individuals	Mean $\delta^{15}N$ (‰)	Mean $\delta^{15}N$ (‰)
Overall	10	19.7	44	20.0	-0.3
F&P	-	-	4	19.3	-
Neonatal	3	20.9	15	21.0	-0.1
C1	4	20.1	15	19.9	0.2
C2	2	18.3	7	18.6	-0.3
C3	1	17.9	3	20.0	-2.1

The difference in mean $\delta^{15}N$ values between the overall skin scurvy and non-scurvy samples was 0.0‰. The difference in mean $\delta^{15}N$ values between the F&P skin scurvy and non-scurvy samples was -1.2‰. The difference in mean $\delta^{15}N$ values between the neonatal skin scurvy and non-scurvy samples was 0.3‰. The difference in mean $\delta^{15}N$ values between the C1 skin scurvy and non-scurvy samples was 0.2‰. The difference in mean $\delta^{15}N$ values between the C2 skin scurvy and non-scurvy samples was -1.7‰. The difference in mean $\delta^{15}N$ values between the C3 skin scurvy and non-scurvy samples was 0.1‰.

Table 44: Differences between mean $\delta^{15}N$ values of the scurvy and non-scurvy skin samples, both as an overall sample and within each age cohort.

	Scurvy Samples		Non-Scurvy Samples		Δ Scurvy - Non-Scurvy
Age Cohort	Number of Individuals	Mean $\delta^{15}N$ (‰)	Number of Individuals	Mean $\delta^{15}N$ (‰)	Mean $\delta^{15}N$ (‰)
Overall	19	21.1	59	21.1	0
F&P	1	18.7	8	19.9	-1.2
Neonatal	5	21.5	23	21.2	0.3
C1	6	21.6	16	21.4	0.2
C2	4	20.4	7	22.1	-1.7
C3	3	21.1	5	21.0	0.1

Intra-tissue Stable Carbon and Nitrogen Isotope Values

Bone

The overall bone collagen cohorts exhibited a greater range in $\delta^{15}N$ values (5.8‰) than in $\delta^{13}C$ values (1.9‰), with the same trend being exhibited in both the scurvy and non-scurvy cohorts (3.6‰ vs. 1.3‰ and 5.8‰ vs. 1.7‰, respectively) (Table 45). Both the overall scurvy and non-scurvy cohorts cluster loosely around a linear trend line (r^2=0.526 and 0.188, respectively) (Figure 45). As $\delta^{13}C$ values increase, or become less negative, $\delta^{15}N$ values also tend to increase.

Table 45: Range of $\delta^{13}C$ and $\delta^{15}N$ values for bone collagen, with the overall, scurvy, and non-scurvy ranges. The highest range value for each grouping has been bolded and italicized.

		Bone Collagen	
		$\delta^{13}C$ (‰)	$\delta^{15}N$ (‰)
Entire Sample	Overall	1.9	***5.8***
	Scurvy	1.3	***3.6***
	Non	1.7	***5.8***
F&P	Overall	0.9	0.2
	Scurvy	-	
	Non	-	
Neo	Overall	0.6	***2.4***
	Scurvy	***0.3***	1.1
	Non	0.3	***0.9***
C1	Overall	1.7	***4.2***
	Scurvy	***1.1***	2.9
	Non	1.5	***4.2***
C2	Overall	0.4	***1.7***
	Scurvy	***0.4***	0.8
	Non	***0.2***	1.2
C3	Overall	0.4	***0.9***
	Scurvy	***0.3***	0.2
	Non	-	
"-" indicates not enough data available to calculate the $\delta^{13}C$ and $\delta^{15}N$ values ranges			

The F&P cohort for bone collagen contained only two individuals, one each from the scurvy and non-scurvy cohort. The overall F&P cohort exhibited a greater range in $\delta^{13}C$ values than in $\delta^{15}N$ values (0.9‰ and 0.2‰, respectively). With the limited data available for this age cohort, no trend line or other data regarding trends could be determined. The neonatal cohort for bone collagen contained only four individuals, two with scurvy and two without scurvy. This

cohort overall, as well as both the scurvy and non-scurvy cohorts, exhibited a greater range in $\delta^{15}N$ values than in $\delta^{13}C$ values (2.4‰ vs. 0.6‰, 1.1‰ vs. 0.3‰, and 0.9‰ vs. 0.3‰, respectively). Again, the limited data available for this cohort did not allow for trend line determinations. The overall C1 cohort, as well as the scurvy and non-scurvy cohorts, exhibited a greater range in $\delta^{15}N$ values than in $\delta^{13}C$ values (4.2‰ vs. 1.7‰, 2.9‰ vs. 1.1‰, and 4.2‰ vs. 1.5‰, respectively). Due to the small sample size (n=3) of the scurvy cohort, the trend line provides little useful information. The non-scurvy cohort, with a slightly larger sample size (n=7), loosely clusters around a trend line (r^2=0.135). As with the overall cohorts, as $\delta^{13}C$ values increase $\delta^{15}N$ values also tend to increase (Figure 14). The overall C2 cohort and both scurvy and non-scurvy cohorts exhibited a greater range in $\delta^{15}N$ values than in $\delta^{13}C$ values (1.7‰ vs. 0.4‰, 0.8‰ vs. 0.4‰, and 1.2‰ vs. 0.2‰, respectively). Small sample sizes for both the scurvy and non-scurvy cohorts (n=3 and 2, respectively) render the trend lines of minimal use (Figure 15). The overall C3 cohort contained three individuals, two with scurvy and one without scurvy. This cohort overall exhibited a greater range in $\delta^{15}N$ values than in $\delta^{13}C$ values (0.9‰ vs. 0.4‰), while the scurvy cohort exhibited the opposite (0.3‰ vs. 0.2‰). With the limited data available for this age cohort, no trend line or other data regarding trends could be determined.

Hair

All hair overall cohorts (first, second, and third hair segments) exhibited a greater range in $\delta^{15}N$ values than $\delta^{13}C$ values (Table 46). For all hair overall cohorts, the scurvy and non-scurvy cohorts loosely clustered around trend lines and as $\delta^{13}C$ values increased $\delta^{15}N$ tended to also increase (Figures 17 – 19).

Table 46: Range of $\delta^{13}C$ and $\delta^{15}N$ values for all hair sample groups (first, second, and third hair segments) with the overall, scurvy, and non-scurvy. The highest range value for each grouping has been bolded and italicized.

		1st Hair Segment		2nd Hair Segment		3rd Hair Segment	
		$\delta^{13}C$ (‰)	$\delta^{15}N$ (‰)	$\delta^{13}C$ (‰)	$\delta^{15}N$ (‰)	$\delta^{13}C$ (‰)	$\delta^{15}N$ (‰)
Entire Sample	Overall	5.0	***8.5***	2.4	***8.1***	3.3	***6.3***
	Scurvy	2.8	***6.9***	2.3	***6.2***	2.5	***3.6***
	Non-scurvy	5.0	***8.5***	2.4	***8.1***	2.5	***6.3***
F&P	Overall	-	-	-	-	-	-
	Scurvy	-	-	-	-	-	-
	Non-scurvy	2.8	***5.7***	1.5	***2.5***	1.1	***1.5***
Neo	Overall	4.7	***7.4***	1.3	***6.7***	-	-
	Scurvy	1.1	***3.6***	1.0	***3.5***	-	-
	Non-scurvy	4.7	***7.4***	1.0	***6.7***	1.7	***2.8***
C1	Overall	3.5	***6.8***	2.4	***6.6***	3.3	***5.5***
	Scurvy	0.9	***5.6***	1.6	***3.9***	2.5	***3.6***
	Non-scurvy	3.5	***6.8***	2.3	***6.6***	2.5	***5.2***
C2	Overall	1.0	***5.2***	1.3	***2.5***	1.4	***3.2***
	Scurvy	0.6	***2.1***	0.7	***2.0***	0.8	***1.4***
	Non-scurvy	1.0	***5.2***	1.3	***2.3***	1.2	***3.2***
C3	Overall	1.9	***2.6***	1.1	***2.2***	1.0	***2.2***
	Scurvy	1.6	***1.9***	1.1	***1.8***	***0.8***	0.2
	Non-scurvy	0.9	***2.3***	0.9	***2.0***	0.9	***2.2***

The F&P cohort contained only non-scurvy individuals for hair. All hair cohorts (first, second, and third hair segments) from the F&P cohort exhibited a greater range in $\delta^{15}N$ values than $\delta^{13}C$ (Table 46). As $\delta^{13}C$ values increase within the first hair segment $\delta^{15}N$ tends to decrease, however, in the second hair segment the opposite is exhibited (Figure 94). The third

hair segment contained only three individuals, therefore, no useful data regarding trends could be determined.

All hair cohorts (first, second, and third hair segments) from the neonatal cohort exhibited a greater range in $\delta^{15}N$ values than $\delta^{13}C$ (Table 46). As $\delta^{13}C$ values increase within the first and second hair segments for scurvy individuals, $\delta^{15}N$ tends to decrease, while the opposite is exhibited in the non-scurvy individuals. The third hair segment contained only non-scurvy individuals and exhibited increasing $\delta^{15}N$ values as $\delta^{13}C$ values increased (Figure 95).

All hair cohorts (first, second, and third hair segments; scurvy and non-scurvy) from the C1 cohort exhibited a greater range in $\delta^{15}N$ values than $\delta^{13}C$ (Table 46). As $\delta^{13}C$ values increased for all groupings $\delta^{15}N$ tended to also increase. The scurvy cohort for the third hair segment contained only three individuals, therefore, no useful data regarding trends could be determined.

All hair cohorts (first, second, and third hair segments; scurvy and non-scurvy) from the C2 cohort exhibited a greater range in $\delta^{15}N$ values than $\delta^{13}C$ values (Table 46). As $\delta^{13}C$ values increased $\delta^{15}N$ values tended to also increase for all scurvy cohorts as well as the non-scurvy cohort for the third hair segment, while the opposite was exhibited for the non-scurvy cohorts for the first and second hair segments (Figure 97). The scurvy cohort for the second and third hair segments contained only three individuals each, therefore, no useful data regarding trends could be determined.

All hair cohorts (first, second, and third hair segments; scurvy and non-scurvy) from the C3 cohort exhibited a greater range in $\delta^{15}N$ values than $\delta^{13}C$ values, except the scurvy cohort for the third hair segment which exhibited the opposite (Table 98). As $\delta^{13}C$ values increased $\delta^{15}N$

values tended to also increase for all non-scurvy cohorts. The scurvy cohort for this group contained only three individuals in each hair sample, therefore, no useful data regarding trends could be determined.

Nail

All proximal nail segment overall cohorts exhibited a greater range in $\delta^{15}N$ values than $\delta^{13}C$ (Table 47). For proximal nail segment cohorts, the scurvy and non-scurvy cohorts loosely clustered around trend lines and as $\delta^{13}C$ values increased $\delta^{15}N$ tended to also increase (Figures 42).

Table 47: Range of $\delta^{13}C$ and $\delta^{15}N$ values for all proximal nail segment cohorts, with the overall, scurvy, and non-scurvy ranges for all age cohorts, as well as the overall sample. The highest range value for each grouping has been bolded and italicized.

		Proximal Nail Segment	
		$\delta^{13}C$ (‰)	$\delta^{15}N$ (‰)
Entire Sample	Overall	4.4	***9.0***
	Scurvy	2.6	***4.1***
	Non-scurvy	4.1	***9.00***
F&P	Overall	-	-
	Scurvy	-	-
	Non-scurvy	1.8	***4.0***
Neo	Overall	2.3	***3.5***
	Scurvy	1.4	***1.7***
	Non-scurvy	2.0	***3.5***
C1	Overall	3.5	***9.0***
	Scurvy	0.4	***3.0***
	Non-scurvy	3.5	***9.0***
C2	Overall	2.1	***3.2***
	Scurvy	0.8	***0.9***
	Non-scurvy	2.0	***3.2***
C3	Overall	0.6	***2.7***
	Scurvy	-	-
	Non-scurvy	0.6	***1.8***

The F&P cohort contained only non-scurvy individuals for nail. The non-scurvy proximal nail segments from the F&P cohort exhibited a greater range in $\delta^{15}N$ values than $\delta^{13}C$ (Table 47). The proximal nail segment $\delta^{13}C$ values clustered closely around a trend line (Figure 44). As $\delta^{13}C$ values increased within the proximal nail segment $\delta^{15}N$ tended to also increase.

All nail cohorts from the neonatal cohort exhibited a greater range in $\delta^{15}N$ values than $\delta^{13}C$ (Table 47). The non-scurvy individuals clustered loosely around a trend line (Figure 45). As $\delta^{13}C$ values increased for the non-scurvy cohort, $\delta^{15}N$ values tended to decrease. The scurvy cohort for the neonatal proximal nail segment contained only three individuals, therefore, no useful data regarding trends could be determined.

All nail cohorts from the C1 cohort exhibited a greater range in $\delta^{15}N$ values than $\delta^{13}C$ (Table 47). The scurvy and non-scurvy individuals closely clustered around their respective trend lines (Figure 46). As $\delta^{13}C$ values increased for scurvy proximal nail segment, $\delta^{15}N$ tended to also increase. As the $\delta^{13}C$ values increased for non-scurvy proximal nail segment, $\delta^{15}N$ tended to decrease.

All nail cohorts from the C2 cohort exhibited a greater range in $\delta^{15}N$ values than $\delta^{13}C$ values (Table 47). The non-scurvy individuals clustered closely around their trend line for the (Figure 647). As $\delta^{13}C$ values increased for the non-scurvy cohort, $\delta^{15}N$ values tended to also increase. The scurvy cohort for the proximal nail segment contained only two individuals, therefore, no useful data regarding trends could be determined.

The C3 non-scurvy proximal nail segment cohort exhibited a greater range in $\delta^{15}N$ values than $\delta^{13}C$ values (Table 47). Both the scurvy and non-scurvy cohorts contained only one and three individuals, respectively, therefore, no useful data regarding trends could be determined.

Skin

The overall skin samples (including the scurvy and non-scurvy cohorts) exhibited a greater range in $\delta^{15}N$ values than $\delta^{13}C$ values (Table 48). The scurvy and non-scurvy overall

cohorts loosely clustered around trend lines, with the scurvy individuals clustered more closely (Figure 49). For the scurvy cohort, as $\delta^{13}C$ values increased $\delta^{15}N$ values also tended to increase, however, for the non-scurvy cohort the opposite was exhibited.

Table 48: Range of $\delta^{13}C$ and $\delta^{15}N$ values for all skin groups, with the overall, scurvy, and non-scurvy ranges for all age cohorts, as well as the overall sample. The highest range value for each grouping has been bolded and italicized.

		$\delta^{13}C$ (‰)	$\delta^{15}N$ (‰)
Entire Sample	Overall	4.2	***6.9***
	Scurvy	3.5	***3.8***
	Non-scurvy	4.2	***6.9***
F&P	Overall	2.2	3.1
	Scurvy	-	-
	Non-scurvy	1.8	***3.1***
Neo	Overall	4.0	***5.6***
	Scurvy	***2.2***	2.1
	Non-scurvy	3.6	***5.6***
C1	Overall	3.1	***5.2***
	Scurvy	***2.6***	2.3
	Non-scurvy	2.3	***5.2***
C2	Overall	3.6	***4.7***
	Scurvy	***2.6***	2.4
	Non-scurvy	***3.6***	2.7
C3	Overall	3.5	***4.4***
	Scurvy	***1.0***	0.8
	Non-scurvy	3.5	***4.4***

"-" indicates not enough data available to calculate the range of $\delta^{13}C$ and $\delta^{15}N$ values.

The F&P cohort exhibited a greater range in $\delta^{15}N$ values than $\delta^{13}C$ values (Table 48). The non-scurvy cohort clustered loosely around a trend line with increasing $\delta^{13}C$ values exhibiting

increasing $\delta^{15}N$ values also (Figure 51). The scurvy cohort contained only one individual, therefore, no trend line or other data regarding trends could be determined. The overall and non-scurvy neonatal cohorts exhibited a greater range in $\delta^{15}N$ values than $\delta^{13}C$ values, while the scurvy cohort exhibited the opposite (Table 48). The scurvy and non-scurvy cohorts loosely clustered around their respective trend lines (Figure 52). For the scurvy cohort as $\delta^{13}C$ values increased $\delta^{15}N$ values also increased, while the non-scurvy cohort exhibited the opposite. The overall and non-scurvy C1 cohorts exhibited a greater range in $\delta^{15}N$ values than $\delta^{13}C$ values, while the scurvy cohort exhibited the opposite (Table 48). The scurvy and non-scurvy cohorts loosely clustered around their respective trend line and as $\delta^{13}C$ values for both cohorts increased $\delta^{15}N$ values also increased (Figure 53). The overall sample for the C2 cohort exhibited a greater range in $\delta^{15}N$ values than $\delta^{13}C$ values, while the scurvy and non-scurvy cohorts exhibited the opposite (Table 48). The scurvy and non-scurvy cohorts clustered closely around their respective trend lines (Figure 54). For the scurvy cohort, as $\delta^{13}C$ values increased $\delta^{15}N$ values also increased, while the non-scurvy cohort exhibited the opposite. The overall and non-scurvy C3 cohorts exhibited a greater range in $\delta^{15}N$ values than $\delta^{13}C$ values, while the scurvy cohort exhibited the opposite (Table 48). The non-scurvy cohort clustered loosely around a trend line and as $\delta^{13}C$ values increased $\delta^{15}N$ values tended to decrease (Figure 55). The scurvy cohort contained only three individuals, therefore, no trend line or other data regarding trends could be determined.

Inter-tissue Spacing

Inter-tissue comparisons via Mann-Whitney U t-tests were conducted for both $\delta^{13}C$ and $\delta^{15}N$ values in order to determine if statically significant differences were present between the tissues. Overall bone collagen $\delta^{13}C$ and $\delta^{15}N$ values were compared to the overall first hair segment, proximal nail segment, and skin $\delta^{13}C$ and $\delta^{15}N$ values. The overall first hair segment $\delta^{13}C$ and $\delta^{15}N$ values were likewise compared to the overall proximal nail segment and skin $\delta^{13}C$ and $\delta^{15}N$ values. Finally, the proximal nail segment and skin $\delta^{13}C$ and $\delta^{15}N$ values were compared. This same pattern of comparison was then applied to the overall scurvy and non-scurvy cohorts for the tissues. These comparisons were not conducted among the different age cohorts because of the small sample sizes available in some of the cohorts. Additionally, the inter-tissue spacing results for each comparison was calculated. Inter-tissue spacing was also calculated for each age cohort between mean bone collagen and mean first hair segment $\delta^{13}C$ and $\delta^{15}N$ values.

Overall Carbon Comparisons

When the overall bone collagen $\delta^{13}C$ values were compared with all other overall tissue $\delta^{13}C$ values separately, all of the Mann-Whitney U t-tests resulted in a p-value of < 0.001, indicating statistically significant differences between overall bone collagen $\delta^{13}C$ values and all other overall tissue $\delta^{13}C$ values. When the overall first hair segment $\delta^{13}C$ values were compared with the proximal nail segment and skin $\delta^{13}C$ values, each result was statistically significant, ($p = 0.002$ and $p < 0.001$, respectively). The comparison of the overall proximal nail segment and

skin $\delta^{13}C$ values did not yield statistically significant results, with a p-values of 0.300. The p-values for the overall $\delta^{13}C$ value inter-tissue comparisons can be found in Table 49.

Table 49: Results of the Mann-Whitney U t-tests of each overall tissue group with all other overall tissue groups for $\delta^{13}C$ values. Statistically significant results are bolded and italicized.

	Bone Collagen	1st Hair Segment	Proximal Nail Segment
1st Hair Segment	***<0.001***		
Proximal Nail Segment	***<0.001***	***0.002***	
Skin	***<0.001***	***<0.001***	0.300

When comparing the mean $\delta^{13}C$ values for overall bone collagen to the overall first hair segment, proximal nail segment, and skin mean $\delta^{13}C$ values for inter-tissue spacing, it was found that the tissues are spaced 0.7‰, 1.0‰, and 1.2‰, respectively. When comparing the mean $\delta^{13}C$ values for the overall first hair segment to the overall proximal nail segment and skin mean $\delta^{13}C$ values for inter-tissue spacing, it was found that the tissues are spaced 0.3‰ and 0.5‰, respectively. When comparing the overall proximal nail segment and skin mean $\delta^{13}C$ values for inter-tissue spacing, it was found that the tissues are spaced -0.2‰. The overall inter-tissue spacing results can be viewed in Appendix I. When divided by age cohorts, the inter-tissue spacing results provide a more detailed view of the tissue spacing in these juveniles. The mean $\delta^{13}C$ age cohort inter-tissue spacing results showed an enrichment of bone collagen over the first hair segment. The F&P cohort mean bone collagen enrichment was 1.1‰; the neonatal cohort mean bone collagen enrichment was 0.6‰; the C1 cohort mean bone collagen enrichment was

0.6‰; the C2 cohort mean bone collagen enrichment was 0.7‰; the C3 cohort mean bone collagen enrichment was 0.6‰. The inter-tissue spacing for age cohort mean $\delta^{13}C$ is shown in Figure 74 and values can be viewed in Appendix J. The $\delta^{13}C$ inter-tissue spacing values presented here (overall and age cohorts) fall within one standard deviation of the value published by Williams (2005); however, only the C1 cohort falls within one standard deviation of corresponding cohort value published by Norris (2012). The overall and F&P cohorts both fall within two standard deviations of the overall value found in Norris (2012), while the remainder of the cohorts in this study fall outside of two standard deviations of the corresponding cohort inter-tissue spacing values found by Norris (2012).

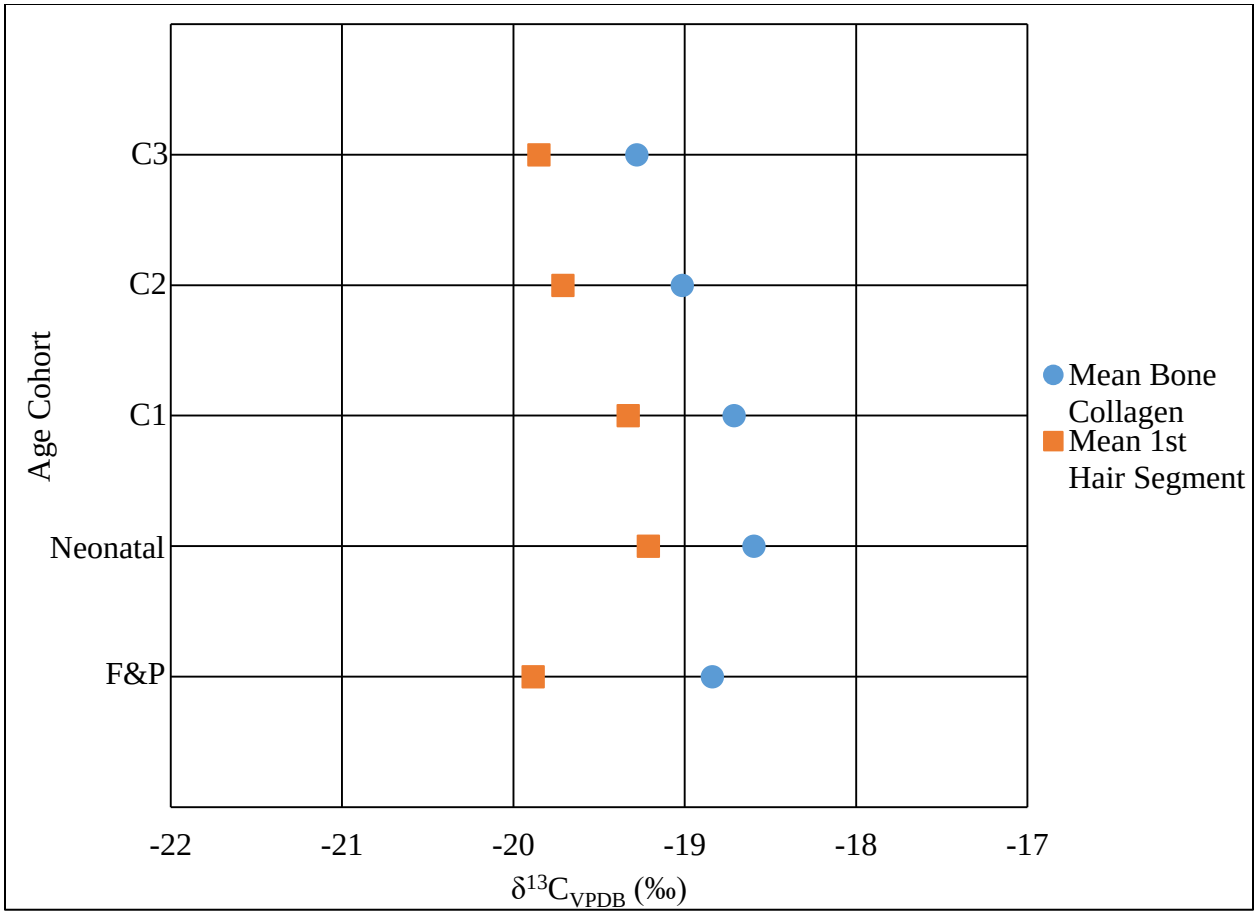

Figure 74: Inter-tissue spacing for mean bone collagen and first hair segment $\delta^{13}C$ values for each age cohort.

Overall Nitrogen Comparisons

When the overall bone collagen $\delta^{15}N$ values were compared with all other overall tissue $\delta^{15}N$ values separately, the comparison with the overall first hair segment $\delta^{15}N$ values was not statistically significant ($p = 0.678$) while the comparisons with the overall proximal nail segment and skin $\delta^{15}N$ values were statistically significant ($p = 0.011$ and $p < 0.001$, respectively). When the overall first hair segment $\delta^{15}N$ values were compared with the proximal nail segment and

skin $\delta^{15}N$ values, each result was statistically significant ($p < 0.001$). The comparison of the overall proximal nail segment and skin $\delta^{15}N$ values were also statistically significant ($p < 0.001$). The p-values for the overall $\delta^{15}N$ value inter-tissue comparisons can be found in Table 50.

Table 50: Results of the Mann-Whitney U t-tests of each overall tissue group with all other overall tissue groups for $\delta^{15}N$ values. Statistically significant results are bolded and italicized.

	Bone Collagen	1st Hair Segment	Proximal Nail Segment
1st Hair Segment	0.678		
Proximal Nail Segment	***0.011***	***< 0.001***	
Skin	***< 0.001***	***< 0.001***	***< 0.001***

When comparing the mean $\delta^{15}N$ values for overall bone collagen to the overall first hair segment, proximal nail segment, and skin mean $\delta^{15}N$ values for inter-tissue spacing, it was found that the tissues are spaced 0.2‰, -1.1‰, and -2.2‰, respectively. When comparing the mean $\delta^{15}N$ values for the overall first hair segment to the overall proximal nail segment and skin mean $\delta^{15}N$ values for inter-tissue spacing, it was found that the tissues are spaced -1.3‰ and -2.4‰, respectively. When comparing the overall proximal nail segment and skin mean $\delta^{15}N$ values for inter-tissue spacing, it was found that the tissues are spaced 1.1‰. The inter-tissue spacing results can be viewed in Appendix I. When divided by age cohorts, the inter-tissue spacing results provide a more detailed view of the tissue spacing in these juveniles. The mean $\delta^{15}N$ age cohort inter-tissue spacing results showed an enrichment of bone collagen over the first hair segment. The F&P cohort mean bone collagen enrichment was 0.5‰; the neonatal cohort mean

bone collagen enrichment was 0.3‰; the C1 cohort mean bone collagen enrichment was 0.7‰; the C2 cohort mean bone collagen enrichment was 0.0‰; the C3 cohort mean bone collagen enrichment was 0.1‰. The inter-tissue spacing for age cohort mean $\delta^{15}N$ is shown in Figure 75 and values can be viewed in Appendix J. The $\delta^{15}N$ inter-tissue spacing values presented here (overall and age cohorts) fall within one standard deviation of the value published by Williams (2005).

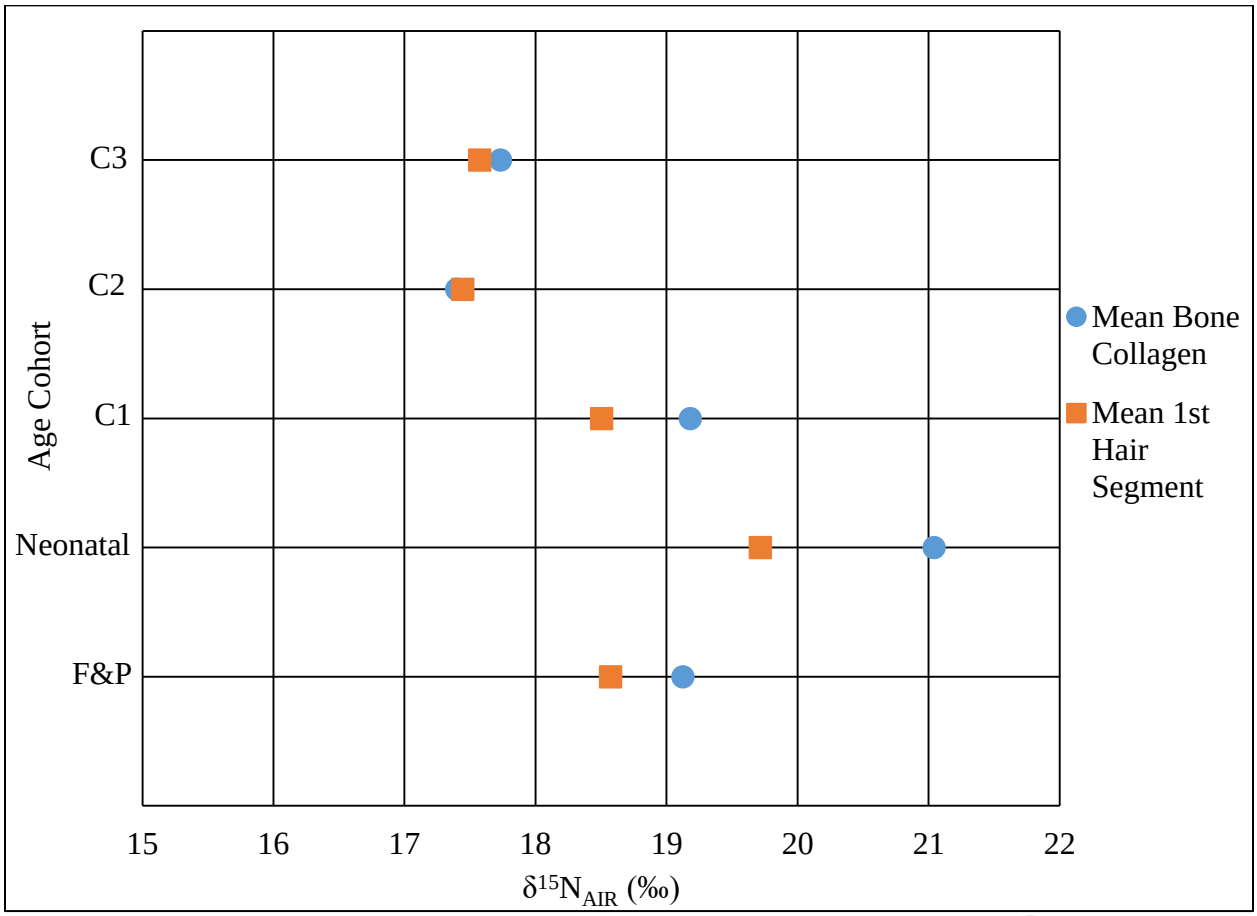

Figure 75: Inter-tissue spacing for mean bone collagen and first hair segment $\delta^{15}N$ values for each age cohort.

Scurvy and Non-scurvy Carbon Comparisons

When the scurvy bone collagen $\delta^{13}C$ values were compared with the scurvy and non-scurvy first hair segment, proximal nail segment, and skin $\delta^{13}C$ values, each Mann-Whitney U t-test produced a statistically significant result with p-values ranging from < 0.001 to 0.015. The non-scurvy bone collagen cohort also produced all statistically significant results when compared to the scurvy and non-scurvy cohort of all other tissues, with p-values ranging from < 0.001 to 0.003. When the scurvy first hair segment $\delta^{13}C$ values were compared with scurvy proximal nail segment and skin $\delta^{13}C$ values, neither result was statistically significant ($p = 0.261$ and 0.076, respectively). When the non-scurvy first hair segment $\delta^{13}C$ values were compared with the non-scurvy proximal nail segment and skin $\delta^{13}C$ values, each result was statistically significant ($p = 0.019$ and 0.006, respectively). When the scurvy and non-scurvy proximal nail segment $\delta^{13}C$ values were compared with the scurvy and non-scurvy skin $\delta^{13}C$ values, none of the results were statistically significant with p-values ranging from 0.314 to 0.810. The p-values for the overall $\delta^{13}C$ value inter-tissue comparisons can be found in Table 51.

Table 51: Scurvy and non-scurvy inter-tissue Mann-Whitney U t-test results for $\delta^{13}C$ with statistically significant results italicized and bolded.

		Bone Collagen		1st Hair Segment		Proximal Nail Segment	
		Scurvy	Non-scurvy	Scurvy	Non-scurvy	Scurvy	Non-scurvy
1st Hair Segment	Scurvy	***0.015***	***0.003***				
	Non-scurvy	***0.002***	***<0.001***				
Proximal Nail Segment	Scurvy	***0.007***	***0.002***	0.261	0.291		
	Non-scurvy	***<0.001***	***<0.001***	***0.019***	***0.005***		
Skin	Scurvy	***0.001***	***<0.001***	0.076	0.054	0.565	0.810
	Non-scurvy	***<0.001***	***<0.001***	***0.006***	***<0.001***	0.314	0.364

When comparing the mean $\delta^{13}C$ values for scurvy bone collagen to the scurvy first hair segment, proximal nail segment, and skin mean $\delta^{13}C$ values for inter-tissue spacing, it was found that the tissues are spaced 0.5‰, 0.8‰, and 1.1‰, respectively. When comparing the mean $\delta^{13}C$ values for the scurvy first hair segment to the scurvy proximal nail segment and skin mean $\delta^{13}C$ values for inter-tissue spacing, it was found that the tissues are spaced 0.3‰ and 0.6‰, respectively. When comparing the scurvy proximal nail segment and skin mean $\delta^{13}C$ values for inter-tissue spacing, it was found that the tissues are spaced -0.3‰. The inter-tissue spacing results can be viewed in Appendix K (Table 64).

When comparing the mean $\delta^{13}C$ values for non-scurvy bone collagen to the non-scurvy first hair segment, proximal nail segment, and skin mean $\delta^{13}C$ values for inter-tissue spacing, it was found that the tissues are spaced 0.7‰, 1.0‰, and 1.3‰, respectively. When comparing the mean $\delta^{13}C$ values for the non-scurvy first hair segment to the non-scurvy proximal nail segment and skin mean $\delta^{13}C$ values for inter-tissue spacing, it was found that the tissues are spaced 0.3‰

and 0.6‰, respectively. When comparing the non-scurvy proximal nail segment and skin mean $\delta^{13}C$ values for inter-tissue spacing, it was found that the tissues are spaced -0.3‰. The inter-tissue spacing results can be viewed in Appendix K (Table 64).

When comparing the mean $\delta^{13}C$ values for scurvy bone collagen to the non-scurvy first hair segment, proximal nail segment, and skin $\delta^{13}C$ values for inter-tissue spacing, it was found that the tissues are spaced 0.6‰, 0.9‰, and 1.2‰, respectively. When comparing the mean $\delta^{13}C$ values for the scurvy first hair segment to the non-scurvy proximal nail segment and skin mean $\delta^{13}C$ values for inter-tissue spacing, it was found that the tissues are spaced 0.4‰ and 0.7‰, respectively. When comparing the scurvy proximal nail segment and non-scurvy skin mean $\delta^{13}C$ values for inter-tissue spacing, it was found that the tissues are spaced -0.2‰. The inter-tissue spacing results can be viewed in Appendix K (Table 64).

When comparing the mean $\delta^{13}C$ values for non-scurvy bone collagen to the scurvy first hair segment, proximal nail segment, and skin mean $\delta^{13}C$ values for inter-tissue spacing, it was found that the tissues are spaced 0.6‰, 0.9‰, and 1.2‰, respectively. When comparing the mean $\delta^{13}C$ values for the non-scurvy first hair segment to the scurvy proximal nail segment and skin mean $\delta^{13}C$ values for inter-tissue spacing, it was found that the tissues are spaced 0.2‰ and 0.5‰, respectively. When comparing the non-scurvy proximal nail segment and skin mean $\delta^{13}C$ values for inter-tissue spacing, it was found that the tissues are spaced -0.4‰. The inter-tissue spacing results can be viewed in Appendix K (Table 64).

Scurvy and Non-scurvy Nitrogen Comparisons

When the scurvy bone collagen $\delta^{15}N$ values were compared with the scurvy and non-scurvy first hair segment and scurvy proximal nail segment $\delta^{15}N$ values, each Mann-Whitney U t-test produced non-statistically significant results with p-values ranging from 0.129 to 0.905. When compared to the non-scurvy proximal nail segment and scurvy and non-scurvy skin $\delta^{15}N$ values, each t-test produced a statistically significant result with p-values ranging from < 0.001 to 0.014. When the non-scurvy bone collagen $\delta^{15}N$ values were compared with the scurvy and non-scurvy first hair segment and proximal nail segment $\delta^{15}N$, each t-test produced non-statically significant results with p-values ranging from 0.130 to 0.514. When the scurvy and non-scurvy first hair segment $\delta^{15}N$ values were compared with the scurvy proximal nail segment $\delta^{15}N$, the t-tests produced non-statistically significant results (p = 0.113 and 0.062, respectively). When the scurvy and non-scurvy first hair segment $\delta^{15}N$ values were compared with the non-scurvy proximal nail segment and scurvy and non-scurvy skin $\delta^{15}N$ values, each t-test produced statistically significant results with p-values ranging from < 0.001 to 0.006. When the scurvy and non-scurvy proximal nail segment $\delta^{15}N$ values were compared with the scurvy and non-scurvy skin $\delta^{15}N$ values, each t-test produced statistically significant results with p-values ranging from 0.001 to 0.016. The p-values for the scurvy and non-scurvy inter-tissue comparisons can be found in Table 52.

Table 52: Scurvy and non-scurvy inter-tissue Mann-Whitney U t-test results for $\delta^{15}N$ with statistically significant results italicized and bolded.

		Bone Collagen		1st Hair Segment		Proximal Nail Segment	
		Scurvy	Non-scurvy	Scurvy	Non-scurvy	Scurvy	Non-scurvy
1st Hair Segment	Scurvy	0.905	0.478				
	Non-scurvy	0.869	0.514				
Proximal Nail Segment	Scurvy	0.129	0.336	0.113	0.062		
	Non-scurvy	***0.014***	0.130	***0.006***	***<0.001***		
Skin	Scurvy	***<0.001***	***0.004***	***<0.001***	***<0.001***	***0.011***	***0.014***
	Non-scurvy	***<0.001***	***0.001***	***<0.001***	***<0.001***	***0.016***	***0.001***

When comparing the mean $\delta^{15}N$ values for scurvy bone collagen to the scurvy first hair segment, proximal nail segment, and skin mean $\delta^{15}N$ values for inter-tissue spacing, it was found that the tissues are spaced 0.1‰, -1.0‰, and -2.4‰, respectively. When comparing the mean $\delta^{15}N$ values for the scurvy first hair segment to the scurvy proximal nail segment and skin mean $\delta^{15}N$ values for inter-tissue spacing, it was found that the tissues are spaced -1.1‰ and -2.5‰, respectively. When comparing the scurvy proximal nail segment and skin mean $\delta^{15}N$ values for inter-tissue spacing, it was found that the tissues are spaced 1.4‰. The inter-tissue spacing results can be viewed in Appendix K (Table 65).

When comparing the mean $\delta^{15}N$ values for non-scurvy bone collagen to the non-scurvy first hair segment, proximal nail segment, and skin mean $\delta^{15}N$ values for inter-tissue spacing, it was found that the tissues are spaced 0.4‰, -0.9‰, and -2.0‰, respectively. When comparing the mean $\delta^{15}N$ values for the non-scurvy first hair segment to the non-scurvy proximal nail segment and skin mean $\delta^{13}C$ values for inter-tissue spacing, it was found that the tissues are

spaced -1.3‰ and -1.1‰, respectively. When comparing the non-scurvy proximal nail segment and skin mean $\delta^{15}N$ values for inter-tissue spacing, it was found that the tissues are spaced 1.1‰. The inter-tissue spacing results can be viewed in Appendix K (Table 65).

When comparing the mean $\delta^{15}N$ values for scurvy bone collagen to the non-scurvy first hair segment, proximal nail segment, and skin mean $\delta^{15}N$ values for inter-tissue spacing, it was found that the tissues are spaced 0.0‰, -2.4‰, and -2.4‰, respectively. When comparing the mean $\delta^{15}N$ values for the scurvy first hair segment to the non-scurvy proximal nail segment and skin mean $\delta^{13}C$ values for inter-tissue spacing, it was found that the tissues are spaced -1.4‰ and -2.5‰, respectively. When comparing the scurvy proximal nail segment and non-scurvy skin mean $\delta^{15}N$ values for inter-tissue spacing, it was found that the tissues are spaced 1.1‰. The inter-tissue spacing results can be viewed in Appendix K (Table 65).

When comparing the mean $\delta^{15}N$ values for non-scurvy bone collagen to the scurvy first hair segment, proximal nail segment, and skin mean $\delta^{15}N$ values for inter-tissue spacing, it was found that the tissues are spaced 0.5‰, -0.6‰, and -2.0‰, respectively. When comparing the mean $\delta^{15}N$ values for the non-scurvy first hair segment to the scurvy proximal nail segment and skin mean $\delta^{15}N$ values for inter-tissue spacing, it was found that the tissues are spaced -1.0‰ and -2.4‰, respectively. When comparing the non-scurvy proximal nail segment and scurvy skin mean $\delta^{15}N$ values for inter-tissue spacing, it was found that the tissues are spaced 1.4‰. The inter-tissue spacing results can be viewed in Appendix K (Table 65).

Outliers and Inter-tissue Spacing

Five of the outliers identified previously contributed both bone collagen and hair to this study. These were the first hair segment $\delta^{13}C$ value for burials 23 and 260, the bone collagen and second hair segment $\delta^{13}C$ values for burial 71, and the bone collagen $\delta^{15}N$ values for burials 520 and 582. The $\delta^{13}C$ and $\delta^{15}N$ values for these juveniles are examined to evaluate possible differences in inter-tissue spacing of outliers.

The $\delta^{13}C$ value of the first hair segment of burial 23 was indicated as an outlier by SPSS (Figures 31 and 32). This tissue had a $\delta^{13}C$ value of -21.2‰, which is more depleted in $\delta^{13}C$ than both its bone collagen and second hair segment $\delta^{13}C$ values, as well as the mean C1 cohort bone collagen and first hair segment $\delta^{13}C$ values (Figure76). The inter-tissue spacing between burial 23's bone collagen $\delta^{13}C$ value and first and second hair segments are 2.4‰ and 1.0‰, respectively. The mean C1 cohort bone collagen $\delta^{13}C$ value is 2.5‰ and 1.1‰ enriched over burial 23's first and second hair segment $\delta^{13}C$ values, respectively. Burial 23's bone collagen $\delta^{13}C$ value is enriched 0.5‰ over the mean C1 first hair segment $\delta^{13}C$ value. The $\delta^{13}C$ inter-tissue spacing values can be found in Appendix L (Table 66). Although none of the $\delta^{15}N$ values for burial 23 presented as outliers, the inter-tissue spacing results are still presented here for reference (Figure 77). The bone collagen $\delta^{15}N$ value for burial 23 is more enriched than both the first and second hair segments, as well as the mean C1 first hair segment $\delta^{15}N$ value (2.9‰, 2.8‰, and 1.2‰, respectively). The mean C1 bone collagen $\delta^{15}N$ value is more enriched than burial 23's first and second hair segment $\delta^{15}N$ values (2.4‰ and 2.3‰, respectively). The $\delta^{15}N$ inter-tissue spacing values can be found in Appendix L (Table 67).

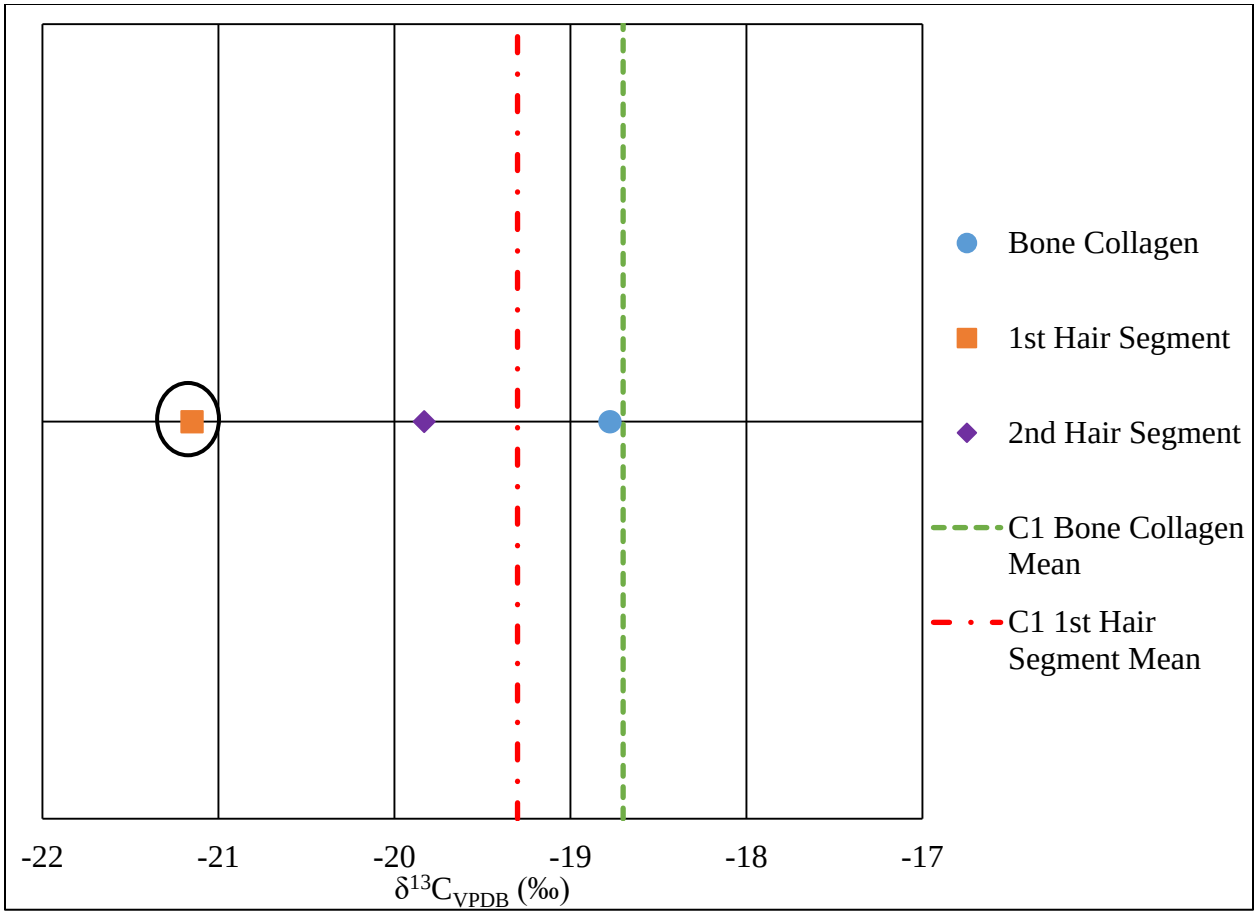

Figure 76: Inter-tissue spacing between bone collagen and hair segment $\delta^{13}C$ values for burial 23, with the outlier value circled and mean C1 cohort bone collagen and first hair segment $\delta^{13}C$ values indicated.

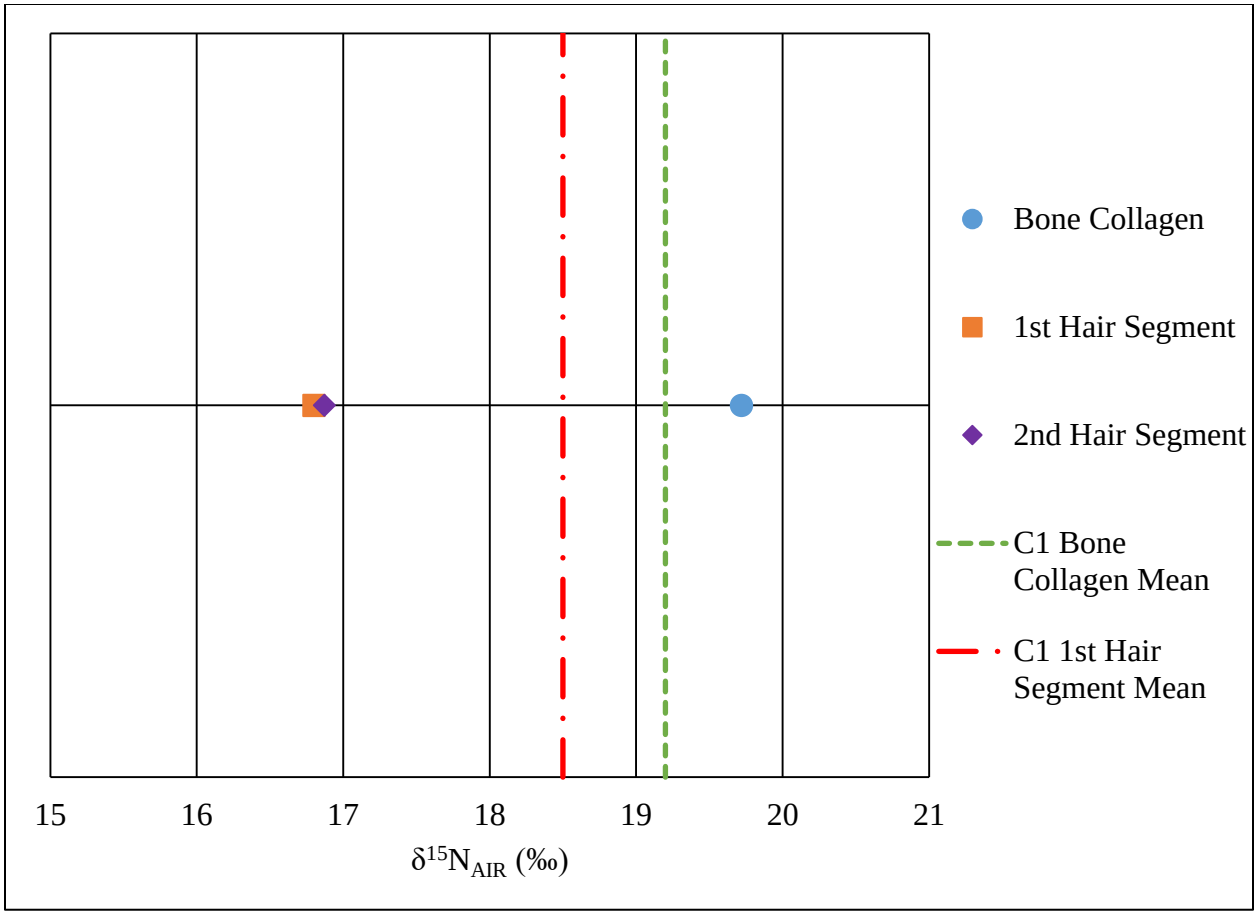

Figure 77: Inter-tissue spacing between bone collagen and hair segment $\delta^{15}N$ values for burial 23 and the mean C1 cohort bone collagen and first hair segment $\delta^{15}N$ values.

The $\delta^{13}C$ values of bone collagen and the second hair segment of burial 71 were indicated as outliers by SPSS (Figures 13 and 33). The bone collagen $\delta^{13}C$ value was -17.6‰ and the second hair segment $\delta^{13}C$ value was -18.1‰. The bone collagen $\delta^{13}C$ value is more enriched than the hair segments and mean C1 bone collagen and first hair segment $\delta^{13}C$ values, while the second hair segment is more depleted in $\delta^{13}C$ than the bone collagen and third hair segment $\delta^{13}C$ values and more enriched than the first hair segment and mean C1 bone collagen and first hair segment $\delta^{13}C$ values (Figure 78). The inter-tissue spacing between burial 71's bone collagen $\delta^{13}C$ value and first, second, and third hair segments are 0.7‰, 0.5‰, and 0.3‰, respectively.

The mean C1 cohort bone collagen $\delta^{13}C$ value is -0.4‰, -0.6‰, and -0.8‰ depleted from burial 71's first, second, and third hair segment $\delta^{13}C$ values, respectively. Burial 71's bone collagen $\delta^{13}C$ value is enriched 1.7‰ over the mean C1 first hair segment $\delta^{13}C$ value. The $\delta^{13}C$ inter-tissue spacing values can be found in Appendix L (Table 66). Although none of the $\delta^{15}N$ values for burial 71 presented as outliers, the inter-tissue spacing results are still presented here for reference (Figure 79). The bone collagen $\delta^{15}N$ value for burial 71 is more enriched than the first, second, and third hair segments, as well as the mean C1 first hair segment $\delta^{15}N$ value (1.8‰, 1.6‰, 1.8‰, and 1.6‰, respectively). The mean C1 bone collagen $\delta^{15}N$ value is more enriched than burial 71's first, second, and third hair segment $\delta^{15}N$ values (0.9‰, 0.7‰, and 0.9‰, respectively). The $\delta^{15}N$ inter-tissue spacing values can be found in Appendix L (Table 67).

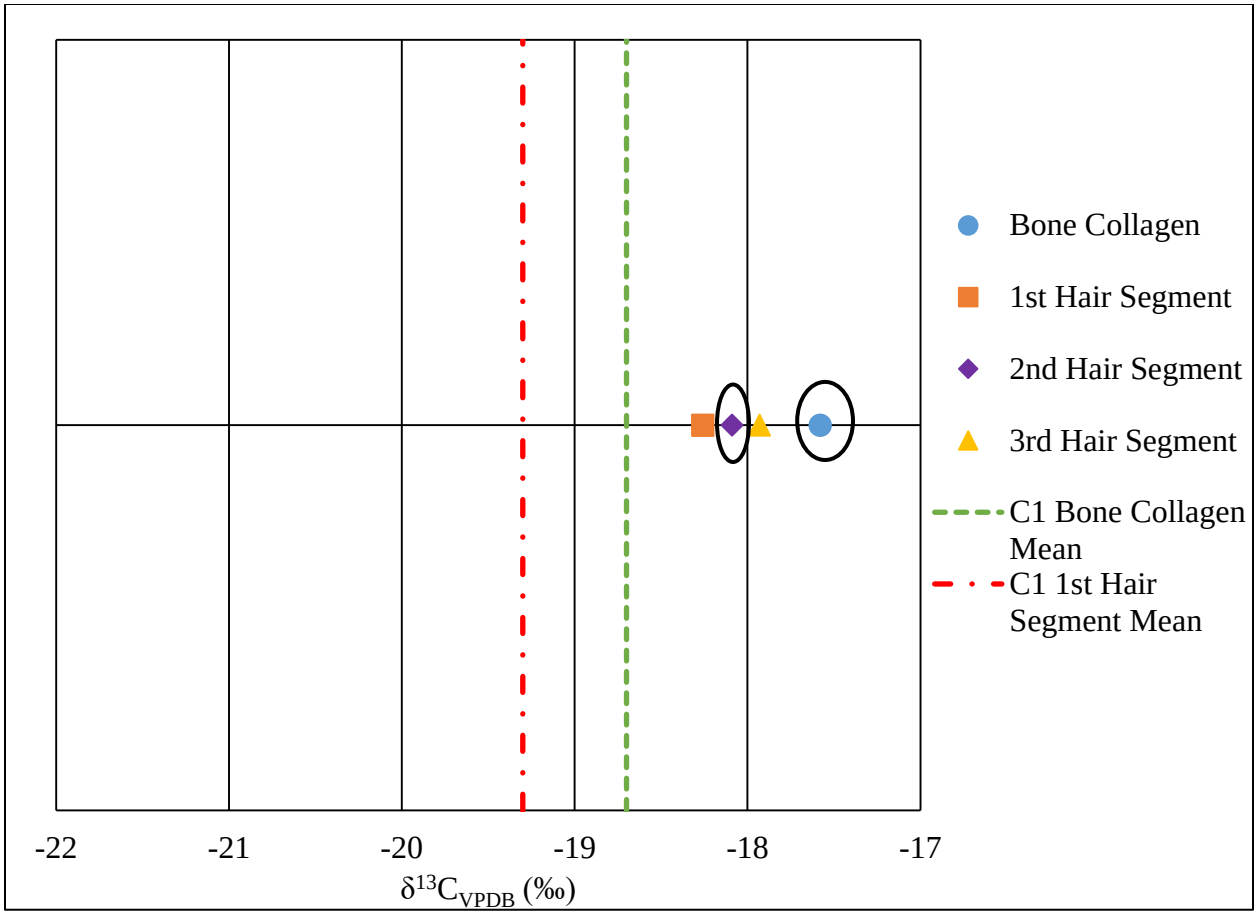

Figure 78: Inter-tissue spacing between bone collagen and hair segment $\delta^{13}C$ values for burial 71, with the outlier values circled and mean C1 cohort bone collagen and first hair segment $\delta^{13}C$ values indicated.

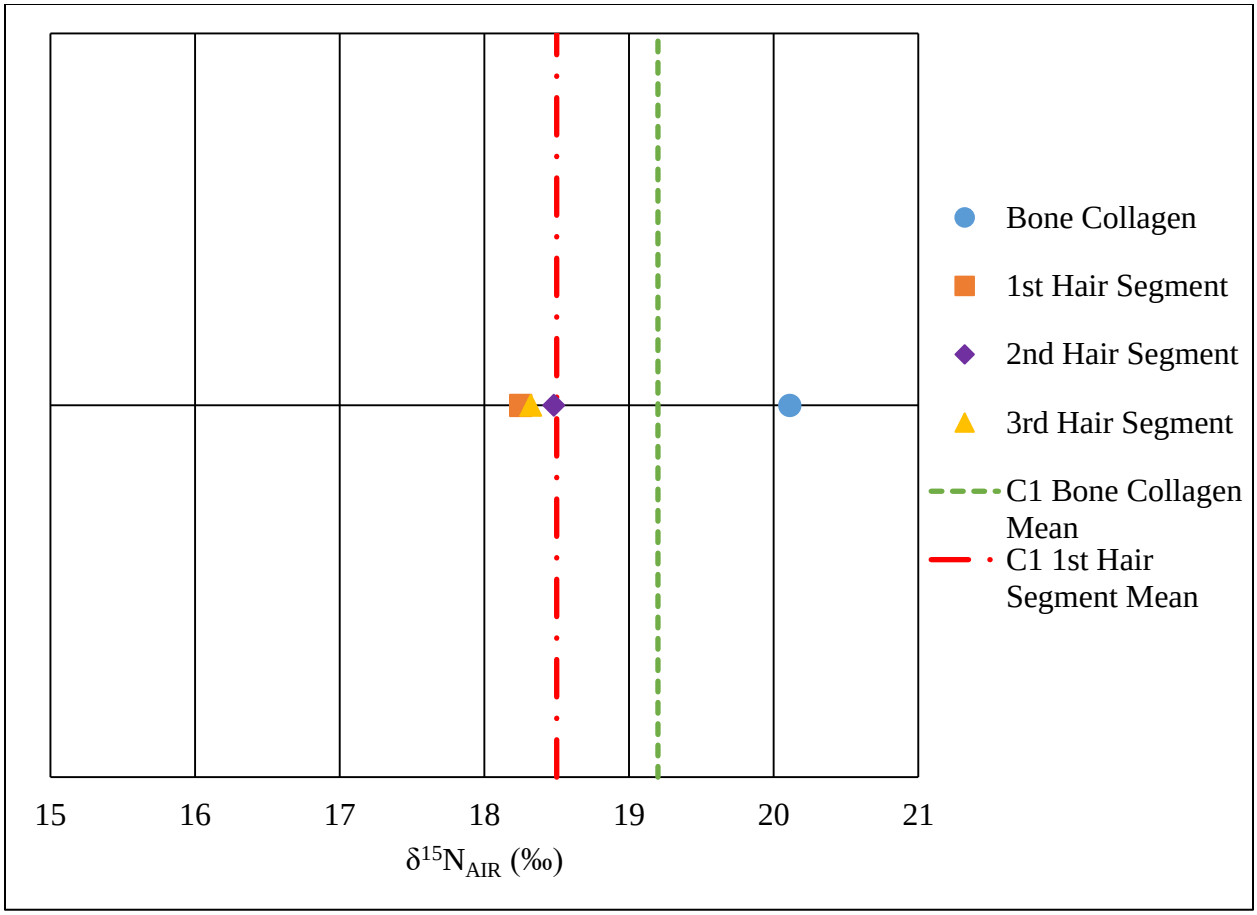

Figure 79: Inter-tissue spacing between bone collagen and hair segment $\delta^{15}N$ values for burial 71 and the mean C1 cohort bone collagen and first hair segment $\delta^{15}N$ values.

The $\delta^{13}C$ value of the first hair segment of burial 260 was indicated as an outlier by SPSS (Figure 39). This tissue had a $\delta^{13}C$ value of -21.1‰, which is more depleted in $\delta^{13}C$ than both its bone collagen and second and third hair segment $\delta^{13}C$ values, as well as the mean C1 cohort bone collagen and first hair segment $\delta^{13}C$ values (Figure 80). The inter-tissue spacing between burial 260's bone collagen $\delta^{13}C$ value and first, second, and third hair segments are 1.6‰, 0.9‰, and 0.6‰, respectively. The mean C1 cohort bone collagen $\delta^{13}C$ value is 1.8‰, 1.1‰, and 0.8‰ enriched over burial 260's first, second, and third hair segment $\delta^{13}C$ values, respectively. Burial 260's bone collagen $\delta^{13}C$ value is enriched 0.4‰ over the mean C1 first hair segment $\delta^{13}C$ value.

The $\delta^{13}C$ inter-tissue spacing values can be found in Appendix L (Table 66). Although none of the $\delta^{15}N$ values for burial 260 presented as outliers, the inter-tissue spacing results are still presented here for reference (Figure 81). The bone collagen $\delta^{15}N$ value for burial 260 is more enriched than the third hair segment $\delta^{15}N$ value and the mean C1 first hair segment $\delta^{15}N$ value, but more depleted than the first and second hair segment $\delta^{15}N$ values (0.3‰, 0.3‰, -1.1‰, and -0.9‰, respectively). The mean C1 bone collagen $\delta^{15}N$ value more enriched than burial 260's third hair segment $\delta^{15}N$ value (0.1‰), and more depleted in $\delta^{15}N$ than the first and second hair segment $\delta^{15}N$ values (-1.3‰ and -1.1‰, respectively). The $\delta^{15}N$ inter-tissue spacing values can be found in Appendix L (Table 67).

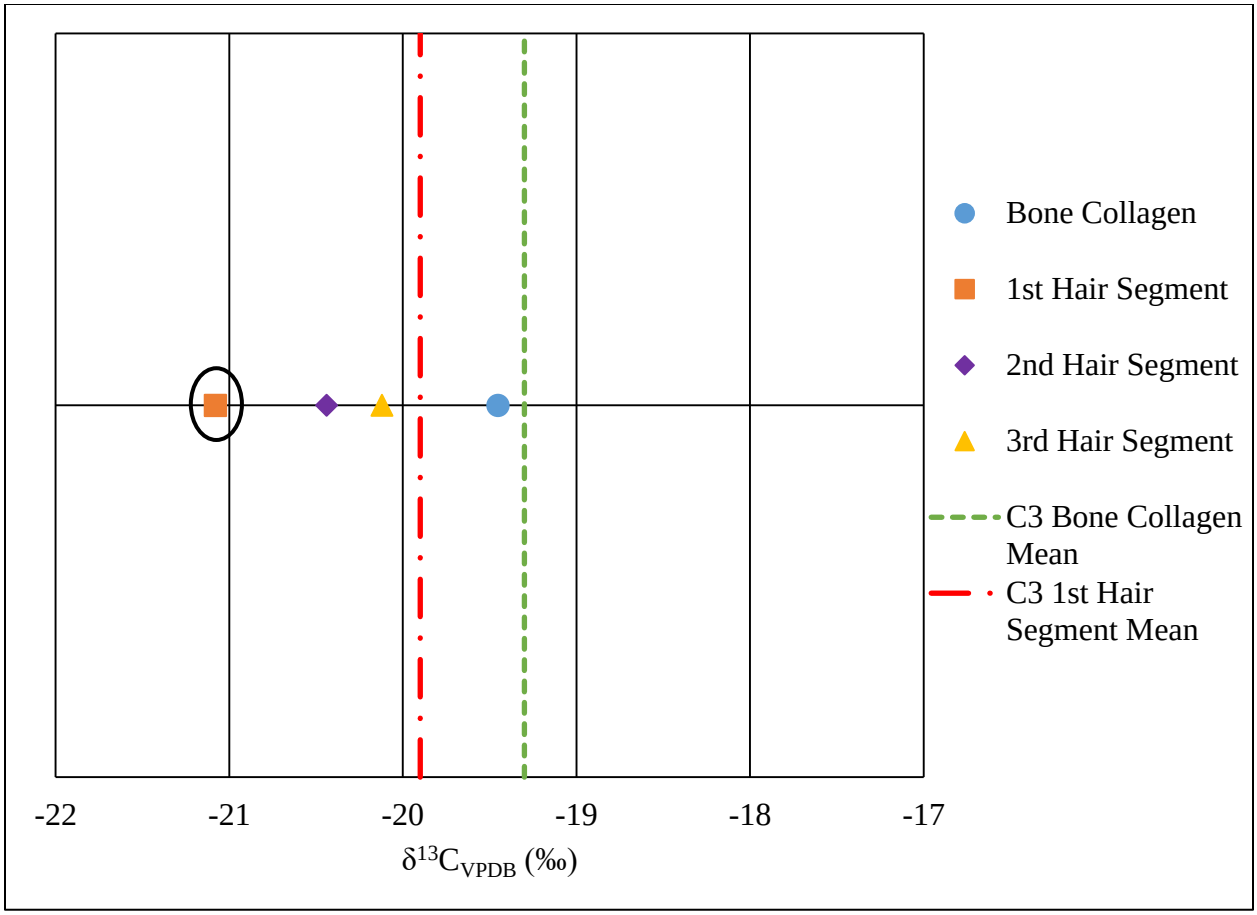

Figure 80: Inter-tissue spacing between bone collagen and hair segment $\delta^{13}C$ values for burial 260, with the outlier value circled and mean C1 cohort bone collagen and first hair segment $\delta^{13}C$ values indicated.

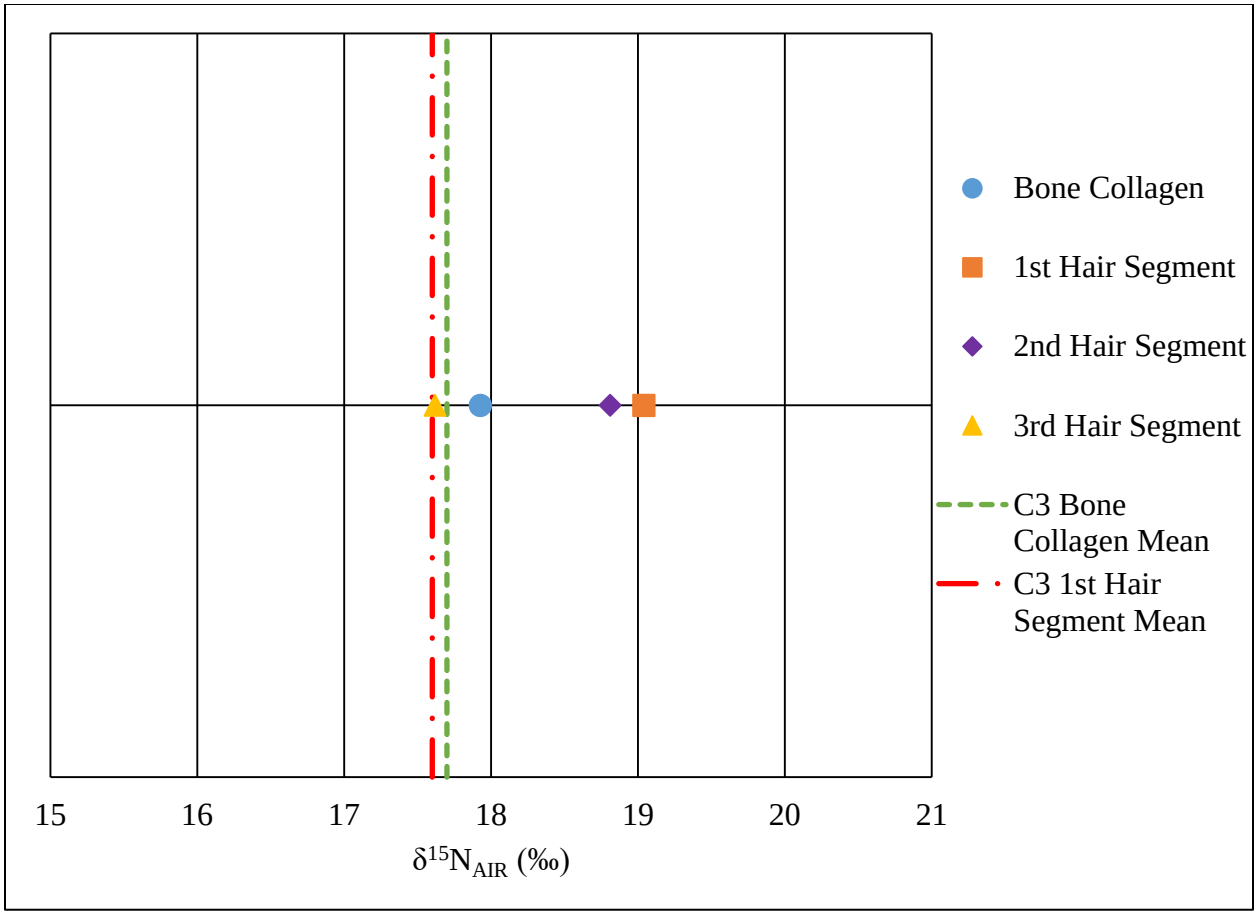

Figure 81: Inter-tissue spacing between bone collagen and hair segment $\delta^{15}N$ values for burial 260 and the mean C1 cohort bone collagen and first hair segment $\delta^{15}N$ values.

The $\delta^{15}N$ value for bone collagen of burial 520 was indicated as an outlier by SPSS (Figure 57). This tissue had a $\delta^{15}N$ value of 18.1‰, which is more enriched in $\delta^{15}N$ than the first, second, and third hair segment $\delta^{15}N$ values, as well as the mean C1 cohort first hair segment $\delta^{15}N$ values (Figure 82). The inter-tissue spacing between burial 520's bone collagen $\delta^{15}N$ value and first, second, and third hair segments are 1.5‰, 1.7‰, and 1.4‰, respectively. The mean C1 cohort bone collagen $\delta^{15}N$ value is 0.8‰, 1.0‰, and 0.7‰ enriched over burial 520's first, second, and third hair segment $\delta^{15}N$ values, respectively. Burial 520's bone collagen $\delta^{15}N$ value is enriched 0.7‰ over the mean C1 first hair segment $\delta^{15}N$ value. The $\delta^{15}N$ inter-tissue spacing

values can be found in Appendix L (Table 67). Although none of the $\delta^{13}C$ values for burial 520 presented as outliers, the inter-tissue spacing results are still presented here for reference (Figure 83). The bone collagen $\delta^{13}C$ value for the burial 520 is more enriched than the first, second, and third hair segments, as well as the mean C1 mean first hair $\delta^{13}C$ value (1.0‰, 1.0‰, 1.2‰, and 0.5‰, respectively). The mean C1 bone collagen $\delta^{13}C$ value is more enriched than burial 520's first, second, and third hair segment $\delta^{13}C$ values (1.2‰, 1.2‰, and 1.4‰, respectively). The $\delta^{13}C$ inter-tissue spacing values can be found in Appendix L (Table 66).

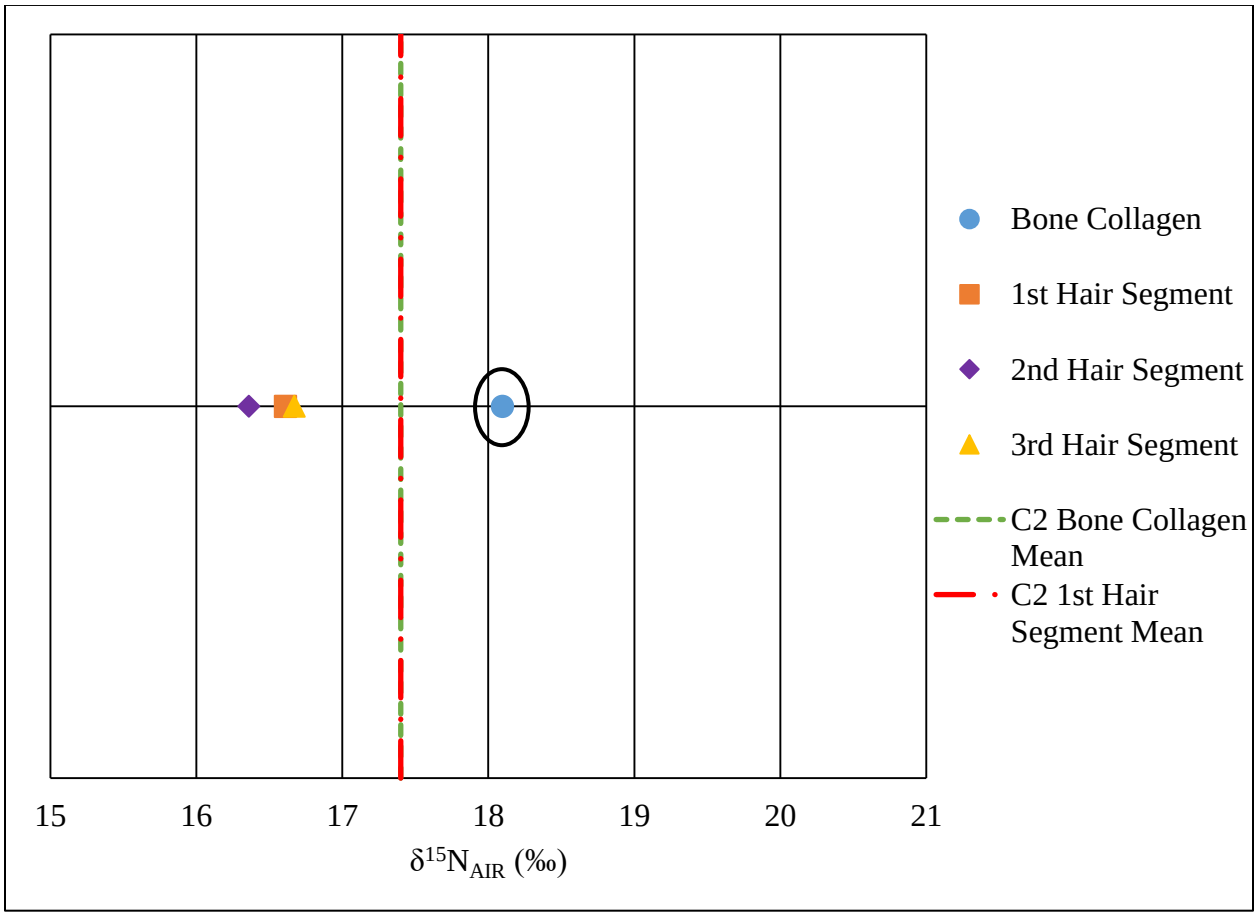

Figure 82: Inter-tissue spacing between bone collagen and hair segment $\delta^{15}N$ values for burial 520, with the outlier value circled and mean C1 cohort bone collagen and first hair segment $\delta^{15}N$ values indicated.

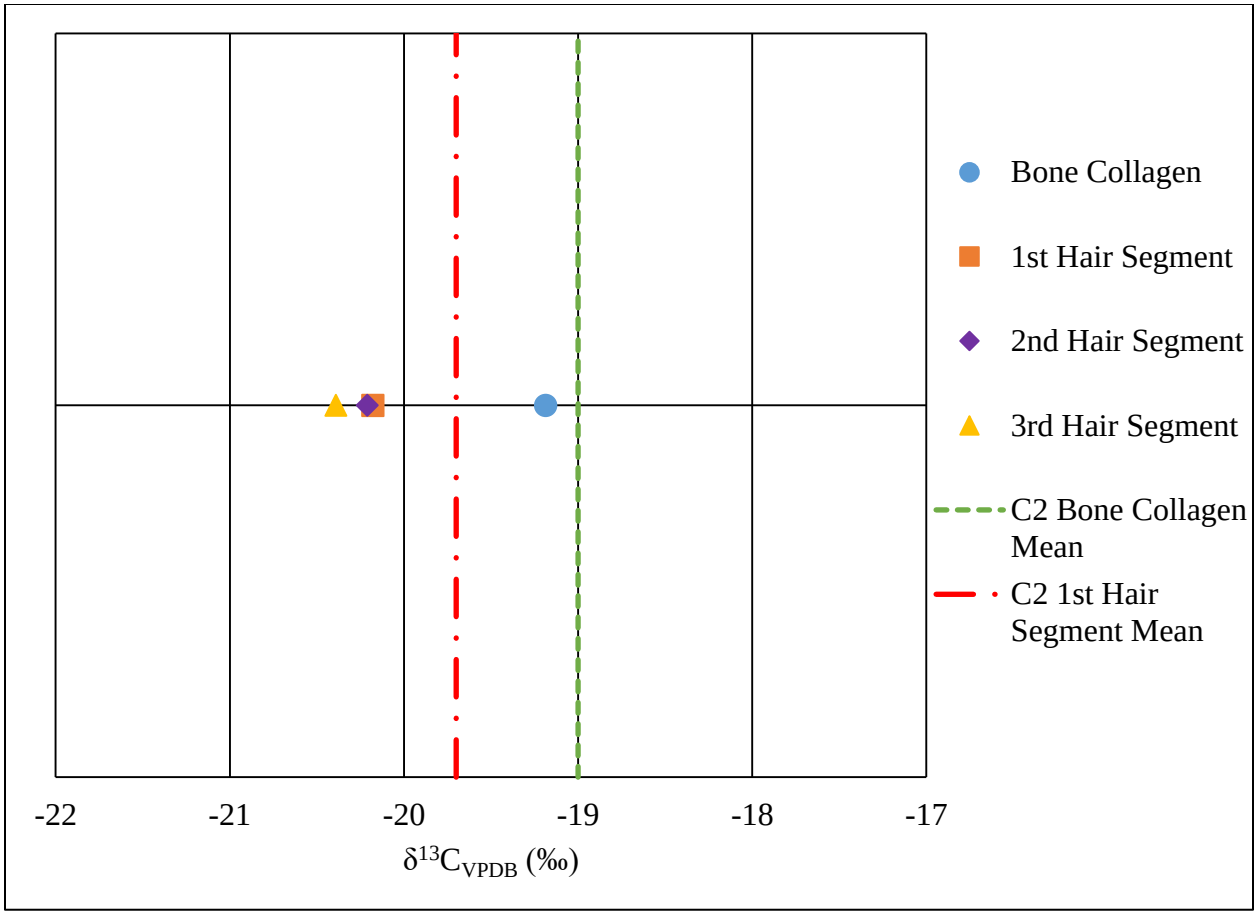

Figure 83: Inter-tissue spacing between bone collagen and hair segment $\delta^{13}C$ values for burial 520 and the mean C1 cohort bone collagen and first hair segment $\delta^{13}C$ values.

The $\delta^{15}N$ value for bone collagen of burial 582 was indicated as an outlier by SPSS (Figure 57). This tissue had a $\delta^{15}N$ value of 16.4‰, which is more enriched in $\delta^{15}N$ than the first hair segment, and depleted in $\delta^{15}N$ in relation to the mean C1 cohort bone collagen and first hair segment $\delta^{15}N$ values (Figure 84). The inter-tissue spacing between burial 582's bone collagen $\delta^{15}N$ value and first hair segment is 0.2‰. The mean C1 cohort bone collagen $\delta^{15}N$ value is 1.2‰ enriched over burial 582's first hair segment $\delta^{15}N$ value. Burial 582's bone collagen $\delta^{15}N$ value is depleted in $\delta^{15}N$ by -1.0‰ relative to the mean C1 first hair segment $\delta^{15}N$ value. The $\delta^{15}N$ inter-tissue spacing values can be found in Appendix L (Table 67). Although none of the

$\delta^{13}C$ values for burial 582 presented as outliers, the inter-tissue spacing results are still presented here for reference (Figure 85). The bone collagen $\delta^{13}C$ value for burial 582 is more enriched than the first hair segment and mean C1 first hair segment $\delta^{13}C$ value (0.5‰ and 0.5‰, respectively). The mean C1 bone collagen $\delta^{13}C$ value is more enriched than burial 582's first hair segment $\delta^{13}C$ value (0.7‰). The $\delta^{13}C$ inter-tissue spacing values can be found in Appendix L (Table 66).

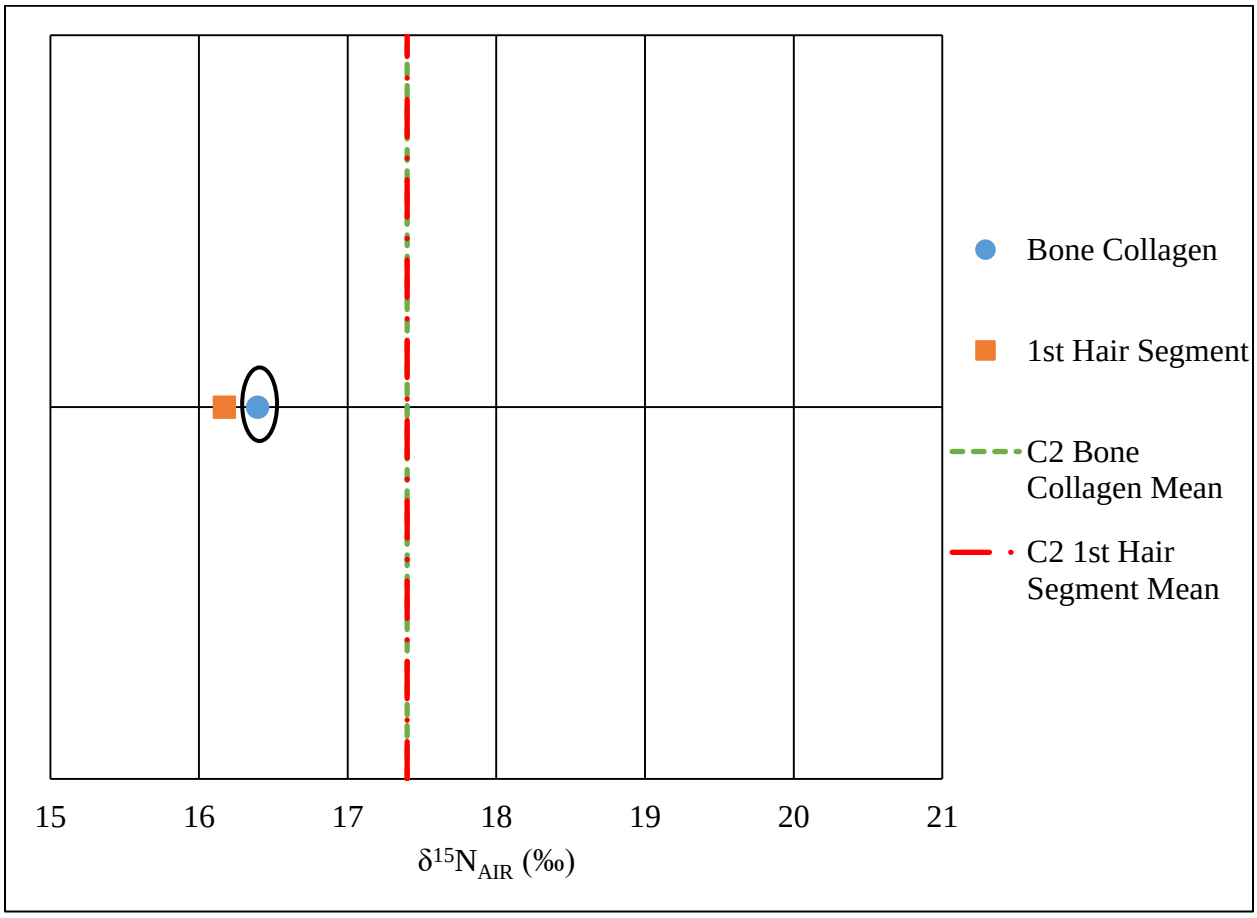

Figure 84: Inter-tissue spacing between bone collagen and hair segment $\delta^{15}N$ values for burial 582, with the outlier value circled and mean C1 cohort bone collagen and first hair segment $\delta^{15}N$ values indicated.

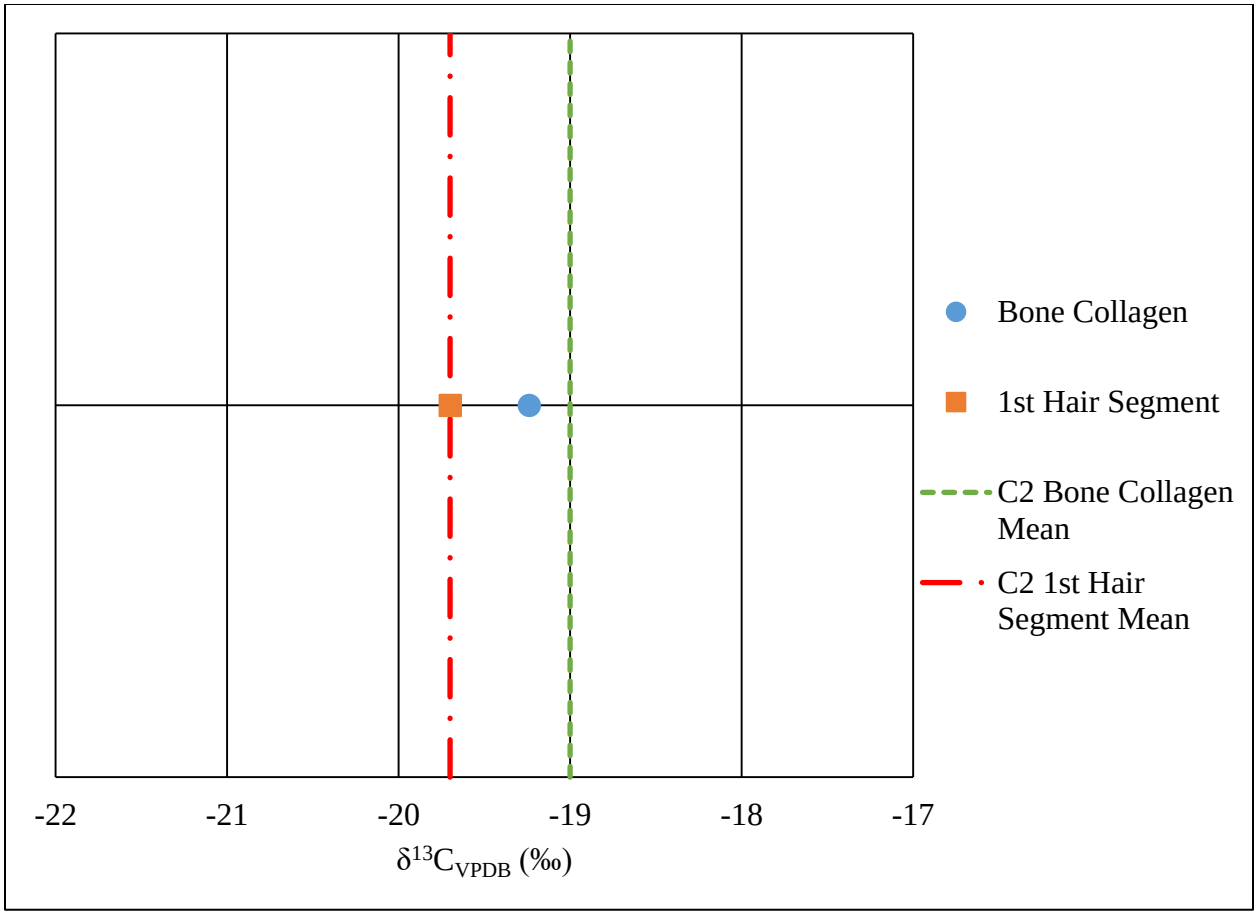

Figure 85: Inter-tissue spacing between bone collagen and hair segment $\delta^{13}C$ values for burial 582 and the mean C1 cohort bone collagen and first hair segment $\delta^{13}C$ values.

CHAPTER 5: DISCUSSION

The initial analysis of $\delta^{13}C$ and $\delta^{15}N$ values for this study included four tissues (bone collage, hair, nail, and skin), however, only bone collagen and hair will be discussed here. Nail was removed from further analysis because nail growth is highly variable from individual to individual and nail to nail due to health status and rate of keratinization (de Berker, 2013; Hamilton et al., 1955; Levit and Scher, 2001; Williams, 2008; Wu et al., 2012; Yaemsiri et al., 2010). Few studies (e.g. Johns, 2012; Norris, 2012; Williams, 2008; Williams, 2005) currently exist that employ the use of skin $\delta^{13}C$ and $\delta^{15}N$ values, with none that have specifically analyzed preservation values to avoid using degraded or contaminated samples; therefore, it was not possible to ensure that the skin samples within this study were not degraded or contaminated, thus the skin samples were removed from further analysis. Bone collagen and hair segments are discussed in regards to inter-tissue spacing and the initial goals of this study involving detecting scurvy isotopically.

Inter-tissue Spacing

The $\delta^{13}C$ and $\delta^{15}N$ inter-tissue spacing results from this study between bone collagen and hair all fall within the published findings of Williams (2005), but do not all fall within those published by Norris (2012). When the overall bone collagen cohort was compared to the overall first hair segment, the difference in mean $\delta^{13}C$ values was statistically significant ($p < 0.001$). These two tissues were spaced 0.7‰, with bone collagen being more enriched in $\delta^{13}C$ than hair. When bone collagen and hair were divided into overall scurvy and non-scurvy cohorts

(disregarding age), the same statistically significant results were found, though with slightly different p-values. The tissue spacing values ranged from 0.5‰ to 0.7‰. These tissue spacing values are not close to that reported by Williams (2005) of 0.5‰, but they are within one standard deviation of this value. The reason this difference in inter-tissue spacing values was found is most likely due to Williams (2005) not dividing her juvenile sample into age cohorts to account for differences in turnover rates, which affect fractionation and subsequently inter-tissue spacing.

When the bone collagen and first hair segment results were divided into age cohorts, a little more variation was found in tissue spacing values. The range here was 0.6‰ to 1.1‰. These results were more closely associated with those bone collagen-to-hair inter-tissue spacing values found by Norris (2012). While Norris (2012) did not include any F&P or neonatal individuals in her study, her inter-tissue spacing results for juveniles aged 1 to 15 years correspond well with the C1, C2, and C3 cohort inter-tissue spacing results in this study. The C1 cohort had a bone collagen to first hair segment value of 0.6‰, while Norris (2012) found a value of 0.72 ± 0.29‰; the C2 cohort had a bone collagen to first hair segment value of 0.7‰ with Norris's (2012) 5 to 10 year old cohort having a value of 0.98 ± 0.11‰; and the C3 cohort had a bone to first hair segment value of 0.6‰, Norris (2012) reported a value of 1.49 ± 0.44‰ in 11 to 15 year olds. The current study includes six additional individuals who exhibit skeletal indicators of scurvy, which may account for the slight differences between the two studies, as they were both conducted on roughly the same sample set.

The $\delta^{15}N$ tissue-spacing values from this study are similar to those found by Williams (2005). Williams (2005) found in her study that bone collagen and hair are spaced 0.5 ± 1.3‰,

while the current study found tissue spacing values between 0.0‰ and 0.7‰. All of the values found within this study, however, do fall well within the standard deviation provided by Williams (2005).

Some anomalous inter-tissue spacing values were found when several outliers were analyzed specifically for bone collagen to hair differences. While the $\delta^{13}C$ values of bone collagen were enriched over each hair segment $\delta^{13}C$ value, one outlier had extreme enrichment over the first hair segment and one had less than expected enrichment. The $\delta^{13}C$ of bone collagen of burial 23 was enriched 2.4‰ over the first hair segment, which is more than both Williams (2005) and Norris (2012) report in their findings. This individual did not show such extreme enrichment of bone collagen over the second hair segment (1.0‰). Since bone collagen is a long-term tissue, this change would be a result of a depletion in $\delta^{13}C$ of the first hair segment, which would indicate a change in diet between the second-to-last and last month of life for this individual. While this juvenile was not diagnosed with skeletal indicators of scurvy, it is possible that they experienced an acute onset of another disease causing a change in diet or crash of their $\delta^{13}C$ values. One other possible explanation for the sudden change in $\delta^{13}C$ value for the first hair segment could be related to a change in diet related to weaning, as this individual was approximately 2 years of age. However, several studies on the Kellis 2 juvenile sample indicate that weaning in this society was a slow process that began at around 6 months of age and was complete around 3 years and included C_4 foods, which would cause an enrichment of $\delta^{13}C$ values (e.g. Dupras, 1999; Dupras and Tocheri, 2007; Dupras et al., 2001; Williams, 2008). This depleted $\delta^{13}C$ value for hair does not follow the typical enrichment pattern seen as a result of weaning in this sample, therefore it is more likely that a sudden change to a more C_3-based

"illness" diet (Williams, 2008), possibly brought on by an acute illness, is a more likely explanation.

The other outlier with a bone collagen to first hair segment enrichment pattern outside of the expected range was burial 582. This individual provided only one hair segment, so no patterns over time can be explored, however, in their last month of life, their bone collagen $\delta^{13}C$ value was only enriched over hair by only 0.5‰, which is low according to both Williams (2005) and Norris (2012). This would indicate this juvenile was consuming more C_4 foods in their last month of life than they had over the course of their life (as determined by their bone collagen $\delta^{13}C$ value). However, since only one hair segment was available for analysis, it is not possible to see if this incorporation of C_4 foods was a gradual process or sudden at the end of their life.

The majority of the $\delta^{15}N$ inter-tissue spacing values between bone collagen and hair for the outliers identified above fall within one standard deviation of the value given by Williams (2005). Burial 23 again falls outside of one standard deviation from this value, however, unlike with the $\delta^{13}C$ values, there is no significant change from the second to the first hair segment, indicating that $\delta^{15}N$ values of their hair did not change significantly in their last two months of life. While their diet may have changed, as evidenced by the changing $\delta^{13}C$ values, the factors that affect $\delta^{15}N$ values (e.g. trophic level, physiological stress) did not drastically change during those two months.

Burial 260, however, shows a drastic enrichment of hair $\delta^{15}N$ values over bone collagen in the second and last month of life. Both the second and first hair segments have $\delta^{15}N$ values that are more enriched than bone collagen, which is opposite of the expected pattern based on Williams's (2005) research. This individual was approximately 15 years old at the time of death,

so the enriched $\delta^{15}N$ value over the last two months of life is not due to breastfeeding as could be possible in much younger individuals. The inclusion of significantly more meat in the diet of this individual, while possible, is not likely to have occurred enough over the entirety of two months to cause such an increase in $\delta^{15}N$ values. Therefore, the most likely cause for the increase in $\delta^{15}N$ values within the first and second hair segments of this individual is physiological stress. This individual was diagnosed as having skeletal indicators of scurvy, which is a physiological stressor. While Olsen (2013) indicated that metabolic diseases do not affect $\delta^{15}N$ values, D'Ortenzio et al. (2015) found that long-term illnesses do cause an increase in $\delta^{15}N$ values. If burial 260 experienced scurvy for a prolonged amount of time, it is possible that it acted more like a long-term illness on their $\delta^{15}N$ values, thus causing the increase seen in the second-to-last month of life. In order to determine if this enrichment of hair $\delta^{15}N$ values was sudden, it would be necessary to look at more hair segments; unfortunately, this individual has provided only the three analyzed hair segments.

The last outlier with interesting $\delta^{15}N$ inter-tissue spacing values is burial 520. The values for this individual are not remarkable in and of themselves, as each value falls within one standard deviation of the published values (e.g. Williams, 2005). However, when taking into account that they were diagnosed as having skeletal indicators of scurvy and then comparing their inter-tissue spacing $\delta^{15}N$ values to those of burial 260, they warrant further discussion. During the last month of life, burial 520's bone collagen was enriched over hair by 1.5‰. Since this individual is known to have scurvy, it would be expected that their hair $\delta^{15}N$ values would show an increase due to the physiological stress of the disease. From the third to the second hair segment the $\delta^{15}N$ value decreased, which is not typical of physiological stress. However, it then

increased between the second and first hair segments, indicating a change in this individual between those two months. Burial 520 was approximately 8 year of age at the time of death, indicating again that breastfeeding would not be the cause for this increase in $\delta^{15}N$ value. As with burial 260, it is also unlikely that enough animal protein was consumed over their last two months of life to affect their $\delta^{15}N$ values to this extent. Therefore, it is again likely that physiological stress is the cause for this increase from the second to first hair segment. Since this individual shows skeletal indicators of scurvy, it is probable that the disease caused this increase in $\delta^{15}N$ value in the first hair segment just prior to death.

Intra-tissue Scurvy and Non-scurvy Comparisons

While it was expected that the scurvy cohorts, due to physiological stress of the disease, would have differing $\delta^{13}C$ and $\delta^{15}N$ values from the non-scurvy cohorts, this was not the result found within this study. The comparison of $\delta^{13}C$ and $\delta^{15}N$ values between overall scurvy and non-scurvy cohorts within bone collagen and hair were unable to detect statistically significant differences within this sample (Appendix F). Likewise, when each tissue was divided by both age cohort and scurvy status, none of the t-test results were statistically significant (Appendix G). The non-statistically significant differences in mean $\delta^{13}C$ and $\delta^{15}N$ values between the scurvy and non-scurvy cohorts for bone collagen and hair indicate that the use of these isotopes and methods is not applicable for the detection of scurvy.

It is possible that scurvy, a metabolic disease, may not sufficiently affect $\delta^{13}C$ or $\delta^{15}N$ values to the point of detection, as indicated by Olsen (2013). However, as discussed previously, such as in regards to burial 260, some differences in $\delta^{13}C$ and/or $\delta^{15}N$ values of scurvy

individuals may exist, especially if it was present for an extended period of time and acted as a long-term illness. If this is the case, it would mean that the non-scurvy cohorts' $\delta^{13}C$ and $\delta^{15}N$ values were also being affected in similar ways during the time periods represented by their bone collagen and hair. Since all of the juveniles within this sample are non-survivors, they were all suffering from end of life events, which would be expected to be revealed in their $\delta^{13}C$ and $\delta^{15}N$ values. This is an example of the Osteological Paradox (Wood et al., 1992).

The osteological paradox essentially states that all archaeological assemblages are composed of individuals that, for one reason or another, are non-survivors, thus making it difficult to accurately determine "healthy" and "unhealthy" individuals within the sample (Wood et al., 1992). As with all bioarchaeological studies, the osteological paradox is relevant to this current study, as the entire sample is composed of juveniles that did not survive childhood, as previously stated. The fact that some individuals exhibit skeletal indicators of scurvy while others do not, does not automatically indicate that one group was "healthier" than the other. When discussing bone collagen, while it is a composite of $\delta^{13}C$ and $\delta^{15}N$ values over time, in juveniles this time frame is greatly shortened (Kinaston et al., 2009) and may reflect end-of-life processes, especially in very young individuals. The use of incremental sampling, such as with hair segments, may possibly mitigate the mortality bias described by the osteological paradox by providing isotopic signatures from time periods that were survived (King et al., 2018), even if those time periods are on the order of months. However, end-of-life processes within hair must be taken into consideration for the first hair segment (closest to the scalp). This segment of hair, as long as it is in the anagen phase (Williams et al., 2011), represents the last month of life (O'Connell and Hedges, 1999; Pollard et al., 2007), and therefore may have some inherent

mortality bias, especially when comparing groups in regards to specific states of "health" (e.g. scurvy vs. non-scurvy). As described above, no statistically significant results from intra-tissue $\delta^{13}C$ or $\delta^{15}N$ value t-tests between scurvy and non-scurvy cohorts were found. This lack of distinction could be the result of scurvy not affecting $\delta^{13}C$ or $\delta^{15}N$ values enough to differentiate them from non-scurvy cohorts, or it could be the result of the non-scurvy cohorts experiencing physiological stressors at the end of their lives causing $\delta^{13}C$ and $\delta^{15}N$ to react similarly to scurvy.

Hair Segments Comparisons

The mean $\delta^{13}C$ and $\delta^{15}N$ values for each age cohort were compared to determine if the onset of scurvy could be detected isotopically. Some patterns were found in the changes of both $\delta^{13}C$ and $\delta^{15}N$ values, but indicators of the onset of scurvy were not found in this sample. These patterns are briefly discussed here, however, they were not useful in bridging the gap between clinical symptoms and skeletal indicators of scurvy.

None of the mean hair segment $\delta^{13}C$ values within each age and scurvy-status cohort were statistically significant, indicating that no significant change over the last three months of life occurred within any age cohort. The scurvy cohorts did not exhibit any pattern in regards to enrichment between the hair segments, with some age cohorts showing enrichment of $\delta^{13}C$ over the last three months of life and others showing depletion of $\delta^{13}C$ during this time period. The non-scurvy cohorts, however, did exhibit a pattern in regards to the change between the second and first hair segment. For each age cohort, the mean $\delta^{13}C$ values decreased between the second and first hair segments, excluding the C1 cohort whose mean $\delta^{13}C$ value remained the same. This decrease indicates a shift toward a more C_3 food-based diet. While these individuals did not have

skeletal indicators of scurvy, they may have been suffering from other illnesses that prompted a change to an "illness" diet as described by Williams (2008). The lack of consistent patterning within the scurvy cohorts, however, does not help to identify an isotopic signature of the disease. In order to determine if hair segment analysis is a viable method for detecting the onset of diseases, it may be necessary to analyze more than three segments of hair to gain more time-depth of isotopic signatures for these juveniles.

Within the mean $\delta^{15}N$ hair segment comparisons, no statistically significant differences were found within each age and scurvy-status cohort, again indicating that no significant changes took place over the last three months of life for these juveniles. The scurvy cohorts did exhibit a pattern between the second and first hair segments, with the mean $\delta^{15}N$ values increasing between these two segments. It is likely that this increase represents the physiological stress experienced by these juveniles in the last two months of life. Some of the non-scurvy age cohorts also indicate an increase in mean $\delta^{15}N$ values during this timeframe, indicating that this increase may not be the result of scurvy, but rather the end-of-life processes experienced by these juveniles. As with the $\delta^{13}C$ values, analysis of more hair segments would aid in determining if the onset of scurvy can be detected using this tissue.

Summary

This study was undertaken in order to determine if analysis of $\delta^{13}C$ and $\delta^{15}N$ values could detect scurvy and non-scurvy cohorts in juveniles from the Kellis 2 cemetery in the Dakhleh Oasis, Egypt. While four tissues were initially investigated for this study (bone collage, hair, nail, and skin), only bone collagen and hair were discussed here. The $\delta^{13}C$ and $\delta^{15}N$ bone

collagen-to-hair inter-tissue spacing results all fall within those published by Williams (2005), however, not all of the $\delta^{13}C$ results are within one or even two standard deviations of those published by Norris (2012). Five outliers were further analyzed in regards to their bone collagen-to-hair inter-tissue spacing values, with interesting results found for both $\delta^{13}C$ and $\delta^{15}N$ values that warrant further investigation. When the intra-tissue scurvy and non-scurvy cohorts were compared, it was found that no statistically significant differences exist between the two cohorts, neither in overall groupings nor in age cohorts. The Osteological Paradox (Wood et al., 1992) is helpful in explaining this lack of difference, as the non-scurvy cohorts are non-survivors and therefore were likely experiencing physiological stressors at the end of their lives that caused changes to their $\delta^{13}C$ and $\delta^{15}N$ values and thus masked any differences from the scurvy cohorts. No significant differences or patterns were found between the three hair segments analyzed in this study. In order to determine if it is possible to detect early isotopic signals of scurvy, additional hair segments would need to be analyzed in order to view a larger time-depth period. While this study was not able to explicitly distinguish scurvy and non-scurvy cohorts isotopically, the inter-tissue spacing results do provide some insight into possible changes caused by the disease and provided some future directions that warrant analysis on this sample.

CHAPTER 6:
CONCLUSION, LIMITATIONS AND FUTURE DIRECTIONS

This thesis was focused on the exploration of analyzing $\delta^{13}C$ and $\delta^{15}N$ values as a method of detecting juveniles with scurvy. A total of 148 juveniles from the Dakhleh Oasis, Egypt, were sampled for this study, with each providing at least one tissue sample (bone collage, hair, nail, or skin). The sample was divided by scurvy status (e.g. scurvy and non-scurvy) and age cohorts (F&P, neonatal, C1, C2, C3). Both intra- and inter-tissue differences between bone collagen and hair were utilized to determine if analysis of $\delta^{13}C$ and $\delta^{15}N$ values is a viable method for detecting the presence of scurvy within this sample. Hair segment comparisons were also conducted in order to attempt to locate an early isotopic signature of scurvy to help bridge the gap between clinical symptoms and skeletal indicators of the disease.

The intra-tissue comparisons within the overall bone collagen and hair segments produced non-statistically significant results. Likewise, when each tissue was divided by age cohorts as well as scurvy status, the t-tests did not indicate any statistically significant differences. This lack of differentiation between the scurvy and non-scurvy cohorts indicates that the disease is not detectable within $\delta^{13}C$ and $\delta^{15}N$ values in intra-tissue analysis within bone collagen and the first three hair segments. Therefore, it was concluded that isotopic analyses of $\delta^{13}C$ and $\delta^{15}N$ is not a viable method for detecting scurvy within this sample. While the exact cause for this lack of differentiation is unknown, it is possible that both scurvy and non-scurvy cohorts were each experiencing end-of-life stressors that were reflected in their $\delta^{13}C$ and $\delta^{15}N$ values, and thus masked any possible differences specifically caused by scurvy.

The comparisons of mean $\delta^{13}C$ and $\delta^{15}N$ values among the hair segments did not indicate a definitive onset of scurvy. While patterns were found within both $\delta^{13}C$ and $\delta^{15}N$ values, they were not consistent as to which scurvy-status cohort they affected. Additionally, using only three hair segments did not provide enough time-depth to establish a pattern within the $\delta^{13}C$ and $\delta^{15}N$ values for each individual. The short amount of time viewed in this study using three hair segments (three months maximum) was not long enough to see if any real changes to trends occurred during that time frame prior to death. In order to determine if $\delta^{13}C$ and $\delta^{15}N$ values can be used to detect the onset of scurvy, and therefore bridge the gap between clinical symptoms and skeletal indicators of the disease, hair segments that extend beyond three months will need to be analyzed.

The most significant information from this study was found within the inter-tissue spacing results between the $\delta^{13}C$ and $\delta^{15}N$ values of bone collagen and hair. The $\delta^{13}C$ and $\delta^{15}N$ inter-tissue spacing values between bone collagen and hair were found to fall within the published values of Williams (2005), even though this study did not divide the sample by age cohorts. Conversely, only the C1 $\delta^{13}C$ inter-tissue spacing value was within the published results of Norris (2012), who *did* separate the sample by age cohorts which coincided directly with those in the current study. The C2 and C3 cohort $\delta^{13}C$ inter-tissue spacing values fell outside of two standard deviations of those found in Norris (2012) for the same cohorts. The samples for both the current study and Norris (2012) came from the same skeletal assemblage and were almost identical for the C1, C2, and C3 cohorts, however, the current study contained six additional juveniles with skeletal indicators of scurvy. While this number of additional scurvy juveniles is small, it may have been enough to alter the inter-spacing results, indicating that scurvy status

may have an effect when comparing long-term and short-term tissues. Several outliers were identified by variations in their $\delta^{13}C$ and $\delta^{15}N$ inter-tissue spacing values found that warrant further investigation to determine in the future using different analytical approaches.

This study has shown that $\delta^{13}C$ and $\delta^{15}N$ values are not useful in detecting the presence of scurvy within a skeletal sample, neither in bone collagen nor hair. Additionally, the analysis of only three hair segments, equivalent to the last three months of life, does not provide enough time-depth to determine if early signals of scurvy can be seen in $\delta^{13}C$ and $\delta^{15}N$ values. Since the non-scurvy cohorts within this study were also non-survivors of childhood, it is likely that their $\delta^{13}C$ and $\delta^{15}N$ values were also being affected by end-of-life processes as well. The results of the inter-tissue bone collagen-to-hair spacing, however, do provide some insight into possible ways that scurvy was affecting this juvenile population. The outliers that were examined here present opportunities for further research to investigate the patterns and variations seen in the current study. Additionally, this study supplements previously published information on inter-tissue spacing of bone collagen and hair and indicates that health status, in addition to age, may also affect inter-tissue spacing.

Limitations and Future Directions

Some of the limitations present within this study are endemic to bioarchaeological studies of past societies. The unbalanced sample sizes within age cohorts, for example between the F&P cohort (n = 37) and the C3 cohort (n = 12); drastically different numbers of scurvy and non-scurvy individuals, both overall and within age cohorts; and small sample sizes within some cohorts, bring some questions of validity to the interpretations made, especially when those

cohorts were involved. These unequal cohort sizes also bring into question how the data should be interpreted. For example, is the high number of scurvy individuals within the neonatal and C1 cohorts due to prevalent micronutrient deficient diets within these cohorts, or is the low number of scurvy individuals within the C2 and C3 cohorts due to smaller sample sizes or even sampling errors? In this instance, it was found that the percentages of scurvy individuals within each of these four cohorts was similar (~25%), alleviating some of the questions in relation to these differences. These limitations, however, may not be possible to overcome due to the limitations regarding sample sizes present in archaeological assemblages. One last limitation shared among bioarchaeological isotopic studies involves the rate of turnover for bone collagen. While the rate of turnover for adult bone collagen is currently believed to be between 10 and 20 years (Katzenberg, 2008), the rate of turnover for juvenile bone collagen is not clearly known, especially for very young individuals, though it is believed to be much faster than the adult turnover rate due to juveniles' constant state of growth (Hedges et al., 2005). Further understanding of bone collagen turnover rates would aid in interpreting the results, not only of this study, but all studies that utilize juvenile bone collagen.

Another limitation found during the course of this study was the classification of individuals within a single cohort (C1) who were in different life stages (regarding the probability of whether they were still breastfeeding or had been completely weaned from breastmilk) at their time of death. Since $\delta^{13}C$ and $\delta^{15}N$ values are sensitive to dietary inputs, grouping individuals together that most likely were consuming different diets makes interpretation of the data unnecessarily difficult. One way to alleviate this difficulty in future studies would be to reorganize the individuals within the C1 cohort based on their probable

breastfeeding/weaning status. One other limitation within this study is the unknown scurvy status of the adult female population of the cemetery. This information is especially important when analyzing the F&P and neonatal cohorts (as well as younger C1 cohort individuals) because these individuals are uniquely tied to their mother's status, both in terms of disease/physiological stress loads and isotopic signatures. A study of the prevalence, or lack thereof, of scurvy within the adult female population in the Kellis 2 cemetery would provide an avenue of better understanding the maternal and fetal/perinatal link within this sample (Kinaston et al., 2009). An investigation of the adult female population's prevalence of scurvy would also allow for a comparison with the C3 cohort to investigate possible reasons for this cohort's hair $\delta^{15}N$ values that tend to rise above that of the adult female average.

In addition to the above proposed research changes and further investigations, additional research of individuals with scurvy within the juveniles from the Kellis 2 cemetery may be able to better illuminate the changes to $\delta^{13}C$ and $\delta^{15}N$ values caused by the physiological stress of disease. One such way to investigate this connection is to sample, whenever possible, more segments of hair in order to look further back into individual lives, both those with and without skeletal indicators of scurvy. This would possibly allow for differentiation between scurvy and non-scurvy $\delta^{13}C$ and $\delta^{15}N$ values, if analyses can be completed either before scurvy individuals acquired the disease or before non-scurvy individuals began to experience end-of-life physiological stressors. Additionally, since micronutrient deficiencies rarely present in isolation, a differential diagnosis should be completed on all scurvy individuals in order to determine what, if any, additional disease loads they were enduring in the months prior to death. Furthermore, studies using techniques such as laser ablation of dentition would provide information from an

intermediate time frame between bone collagen and hair that may help to elucidate more specific information about the isotopic difference between the scurvy and non-scurvy cohorts within this study, especially on those individuals that were classified as outliers.

During the course of this study, it was found that some of the non-scurvy outliers lost their outlier status when they were grouped with their corresponding scurvy cohort. This indicates that those individuals are more isotopically similar to the scurvy individuals than the corresponding non-scurvy individuals. As previously stated, nutritional deficiencies generally do not present alone, and this loss of outlier status could indicate either that the individuals were suffering from scurvy that had not progressed to skeletal lesion manifestation or that they were affected with a disease or diseases that affect stable carbon and nitrogen isotopic values similarly to scurvy. Additionally, interesting information was found in regards to scurvy individuals of typical breastfeeding/weaning ages for the Dakhleh Oasis that warrants further research, as it is possible that the isotopic signatures of scurvy individuals in this study were affected by a buffering effect of breastfeeding that masked significant differences from non-scurvy individuals.

APPENDIX A: TISSUES SAMPLED FOR EACH INDIVIDUAL

Table 53: List of all individuals included in this study, indicating their age cohort, scurvy status, and which tissues were sampled (indicated by an "x").

Sample ID	Age Cohort[1]	Scurvy Y/N	Tissues Sampled			
			Bone	Hair	Nail	Skin
K2-B3	C1	Y				x
15	Neonatal	N		x	x	x
K2-B23	C1	N	x	x	x	x
24	C2	Y		x	x	x
36	F&P	N		x		x
K2-B38	C2	N	x			
49	C2	N		x		
51	F&P	N		x		
54	F&P	N		x		x
56	Neonatal	N		x		
57	Neonatal	N		x		x
63	Neonatal	N		x		x
64	C2	N		x	x	x
65	F&P	N		x		x
70	C1	N	x	x	x	x
71	C1	N	x	x		
K2-B74	Neonatal	Y		x		
86	C1	N	x	x	x	
94	Neonatal	N		x	x	x
95	Neonatal	N		x	x	x
96	F&P	N		x		x
97	C2	N		x	x	
103	Neonatal	N		x	x	x
104	Neonatal	N		x	x	
108	C1	N	x	x	x	x
113	Neonatal	N		x	x	x
115	Neonatal	N		x	x	
123	F&P	N		x		
125	Neonatal	N		x		x
130	F&P	N		x		
133	Neonatal	N		x		x
147	F&P	N		x		
149	C3	N		x		x

Sample ID	Age Cohort[1]	Scurvy Y/N	Tissues Sampled			
			Bone	Hair	Nail	Skin
163	C2	N		x		x
164	Neonatal	N		x		
173	C3	N		x		
180	F&P	N		x		
K2-B187	C3	N	x			
197	F&P	N		x		
206	Neonatal	N		x		x
209	F&P	N		x		
237	Neonatal	N		x		x
239	C3	N		x	x	x
243	C3	N		x		
258	C2	Y		x		x
K2-260	C3	Y	x	x		x
263	C3	N		x		x
276	F&P	N		x	x	
278	C1	N		x	x	x
288	C3	N		x	x	x
K2-B290	C3	Y		x	x	x
292	F&P	N		x		x
K2-B295	C3	Y	x	x		x
K2-B299	C1	Y	x	x	x	x
302	C3	N		x		
316	F&P	N		x		
318B	F&P	N		x		x
323	C1	N		x		x
K2-B325*	Neonatal	N	x			
K2-B326	C1	Y	x			
328	C1	Y		x	x	x
330	C1	N		x		x
331	Neonatal	N		x		x
334	F&P	N		x		x
335	Neonatal	N		x	x	x
K2-336	C2	Y	x	x		x
337	F&P	N		x		
338	F&P	N		x		

Sample ID	Age Cohort[1]	Scurvy Y/N	Tissues Sampled			
			Bone	Hair	Nail	Skin
342	Neonatal	N		x		
347	Neonatal	Y		x	x	x
349	C2	N		x	x	x
351	C1	Y		x		x
K2-B353	Neonatal	Y			x	
356	Neonatal	Y		x		x
357	C1	N		x	x	x
358	C1	N		x	x	x
K2-B359	C2	Y	x			
360	C2	N		x		x
362	C1	N		x		x
370	C2	N		x	x	x
374	C2	N		x	x	x
378	Neonatal	N		x		x
K2-B383	C1	Y		x		
386	F&P	N		x		
K2-B390	Neonatal	Y				x
396	C1	N		x	x	
K2-B404	Neonatal	Y			x	
K2-B419	F&P	Y				x
428	F&P	N		x		
K2-B435	Neonatal	N	x			
K2-B436	F&P	N	x	x		x
K2-B449	F&P	Y	x			
K2-464	C1	N	x			
468	C3	N		x	x	x
472	F&P	N		x		
476	Neonatal	N		x		
483	Neonatal	N		x		x
484	F&P	N		x		
487	C1	N		x		x
K2-490	C1	N	x	x		x
495	F&P	N		x		
508	F&P	N		x		
513B	F&P	N		x		

Sample ID	Age Cohort[1]	Scurvy Y/N	Tissues Sampled			
			Bone	Hair	Nail	Skin
519	C1	Y	x	x	x	x
K2-520	C2	Y	x	x	x	x
K2-525	Neonatal	N	x			
534	C1	N		x		
538	Neonatal	N		x	x	x
542	Neonatal	N		x		x
K2-545	Neonatal	Y	x			
551	Neonatal	N		x		x
560	C1	Y		x	x	x
562	C1	N		x		x
K2-B565	Neonatal	Y		x		
568	F&P	N		x		
571	Neonatal	N		x		x
K2-B575A	Neonatal	Y				x
577	F&P	N		x		
579	C1	N		x		x
580	Neonatal	N		x		x
K2-B582	C2	N	x	x	x	
583A	C2	N		x	x	x
583B	C1	N		x	x	
584	C1	N		x	x	
587	Neonatal	N		x	x	
K2-590	Neonatal	Y	x	x		
593A	C1	N		x	x	
596	Neonatal	N		x	x	
599	F&P	N		x	x	
600	Neonatal	N		x	x	x
602	Neonatal	N		x	x	x
603	Neonatal	N		x	x	
605	F&P	N		x		
606	F&P	N		x		
608	F&P	N		x		x
609	F&P	N		x	x	
610	F&P	N		x		

Sample ID	Age Cohort[1]	Scurvy Y/N	Tissues Sampled			
			Bone	Hair	Nail	Skin
614	F&P	N		x		
616	F&P	N		x		
K2-B617	C1	Y		x		
618	F&P	N		x		
619	C1	N		x	x	x
620	C1	N		x	x	
621	Neonatal	N		x	x	x
K2-B622	Neonatal	Y		x		
624	C1	N		x	x	x
626	Neonatal	Y		x		x
628	C1	N		x	x	x
629	F&P	N		x		

[1]Age categories are as follows: F&P – 16 to 40 weeks gestation; Neo – 41 weeks gestation to 12 months; C1 – 1 to 4 years; C2 – 5 to 10 years; C3 – 11 to 15 years

*This individual was excluded from further evaluation due to multiple preservation factors indicating poor preservation and accuracy of stable isotopic data.

APPENDIX B: INDICATORS OF SCURVY

Table 54: List of scurvy individuals detailing which indicators those individuals exhibited that led to a diagnosis of scurvy by Dr. Sandra Wheeler.

ID #	CO/Orbital Porosity presence[1]	CO Activity [2]	PH/Vault Porosity presence[3]	PH Activity [4]	Skull Lysis [5]	Skull New Bone Proliferation[6]	Periostosis /NBF (post-cranial)[7]
3	1	1	1	1	0	1	1
24	1	1	0	0	0	0	1
74	1	1	0	0	1	1	1
258	1	1	1	1	0	1	
260	1	3	1	2	0	1	
290	1	3	1	1	0	1	1
295	1	1	0	0	1	1	
299	1	1	1	1	0	1	
326	1	1	0	0	0	1	
328	1	1	1	1	0	1	
336	1	1	1	1	0	1	1
347	1	1	1	1	0	1	
351	1	1	1	1	0	1	1
353	1	1	0	0	0	1	1
356	1	1	1	1	1	1	1
359	1	1	0	0	0	1	
383	1	1	1	1	0	1	
390	1	1	1	1	1	1	1
404	1	1	1	1	0	1	
419			0	0	1	1	
449			0	0	0	1	1
519	1	1	0	0	0	1	1
520	1	1	1	1	0	1	
545			0	0	0	1	1
560	1	3	1	1	0	1	1
565	1	1	1	1	0	1	1
575 A			0	0	1	1	
590	1	1	1	3	0	1	1
617	1	1	0	0	1	1	1
622	1	1	1	1	0	1	1

ID #	CO/Orbital Porosity presence[1]	CO Activity [2]	PH/Vault Porosity presence[3]	PH Activity [4]	Skull Lysis [5]	Skull New Bone Proliferation[6]	Periostosis /NBF (post-cranial)[7]
626	1	1	1	1	1	1	1
	[1]1=present	[2]1=active	[3]0=absent, 1=present	[4]1=active, 3=healed	[5]0= absent, 1= present	[6]0=absent, 1=present	[7]1=present

APPENDIX C: PHOTOGRAPHS OF SKELETAL LESIONS INDICATING THE PRESENCE OF SCURVY

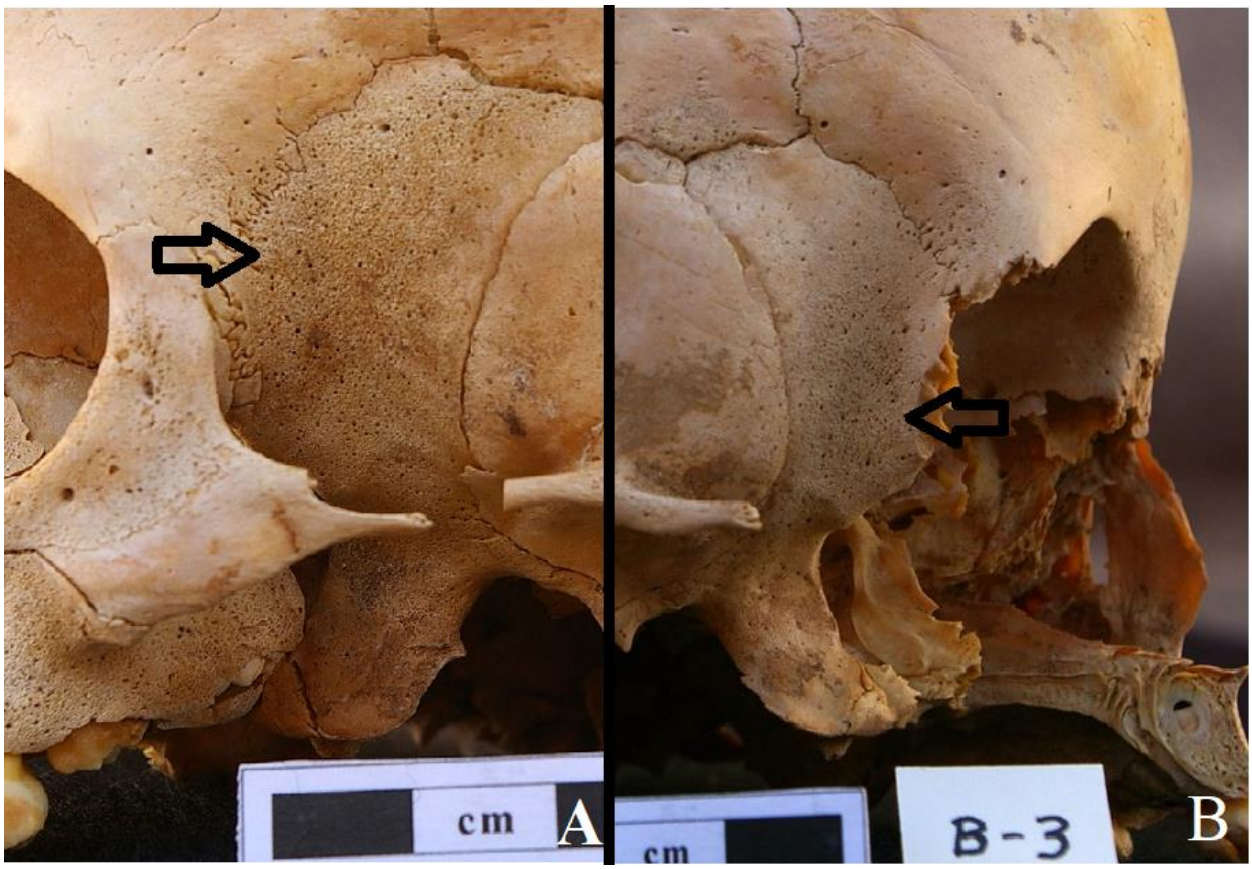

Figure 86: Example of fine porosity on the lateral aspect of the greater wing of the sphenoid of burial 3 (arrows), showing bilateral affliction of both the left (A) and right (B) sides.

Figure 87: Example of cribra orbitalia in the healing stage of burial 260, showing bilateral affliction.

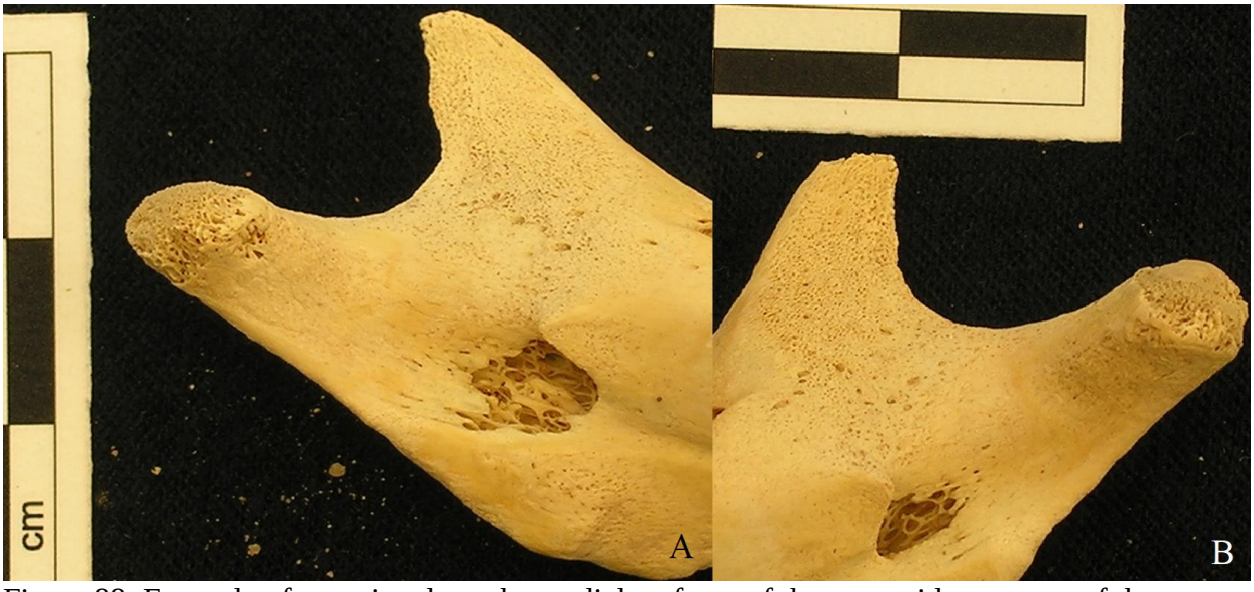

Figure 88: Example of porosity along the medial surfaces of the coronoid processes of the mandible of burial 617, showing bilateral affliction of the left (A) and right (B).

Figure 89: Example of porosity on the mandibular ramus of burial 390, showing bilateral affliction of the left (A) and right (B).

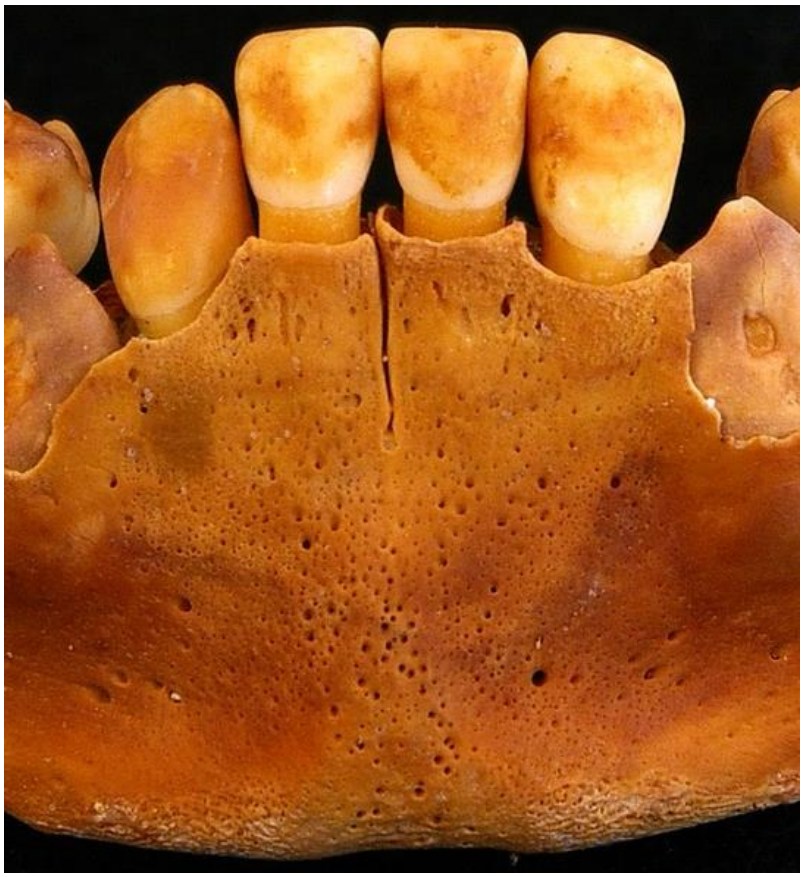
Figure 90: Example of porosity on the anterior mandible of burial 299.

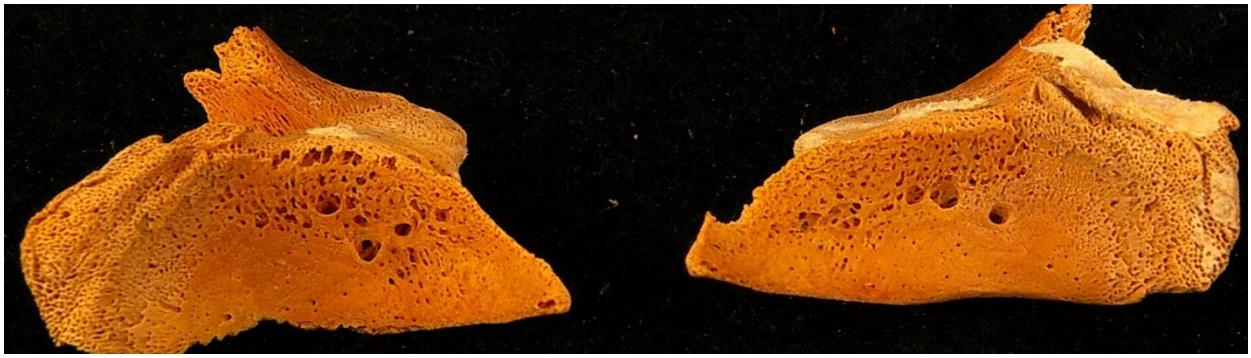

Figure 91: Example of porosity and new bone formation on the orbital surface of the greater wings of the sphenoid of burial 419, showing bilateral affliction.

Figure 92: Example of porosity of the posterior left maxilla above the alveolar bone (circled area) of burial 575A.

Figure 93: Example of porosity of the infra-spinous process (circled in A) and supra-spinous process (arrows in B) of the right scapula of burial 565.

APPENDIX D: TISSUE PRESERVATION VALUES

Table 55: Summary of preservation values for tissue samples prepared by the author. Values outside of published ranges are indicated by an asterisk (*), and the excluded individual is bolded and italicized.

Sample ID	Tissue Type	Collagen Yield (%)	%C Weight	%N Weight	C:N Ratio
23	Bone	16.34	41.48	15.12	3.20
38	Bone	17.65	43.29	15.82	3.19
187	Bone	18.46	43.32	15.91	3.18
260	Bone	14.94	43.33	15.97	3.17
295	Bone	12.66	43.53	15.83	3.21
299	Bone	5.78	42.24	15.21	3.24
325	***Bone***	***3.79****	***14.65****	***4.75****	***3.60***
326	Bone	36.06	43.86	16.09	3.18
336	Bone	7.32	43.17	15.83	3.18
359	Bone	17.15	42.90	15.75	3.18
435	Bone	0.46*	39.25	12.76	3.59
436	Bone	9.65	44.51	16.25	3.20
449	Bone	1.24*	37.12	13.41	3.23
464	Bone	18.50	43.58	15.98	3.18
490	Bone	24.84	44.29	16.30	3.17
520	Bone	21.16	43.14	15.84	3.18
525	Bone	1.70*	44.51	16.12	3.22
545	Bone	11.05	43.37	15.71	3.22
582	Bone	11.79	41.39	15.24	3.17
590	Bone	30.07	43.91	16.17	3.17
74-1	Hair	-	43.00	13.61	3.69
290-1	Hair	-	45.56	14.47	3.67
290-2	Hair	-	44.38	14.30	3.62
383-1	Hair	-	41.66	13.54	3.59
383-2	Hair	-	42.44	13.93	3.55
565-1	Hair	-	42.50	14.03	3.53
590-1	Hair	-	43.87	14.48	3.53
617-1	Hair	-	44.49	14.71	3.53
617-2	Hair	-	44.68	14.78	3.53
622-1	Hair	-	43.04	14.03	3.58
622-2	Hair	-	44.04	14.30	3.59
290	Nail	-	43.78	13.22	3.86*
353	Nail	-	42.18	13.23	3.72
404	Nail	-	43.09	13.43	3.74

Sample ID	Tissue Type	Collagen Yield (%)	%C Weight	%N Weight	C:N Ratio
3	Skin	-	43.24	14.38	3.51
290	Skin	-	46.59	15.35	3.54
390	Skin	-	31.43	9.34	3.93
419	Skin	-	46.4	15.15	3.57
575A	Skin	-	51.48	12.38	4.85*

APPENDIX E: STABLE CARBON AND NITROGEN ISOTOPE DATA

Table 56: Bone collagen $\delta^{13}C$ and $\delta^{15}N$ values.

Sample ID	Age	Bone Collagen	
		$\delta^{13}C$	**$\delta^{15}N$**
449*	F&P	-18.4	19.0
436*	F&P	-19.3	19.2
545*	Neo	-18.3	19.8
590*	Neo	-18.6	20.9
435*	Neo	-18.9	21.3
525*	Neo	-18.6	22.2
299*	C1	-18.2	20.8
326*	C1	-19.3	18.2
519	C1	-19.3	17.9
23*	C1	-18.8	19.7
70	C1	-18.9	21.6
71	C1	-17.6	20.1
86	C1	-18.7	18.2
108	C1	-18.4	19.7
464*	C1	-19.1	17.4
490*	C1	-18.9	18.1
336*	C2	-18.8	17.3
359*	C2	-18.9	17.6
520*	C2	-19.2	18.1
38*	C2	-19.0	17.6
582*	C2	-19.2	16.4
260*	C3	-19.5	17.9
295*	C3	-19.2	18.1
187*	C3	-19.1	17.2
*samples prepared by author; all others prepared by Dr. Lana Williams			

Table 57: First hair segment, second hair segment, and third hair segment $\delta^{13}C$ and $\delta^{15}N$ values for each individual.

Sample ID	Age	Hair Segments					
		1st: 0-1cm		2nd: 1-2cm		3rd: 2-3cm	
		$\delta^{13}C$	$\delta^{15}N$	$\delta^{13}C$	$\delta^{15}N$	$\delta^{13}C$	$\delta^{15}N$
36	F&P	-20.9	19.6				
54	F&P	-19.4	18.7				
65	F&P	-20.3	20.5				
96	F&P	-19.1	18.2				
123	F&P	-19.9	20.1				
130	F&P	-21.7	17.2				
180	F&P	-20.6	19.6				
197	F&P	-19.4	18.5	-19.3	18.2		
209	F&P	-19.6	19.3				
276	F&P	-19.2	18.4	-19.2	18.4		
292	F&P	-21.6	20.1				
316	F&P	-21.3	17.5				
318B	F&P	-20.3	16.1				
334	F&P	-19.1	16.1	-19.4	16.6		
337	F&P	-19.2	18.2				
338	F&P	-19.5	17.7				
386	F&P	-19.4	18.6				
428	F&P	-21.0	21.8				
436	F&P	-19.8	18.7				
472	F&P	-20.2	18.2				
484	F&P	-19.3	20.2				
495	F&P	-19.7	19.2				
513B	F&P	-19.4	18.7				
568	F&P	-19.0	18.5				
577	F&P	-18.9	18.8	-19.0	18.6	-18.4	17.7
599	F&P	-20.1	16.4	-20.5	16.4		
605	F&P	-19.1	18.8	-19.0	18.9	-19.0	19.2
606	F&P	-19.7	17.9	-19.6	17.8	-19.5	18.1
608	F&P	-20.2	17.4				
609	F&P	-19.7	18.4				
610	F&P	-21.2	19.0				
614	F&P	-19.4	19.4				

Sample ID	Age	Hair Segments					
		1st: 0-1cm		2nd: 1-2cm		3rd: 2-3cm	
		$\delta^{13}C$	$\delta^{15}N$	$\delta^{13}C$	$\delta^{15}N$	$\delta^{13}C$	$\delta^{15}N$
629	F&P	-20.2	17.3				
74*	Neo	-18.6	20.4				
347	Neo	-18.3	19.6	-18.2	19.6		
356	Neo	-19.2	19.2	-19.1	19.9		
565*	Neo	-19.4	21.0				
590*	Neo	-18.9	20.2				
622*	Neo	-19.0	18.5	-18.8	18.5		
626	Neo	-19.2	22.1	-19.2	22.0		
15	Neo	-19.7	20.8				
51	Neo	-19.1	18.8	-19.2	18.4	-19.4	18.0
56	Neo	-18.8		-19.1		-19.4	
57	Neo	-18.8	17.6	-19.5	17.9	-19.9	18.0
63	Neo	-18.9	21.6	-18.8	21.8		
94	Neo	-18.8	21.0				
95	Neo	-19.0	21.9	-19.5	21.3		
103	Neo	-20.1	17.3				
104	Neo	-18.9	16.2	-19.1	16.7		
113	Neo	-19.2	19.0	-19.0	18.6	-19.0	18.1
115	Neo	-19.8	17.2				
125	Neo	-18.8	20.9				
133	Neo	-18.8	20.0				
147	Neo	-19.0	20.4	-19.3	19.5	-19.3	20.2
164	Neo	-19.6	18.3				
206	Neo	-20.8	20.8				
237	Neo	-19.1	20.8				
331	Neo	-19.7	20.2				
335	Neo	-19.0	18.9	-18.8	18.7		
342	Neo	-19.5	17.9				
378	Neo	-18.2	19.2				
476	Neo	-19.6	19.7				
483	Neo	-19.5	19.9				
508	Neo	-19.7	18.2				
538	Neo	-18.0	20.7	-18.6	20.6	-18.2	20.8
542	Neo	-18.7	19.5				

Sample ID	Age	Hair Segments					
		1st: 0-1cm		2nd: 1-2cm		3rd: 2-3cm	
		$\delta^{13}C$	$\delta^{15}N$	$\delta^{13}C$	$\delta^{15}N$	$\delta^{13}C$	$\delta^{15}N$
551	Neo	-18.9	19.5	-18.5	19.5		
571	Neo	-18.5	23.6	-18.5	23.4		
580	Neo	-19.0	16.9				
587	Neo	-19.8	21.1				
596	Neo	-22.7	20.1				
600	Neo	-19.3	20.6				
602	Neo	-18.7	21.4				
603	Neo	-19.2	16.8				
621	Neo	-19.2	20.4	-19.1	20.5		
299	C1	-19.2	19.3	-19.0	19.4	-18.7	19.9
328	C1	-18.8	20.3	-18.9	19.7	-19.2	19.3
351	C1	-19.7	16.5				
383*	C1	-19.3	16.4	-19.4	16.4		
519	C1	-19.7	15.2	-20.5	15.8	-21.2	16.3
560	C1	-19.0	20.8				
617*	C1	-19.7	17.5	-19.7	17.9		
23	C1	-21.2	16.8	-19.8	16.9		
70	C1	-18.8	20.9	-18.6	21.0		
71	C1	-18.3	18.3	-18.1	18.5	-17.9	18.3
86	C1	-19.8	18.1	-19.7	17.7		
108	C1	-19.2	18.0				
278	C1	-19.1	18.6	-19.2	18.1	-20.4	18.3
323	C1	-19.5	20.0				
330	C1	-17.9	18.4	-18.6	17.3	-19.4	17.6
357	C1	-18.9	20.9				
358	C1	-19.4	18.3	-19.6	17.8	-19.9	18.1
362	C1	-19.8	17.4	-19.6	17.6		
396	C1	-19.0	17.6	-19.3	17.3	-19.5	16.6
487	C1	-17.7	19.0	-18.1	18.5	-18.9	17.9
490	C1	-19.2	16.2	-20.0	15.3		
534	C1	-18.9	17.9	-19.2	18.5	-19.0	19.6
562	C1	-20.3	17.9	-20.0	18.0		
579	C1	-19.7	18.8	-19.2	20.0	-18.9	19.8
583B	C1	-19.8	20.1	-19.3	19.9	-19.2	20.0

Sample ID	Age	Hair Segments					
		1st: 0-1cm		2nd: 1-2cm		3rd: 2-3cm	
		$\delta^{13}C$	$\delta^{15}N$	$\delta^{13}C$	$\delta^{15}N$	$\delta^{13}C$	$\delta^{15}N$
593A	C1	-19.0	18.8	-19.1	17.6	-20.4	17.9
619	C1	-20.9	15.1				
620	C1	-19.4	20.4	-20.4	20.2	-19.9	20.1
624	C1	-19.4	21.9	-19.4	21.9	-19.6	21.8
628	C1	-19.5	20.1				
24	C2	-19.6	18.2	-19.5	18.4	-19.6	18.1
258	C2	-19.7	18.7				
336	C2	-19.9	16.8	-19.9	16.5	-20.1	16.8
520	C2	-20.2	16.6	-20.2	16.4	-20.4	16.7
49	C2	-19.5	15.3	-19.6	15.9	-19.7	15.5
64	C2	-19.7	19.1	-19.6	17.5		
97	C2	-19.6	16.7	-19.6	17.3	-19.3	18.7
163	C2	-20.2	20.5				
349	C2	-19.4	17.9				
360	C2	-19.6	16.5	-19.2	16.1	-19.1	16.2
370	C2	-19.8	17.5				
374	C2	-19.2	17.2	-19.1	17.6	-19.0	17.4
582	C2	-19.7	16.2				
583A	C2	-19.7	18.0	-19.6	18.2		
584	C2	-20.0	16.6	-20.4	17.3	-20.2	16.3
260	C3	-21.1	19.0	-20.4	18.8	-20.1	17.6
290*	C3	-20.3	17.1	-19.9	17.0		
295	C3	-19.5	17.5	-19.3	17.4	-19.3	17.4
149	C3	-20.1	16.4	-20.2	16.6	-20.0	16.8
173	C3	-19.7	16.6				
239	C3	-19.8	18.7	-19.3	18.6	-19.1	19.0
243	C3	-19.2	18.1	-19.3	18.2	-19.5	18.0
263	C3	-19.5	16.8				
288	C3	-19.6	17.4	-19.4	18.0	-19.7	17.8
302	C3	-19.7	18.6	-19.8	18.5	-19.6	17.6
468	C3	-19.8	17.1	-19.7	17.9	-19.7	17.5
*samples prepared by author; all others prepared by Dr. Lana Williams							

Table 58: Proximal nail segment $\delta^{13}C$ and $\delta^{15}N$ values.

Sample ID	Age	Proximal Nail Segment	
		$\delta^{13}C$	**$\delta^{15}N$**
276	F&P	-19.5	19.5
599	F&P	-20.5	17.2
608	F&P	-19.3	19.4
609	F&P	-18.7	21.2
347	Neo	-18.1	20.6
353*	Neo	-19.5	20.2
404*	Neo	-19.1	21.9
15	Neo	-19.2	20.6
94	Neo	-20.4	22.0
95	Neo	-19.7	21.7
103	Neo	-19.3	21.5
104	Neo	-19.5	18.8
113	Neo	-19.6	19.1
115	Neo	-19.9	22.3
335	Neo	-19.2	19.8
538	Neo	-19.6	20.8
587	Neo	-19.6	21.8
596	Neo	-19.6	21.3
600	Neo	-19.7	21.5
602	Neo	-19.4	22.3
603	Neo	-19.2	21.8
621	Neo	-18.4	20.1
299	C1	-19.6	20.2
328	C1	-19.5	20.9
519	C1	-19.9	18.1
560	C1	-19.7	21.1
23	C1	-20.4	17.6
70	C1	-19.5	21.2
86	C1	-20.4	18.9
108	C1	-19.0	20.3
278	C1	-19.3	18.5
357	C1	-19.7	20.7
358	C1	-20.2	19.2
396	C1	-22.5	24.5

Sample ID	Age	Proximal Nail Segment	
		$\delta^{13}C$	$\delta^{15}N$
583B	C1	-20.0	20.9
593A	C1	-20.5	18.5
619	C1	-20.3	15.5
620	C1	-20.0	20.5
624	C1	-19.3	22.2
628	C1	-20.7	21.3
24	C2	-19.9	18.7
520	C2	-20.7	17.8
64	C2	-19.9	18.6
97	C2	-18.6	20.9
349	C2	-20.2	17.7
370	C2	-20.1	18.0
374	C2	-20.6	18.1
582	C2	-19.9	18.0
583A	C2	-20.1	19.0
584	C2	-20.6	18.1
290*	C3	-20.7	17.9
239	C3	-20.8	20.6
288	C3	-20.2	18.8
468	C3	-20.2	20.5
*samples prepared by author; all others prepared by Dr. Lana Williams			

Table 59: Skin $\delta^{13}C$ and $\delta^{15}N$ values.

Sample ID	Age	Skin	
		$\delta^{13}C$	$\delta^{15}N$
419*	F&P	-19.6	18.7
36	F&P	-21.4	19.9
54	F&P	-20.0	20.0
65	F&P	-20.5	20.6
96	F&P	-20.1	20.3
292	F&P	-20.6	20.9
318B	F&P	-21.8	19.3
334	F&P	-20.5	17.8
436	F&P	-21.0	20.1
347	Neo	-18.7	21.6
356	Neo	-19.9	21.2
390*	Neo	-18.7	21.6
575A*	Neo	-20.9	20.4
626	Neo	-20.1	22.5
15	Neo	-19.9	21.3
57	Neo	-21.6	19.3
63	Neo	-19.8	22.4
94	Neo	-19.5	21.7
95	Neo	-19.4	22.1
103	Neo	-20.0	20.5
113	Neo	-19.6	20.2
125	Neo	-22.7	24.7
133	Neo	-20.1	21.2
206	Neo	-20.7	21.1
237	Neo	-19.8	21.0
331	Neo	-19.7	20.7
335	Neo	-19.3	19.5
378	Neo	-19.1	20.2
483	Neo	-20.9	19.9
538	Neo	-19.5	21.5
542	Neo	-19.6	21.3
551	Neo	-20.0	21.9
571	Neo	-19.2	23.0
580	Neo	-20.1	19.1

Sample ID	Age	Skin	
		$\delta^{13}C$	$\delta^{15}N$
600	Neo	-19.1	21.8
602	Neo	-19.1	22.2
621	Neo	-19.4	20.3
3*	C1	-19.2	22.3
299	C1	-21.7	20.2
328	C1	-19.1	22.5
351	C1	-20.2	21.5
519	C1	-19.1	21.0
560	C1	-19.4	22.3
23	C1	-20.3	21.9
70	C1	-19.6	22.4
108	C1	-19.5	21.4
278	C1	-20.7	22.7
323	C1	-19.0	21.7
330	C1	-18.6	20.6
357	C1	-20.4	23.4
358	C1	-19.0	21.0
362	C1	-20.9	20.3
487	C1	-20.2	22.6
490	C1	-20.2	20.5
562	C1	-20.9	18.2
579	C1	-18.9	22.1
619	C1	-20.1	19.5
624	C1	-19.7	22.9
628	C1	-20.5	20.8
24	C2	-20.6	20.8
258	C2	-19.6	21.2
336	C2	-22.2	18.8
520	C2	-20.1	20.7
64	C2	-20.0	22.5
163	C2	-19.2	21.5
349	C2	-20.3	21.8
360	C2	-18.8	21.7
370	C2	-19.3	22.7
374	C2	-18.8	20.8

Sample ID	Age	Skin	
		$\delta^{13}C$	$\delta^{15}N$
370	C2	-19.3	22.7
374	C2	-18.8	20.8
583A	C2	-22.4	23.5
260	C3	-20.3	21.5
290*	C3	-19.6	20.7
295	C3	-20.6	21.2
149	C3	-21.0	20.2
239	C3	-20.5	20.9
263	C3	-19.8	19.5
288	C3	-22.0	23.9
468	C3	-18.5	20.4
*samples prepared by author; all others prepared by Dr. Lana Williams			

APPENDIX F: OVERALL INTRA-TISSUE MANN-WHITNEY U T-TEST RESULTS

Table 60: Mann-Whitney U t-test results for intra-tissue comparisons of scurvy and non-scurvy samples within each tissue.

Tissue	**p-values**	
	$\delta^{13}C$	**$\delta^{15}N$**
Bone Collagen	0.705	0.622
1st Hair Segment	0.667	0.879
2nd Hair Segment	0.443	0.761
3rd Hair Segment	0.160	0.265
Proximal Nail Segment	0.631	0.518
Skin	0.744	0.907

APPENDIX G: AGE COHORT INTRA-TISSUE MANN-WHITNEY U T-TEST RESULTS

Table 61: Mann-Whitney U t-test results for age cohort intra-tissue comparisons of scurvy and non-scurvy samples within each tissue.

Tissue	Age Cohort	p-values	
		$\delta^{13}C$	$\delta^{15}N$
Bone Collagen	F&P	0.317	0.317
	Neonatal	0.221	0.121
	C1	0.302	0.819
	C2	0.374	0.374
	C3	0.221	0.221
1st Hair Segment	Neonatal	0.361	0.499
	C1	0.980	0.418
	C2	0.290	0.557
	C3	0.258	0.357
2nd Hair Segment	Neonatal	0.567	0.627
	C1	0.709	0.502
	C2	0.410	0.909
	C3	0.431	0.796
3rd Hair Segment	C1	0.942	0.772
	C2	0.180	0.456
	C3	0.737	0.402
Proximal Nail Segment	Neonatal	0.073	0.812
	C1	0.242	0.958
	C2	0.595	0.793
	C3	0.637	0.180
Skin	F&P	0.120	0.245
	Neonatal	0.787	0.471
	C1	0.605	0.854
	C2	0.185	0.018
	C3	0.655	0.297

APPENDIX H: HAIR SEGMENT SCATTER PLOTS

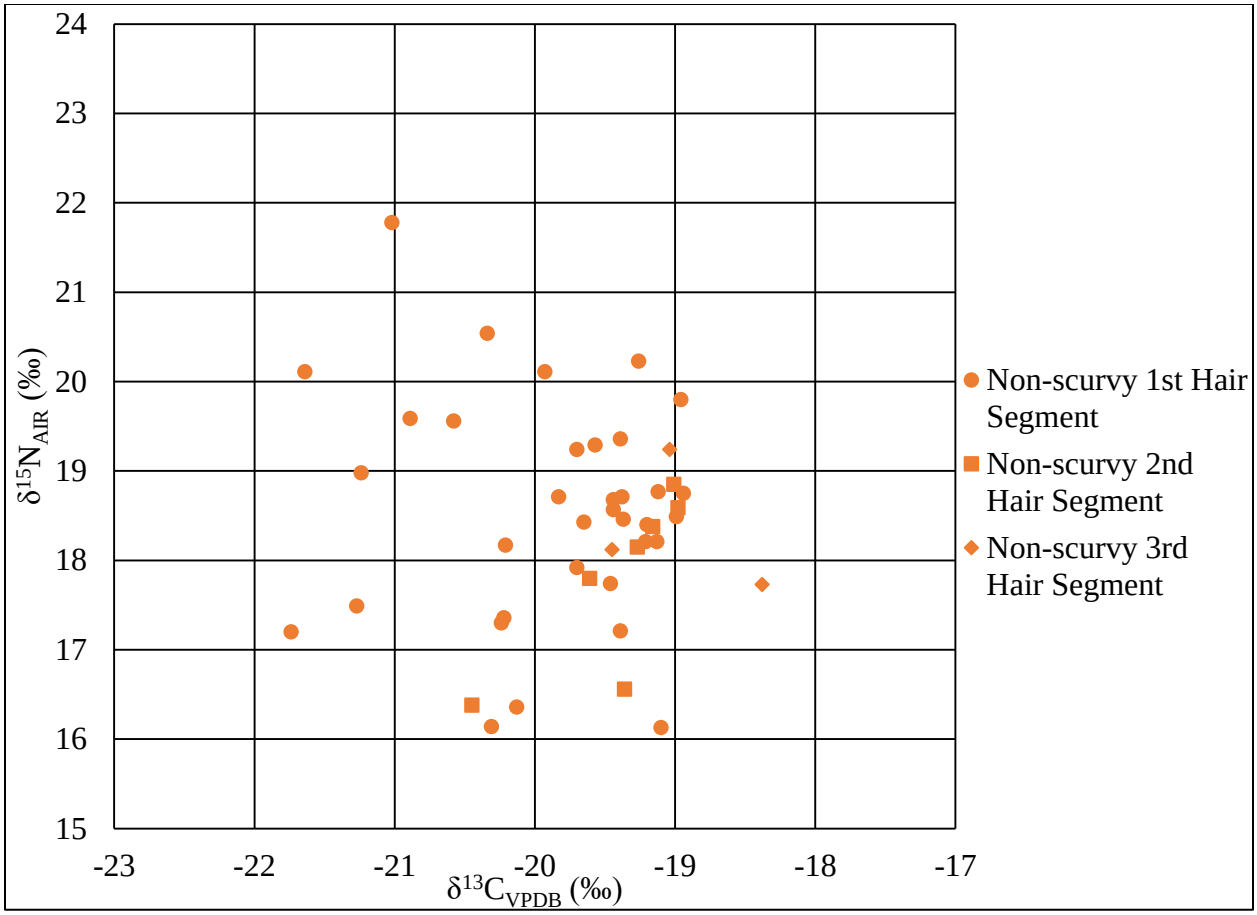

Figure 94: Scatter plot of $\delta^{13}C$ and $\delta^{15}N$ values for first, second, and third hair segments of all juveniles in the F&P cohort.

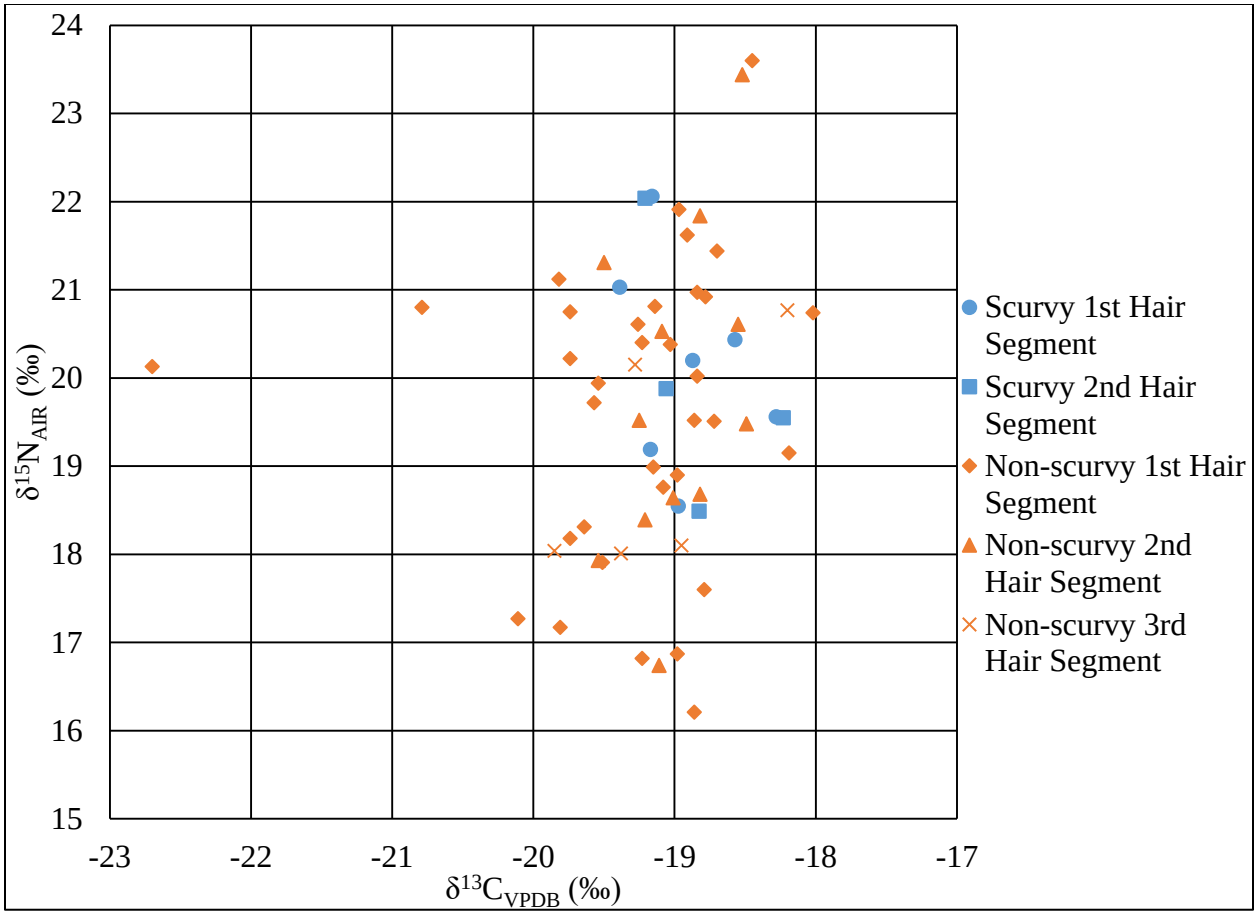

Figure 95: Scatter plot of $\delta^{13}C$ and $\delta^{15}N$ values for first, second, and third hair segments of all juveniles in the neonatal cohort.

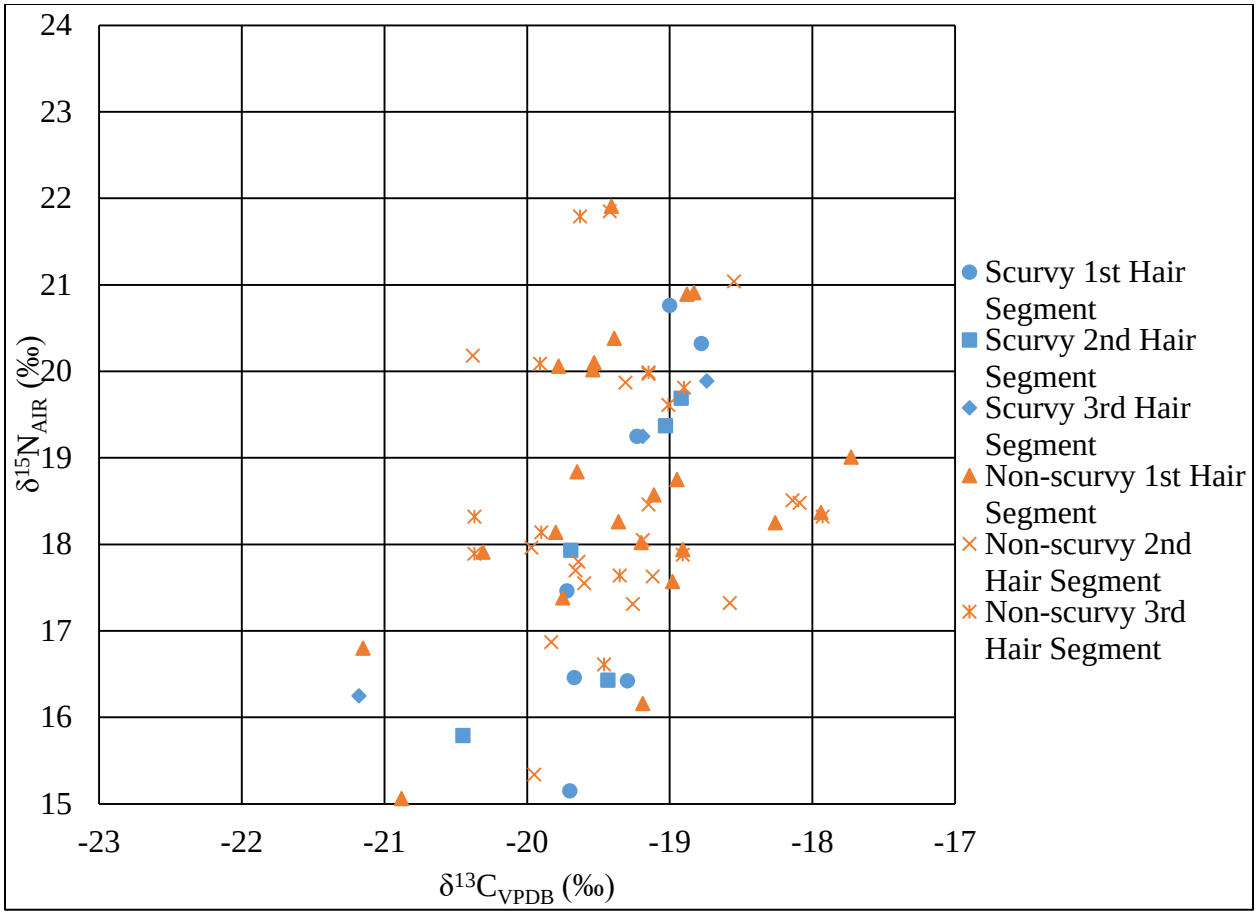

Figure 96: Scatter plot of $\delta^{13}C$ and $\delta^{15}N$ values for first, second, and third hair segments of all juveniles in the C1 cohort.

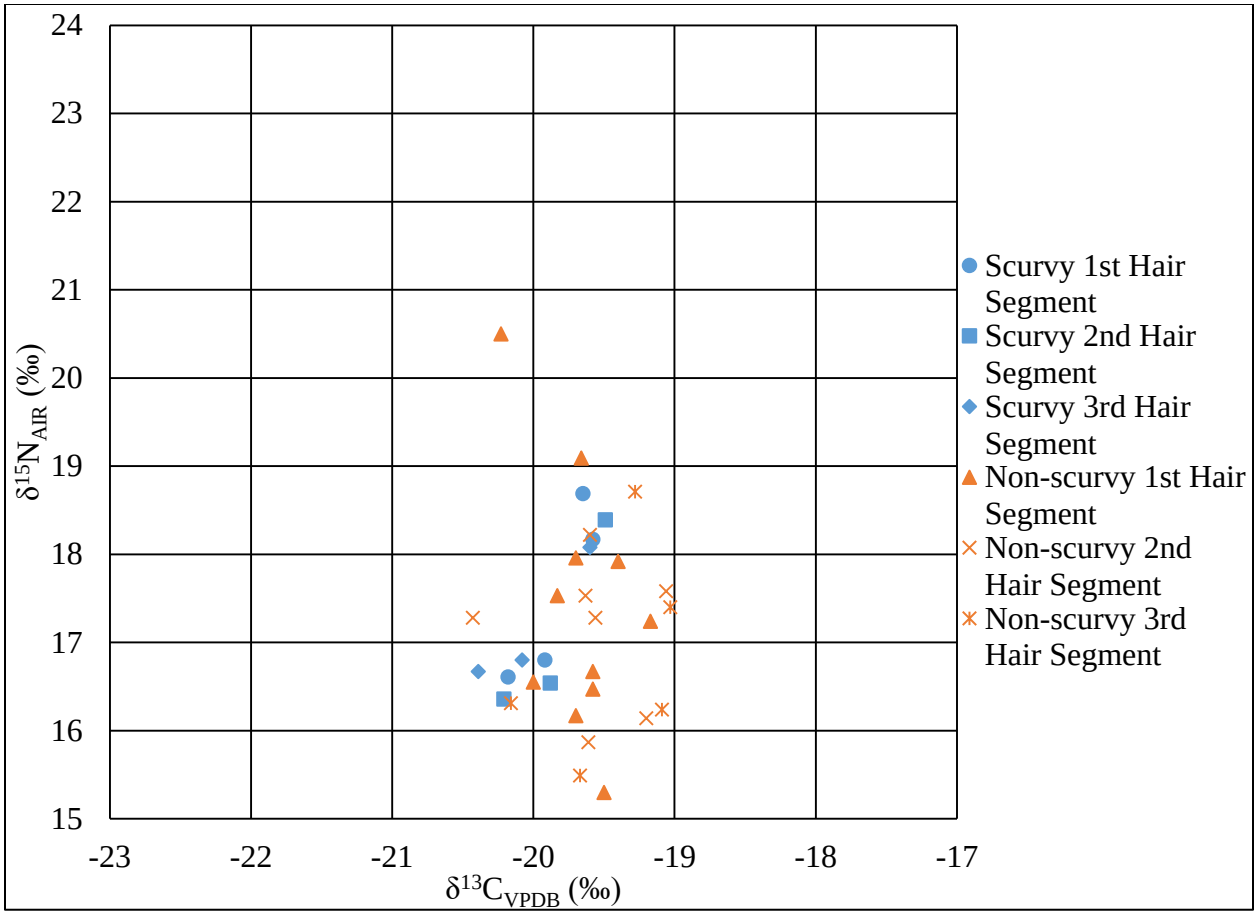

Figure 97: Scatter plot of $\delta^{13}C$ and $\delta^{15}N$ values for first, second, and third hair segments of all juveniles in the C2 cohort.

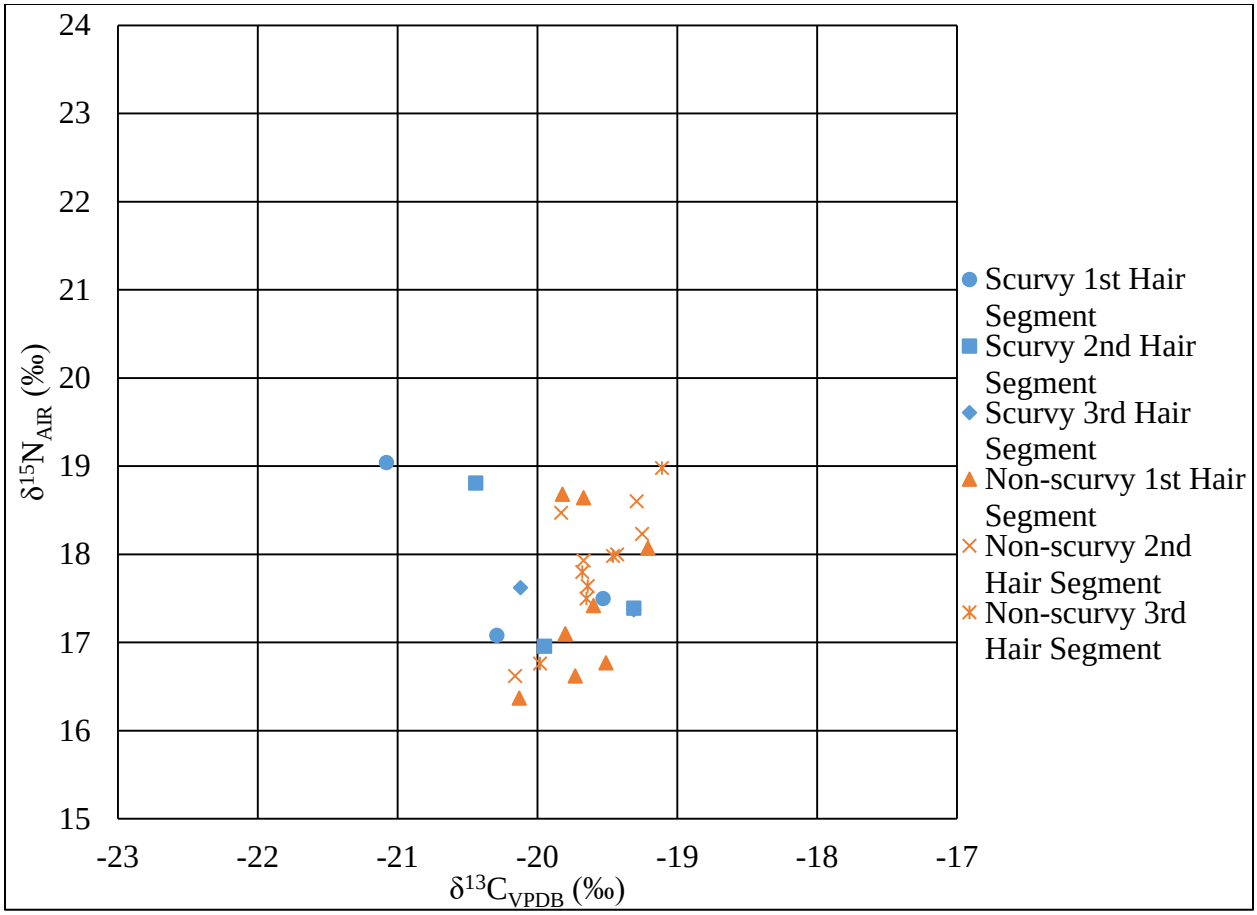

Figure 98: Scatter plot of $\delta^{13}C$ and $\delta^{15}N$ values for first, second, and third hair segments of all juveniles in the C3 cohort.

APPENDIX I: OVERALL INTER-TISSUE SPACING VALUES

Table 62: Overall inter-tissue (Δ) spacing values for $\delta^{13}C$ and $\delta^{15}N$ between bone collagen (BC), the first hair segment (H1), proximal nail segment (N), and skin (S).

	Δ_{BC-H1} (‰)	**Δ_{BC-N} (‰)**	**Δ_{BC-S} (‰)**	**Δ_{H1-N} (‰)**	**Δ_{H1-S} (‰)**	**Δ_{S-N} (‰)**
$\delta^{13}C$	0.7	1	1.2	0.3	0.5	-0.2
$\delta^{15}N$	0.2	-1.1	-2.2	-1.3	-2.4	1.1

APPENDIX J: AGE COHORT INTER-TISSUE SPACING VALUES

Table 63: Age cohort inter-tissue (Δ) spacing values for $\delta^{13}C$ and $\delta^{15}N$ between bone collagen (BC) and the first hair segment (H1).

	ΔBC-H1 (‰)	
	$\delta^{13}C$	**$\delta^{15}N$**
F&P	1.1	0.5
Neonatal	0.6	0.3
C1	0.6	0.7
C2	0.7	0.0
C3	0.6	0.1

APPENDIX K: SCURVY AND NON-SCURVY COHORT INTER-TISSUE SPACING VALUES

Table 64: Overall scurvy and non-scurvy cohort inter-tissue (Δ) spacing values for $\delta^{13}C$ between bone collagen (BC), the first hair segment (H1), proximal nail segment (N), and skin (S).

	Δ_{BC-H1} (‰)	**Δ_{BC-N} (‰)**	**Δ_{BC-S} (‰)**	**Δ_{H1-N} (‰)**	**Δ_{H1-S} (‰)**	**Δ_{S-N} (‰)**
Scurvy to Scurvy	0.5	0.8	1.1	0.3	0.6	-0.3
Non-scurvy to Non-scurvy	0.7	1.0	1.3	0.3	0.6	-0.3
Scurvy to Non-scurvy	0.6	0.9	1.2	0.4	0.7	-0.2
Non-scurvy to Scurvy	0.6	0.9	1.2	0.2	0.5	-0.4

Table 65: Overall scurvy and non-scurvy cohort inter-tissue (Δ) spacing values for $\delta^{15}N$ between bone collagen (BC), the first hair segment (H1), proximal nail segment (N), and skin (S).

	Δ_{BC-H1} (‰)	**Δ_{BC-N} (‰)**	**Δ_{BC-S} (‰)**	**Δ_{H1-N} (‰)**	**Δ_{H1-S} (‰)**	**Δ_{S-N} (‰)**
Scurvy to Scurvy	0.1	-1.0	-2.4	-1.1	-2.5	1.4
Non-scurvy to Non-scurvy	0.4	-0.9	-2	-1.3	-1.1	1.1
Scurvy to Non-scurvy	0.0	-2.4	-2.4	-1.4	-2.5	1.1
Non-scurvy to Scurvy	0.5	-0.6	-2.0	-1.0	-2.4	1.4

APPENDIX L: INTER-TISSUE SPACING VALUES OF OUTLIERS

Table 66: Inter-tissue (Δ) spacing values for $\delta^{13}C$ for outliers between outlier bone collagen (BC); outlier first (H1), second (H2), and third (H3) hair segments; corresponding age cohort mean bone collagen (ACBC); and corresponding age cohort mean first hair segment (ACH1).

Burial	Δ_{BC-H1} (‰)	Δ_{BC-H2} (‰)	Δ_{BC-H3} (‰)	$\Delta_{ACBC-H1}$ (‰)	$\Delta_{ACBC-H2}$ (‰)	$\Delta_{ACBC-H3}$ (‰)	$\Delta_{BC-ACH1}$ (‰)
23	2.4	1.0	-	2.5	1.1	-	0.5
71	0.7	0.5	0.3	-0.4	-0.6	-0.8	1.7
260	1.6	0.9	0.6	1.8	1.1	0.8	0.4
520	1.0	1.0	1.2	1.2	1.2	1.4	0.5
582	0.5	-	-	0.7	-	-	0.5

Table 67: Inter-tissue (Δ) spacing values for $\delta^{15}N$ for outliers between outlier bone collagen (BC); outlier first (H1), second (H2), and third (H3) hair segments; corresponding age cohort mean bone collagen (ACBC); and corresponding age cohort mean first hair segment (ACH1).

Burial	Δ_{BC-H1} (‰)	Δ_{BC-H2} (‰)	Δ_{BC-H3} (‰)	$\Delta_{ACBC-H1}$ (‰)	$\Delta_{ACBC-H2}$ (‰)	$\Delta_{ACBC-H3}$ (‰)	$\Delta_{BC-ACH1}$ (‰)
23	2.9	2.8	-	2.4	2.3	-	1.2
71	1.8	1.6	1.8	0.9	0.7	0.9	1.6
260	-1.1	-0.9	0.3	-1.3	-1.1	0.1	0.3
520	1.5	1.7	1.4	0.8	1.0	0.7	0.7
582	0.2	-	-	1.2	-	-	-1.0

REFERENCES

Adelman HM, Wallach PM, Gutierrez F, Kreitzer SM, Seleznick MJ, Espinoza CG, Espinoza LR. 1994. Scurvy resembling cutaneous vasculitis. Cutis 54:111-114.

Agarwal A, Shaharyar A, Kumar A, Bhat MS, Mishra M. 2015. Scurvy in pediatric age group – A disease often forgotten? J Clin Orthop Trauma 6:101-107.

Allgaier RL, Vallabh K, Lahri S. 2012. Scurvy: A difficult diagnosis with a simple cure. Afr J Emerg Med 2:20-23.

Alqanatish JT, Alqahtani F, Alsewairi WM, Al-kenaizan S. 2015. Childhood scurvy: An unusual cause of refusal to walk in a child. Pediatr Rheumatol Online J 13:23.

Ambrose SH. 1990. Preparation and characterization of bone and tooth collagen for isotopic analysis. J Archaeol Sci 17:431-451.

Ambrose SH, DeNiro MJ. 1987. Bone nitrogen isotope composition and climate. Nature 325:201.

Ambrose SH, Norr L. 1992. On stable isotopic data and prehistoric subsistence in the Soconusco region. Curr Anthropol 33:401-404.

Aufderheide AC, Cartmell LL, Zlonis M, Horne P. 2003. Chemical dietary reconstruction of Greco-Roman mummies at Egypt's Dakhleh Oasis. J Soc Study Egypt Antiq 30:1-10.

Bagnall RS. 1997. The Kellis agricultural account book. Oxford: Oxbow Books.

Barlow T. 1894. The Bradshaw lecture on infantile scurvy and its relation to rickets. Br Med J 2:1029-1034

Barr BC. 2010. Alfred Fabian Hess. American National Biography. Oxford University Press.

Barth JH. 1986. Measurement of hair growth. Clin Exp Dermatol 11:127-138.

Bean WB. 1980. Nail growth: Thirty-five years of observation. Arch Intern Med 140:73-76.

Bickle DD. 2009. Vitamin D insufficiency/deficiency in gastrointestinal disorders. J Bone Miner Res 22:V50-V54.

Bineesh NP, Singhal RS, Pandit AB. 2005. A study on degradation kinetics of ascorbic acid in drumstick (*Moringa olifera*) leaves during cooking. J Sci Food Agric 85:1953-1958.

Birrell M. 1999. Excavations in the cemeteries of Ismant el-Kharab. In: Hope CA, Mills AJ, editors. Dakhleh Oasis Project: Preliminary Reports on the 1992-1993 and 1993-1994 Field Seasons. Oxford: Oxbow Books. p. 29-41.

Blume HP, Alaily U, Smettan U, Zielinshi J. 1984. Soil types and associations of Southwest Egypt. In: Klitzsch E, Said R, Schrak E, editors. Research in Egypt and Sudan. Berlin: Verlag von Dietrich Reimer. p. 293-302.

Bourbou C. 2014. Evidence of childhood scurvy in a Middle Byzantine Greek population from Crete, Greece (11^{th}-12^{th} centuries A.D.). Int J Paleopathol 5:86-94.

Bowen GE. 2003. Some observations on Christian burial practices at Kellis. In: Bowen GE, Hope CA, Parr BE, editors. The Oasis papers 3: Proceedings of the third international conference of the Dakhleh Oasis Project. Oxford: Oxbow Books. p. 167-182.

Brickley M, Ives R. 2008. The bioarchaeology of metabolic bone disease. Amsterdam: Elsevier.

Brickley M, Ives R. 2006. Skeletal manifestations of infantile scurvy. Am J Phys Anthropol 129:163-172.

Brown M, Ortner DJ. 2011. Childhood scurvy in a medieval burial from Macvanska Mitrovica, Serbia. Int J Osteoarchaeol 21:197-207.

Chambial S, Dwivedi S, Shukla KK, John PJ, Sharma P. 2013. Vitamin C in disease prevention and cure: An overview. Ind J Clin Biochem.

Churcher CS. 1993. Romano-Byzantine and Neolithic diets in the Dakhleh Oasis. Bull Can Mediterr Inst 13: 1-2.

Churcher CS. 1983. Dakhleh Oasis Project paleontology: Interim report on the 1982 field season. J Soc Study Egypt Antiquities 13:178-187.

Cope DJ. 2008. Bent bones: The pathological assessment of two fetal skeletons from the Dakhleh Oasis, Egypt. MA thesis. University of Central Florida: Orlando, Florida.

Cope DJ, Dupras TL. 2011. Osteogenesis imperfecta in the archaeological record: An example from the Dakhleh Oasis, Egypt. Int J Paleopathol 1:188-199.

Corr LT, Richards MP, Grier C, Mackie A, Beattie O, Evershed RP. 2009. Probing dietary change of the Kwädąy Dän Ts'ìnchį individual, an ancient glacier body from British Columbia: II. Deconvoluting whole skin and bone collagen $\delta^{13}C$ values via carbon isotope analysis of individual amino acids. J Archaeol Sci 36:12-18.

Crandall JJ, Klaus HD. 2014. Advancements, challenges, and prospects in the paleopathology of scurvy: Current perspectives on vitamin C deficiency in human skeletal remains. Int J Paleopathol 5:1-8.

D'Ortenzio L, Brickley M, Schwarcz H, Prowse T. 2015. You are not what you eat during physiological stress: Isotopic evaluation of human hair. Am J Phys Anthropol 157:374-388.

Davies MB, Austin J, Partridge DA. 1991. Vitamin C: Its chemistry and biochemistry. Cambridge: Royal Society of Chemistry.

Dawber RPR, Van Neste D. 2004. Hair and scalp disorders: Common presenting signs, differential diagnosis and treatment. London: CRC Press.

de Berker D. 2013. Nail anatomy. Clin Dermatol 31:509-515.

DeNiro MJ. 1987. Stable isotopy and archaeology. Am Sci 75:182-191.

DeNiro MJ. 1985. Postmortem preservation and alteration of *in vivo* bone collagen isotope ratios in relation to palaeodietary reconstruction. Nature 317:806-809.

DeNiro MJ, Epstein S. 1978. Influence of diet on the distribution of carbon isotopes in animals. Geochim Cosmochim Acta 42:495-506.

Doering HW, Gericke R. 1984. Practice and problems of agricultural land use in the South East Sahara. In: Klitzsch E, Said R, Schrank E, editors. Research in Egypt and Sudan. Berlin: Verlag von Dietrich. p. 325-334.

Donoghue HD, Marcsik A, Matheson C, Vernon K, Nuorala E, Molto JE, Greenblatt CL, Spigelman M. 2005. Co-infection of *Mycobacterium tuberculosis* and *Mycobacterium leprae* in human archaeological samples: A possible explanation for the historical decline of leprosy. Proc R Soc Lond B Biol Sci 272:389-394.

Dupras TL. 1999. Dining in the Dakhleh Oasis: Determination of diet from documents and stable isotope analysis. Ph.D. dissertation. McMaster University, Hamilton.

Dupras TL, Schwarcz HP. 2001. Strangers in a strange land: Stable isotope evidence for human migration in the Dakhleh Oasis, Egypt. J Archaeol Sci 28:1199-1208.

Dupras TL, Schwarcz HP, Fairgrieve SI. 2001. Infant feeding and weaning practices in Roman Egypt. Am J Phys Anthropol 115:204-212.

Dupras TL, Tocheri MW. 2007. Reconstructing infant weaning histories at Roman period Kellis, Egypt using stable isotope analysis of dentition. Am J Phys Anthropol 134:63-74.

East KE. 2015. Exploring social identity through stable isotope analysis in the Kellis 2 cemetery. MA thesis. University of Central Florida: Orlando, Florida.

Ebling FJG. 1988. The hair cycle and its regulation. Clin Dermatol 6:67-73.

El-Harake WA, Furman MA, Cook B, Nair KS, Kukowski J, Brodsky IG. 1998. Measurement of dermal collagen synthesis rate in vivo in humans. Am J Physiol 274:E586-E591.

Fairgrieve SI, Molto JE. 2000. Cribra orbitalia in two temporally disjunct population samples from the Dakhleh Oasis, Egypt. Am J Phys Anthropol 111:319-331.

Finucane BC. 2007. Mummies, maize, and manure: Multi-tissue stable isotope analysis of late prehistoric human remains from the Ayacucho Valley, Perú. J Archaeol Sci 34:2115-2124.

Forslind B, Lindberg M. 2004. An introduction to the book. In: Forslind B, Lindberg M, editors. Skin, hair, and nails: Structure and function. New York: Marcel Dekker, Inc. pg. 1-10.

Fossitt DD, Kowalski TJ. 2014. Classic skin findings of scurvy. Mayo Clin Proc 89:e61.

Freinkel RK, Woodley DT. 2001. Introduction. In: Freinkel RK, Woodley DT, editors. The biology of the skin. New York: The Parthenon Publishing Group. pg. 15-17.

Giddy LL. 1987. Egyptian oases: Bahariya, Dakhla, Farafara and Kharga during Pharaonic times. London: Aris & Phillips Ltd.

Gilchrist ML, Buxton LHD. 1939. The relation of finger-nail growth to nutritional status. J Anat 73:575-582.

Grauer AL. 2012. A companion to paleopathology. Chichester: Wiley-Blackwell.

Grolmusová Z, Rapčanová A, Michalko J, Čech P, Veis P. 2014. Stable isotope composition of human fingernails from Slovakia. Sci Total Environ 496:226-232.

Haake A, Scott GA, Holbrook KA. 2001. Structure and function of the skin: Overview of the epidermis and dermis. In: Freinkel RK, Woodley DT, editors. The biology of the skin. New York: The Parthenon Publishing Group. pg. 19-46.

Hallberg L, Brune M, Rossander L. 1989. The role of vitamin C in iron absorption. Int J Vitam Nutr Res Suppl 30:103-108.

Hamilton JB, Terada H, Mestler GE. 1955. Studies of growth throughout the lifespan in Japanese: Growth and size of nails and their relationship to age, sex, heredity, and other factors. J Gerontol 10:401-415.

Heaton THE, Vogel JC, von la Chevallerie G, Collett G. 1986. Climatic influence on the isotopic composition of bone nitrogen. Nature 322:822-823.

Hedges REM, Reynard LM. 2007. Nitrogen isotopes and the trophic level of humans in archaeology. J Archaeol Sci 34:1240-1251.

Hedges REM, Stevens RE, Koch PL. 2005. Isotopes in bones and teeth. In: Leng MJ, editor. Isotopes in paleoenvironmental research. Netherlands: Springer. p. 117-145.

Honch NV, McCullagh JSO, Hedges REM. 2012. Variation of bone collagen amino acid $\delta^{13}C$ values in archaeological humans and fauna with different dietary regimes: Developing frameworks of dietary discrimination. Am J Phys Anthropol 148:495-511.

Hope CA. 2003. The excavations at Ismant El-Kharab from 2000-2002. In: Bowen GE, Hope CA, editors. The oasis paper 3: The proceedings of the third international conference of the Dakhleh Oasis Project. Oxford: Oxbow Books. p. 207-289.

Hope CA. 2001. Observations on the dating of the occupation at Ismant el-Kharab. In: Marlow CA, Mills AJ, editors. The Oasis papers. I. The proceedings of the First Conference of the Dakhleh Oasis Project. Oxford: Oxbow Books. p. 43-59.

Innis MD. 2012. Malnutrition, liver dysfunction, subdural and retinal haemorrhages and encephalopathy in children resulting from a deficiency or abnormality of vitamins C, D and K. J Orthomol Med 27:117-122.

Jeejeebhoy KN, Duerksen DR. 2018. Malnutrition in gastrointestinal disorders: Detection and nutritional assessment. Gastroenterol Clin N Am 47:1-22.

Johns N. 2012. Stable isotopes and multiple tissue analysis: Reconstructing life histories for individuals from the Dakhleh Oasis, Egypt. MA thesis. University of Central Florida: Orlando, Florida.

Jutkus RAL, Li N, Taylor LS, Mauer LJ. 2015. Effect of temperature and initial moisture content on the chemical stability and color change of various forms of vitamin C. Int J Food Prop 18:862-879.

Kaewsuksaeng S, Urano Y, Aiamla-or S, Shigyo M, Yamauchi N. 2011. Effect of UV-B irradiation on chlorophyll-degrading enzyme activities and postharvest quality in stored lime (*Citrus latifolia* Tan.) fruit. Postharvest Biol Technol 61:124-130.

Katzenberg MA. 2008. Stable isotope analysis: A tool for studying past diet, demography, and life history. In: Katzenberg MA, Saunders SR, editors. Biological anthropology of the human skeleton, 2nd ed. New Jersey: John Wiley & Sons, Inc.

Katzenberg MA, Lovell NC. 1999. Stable isotope variation in pathological bone. Int J Osteoarchaeol 9:316-324.

Kinaston RL, Buckley HR, Halcrow SE, Spriggs MJT, Bedford S, Neal K, Gray A. 2009. Investigating foetal and perinatal mortality in prehistoric skeletal samples: A case study from a 3000-year-old Pacific Island cemetery site. J Archaeol Sci 36:2780-2787.

King CL, Millard AR, Gröcke DR, Standen VG, Arriaza BT, Halcrow SE. 2018. A comparison of using bulk and incremental isotopic analyses to establish weaning practices in the past. Sci Technol Archaeol Res 3:126-134.

Klaus HD. 2015. Paleopathological rigor and differential diagnosis: Case studies involving terminology, description, and diagnostic frameworks for scurvy in skeletal remains. Int J Paleopathol. http://dx.doi.org/10.1016/j.ijpp.2015.10.002.

Kligman AM. 1959. The human hair cycle. J Invest Dermatol 33:307-316.

Krueger HW, Sullivan CH. 1984. Models for carbon isotope fractionation between diet and bone. Stable Isotopes in Nutrition 258:205-220.

Lamb AL. 2016. Stable isotope analysis of soft tissues from mummified human remains. Environ Archaeol 21:271-284.

Lambert JB. 1997. Traces of the past: Unraveling the secrets of archaeology through chemistry. Cambridge: Perseus Publishing.

Lee-Thorp JA. 2008. On isotopes and old bones. Archaeometry 50: 925-950.

Lee-Thorp JA, Sealy JC, van der Merwe NJ. 1989. Stable carbon isotope ratio differences between bone collagen and bone apatite, and their relationship to diet. J Archaeol Sci 16:585-599.

Levit EK, Scher RK. 2001. Basic science of the nail unit. In: Freinkel RK, Woodley DT, editors. The biology of the skin. New York: The Parthenon Publishing Group. pg. 101-112.

Lind J. 1753. A treatise of the scurvy. Edinburgh. Eighteenth Century Collections Online. Gale.

Longin R. 1971. New method of collagen extraction for radiocarbon dating. Nature 230:241-242.

Lubec G. 1987. Structural stability of hair over three thousand years. J Archaeol Sci 14:113-120.

Mathews S. 2008. Diagnosing anencephaly in archaeology: A comparative analysis of nine clinical specimens from the Smithsonian Institution National Museum of Natural History, and one from the archaeological site of Kellis 2 cemetery in Dakhleh Oasis, Egypt. MA thesis. University of Central Florida: Orlando, Florida.

McKeag NA, McKinley MC, Woodside JV, Harbinson MT, McKeown PP. 2012. The role of micronutrients in heart failure. J Acad Nutr Diet 112:870-886.

Mekota AM, Frupe G, Ufer S, Cuntz U. 2009. Identifying starvation episodes using stable isotopes in hair: Forensic approach on serial hair analysis. Rechtsmedizin 19:431-440.

Milner N, Craig OE, Bailey GN, Pedersen K, Andersen SH. 2004. Something fishy in the Neolithic? A re-evaluation of stable isotope analysis of Mesolithic and Neolithic coastal populations. Antiquity 78:9-22.

Molto JE. 2002. Leprosy in Roman period skeletons from Kellis 2, Dakhleh, Egypt. In: Roberts CA, Lewis ME, Manchester K, editors. The past and present of leprosy: Archaeological, historical, palaeopathological and clinical approaches. Oxford: Archaeopress. p. 179-192.

Nadiger HA. 1980. Role of vitamin E in the aetiology of phrynoderma (follicular hyperkeratosis) and its interrelationship with B-complex vitamins. Br J Nutr 44:211-214.

Netter FH. 2019. Atlas of human anatomy, 7th ed. Philadelphia: Elsevier.

Nolan JD, Johnston IM, Walters JRF. 2015. Basic science: Physiology of malabsorption. Surg 30:268-274.

Noordin S, Baloch N, Salat MS, Memon AR, Ahmad T. 2012. Skeletal manifestations of scurvy: A case report from Dubai. Case Rep Orthop 2012:1-5.

Norris AL. 2012. Age as a factor in inter-tissue spacing of stable carbon isotope values in juvenile human remains from the Dakhleh Oasis, Egypt. MA thesis. University of Central Florida: Orlando, Florida.

Nunes MCN, Brecht JK, Morais AMMB, Sargent SA. 1998. Controlling temperature and water loss to maintain ascorbic acid levels in strawberries during postharvest handling. J Food Sci 63:1033-1036.

O'Connell TC, Hedges REM. 1999. Isotopic comparison of hair, nail, and bone: Modern analyses. J Archaeol Sci 28:1247-1255.

O'Connell TC, Hedges REM, Healey MA, Simpson AHRW. 2001. Isotopic comparison of hair, nail and bone: Modern analyses. J Archaeol Sci 28:1247-1255.

Olsen KC. 2013. A multi-isotope investigation of two medieval German populations: Insight into the relationship among diet, disease, and tissue isotopic compositions. Ph.D. dissertation. University of Western Ontario: London, Ontario, Canada.

Orentreich N, Markofsky J, Vogelman JH. 1979. The effect of aging on the rate of linear nail growth. J Invest Dermatol 73:126-130.

Ortner DJ, Butler W, Cafarella J, Milligan L. 2001. Evidence of probable scurvy in subadults from archaeological sites in North America. Am J Phys Anthropol 114:343-351.

Ortner DJ, Ericksen MF. 1997. Bone changes in the human skull probably resulting from scurvy in infancy and childhood. Int J Osteoarchaeol 7:212-220.

Page KE. 2014. Bioarchaeological assessment of diet and changes in femoral and humeral stable isotopic values among subadults at medieval Alytus, Lithuania. MA thesis. University of Central Florida: Orlando, Florida.

Paus R, Cotsarelis G. 1999. The biology of hair follicles. N Engl J Med 341:491-497.

Pimentel L. 2003. Scurvy: Historical review and current diagnostic approach. Am J Emerg med 21:328-332.

Polat AV, Bekci T, Say F, Bolukbas E, Selcuk MB. 2015. Osteoskeletal manifestations of scurvy: MRI and ultrasound findings. Skeletal Radiol 44:1161-1164.

Pollard M, Batt C, Stern B, Young SMM. 2007. Analytical chemistry in archaeology. Cambridge: Cambridge University Press.

Popovich D, McAlhany A, Adewumi AO, Barnes MM. 2009. Scurvy: Forgotten but definitely not gone. J Pediatr Health Care 23:405-415.

Price M. 1985. Introducing groundwater. London: George Allen & Unwin.

Rameshkumar A, Sivasudha T, Jeyadevi R, Ananth DA, Pradeepha G. 2012. Effect of environmental factors (air and UV-C irradiation) on some fresh fruit juices. Eur Food Res Technol 234:1063-1070.

Rumberger JD. 2016. Diet and migration in coastal Oaxaca: Identifying effects of political and social collapse through the utilization of stable isotope analysis. MA thesis. University of Central Florida: Orlando, Florida.

Saitoh M, Uzuka M, Sakamoto M. 1970. Human hair cycle. J Invest Dermatol 54:65-81.

Sandström B. 2001. Micronutrient interactions: Effects on absorption and bioavailability. Br J Nutr 85 Suppl 2:S181-S185.

Scanlon VC, Sanders T. 2007. Essentials of anatomy and physiology. 5th ed. Philadelphia: F.A. Davis Company.

Scheuer L, Black S. 2000. Developmental Juvenile Osteology. Amsterdam: Elsevier Academic Press.

Schoeninger MJ, Moore K. 1992. Bone stable isotope studies in archaeology. J World Prehistory 6:247-296.

Schoeninger MJ, Moore KM, Murray ML, Kingston JD. 1989. Detection of bone preservation in archaeological and fossil samples. Appl Geochem 4:281-292.

Schwarcz HP, Dupras TL, Fairgrieve SI. 1999. ^{15}N enrichment in the Sahara: In search of a global relationship. J Archaeol Sci 26:629-636.

Shalin M. 1985. Hydrology of the Nile Basin. Amsterdam: Elsevier.

Snoddy AME, Halcrow SE, Buckley HR, Standen VG, Arriaza BT. 2017. Scurvy at the agricultural transition in the Atacama desert (ca 3600-3200 BP): Nutritional stress at the maternal-foetal interface? Int J Paleopathol 18:108-120.

Song EK, Kang S. 2018. Vitamin C deficiency, high-sensitivty C-reactive protein, and cardiac event-free survival in patients with heart failure. J Cardiovasc Nurs 33:6-12.

Stark RJ. 2014. A proposed framework for the study of paleopathological cases of subadult scurvy. Int J Paleopathol 5:18-26.

Stevens RE, Lightfoot E, Hamilton J, Cunliffe B, Hedges REM. 2010. Stable isotope investigations of the Danebury hillfort pit burials. Oxf J Archaeol 29:407-428.

Stewart JD, Molto JE, Reimer PJ. 2003. The chronology of Kellis 2: The interpretative significance of radiocarbon dating of human remains. In: Bowen GE, Hope CA, editors. The Oasis papers 3: Proceedings from the third international conference of the Dakhleh Oasis Project. Oxford: Oxbow Books. p. 373-382.

Strange MR. 2006. The effect of pathology on the stable isotopes of carbon & nitrogen: Implications for dietary reconstruction. MA thesis. Binghamton University: Binghamton, New York.

Thanheiser U, Walter J, Hope CA. 2002. Roman agriculture and gardening in Egypt as seen from Kellis. In: Hope CA, Bowen GE. Dakhleh Oasis Project: Preliminary reports on the 1994-1995 to 1998-1999 field seasons. Oxford: Oxbow Books. p. 299-310.

Tieszen LL, Boutton TW, Tesdahl KG, Slade NA. 1983. Fractionation and turnover of stable carbon isotopes in animal tissues: Implications for $\delta^{13}C$ analysis of diet. Oecologia 57:32-37.

Tocheri MW, Dupras TL, Sheldrick P, Molto JE. 2005. Roman period fetal skeletons from the east cemetery (Kellis 2) of Kellis, Egypt. Int J Osteoarchaeol 15:326-341.

Vagianos K, Bector S, McConnell J, Bernstein CN. 2007. Nutrition assessment of patients with inflammatory bowel disease. JPEN J Parenter Enteral Nutr 31:311-319.

Valšíková M, Mezeyová I, Rehuš M, Šlosár M. 2016. Changes of vitamin C content in celery and parsley herb after processing. Potravinarstvo 10:637-642.

van Klinken GJ. 1999. Bone collagen quality indicators for palaeodietary and radiocarbon measurements. J Archaeol Sci 26:687-695.

Webb EC, White CD, Van Uum S, Longstaffe FJ. 2015. Integrating cortisol and isotopic analyses of archaeological hair: Elucidating juvenile ante-mortem stress and behaviour. Int J Paleopathol 9:28-37.

Westgate GE, Botchkareva NV, Tobin DJ. 2013. The biology of hair diversity. Int J Cosmet Sci 35:329-336.

Wheeler SM. 2009. Bioarchaeology of infancy and childhood at the Kellis 2 cemetery, Dakhleh Oasis, Egypt. Ph.D. dissertation. University of Western Ontario: London, Ontario, Canada.

White CD. 1991. Isotopic analysis of multiple human tissues from three ancient Nubian populations. Ph.D. dissertation. University of Toronto: Toronto, Ontario, Canada.

White CD, Armelagos GJ. 1997. Osteopenia and stable isotope ratios in bone collagen of Nubian female mummies. Am J Phys Anthropol 103:185-199.

White CD, Longstaffe FJ, Law KR. 1999. Seasonal stability and variation in diet as reflected in human mummy tissues from the Kharga Oasis and the Nile Valley. Palaeogeogr Palaeoclimatol Palaeoecol 147:209-222.

White CD, Schwarcz HP. 1994. Temporal trends in stable isotopes for Nubian mummy tissues. Am J Phys Anthropol 93:165-187.

Williams JS. 2005. Investigating diet and dietary change using the stable isotopes of carbon and nitrogen in mummified tissues from Puruchuco-Huaquerones, Peru. Ph.D. dissertation. University of Calgary: Calgary, Alberta, Canada.

Williams LJ, White CD, Longstaffe FJ. 2011. Improving stable isotopic interpretations made from human hair through reduction of growth cycle error. Am J Phys Anthropol 145:125-136.

Williams LJ. 2008. Investigating seasonality of death at Kellis 2 cemetery using solar alignment and isotopic analysis of mummified tissues. Ph.D. dissertation. University of Western Ontario: London, Ontario, Canada.

Wood JW, Milner GR, Harpending HC, Weiss KM. 1992. The osteological paradox: Problems of inferring prehistoric health from skeletal samples. Curr Anthropol 33:343-370.

Wu Z, Xu J, Jiao Y, Fan S, He K, Qin L. 2012. Fingernail growth rate and macroelement levels determined by ICP-OES in healthy Chinese college students. Pol J Environ Stud 21:1067- 1070.

Yaemsiri S, Hou N, Slining MM, He K. 2010. Growth rate of human fingernails and toenails in healthy American young adults. J Eur Acad Dermatol Venereol 24:420-423.